Universität Rostock

Traditio et Innovatio

Institute of Physics
Research Report
2010-2012

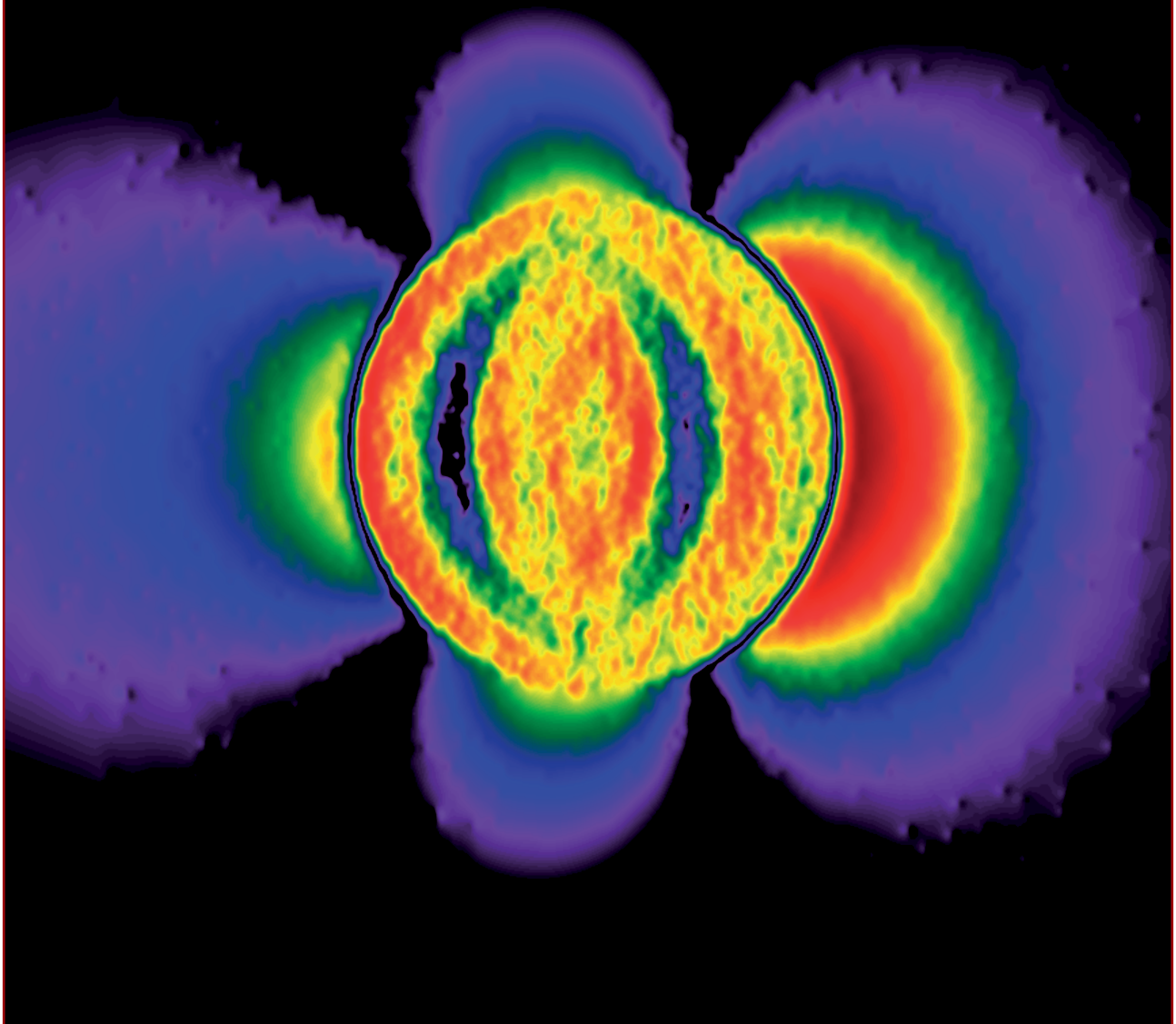

Faculty of Mathematics and Natural Sciences

Institute of Physics

Research Report
2010–2012

University of Rostock
2013

Editor: Institute of Physics
University of Rostock

Editorial Work: Dr. Sergei D. Ivanov, Prof. Dr. Oliver Kühn

CIP Short Title: Research Report 2010–2012
Institute of Physics
University of Rostock
2013

Source of supply: University of Rostock, Institute of Physics, 18051 Rostock
Telephone: +49 (0)381 498-6700
Telefax: +49 (0)381 498-6702
e-mail: institut.physik@uni-rostock.de
http://www.physik.uni-rostock.de

Titlepage: Internal plasma waves in a laser-driven nanoparticle.
Adapted from C. Peltz *et al.*, New J. Phys., **14**, 065011 (2012)

Print: Stadtdruckerei Weidner GmbH Rostock

Contents

Preface

This research report covers the activities of the Institute of Physics at the University of Rostock during the years 2010 - 2012. The tradition of the institute starts in 1874 when Ludwig Matthiessen was appointed to the first chair of Physics, a position he held for more than 30 years. During these years the importance of physics — not at least for the industrial development — led to an expansion of the institute up to the point that a new building was needed. Finally, in 1910 the new physics building by the architect Hermann Schlosser was opened after two years of construction. The 100th anniversary of this event was celebrated with a colloquium in June 2010. However, this occasion was not only for remembering history, but also for looking ahead: At that time the new physics building on the Südstadt campus already took shape. The topping out ceremony (see picture below) has been the latest event in this respect (see also Section 1).

The Institute of Physics in 2012 has its focus on experiment and theory in the areas Optics and Laser Physics, Physics of Nanomaterials, and Physics of Particles and Fields. Expertise in Maritime and Atmospheric Physics is contributed by two adjunct external institutes, i.e. the Baltic See Research Institute and the Leibniz Institute for Atmospheric Physics.

In the reporting period (2010) Professors H.-J. Fitting and H. Schröder retired. In April 2012 we received the sad news, that Prof. Schröder passed away at the age of 67. Five new professors, two of them being junior professors, have been appointed: In Experimental Physics Prof. Sylvia Speller and Jun.-Prof. Boris Hage joined the institute. Prof. Speller's research focuses on "Surfaces and Interfaces" where she investigates systems on the nanometer scale at the border between Physics, Chemistry, and Biology. Jun.-Prof. Hage's "Experimental Quantum Optics" group is concerned with fundamental quantum properties of light. Jointly with the Leibniz Institute for Plasma Science and Technology, Greifswald, the University of Rostock appointed Prof. Jürgen Kolb as a Professor for Bioelectrics. In Theoretical Physics Prof. Stefan Scheel ("Quantum Optics of Macroscopic Systems") and Jun.-Prof. Thomas Fennel ("Theoretical Cluster Physics") have been appointed.

The research at the institute is to a considerable extent based on third party funding, via individual or collaborative grants. Among the collaborative grants the Sonderforschungsbereich (SFB) 652 "Strong Correlations and Collective Effects in Radiation Fields" continued to provide the platform for the joined research of ten groups from the institute, one from the Institute of Chemistry and three from the University of Greifswald. Furthermore, two interdisciplinary projects within the BMBF program "Spitzenforschung und Innovation in den neuen Bundesländern",

Topping-out ceremony for the new Physics buildings on October, 12 2012; from left: Prof. Schareck, Prof. Kühn, Prof. Meiwes-Broer, H. Polzin (Minister of Finance), H.-G. Hufen (Head of BBL). (source: Prof. F. Mitschke)

which had started at the end of 2009, are still ongoing. "Light2Hydrogen" (with participation of the groups of Profs. Meiwes-Broer, Kühn, Lochbrunner) investigates fundamental aspects of photocatalytic water splitting. REMEDIS ("Regional Development of Medical Innovation and Research" with participation of the groups of Profs. Meiwes-Broer and Lochbrunner) focuses on the development of new micro implants. Both projects are strongly connected to the activities of the department "Science and Technology of Life, Light and Matter" (LL&M) of the Interdisciplinary Faculty (INF).

During the period of this report the Bologna process has been completed with the successful start of the first Master courses in 2010. In addition the international Master programme was continued in order to attract students from abroad thus compensating for the future demographic challenges. Starting with the winter semester 2012/2013 the curriculum for physics teachers has been completely restructured. Opportunities for PhD students to broaden their education beyond the specific topic are offered by two graduate schools, i.e. the integrated graduate school of the SFB 652 in the area of light-matter interaction and the graduate school "Physics, Chemistry, and Technology of New Materials". As a means for optimising the graduate education and the information exchange for students, the University of Rostock has established a Graduate Academy in 2011.

The Institute of Physics places emphasis on various outreach activities to communicate science to the society and to raise the interest in studying Physics. In September 2011 the "Highlights of Physics" organised by the BMBF and the DPG

Highlights of Physics 2011: Opening event in the Stadthalle. (source: Prof. K.-H. Meiwes-Broer)

have been held in Rostock (see picture above). The topic "Röntgen and Co." attracted more than 35000 visitors, thus topping previous records of this event. As a new concept the so-called Physics Navigator programme has been introduced. Here students provide answers about study related questions to interested pupils. Further activities include the yearly "Physics Day", the "Long Night of Sciences", "Science and Sail", the "Girls Day" and "Physch", Physics and school (see also Section 2.6)

In the following a brief overview of the institute will be provided. Subsequently, the research activities of the individual groups are presented. Finally, the current activities within the SFB 652 project and of the Department of Light, Life, and Matter are summarised. This report was written not only for statistical purposes, but to trigger interest in study and research at the Institute of Physics of the University of Rostock.

Prof. Dr. Oliver Kühn
Managing Director, Institute of Physics

1 Overview of the Institute

During the period of this report the structure of the **faculty members** changed further according to the gradual replacement of C3/C4 by W2/W3 positions. Furthermore, it was possible to establish two junior research groups led by W1 junior professors. The scientific staff was completed by 5 lecturers (Privatdozenten). PD Dr. Heidi Reinholz has been appointed to a temporary professorship at the J. Kepler-University Linz, Austria (until 09/2011).

	2010	2011	2012
C4 professors	6	5	5
C3 professors	4	3	3
W3 professors	2	2	4
W2 professors	1	1	1
W1 professors	1	1	2

In the reporting period 34 students received their **doctor's degree** (see Section 5.1 for details).

Prof. Sauerbrey receiving his honorary degree from the university's rector Prof. Schareck on May, 7 2010. (source: IT- und Medienzentrum der Universität Rostock)

A particular event has been the acceptance of a **honorary doctoral degree** of the Faculty of Mathematics and Natural Sciences of the University of Rostock by Prof. Dr. Roland Sauerbrey on May, 7 2010. Prof. Sauerbrey is the Scientific Director of the Helmholtz Research Center Dresden-Rossendorf e.V. He has been

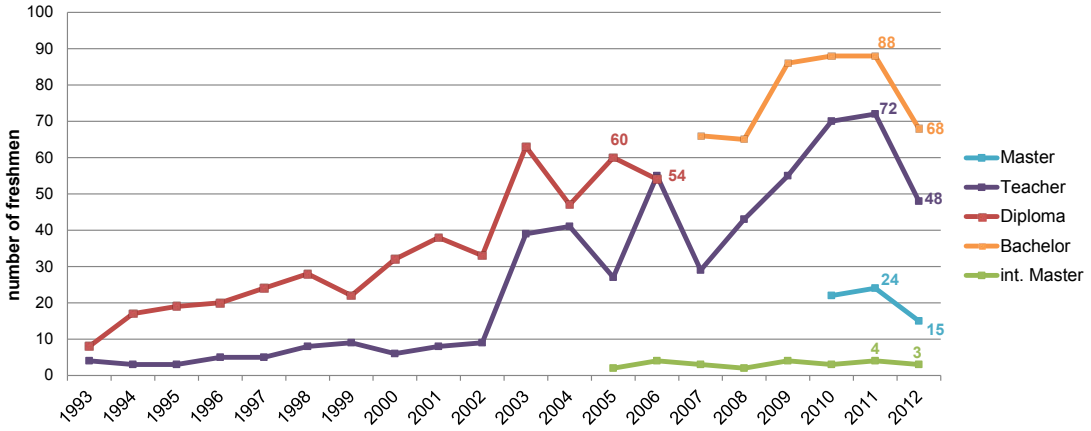

Number of freshmen at the Institute of Physics. Note that the official number of Master students include only those who enroll in the winter term. As of 2012 those students are included who started in the previous summer term.

collaborating with our institute since the 1990s in the area of the interaction of ultra-intense laser field with matter. On occasion of the ceremony Prof. Sauerbrey presented a talk on "The Power of Light" at the university church.

Our institute continues to be an attractive place for studying Physics in Germany. This fact manifests itself in the excellent rankings during the last years. For example, the 2012/2013 CHE ranking of the Zentrum für Hochschulentwicklung places Physics in Rostock into the top-level group in the categories "general study situation", "laboratory equipment", "scientific publications", and "supervision". Concerning the number of **freshmen** the trend of the previous years continued until 2011. In 2012 there has been a drop reflecting the overall demographic situation in Germany.

The research projects of the Institute of Physics received **support by external sources** from various organizations such as Deutsche Forschungsgemeinschaft (DFG), Bundesministerium für Bildung und Forschung (BMBF), European Union (EU) as well as by programs within the scope of the Hochschulbauförderungsgesetz (HBFG) and by industry. The major part of operational expenses of the institute was financed by these external financial sources. Here, the averaged budget per year was about 4.0 Mio Euro in the accounting period.

The construction of the **new buildings** of the Institute of Physics and the Department of Light, Life, and Matter on the Südstadt campus continued during the period of the research report, and the move of the different research groups, which are currently scattered across three different locations, is within reach. The new institute will consist of a laboratory building and a teaching complex, being connected by a bridge over the Campus Street leading from the university library to the LIKAT on the campus. Next to the teaching building there will be the research building of the Department Life, Light and Matter of the Interdisciplinary Faculty. It will host the facilities for interdisciplinary projects focusing on "Complex Molecular Systems".

The locations of the new buildings of the Institute of Physics and the science building of the Department of Light, Life, and Matter on the Südstadt campus. (source: Prof. K.-H. Meiwes-Broer)

2 Research Activities

2.1 Optics and Laser Physics

2.1.1 Nonlinear Optics

Head: Prof. Dr. Fedor Mitschke

Staff:	Dr. Haldor Hartwig	Dipl.-Phys. Christoph Mahnke
	Dr. Alexander Hause	Dipl.-Phys. Philipp Rohrmann
	Dr. Rodislav Driben	
	Hartmut Reichwagen	Theresa Kopplow
MSc Graduates:	Sonia Gholami	
Dipl.-Phys. Graduates:	Daniel Prestin	Jan Riemer
	Philip Rohrmann	Matthias Strauch
St.Ex. Graduates:	Kevin Jacob	Dirk Levetzow
	Sven Levetzow	Katharina Möller
	Susann Vahs	
BSc Graduates:	Jan Froh	Stefan Graunke
	Miriam Hess	Maria Kaupsch
	Sven Kraft	

General Outline of the Field of Research

We study nonlinear dynamical processes in the realm of optics. *Nonlinear* means that optical properties of a material are modified by the irradiated light so that a light beam itself modifies the conditions of its propagation. *Dynamical* refers to short time scales; we routinely deal with femtosecond processes. Lasers are a central concept here in a twofold way: They provide the light required to excite nonlinear processes, but their inner workings involve nonlinear processes too.

During the period of this report our focus has been on the nonlinear interactions which occur when a short pulse of light travels down an optical fiber. Given the right conditions, very special pulses called solitons can arise. A quarter century after their first experimental demonstration solitons have found their way into commercial applications in optical telecommunication. One aspect of our work deals with the fundamental limitations of the data-carrying capacity of fibers, and with ways to extend that limit using soliton concepts. Another aspect is to use the nonlinear interactions in a fiber to generate broadband light; feedback is employed to enhance the process.

Dispersion-Managed Solitons

Solitons in an ordinary fiber are described by the nonlinear Schrödinger equation for which analytic solutions exist. Fibers deployed today are of a different type, however, which is called dispersion-managed fiber. For this fiber there are no closed solutions of the wave equation, and some aspects of the pulse behavior remain unclear. One observation made by many authors mostly in numerical simulations was a peculiar slow oscillation of the parameters describing the pulse shape (width, peak power, etc.). Using a numerical method developed earlier in this group we could identify the cause of this phenomenon as a beat note between constituent parts of the dispersion-managed soliton [1].

Soliton Interaction

Soliton-soliton interaction, first experimentally described by the group head in 1986, remains an issue of some debate when higher-order corrections to the propagation equation must be included. In particular, Raman scattering has a profound influence on the pulse's evolution. In cooperation with the group of P. Russell at the Max Planck Institute for the Science of Light (Erlangen) we investigated the behavior of pulse pairs in the presence of the Raman effect. Issues of stability of the pair which had been the subject of some conjectures before could be settled, and conclusions about larger soliton compounds could be drawn [2, 3].

In the case of dispersion-managed fiber, the interaction of a pair of solitons is considerably modified. Depending on their initial separation and other factors there can be an effective force which is either attractive or repulsive. At least one stable equilibrium point also exists, which is a fact of considerable interest as it allows the formation of stable pairs ('soliton molecules'). The parameter dependence of the force was shown to be of a self-similar, fractal nature [4].

Soliton Molecules

A few years ago we discovered that there exists a stable solution which is a compound state of two bright solitons. This compound, called the soliton molecule, suggests a way to create an optical coding of data that goes beyond the binary format: This would increase the data-carrying capacity of fibers so that the impending capacity bottleneck (called the 'capacity crunch' by some) might be avoided. The two-pulse molecule represents an additional symbol, but for this suggestion to be successful, further symbols are required.

It was therefore a major success when we could demonstrate experimentally that soliton molecules composed of three individual pulses exist and propagate stably. Now four symbols (no pulse, single soliton, two-pulse molecule, three-pulse molecule) have been demonstrated (see Fig. 2.1); this in principle enables transmission of two bits per clock period [5].

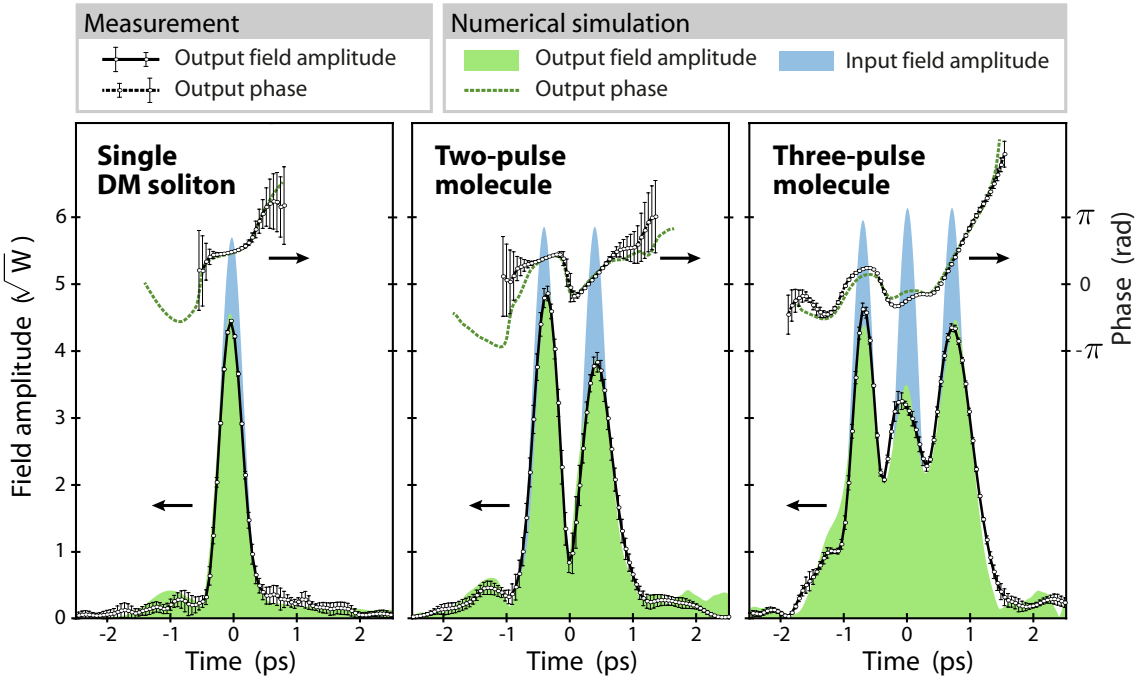

Fig. 2.1: Temporal shape of single dispersion-managed (DM) soliton (left), two-pulse molecule (center) and three-pulse molecule (right). Shown are field amplitude envelopes (lower part, left axis) and phases (upper part, right axis). Points with error bars are experimental data. Together with the absence of a pulse (not shown) these are four symbols, so that two-bit-per-clock transmission becomes possible.

Ultrashort Pulse Measurement Technique Refined

Earlier cooperation between the group of Prof. Stolz, the Institute of Mathematics (Prof. Tasche) and this group resulted in a novel technique to assess amplitude and phase of femtosecond light pulses which was introduced ca. 2007. The technique had already been shown to be superior to competing techniques such as FROG under certain circumstances because it is unaffected by certain ambiguities. In extension of that work an extremely hard test was devised: A pulse structure containing a spectral gap (as opposed to just a null) is challenging to all other techniques, but our method was shown to be able to handle even such extreme case [6].

Photonic Crystal Fiber

We have developed a very simple model for the description of the waveguiding properties which relies only on symmetry and limit considerations. It could be shown that this quite general framework gives a remarkably good approximation so that it is useful for quick estimates [7].

Optical Supercontinuum from a Photonic Crystal Fiber

We have investigated the generation of spatially coherent yet broadband light – now known as optical supercontinuum – in a highly nonlinear photonic crystal fiber. In previous research we had considered hollow-core photonic crystal fibers the core of which was filled with a liquid; in that context we had developed a technique to selectively fill the core while leaving the voids in the cladding alone. This technique enabled an experiment in cooperation with Max Born Institute (Berlin) in which supercontinuum generation with an impressive two-octave width was demonstrated [8].

Supercontinuum generation typically starts with launching a powerful femtosecond light pulse into a fiber where it breaks up in a process known as soliton fission; an ensemble of several solitons plus some linear radiation is generated. We could show recently that the further evolution of the solitons is in fact influenced strongly by the weak linear radiation [9]. In further generalization of this concept of soliton-background interaction we could show in cooperation with authors from the Weierstrass Institute and the Max Born Institute (both Berlin) we could show that conditions for weak radiation strongly affecting strong pulses are not at all unusual, and that the process is related to both rogue wave generation and the concept of an optical event horizon [10].

Akhmediev Breather

In the event that supercontinuum generation is triggered by a picosecond (or longer) pulse, soliton fission is no longer relevant. Instead, modulational instability takes over to create substructure in the pump pulse. There was consensus that here, too, an ensemble of solitons plus some linear radiation is generated; however, the way how solitons arise in this situation was unclear.

We could recently solve this longstanding issue by a detailed study of the process. It turns out that solitons are only generated if at least one additional perturbation is added to the nonlinear Schrödinger equation: Raman scattering is a suitable process [11]. In practice, Raman scattering is always present so that the general consensus was correct, but now the reasons are clear.

Interdisciplinary: Perception of Polarization

Humans do not perceive the state of polarization of light, but K. v. Frisch (at one time a professor of zoology in Rostock) won the Nobel Prize for his demonstration that honey bees actually 'see' polarization states. Meanwhile the same has been demonstrated for various other members of the animal kingdom. In the context of research about sensory capabilities of harbor seals (*phoca vitulina*) the group of Prof. G. Dehnhardt (Dept. of Life Sciences) designed experiments to test polarization vision in these animals. They turned to the group head for discussions, and he was able to contribute useful advice [12].

References

[1] H. Hartwig, M. Böhm, A. Hause and F. Mitschke. "Slow oscillations of dispersion-managed solitons". *Phys. Rev. A*, **81** (2010), 033810.

[2] A. Hause, T. X. Tran, F. Biancalana, A. Podlipensky, P. S. J. Russell and F. Mitschke. "Understanding Raman-shifting multipeak states in photonic crystal fibers: two convergent approaches". *Opt. Lett.*, **35** (2010), 2167–2169.

[3] A. Hause and F. Mitschke. "Soliton Trains in Motion". *Phys. Rev. A*, **82** (2010), 043838.

[4] A. Hause, H. Hartwig and F. Mitschke. "Self-similar interaction of slowly oscillating dispersion-managed solitons". *Phys. Rev. A*, **82** (2010), 053833.

[5] P. Rohrmann, A. Hause and F. Mitschke. "Solitons Beyond Binary: Possibility of Fibre-Optic Transmission of Two Bits per Clock Period". *Sci. Rep.*, **2** (2012), 866.

[6] B. Seifert, A. Hause and F. Mitschke. "A fibre Mach-Zehnder interferometer for the unique phase retrieval of ultrafast pulses with a 1 THz gap". *Appl. Phys. B*, **99** (2010), 423–426.

[7] C. Mahnke and F. Mitschke. "A useful approximation for the cladding index of holey fibers". *Appl. Phys. B*, **99** (2010), 241–245.

[8] J. Bethge, A. Husakou, F. Noack, U. Griebner, G. Steinmeyer, J. Herrmann and F. Mitschke. "Two-octave supercontinuum generation in a water-filled photonic crystal fiber". *Opt. Express*, **18** (2010), 6230–6240.

[9] F. M. R. Driben, N. Zhavoronkov. "Cascaded interactions between Raman induced solitons and dispersive waves in photonic crystal fibers at the advanced stage of supercontinuum generation". *Opt. Express*, **18** (2010), 25993–25998.

[10] A. Demircan, S. Amiranashvili, C. Brée, C. Mahnke, F. Mitschke and G. Steinmeyer. "Rogue events in the group velocity horizon". *Sci. Rep.*, **2** (2012), 850.

[11] C. Mahnke and F. Mitschke. "Possibility of an Akhmediev breather decaying into solitons". *Phys. Rev. A*, **82** (2012), 033808.

[12] F. D. Hanke, L. Miersch, E. J. Warrant, F. Mitschke and G. Dehnhardt. "Are harbour seals (*phoca vitulina*) able to perceive and use polarized light?" *J. Comp. Physiol., A*, (2012). DOI: 10.1007/s00359-012-0762-x.

2.1.2 Theoretical Quantum Optics

Head: Prof. Dr. W. Vogel

Staff:	Dr. Thomas Kiesel	Dr. Andrew A. Semenov
	Dr. Shailendra Kumar Singh	Dr. Jan Sperling
	Dr. Dmytro Yu. Vasylyev	MSc Elizabeth Agudelo Ospina
	Dipl.-Phys. Peter Grünwald	MSc Saleh Rahimi-Keshari
	MSc Frank E. S. Steinhoff	
MSc Graduates:	Melanie Mraz	
BSc Graduates:	Hannes Sobottka	Melanie Mraz
	Alexander Reusch	Stefan Gerke
	Martin Bohmann	Sergej Ryl
	Benjamin Kühn	

Nonclassicality

Since the early days of quantum physics it is of great interest to distinguish quantum phenomena from classical ones. The development of the laser led to the quantum theory of optical coherence. The P_{GS} function of Glauber and Sudarshan led to new insight in the quantum nature of radiation fields. This phase-space distribution represents any classical quantum state as a mixture of coherent states, which are most close to the classical behavior of electromagnetic waves. For nonclassical quantum states negativities of P_{GS} may appear. However, the P_{GS} function may be strongly singular and hence not accessible to experiments.

We could regularize P_{GS} function such that quantum phenomena show up as negativities of a regular P_{Ncl} function [1], the so-called nonclassicality quasiprobability. This new type of quasiprobability distribution can be experimentally reconstructed for any quantum state. This has been demonstrated in cooperation with experimental groups, for the examples of a photon-added thermal state [2], a squeezed-vacuum state [3], and a squeezed ensemble of atoms [4], see Fig. 2.2. We have also developed methods for the direct sampling of this quasiprobability and its statistical errors from measured data [3]. Based on the concept of the nonclassicality quasiprobability, nonclassical effects have also been characterized by the nonclassicality moments [5], which are directly obtained from the experimentally recorded P_{Ncl} functions. We could also clarify the general structure of nonclassicality witnesses [6]. On this basis we have proposed a complete nonclassicality test, which requires the measurement of the photon statistics [7].

In the context of the rapidly developing field of Quantum Technology, it is important to answer the following questions: How strong is a given quantum effect? How useful is it for a certain application? To clarify this, we have introduced an operational quantification of nonclassicality [8]. Perfect operational nonclassicality allows one to realize the quantum-noise-free detection of a properly defined observable. Surprisingly, even a moderately squeezed state can be used for a noise-free

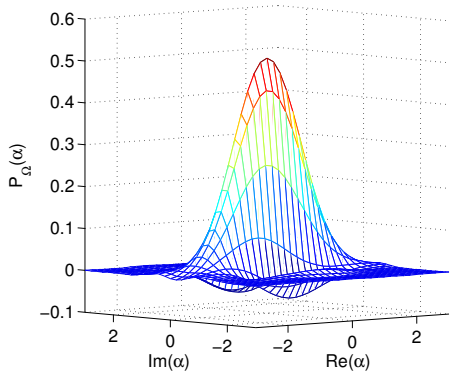

Fig. 2.2: Nonclassicality quasiprobability, $P_\Omega = P_{\mathrm{Ncl}}$, for a squeezed vacuum state [3].

quantum measurement. We have also introduced a quantification of nonclassicality based on the number of superpositions of coherent states. Although these two approaches are different from the fundamental point of view, the main conclusions appear to be consistent.

Entanglement

Entanglement is a nonclassical correlation between two or more quantum systems. Beside other notions of quantum correlations [9, 10], entanglement represents the essential quantum phenomenon of compound systems. Entanglement has been studied in interacting quantum systems, such as atomic resonance fluorescence [11, 12] and turbulent media [13]. However, the detection of entanglement turns out to be a cumbersome problem. For example, entanglement tests in a two-qubit system have been intensively studied [14]. Beyond these low dimensional systems, a rigorous treatment of the entanglement detection was missing.

We introduced a convenient way to characterize entanglement for arbitrary quantum systems. Our approach of entanglement quasiprobabilities – similar to the nonclassicality quasiprobability representation – yields negative values, if and only if the considered state is entangled. In order to get this representation, we introduced the so-called *Separability Eigenvalue Problem*. From its solution we derive the quasiprobability of entanglement. In Fig. 2.3, an example is given for a two-mode squeezed-vacuum state [15].

To measure the strength of quantum correlations, we found that the number of global superpositions is a universal quantifier of entanglement [16]. We introduced a method to construct measurable observables to determine this number [17]. The method has been applied to characterize entangled light from a microcavity system [18].

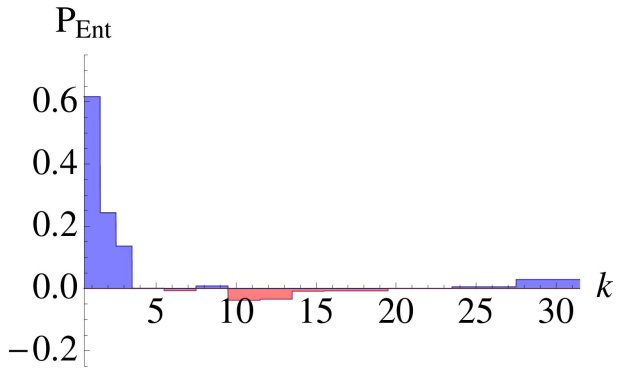

Fig. 2.3: Truncated entanglement quasiprobability, P_{Ent}, of a two-mode squeezed-vacuum state [15]. The negative values uncover entanglement of the state, which is strongly phase-diffused.

Quantum Measurement Theory

The characterization of quantum systems requires a rigorous description of measurements. Otherwise measurement outcomes may indicate fake quantumness, which is solely an effect of incorrect measurement theory [19, 20]. On the other hand, noise, turbulence, and losses may hide nonclassical properties of the system.

For the full quantum state reconstruction phase sensitive measurements are frequently used. We considered the so-called homodyne detection to uncover quantum phenomena in turbulent media [21]. Comparing the statistical errors of different phase-sensitive measurements, we found that the unbalanced homodyne detection yields a higher significance than the balanced one [22].

An ideal detector can perfectly resolve any photon number, which allows one to construct nonclassicality tests [7]. However, these detector systems are often not accessible. Typically one uses a multi-detector system, where each individual detector can only discriminate between the presence (click) and absence (no click) of light. For such detector systems we developed a closed detection theory [20]. In addition, a method to identify nonclassicality based on such detector systems has been introduced [23], cf. Fig. 2.4.

Cavity QED

Fundamental interactions between light and matter can be realized within cavities, where the light-matter coupling is substantially enhanced. We studied the possibility to generate nonclassical light from atom-cavity systems for various scenarious. When coupling multiple leaky cavities in a cascade, it is possible to generate entangled quantum states of light. We could predict for two cavities containing each a two-level atom, that the atoms and the intracavity fields become entangled [24]. Furthermore, a single-mode cavity may optimize squeezing of the fluorescence of the atom out the side of the cavity [25]. The optimal squeezing is much stronger than in the case

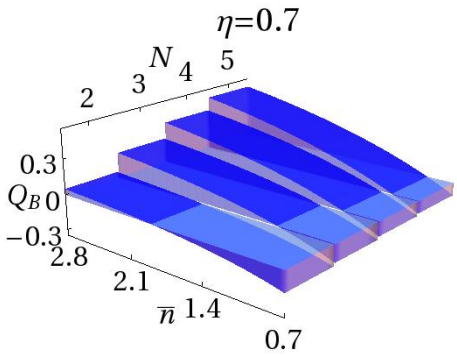

Fig. 2.4: The verification of the nonclassicality of a photon-added thermal state, $Q_{\mathrm{B}} < 0$, is shown for N click detectors, a quantum efficiency $\eta = 0.7$, and a mean thermal photon number $\bar{n}$ [23].

of free-space fluorescence, cf. Fig. 2.5, and it is achieved when the atomic state is purified.

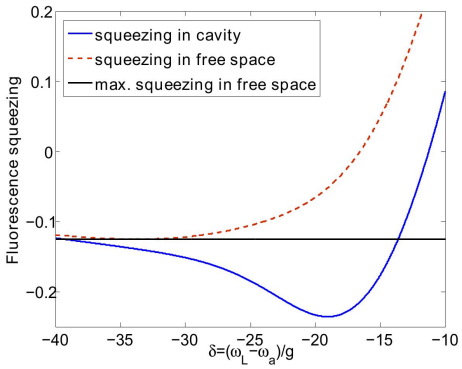

Fig. 2.5: Comparison of the cavity assisted squeezing of the atomic fluorescence (blue solid curve) with the free-space fluorescence squeezing (red dashed line) as a function of the laser-atom detuning δ [25].

In case of two cavity modes, we have studied a scenario in which the frequency gap between the modes is comparable to an atomic Raman-transition. Both modes can be driven by the atom, even though it is only resonant with one mode [26]. The fluorescence of a multi-atom system is entangled in different directions, if the radiation of the system in a single direction shows certain nonclassical features [11, 12]. A similar behavior has been found in semiconductor microcavities, where interacting excitons produce strongly entangled light [18].

Nonclassical Light in the Turbulent Atmosphere

Recent experiments have demonstrated that long-distance quantum communication through the atmosphere is possible even in the case of large losses. We have developed a rigorous theory, which consistently describes the distribution of quantum light through turbulent media and explains the observed phenomena. The corresponding technique has been obtained by a generalization of the similar theory of quantum-light propagation through lossy media [27]. The method has been developed for the case when the turbulence results in random fluctuations of a beam position around the center of aperture [28].

As an example we have considered an experiment where a 144 km quantum channel of 32 dB losses has been used [13]. The Bell parameter, which characterizes nonclassical signatures of light, has been measured. Losses, stray light, and internal dark counts of detectors usually result in a decrease of the Bell parameter. Our analysis of this experiment has shown that turbulent media preserve the value of this parameter much better than glass fibers with the same losses, see Fig. 2.6.

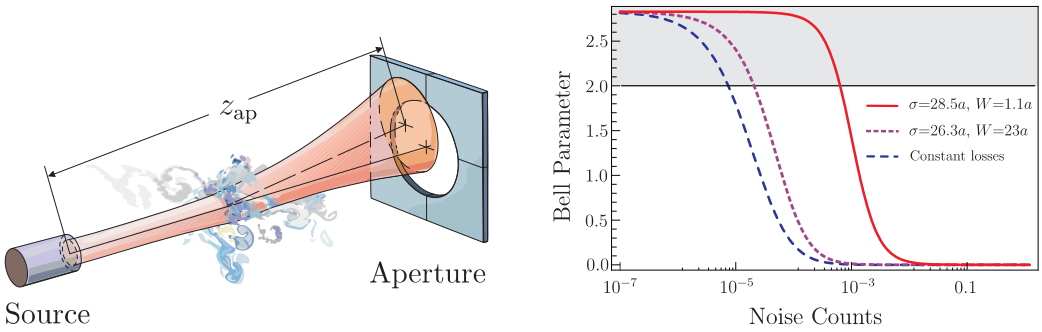

Fig. 2.6: Illustration of the beam wandering phenomenon (left). The Bell parameter (right) is shown in dependence of noise counts for different parameters of beam wandering: σ^2 variance of beam position, W beam spot radius, and a aperture radius. The values of the Bell parameter increases with increasing turbulence. Adapted from [28].

References

[1] T. Kiesel and W. Vogel. "Nonclassicality filters and quasi-probabilities". *Phys. Rev. A*, **82** (2010), 032107.

[2] T. Kiesel and W. Vogel. "Nonclassicality quasiprobability of single-photon-added thermal states". *Phys. Rev. A*, **83** (2011), 032116.

[3] T. Kiesel, W. Vogel, B. Hage and R. Schnabel. "Direct sampling of negative quasiprobabilities of a squeezed state". *Phys. Rev. Lett.*, **107** (2011), 113604.

[4] T. Kiesel, W. Vogel, S. L. Christensen, J.-B. Béguin, J. Appel and E. S. Polzik. "Atomic nonclassicality quasiprobabilities". *Phys. Rev. A*, **86** (2012), 042108.

[5] S. Rahimi-Keshari, T. Kiesel and W. Vogel. "Moments of nonclassicality quasiprobabilities". *Phys. Rev. A*, **85** (2012), 043827.

[6] T. Kiesel and W. Vogel. "Universal nonclassicality witnesses for harmonic oscillators". *Phys. Rev. A*, **85** (2012), 062106.

[7] T. Kiesel and W. Vogel. "Complete nonclassicality test with a photon-number-resolving detector". *Phys. Rev. A*, **86** (2012), 032119.

[8] C. Gehrke, J. Sperling and W. Vogel. "Quantification of nonclassicality". *Phys. Rev. A*, **86** (2012), 052118.

[9] W. Vogel, T. Kiesel and J. Sperling. "Characterizing nonclassicality and entanglement". *Opt. Spectrosc.*, **108** (2010), 197.

[10] A. Miranowicz, P. Horodecki, R. W. Chhajlany, J. Tuziemski and J. Sperling. "Analytical progress on symmetric geometric discord: Measurement-based upper bounds". *Phys. Rev. A*, **86** (2012), 042123.

[11] P. Grünwald and W. Vogel. "Entanglement in atomic resonance fluorescence". *Phys. Rev. Lett.*, **104** (2010), 233602.

[12] P. Grünwald and W. Vogel. "Entanglement in atomic resonance fluorescence". *Phys. Rev. Lett.*, **106** (2011), 119903(E).

[13] A. A. Semenov and W. Vogel. "Entanglement transfer through the turbulent atmosphere". *Phys. Rev. A*, **81** (2010), 023835.

[14] T. Kiesel, W. Vogel, B. Hage and R. Schnabel. "Entangled qubits in a non-Gaussian quantum state". *Phys. Rev. A*, **83** (2011), 062319.

[15] J. Sperling and W. Vogel. "Entanglement quasiprobabilities of squeezed light". *New J. Phys.*, **14** (2012), 055026.

[16] J. Sperling and W. Vogel. "The Schmidt number as a universal entanglement measure". *Physica Scripta*, **83** (2011), 045002.

[17] J. Sperling and W. Vogel. "Determination of the Schmidt number". *Phys. Rev. A*, **83** (2011), 042315.

[18] D. Pagel, H. Fehske, J. Sperling and W. Vogel. "Strongly entangled light from planar microcavities". *Phys. Rev. A*, **86** (2012), 052313.

[19] A. A. Semenov and W. Vogel. "Fake violations of the quantum Bell-parameter bound". *Phys. Rev. A*, **83** (2011), 032119.

[20] J. Sperling, W. Vogel and G. S. Agarwal. "True photocounting statistics of multiple on-off detectors". *Phys. Rev. A*, **85** (2012), 023820.

[21] A. A. Semenov, F. Töppel, D. Y. Vasylyev, H. V. Gomonay and W. Vogel. "Homodyne detection for atmosphere channels". *Phys. Rev. A*, **85** (2012), 013826.

[22] T. Kiesel. "Statistical analysis of sampling methods in quantum tomography". *Phys. Rev. A*, **85** (2012), 052114.

[23] J. Sperling, W. Vogel and G. S. Agarwal. "Sub-Binomial Light". *Phys. Rev. Lett.*, **109** (2012), 093601.

[24] C. Di Fidio and W. Vogel. "Entanglement evolution in a cascaded system with losses". *Physica E*, **42** (2010), 369.

[25] P. Grünwald and W. Vogel. "Optimal Squeezing in Resonance Fluorescence via Atomic-State Purification". *Phys. Rev. Lett.*, **109** (2012), 013601.

[26] P. Grünwald, S. K. Singh and W. Vogel. "Raman-assisted Rabi resonances in two-mode cavity QED". *Phys. Rev. A*, **83** (2011), 063806.

[27] D. Vasylyev, W. Vogel, K. Henneberger and F. Richter. "Propagation of quantized light through bounded dispersive and absorptive media". *Physica Scripta*, **T140** (2010), 014039.

[28] D. Y. Vasylyev, A. A. Semenov and W. Vogel. "Toward Global Quantum Communication: Beam Wandering Preserves Nonclassicality". *Phys. Rev. Lett.*, **108** (2012), 220501.

2.1.3 Experimental Quantum Optics

Head: Jun.-Prof. Dr. Boris Hage

Staff: Dr. Andreas von Czarnowski, Elke Prandke, MSc Melanie Mraz, Semjon Köhnke, Oskar Schlettwein, Hannes Sobottka, Wolfram Stamm

General Outline of the Field of Research

Optical systems are particularly suitable for the fundamental investigation of quantum phenomena as well as their applications. Light with distinct properties can be generated, confined, guided, transmitted and detected easily in many cases. Also, the interaction of light and matter can be well controlled in certain scenarios. Today's communication largely relies on optical channels in the classical regime. Future communication networks will involve some quantum physics for adding communication security or boosting the channel capacity. Hence, studying the quantum properties of optical systems and also the distinction of quantum and classical effects in optics is interesting from a fundamental point of view as well as with respect to technology.

The experimental quantum optics group was started in April 2012 at the University of Rostock. Hence, the results presented here go back to the research groups the head has been working in earlier.

Spatial Mode Quantum Engineering

In quantum optics the light in a single optical mode in a laser beam can be described as a single harmonic oscillator. A mode in a beam is defined by the polarisation, the frequency, the bandwidth, the temporal shape and the transverse spatial shape. For the spatial shape we often use the basis of the *Hermite-Gauß* transverse electromagnetic modes (TEM). Most high quality lasers emit light in the fundamental TEM_{00} mode. Hence, single mode quantum optics, e.g. squeezing, is frequently carried out in the TEM_{00} mode.

The precise transverse position of a scattering particle held by optical tweezers in the TEM_{00} with respect to the tweezers is encoded in the TEM_{01}. For the position readout quantum noise places a fundamental limit on the per photon sensitivity. This is crucial in a biological context, where the optical power must be constrained to avoid damage to the specimen. By using non-classically correlated light in the TEM_{01} we demonstrated that the quantum limit can be surpassed in a biological measurements. In optical tweezers we tracked naturally occurring lipid granules in a yeast cell with sensitivity 2.4 dB beyond the quantum noise limit. This provides information about the viscoelasitc properties of the surrounding cytoplasm [1]. In a separate experiment we demonstrated a dynamic universal mode converter, which

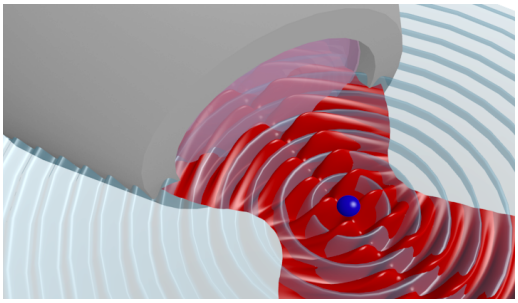

Fig. 2.7: Illustration of a scattering particle in optical tweezers [1]. The trapping field is not shown. The light-blue field represents the scattering field from the particle. As long as the particle is right in the centre the scattered wave does not interfere with the red field mode, which is designed to have a phase flip at the central plane. For small deviations of the particle from its central position the interference signal with the red mode is proportional to the position of the particle. The quantum noise of a position measurement can be traced back to the shot noise of the red mode. Hence, in order to improve the sensitivity with squeezed light its shape must match the red mode.

can in principle convert beams to and from arbitrary modes with very low losses. Therefore it is suitable for the mode conversion of quantum light, where losses have to be as low as possible. Rather than using a phase and amplitude mask in the conversion stage we use several phase-only stages with spatial Fourier transforms in between [2].

A special spatial structure is found in the so-called *vortex beams*. Here, the phase of the wave-front is proportional to the azimuthal coordinate with an integer multiple m of 2π per revolution. In such a beam the photons carry an orbital angular momentum of $m\hbar$. We directly machined so called *spiral phase mirrors* (SPMs) with an ultra-precision single-point diamond turning lathe, which convert an incoming TEM_{00} into a vortex beam upon reflection. We could demonstrate a vortex beam with a topological charge ranging from $m = 1$ to upwards of $m = 100$ and a very high beam quality with this method [3].

Entanglement Engineering

Entanglement is one of the weirdest aspects of quantum mechanics. It plays a crucial role for teleportation, quantum computation and quantum communication. Decoherence effects can destroy the useful entanglement when it is to be distributed to spatially distant locations or stored for some time. When every effort to minimise the decoherence by shielding the entangled system from the environment is not sufficient, an entanglement distillation scheme can be used under certain conditions to partially recover some useful entanglement. We demonstrated an iterative distillation scheme with two successive stages for continuous variables to counter-

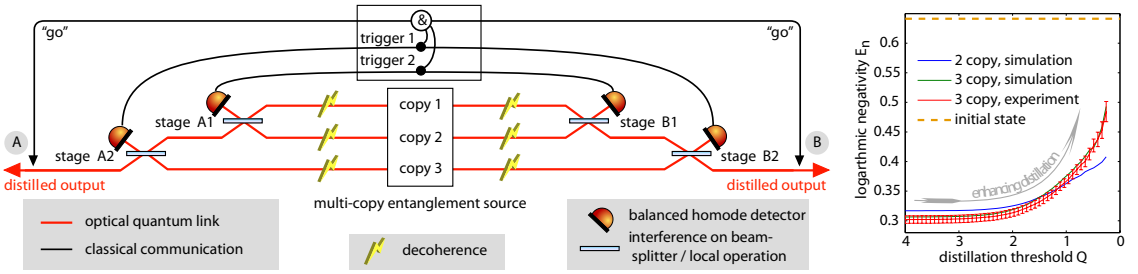

Fig. 2.8: Left: schematic setup of the iterative distillation apparatus [4]. The *distilled outputs* can be used for an arbitrary application or alternatively be fed into yet another distillation stage. Right: The threshold Q determines the strength of the distillation increasing from left to right. The entanglement increases with stronger distillation, However, at the same time the success rate drops to zero at $Q = 0$.

act decoherence caused by phase noise or any other "de-Gaussifying" process [4]. A special instance of entangled states, which no pure entangled states can be distilled from, are called *bound entangled states*. We demonstrated a four-mode bound entangled state in continuous variables [5].

Entanglement can occur in systems which consist of two or more modes. In complex scenarios such as quantum information processing, where entanglement of many modes is required, there can be different topologies of the entanglement. The modes can be entangled pairwise or for certain permutations or even more complex in cluster structures. There are many ways how these modes can be distinguished. The propagation in different directions is one example that is frequently used. In order to handle many modes in a compact way we were using eight different spatial modes of one single beam to carry the entanglement. A crucial component in this setup is the photo-detector, which has to provide the spacial resolution to distinguish the modes. We demonstrated how one can switch between different entanglement topologies by changing a virtual beam splitter network which is linked to the individual pixels of the detector. We could demonstrate up to eight-mode entanglement and a four-mode cluster state [6]. From an operational point of view a quantum communication scheme can be considered efficient when all the quantumness generated by a non-classical resource can be used at the detection stage. In a realistic squeezed/entangled light setup the bandwidth of the non-classical light source often exceeds the useful detector bandwidth. In such a scenario a frequency multiplexing scheme can be implemented, which splits the available bandwidth into a number of segments according to the detector capabilities. We demonstrate the spatial separation of radio frequency side-bands of a single broadband squeezed beam in order to create two-mode squeezed entanglement [7]. This scheme can be extended to an arbitrary number of entangled pairs of modes.

Photons in Phase Space

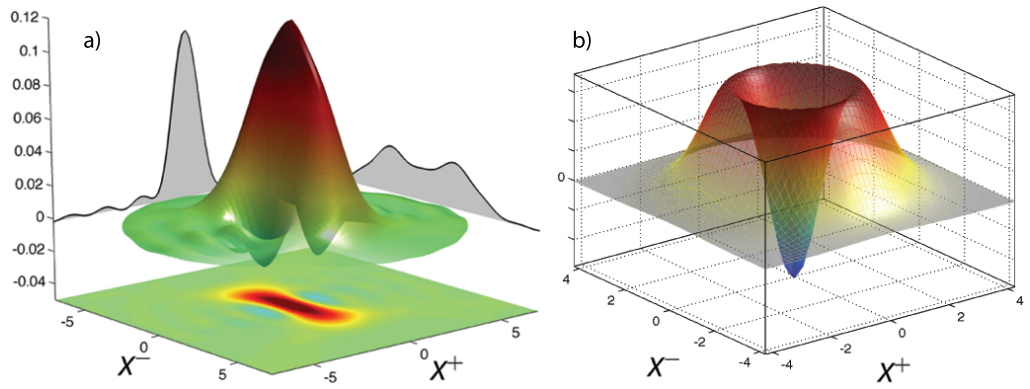

Fig. 2.9: a) Two photon subtracted squeezed state. A squeezed beam was split on a 20:80 beam splitter. The two photon conditioning is based on the BHD signal of the 20% port. The figure shows the Wigner function obtained via quantum state tomography of the 80% port. b) Single photon state. One part of a two-mode squeezed state is used for the single photon conditioning, the Wigner function of the other part is displayed in the figure.

Continuous variable experiments are using *balanced homodyne detectors* (BHDs) which measure the field observables related to phase space representations of the state of a signal field. BHDs cannot count or detect individual photons. However, the equivalence of continuous phase space and discrete photon based representations enables investigation of ensemble photonic properties based on BHD measurements.

We generated a non-Gaussian bipartite entangled state and analysed it with BHDs. For this particular state the entanglement was invisible to Gaussian entanglement criteria but entangled qubits were found in the photon representation. This approach provides extra information about the structure of the entangled state. For this state we found entanglement in qubits of diverse photon numbers although it is symmetric under mode exchange [8]. Besides the photonic structures other powerful quantities can be extracted from phase space distributions. We derived quasiprobabilities from BHD data, which uniquely characterise a state to be quantum or classical [9] The nonlinearity of photon detection and conditional measurement can “de-Gaussify” a Gaussian state of light. We demonstrate a technique for photon-number resolution using only homodyne detection and use it for an ensemble conditional measurement. We reconstructed the statistics of the non-Gaussian one- and two-photon-subtracted squeezed vacuum states [10] as well as single and two photon states [11]. This photon-number measurement relies on ensemble averages. This method prohibits the state preparation. However, its high efficiency, photon-number-resolving capabilities and compatibility with the telecommunications band make it suitable for quantum-information tasks relying on the outcomes of mean values.

References

[1] M. A. Taylor, J. Janousek, V. Daria, J. Knittel, B. Hage, H.-A. Bachor and W. P. Bowen. "Biological measurement beyond the quantum limit". *arXiv*, (2012), 1206.6928. Published online in Nature Photon., DOI: 10.1038/nphoton.2012.346.

[2] J.-F. Morizur, L. Nicholls, P. Jian, S. Armstrong, N. Treps, B. Hage, M. Hsu, W. Bowen, J. Janousek and H.-A. Bachor. "Programmable unitary spatial mode manipulation". *J. Opt. Soc. Am. A*, **27** (2010), 2524–2531.

[3] G. Campbell, B. Hage, B. Buchler and P. K. Lam. "Generation of high-order optical vortices using directly machined spiral phase mirrors". *Appl. Opt.*, **51** (2012), 873–876.

[4] B. Hage, A. Samblowski, J. DiGuglielmo, J. Fiurášek and R. Schnabel. "Iterative Entanglement Distillation: Approaching the Elimination of Decoherence". *Phys. Rev. Lett.*, **105** (2010), 230502.

[5] J. DiGuglielmo, A. Samblowski, B. Hage, C. Pineda, J. Eisert and R. Schnabel. "Experimental Unconditional Preparation and Detection of a Continuous Bound Entangled State of Light". *Phys. Rev. Lett.*, **107** (2011), 240503.

[6] S. Armstrong, J.-F. Morizur, J. Janousek, B. Hage, N. Treps, P. K. Lam and H.-A. Bachor. "Programmable multimode quantum networks". *Nat. Comm.*, **3** (2012), Article number 1026.

[7] B. Hage, A. Samblowski and R. Schnabel. "Towards Einstein-Podolsky-Rosen quantum channel multiplexing". *Phys. Rev. A*, **81** (2010), 062301.

[8] T. Kiesel, W. Vogel, B. Hage and R. Schnabel. "Entangled qubits in a non-Gaussian quantum state". *Phys. Rev. A*, **83** (2011), 062319.

[9] T. Kiesel, W. Vogel, B. Hage and R. Schnabel. "Direct Sampling of Negative Quasiprobabilities of a Squeezed State". *Phys. Rev. Lett.*, **107** (2011), 113604.

[10] H. Chrzanowski, J. Bernu, B. Sparkes, B. Hage, A. Lund, T. Ralph, P. Lam and T. Symul. "Photon-number discrimination without a photon counter and its application to reconstructing non-Gaussian states". *Phys. Rev. A*, **84** (2011), 050302(R).

[11] B. Hage, J. Janoušek, S. Armstrong, T. Symul, J. Bernu, H. M. Chrzanowski, P. K. Lam and H.-A. Bachor. "Demonstrating various quantum effects with two entangled laser beams". *Eur. Phys. J. D*, **63** (2011), 457–461.

2.1.4 Quantum Optics of Macroscopic Systems

Head: Prof. Dr. Stefan Scheel

Staff: Dr. Günter Manzke, Peggy Preuss, Dipl.-Phys. Johannes Fiedler, Dipl.-Phys. Robin Schmidt, Kristine Karstens, Kai Budde

General Outline of the Field of Research

The group *Quantum optics of macroscopic systems* was established at the Institute of Physics in April 2012. The results presented here thus refer to the work performed in the former group of Dr. Scheel at Imperial College London. Our research covers a wide range of different, yet interconnected topics ranging from theoretical quantum optics to applications in atomic physics, quantum information processing, nanoscience or colloidal physics. The research is centred around quantum electrodynamics in dielectric media [1] in which the electromagnetic field is quantised in the presence of absorbing bodies. Based upon this quantisation scheme, we have previously been able to study the propagation of nonclassical light through absorbing optical devices, and to investigate atomic relaxation processes (modified spontaneous emission and spinflip lifetimes) near absorbing dielectrics. Closely connected with these relaxation processes are energy level shifts due to dispersion interactions such as Casimir, Casimir–Polder and van der Waals forces.

Quantum Electrodynamics in Linear and Nonlinear Dielectric Materials

Macroscopic quantum electrodynamics is based on a source-quantity representation of the electromagnetic field in terms of a bosonic vector field that describes collective excitations of field and absorbing matter. In the linear-response approximation, this procedure is exact; it provides a quantum-theoretically consistent quantisation scheme that also fulfils statistical requirements in the form of the linear fluctuation-dissipation theorem. We have shown that even in the presence of linear absorbing media the duality between electric and magnetic fields is a valid symmetry [2].

Nonlinearly responding, absorbing dielectrics have to be treated perturbatively. We have constructed effective nonlinear interaction Hamiltonians [3, 4] that allow one to investigate the interaction of quantised light with nonlinear absorbing dielectric media. With the help of these effective Hamiltonians we were able to compute coincident count rates of spontaneous parametric down-conversion processes in absorbing dielectric media [5].

Ultracold Trapped Neutral Atoms, Atom Chips

With the advent of microfabricated structures (atom chips) that enable one to confine small numbers of neutral atoms near dielectric surfaces, we are now able to

study atom-surface interactions in great detail [6]. Of fundamental importance for trapping atoms are their spin coherence properties. Together with the AG Fortágh in Tübingen we have shown that superconducting substrates can enhance the spin coherence times beyond what is achievable with normal metals [7]. We have investigated the effects of electromagnetic absorption in superconducting surfaces on coherence properties of atomic samples, and we have shown that screening of electromagnetic field fluctuations by the supercurrent [8] is chiefly responsible for them.

Decoherence affects also external degrees of freedom. Atom-surface interactions mediated by electromagnetic field fluctuations give rise to path decoherence of charged or neutral atomic systems near surfaces [9]. In the nonretarded limit (i.e. in near-field), an interpretation of the spatial dependence of the decoherence rate in terms of interactions with image dipole created in the substrate can be given (see Fig. 2.10).

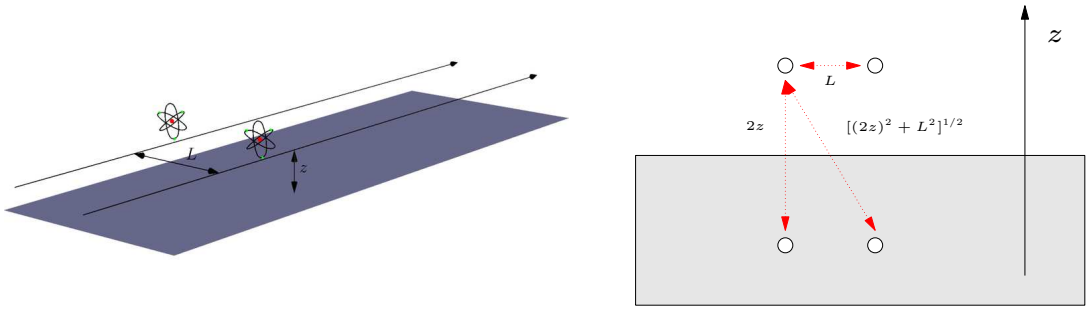

Fig. 2.10: Coherently split beams of electrons or atoms travel parallel to a metallic surface (left). Their decoherence is destroyed by interactions with their image dipoles (right).

Understanding all the mechanisms that can maintain or destroy atomic coherence finally paves the way for coherent manipulation of atomic samples in atom chip devices. Interfacing atomic samples with photonic waveguides can provide strong light-matter interaction. Together with the Centre for Cold Matter at Imperial College London we have investigated the prospects for using such waveguide chips for quantum information processing [10].

Dispersion Forces

Dispersion forces such as Casimir forces between bodies, Casimir–Polder forces between atoms and bodies and van der Waals forces between atomic systems are effective electromagnetic forces that arise as consequences of correlated ground-state fluctuations of the electromagnetic field. Within the general formalism of macroscopic quantum electrodynamics we have shown how universal scaling laws for all dispersion forces can be derived [11]. Similarly, the scaling of the Casimir interaction in a multi-sphere configuration with the number of sphere has been found [12].

Because all dispersion interactions follow from the same physical quantity, namely the quantised Lorentz force, the resulting expressions for the various interactions can be derived from one another, starting from the Casimir force, by diluting one or more macroscopic bodies until they eventually consist only of isolated microscopic particles (atoms or molecules). Making use of that fundamental principle, we have been able to continuously interpolate between Casimir–Polder and van der Waals interactions of atoms and small magnetodielectric spheres [13] which is a step towards understanding size effects in dispersion forces on embedded objects.

In addition to the exchange of virtual photons, for atoms or molecules in excited states, real-photon transitions can contribute substantially and even dominate the Casimir–Polder interaction, for instance in resonating cavities [14]. The most prominent example for the importance of the real-photon transitions are provided by Casimir–Polder interactions with Rydberg atoms [15] where level shifts up to the GHz range are expected at micrometer distances from a metallic surface. The contributions of real photons are also important in the interaction of fullerene molecules with surfaces [16] in molecular interferometry experiments.

Dispersion forces such as the Casimir–Polder interaction show a different distance scaling depending on the nature of the interaction (electrically polarisable, magnetisable, etc.). While the dipole interaction between electrically polarisable objects typically dominates, higher-order perturbative corrections such as magnetic interactions can contribute significantly for some materials. Of particular interest are unusual properties such as chiral responses. We have shown that, in accordance with the Curie dissymmetry principle, the Casimir–Polder potential gains additional contributions if both interacting partners show chiral properties. Moreover, the sign of their interaction depends on their handedness. Combining this effect with the possibility to effectively cancel out the electric Casimir–Polder interaction in resonating cavities, it becomes possible to discriminate between enantiomers in the gas phase [17].

At finite temperature and in thermal nonequlibrium, exchange of real photons is due to absorption and emission of thermal photons. In addition, the exchange of virtual photons occurs only at a discrete set of (Matsubara) frequencies. Rather unexpectedly, we could show that the Casimir–Polder potential can be entirely independent of temperature even if the mean number of thermal photons is large [18]. This statement holds for molecules with small transition frequencies sufficiently close to a metal surface (see Fig. 2.11). This result is largely independent of the geometry of the macroscopic body [20]. This has allowed us to systematically study the level shifts of a particle out of thermal equilibrium with a gold microsphere [19] which enabled us to gain insight into the dispersion interactions at finite temperature beyond numerical means.

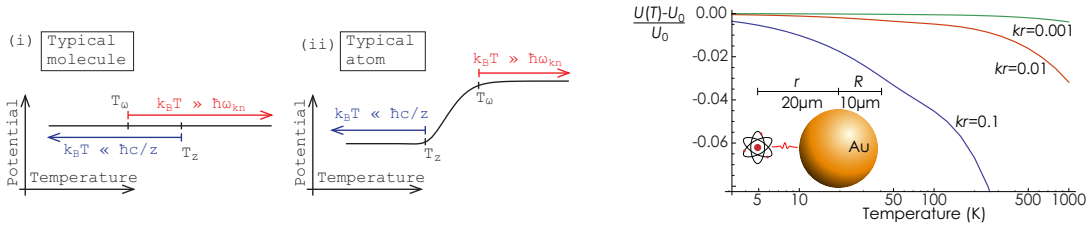

Fig. 2.11: Temperature dependence of the Casimir–Polder potential for a typical molecule vs a typical atom (left). Taken from Ref. [18]. Comparison of the exact thermal Casimir–Polder potential $U(T)$ to the temperature-independent result U_0 of a two-level particle near a gold sphere (right). Taken from Ref. [19].

References

[1] S. Y. Buhmann, D. T. Butcher and S. Scheel. "Macroscopic quantum electrodynamics in nonlocal and nonreciprocal media". *New J. Phys.*, **14** (2012), 083034.

[2] S. Y. Buhmann and S. Scheel. "Macroscopic Quantum Electrodynamics and Duality". *Phys. Rev. Lett.*, **102** (2010), 140404.

[3] J. A. Crosse and S. Scheel. "Effective nonlinear Hamiltonians in dielectric media". *Phys. Rev. A*, **81** (2010), 033815.

[4] J. A. Crosse and S. Scheel. "QED in absorbing nonlinear dielectric media". *Phys. Scripta*, **T140** (2010), 014041.

[5] J. A. Crosse and S. Scheel. "Coincident count rates in absorbing dielectric media". *Phys. Rev. A*, **83** (2010), 023815.

[6] S. Scheel and E. A. Hinds. "Atoms at Micrometer Distances from a Macroscopic Body". In J. Reichel and V. Vuletić, editors, "Atom Chips", pages 119–146. Wiley-VCH, Weinheim (2011).

[7] B. Kasch, H. Hattermann, D. Cano, T. E. Judd, S. Scheel, C. Zimmermann, R. Kleiner, D. Koelle and J. Fortàgh. "Cold atoms near superconductors: atomic spin coherence beyond the Johnson noise limit". *New J. Phys.*, **12** (2010), 065024.

[8] R. Fermani and S. Scheel. "Screening of electromagnetic field fluctuations by s-wave and d-wave superconductors". *J. Phys. B: At. Mol. Opt. Phys.*, **43** (2010), 025001.

[9] S. Scheel and S. Y. Buhmann. "Path decoherence of charged and neutral particles near surfaces". *Phys. Rev. A*, **85** (2012), 030101(R).

[10] R. A. Nyman, S. Scheel and E. A. Hinds. "Prospects for using integrated atom-photon junctions for quantum information processing". *Quant. Inf. Processing*, **10** (2011), 941.

[11] S. Y. Buhmann, S. Scheel and J. R. Babington. "Universal Scaling Laws for Dispersion Interactions". *Phys. Rev. Lett.*, **104** (2010), 070404.

[12] J. R. Babington and S. Scheel. "Casimir forces in multi-sphere configurations". *J. Phys. A: Math. Theor.*, **43** (2010), 215402.

[13] A. Sambale, S. Y. Buhmann and S. Scheel. "Casimir-Polder interaction between an atom and a small magnetodielectric sphere". *Phys. Rev. A*, **81** (2010), 012509.

[14] S. A. Ellingsen, S. Y. Buhmann and S. Scheel. "Casimir–Polder potential and transition rates in resonating cylindrical cavities". *Phys. Rev. A*, **82** (2010), 032516.

[15] J. A. Crosse, S. A. Ellingsen, K. Clements, S. Y. Buhmann and S. Scheel. "Thermal Casimir–Polder shifts in Rydberg atoms near metallic surfaces". *Phys. Rev. A*, **82** (2010), 010901(R).

[16] S. Y. Buhmann, S. Scheel, S. A. Ellingsen, K. Hornberger and A. Jacob. "Casimir–Polder interaction of fullerene molecules with surfaces". *Phys. Rev. A*, **85** (2012), 042513.

[17] D. T. Butcher, S. Y. Buhmann and S. Scheel. "Casimir–Polder forces between chiral objects". *New J. Phys.*, **14** (2012), 113013.

[18] S. A. Ellingsen, S. Y. Buhmann and S. Scheel. "Temperature-Independent Casimir–Polder Forces Despite Large Thermal Photon Numbers". *Phys. Rev. Lett.*, **104** (2010), 223003.

[19] S. A. Ellingsen, S. Y. Buhmann and S. Scheel. "Casimir–Polder energy-level shifts of an out-of-equilibrium particle near a microsphere". *Phys. Rev. A*, **85** (2012), 022503.

[20] S. A. Ellingsen, S. Y. Buhmann and S. Scheel. "Temperature-independent Casimir–Polder forces in arbitrary geometries". *Phys. Rev. A*, **84** (2011), 060501(R).

2.1.5 Semiconductor Optics

Head: Prof. Dr. Heinrich Stolz

Staff:	Dipl.-Phys. Thomas Ahrens	Dipl.-Phys. Martin Borm
	Dr. Gerolf Burau	MSc Stephan Graunke
	MSc Maria Kaupsch	Dr. Frank Kieseling
	Dipl.-Phys. Johannes Kröger	Dr. Günter Manzke
	M. Eng. Stephan Reiß	Dr. Felix Richter
	Dr. Gerd Rudlof	Dipl.-Phys. Dietrich Schneider
	Dipl.-Phys. Rico Schwartz	Dr. Daniel Schwedt
	Dr. Dirk Semkat	Dipl.-Phys. Siegfried Sobkowiak
	MSc Sunipa Som	Dipl.-Phys. Karsten Sperlich
	Dipl.-Ing. Michael Petzold	Christine Schoof
	Prof. Dr. em. Klaus Henneberger	Prof. Dr. em. Dietrich Kremp
MSc Graduates:	Maria Kaupsch	Stephan Graunke
Dipl.-Phys. Graduates:	Johannes Kröger	Siegfried Sobkowiak

General Outline of the Research

The main topics of our research are the study of *fundamental quantum processes in semiconductors* due to electron-hole ($e-h$) pairs and *their interaction with light* on time scales from several hundreds of microseconds down to some femtoseconds (10^{-15} s), especially with respect to future applications in computer and communication technology. Initiated by the *Interdisciplinary Faculty* of the University we recently started together with the clinic of ophthalmology a research project on spatially resolved light scattering from eye structures [1–25].

Bose-Einstein Condensation of Excitons

In semiconductors a new state of matter could be generated by exciting electron-hole pairs with intense laser pulses. This state is similar to that of common matter in many aspects: Bound states, very similar to the hydrogen atom, can build up which are called excitons. These could further form molecules (biexcitons) or even larger aggregates under adequate circumstances. Due to their tiny mass - the exciton mass is about three orders of magnitude smaller than that of the hydrogen atom - excitons should show pronounced quantum properties, like Bose-Einstein condensation or superfluidity already at temperatures of a few Kelvin which is quite different to common matter where temperatures of a few micro Kelvin are necessary. In the focus of this project are the thermodynamical properties of dense exciton systems. Especially, the existence of a theoretically proposed Bose–Einstein condensate (BEC) and its interaction with the light field is of particular interest. All previous studies, however, did not reach sufficiently low temperatures of the exciton system. Here we could make a big step forward by installing a new magneto cryostat system which is unique by allowing direct optical access to the sample space at temperatures down

to 40 mK and magnetic fields up to 7 T [16]. Recently, we achieved a breakthrough by finding strong evidence for a BEC of excitons in high quality cuprous oxide samples. By applying stress to the sample surface via a spherical glass lens we created a potential trap for excitons of a depth of a few meV. By increasing the density of excitons collected in this trap after optical excitation, we observed a transition from a thermal distribution (Fig. 2.12a) to a bimodal one (Fig. 2.12b) with an additional athermal component due to a condensate of excitons [23]. The experimental

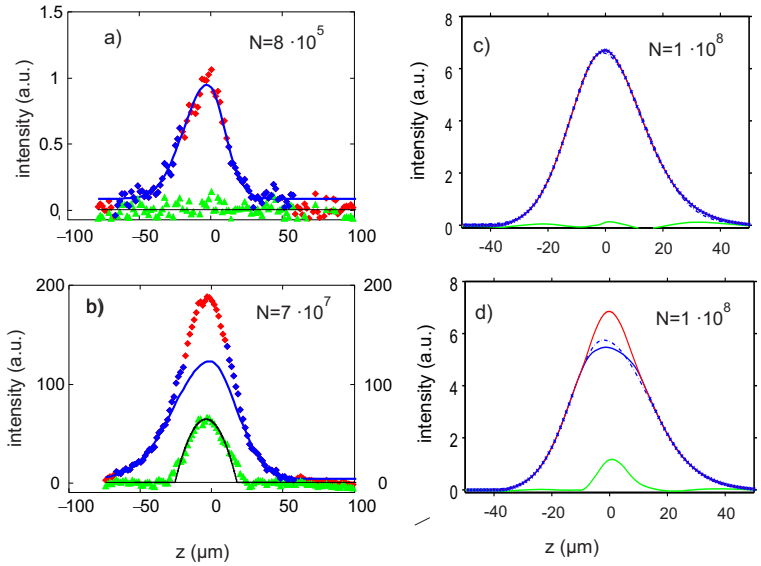

Fig. 2.12: Spatially resolved luminescence spectra of ultracold excitons in a potential trap. Part a and b are experimental data, parts c and d show theoretical results. N is the number of paraexcitons in the trap. In a and b the helium bath temperature is 39 mK, in c and d the local exciton temperature is 0.25 K (c) and 0.15 K (d).

observations are strongly substantiated by recent advances in the **theoretical description of dense excitonic systems**. In close collaboration between theory and experiment, we analyzed the physics of the trapped exciton gas in cuprous oxide. We started with the investigation of a one-component Bose gas of paraexcitons in the frame of the Hartree–Fock–Bogoliubov-Popov approximation, where the condensate density follows from the Gross–Pitaevskii equation in Thomas–Fermi approximation, i.e., by neglecting the kinetic energy of the condensate [19, 24]. To calculate the luminescence spectrum, we applied a local density approximation to the spectral function. Since only states with a wave vector equal to that of the emitted photon contribute to the luminescence, the light emission arises only from the thermally excited states and the condensate remains completely dark in that approximation. Therefore, the usually predicted delta-shaped peak at the chemical potential is absent. The comparison of the calculated spectra with the experiment, performed in [23], has shown the necessity to go beyond the theory developed in [19, 24] in two

aspects: (i) due to the finite extension of the condensate, it has to contribute weakly to the luminescence and (ii) only local thermodynamic equilibrium can be assumed, accounted for by a two-temperature model that leads to a spatial dependence of the chemical potential. Using these assumptions, we could reproduce the experimental spectra qualitatively quite well. Moreover, we have been able to reproduce the most pronounced experimentally found signature of a condensate, the occurrence of a bimodal distribution (see Fig. 2.12c and d).

Recent claims of other groups concerning the observation of a BEC of excitons based on the observation of coherence of the excitonic luminescence, turned out to be highly questionable. By deriving a theory of imaging with partial coherent light, we were able to show in a comment [18] that all coherence effects can be explained already assuming a completely incoherent ensemble.

Resonance Fluorescence from Excitons in GaAs/AlGaAs Quantum Wells: Mott Transition

We have examined the resonance fluorescence from localized excitons in GaAs/AlGaAs quantum wells with increasing excitation power and for different temperatures [4]. We found a nonlinear behaviour of the emitted intensity with increasing laser power, which is explained by our theoretical analysis, see [7] for details, as a transition of the emission from excitonic to electron-hole plasma states due to many-body effects between excited carriers (Mott transition). In [9] we have investigated this Mott transition more in detail from a theoretical point of view, extending and comparing two approaches:

First, a *thermodynamic approach* has been used to investigate the ionization equilibrium between electrons, holes, and excitons, where the abrupt jump of the degree of ionization from 0 to 1 indicates the Mott density. Second, a *spectral approach* based on the semiconductor Bloch equations within linear optical response has been used, considering the quasi-particle properties of carriers and the dynamical screening between electron-hole pairs. We found a strong increase of the excitonic linewidth (FWHM) accompanied by a decrease of the peak absorption as demonstrated in Fig. 2.13. Therefore, the prerequisite of small damping being necessary for the extended quasi-particle approximation in the *thermodynamic approach* is not fulfilled. Moreover, the Mott transition is rather a smooth transition in the region marked by the two dashed vertical lines in Fig. 2.13, than an abrupt one predicted within the *thermodynamic approach*.

Quantum Condensation in Highly Excited Semiconductors

Excitons have been an – unsuccessful – favourite for the experimental realization of Bose–Einstein condensation (BEC) for decades. As already mentioned, their existence is restricted by the Mott transition. For very high densities, a crossover to a BCS-type condensate similar to that in superconductors of weakly interacting $e-h$

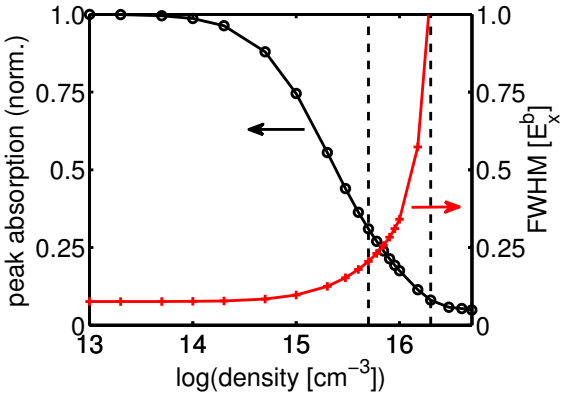

Fig. 2.13: Mott transition in semiconductors. Normalized peak absorption and full-width at half maximum (FWHM) for T=30K as function of the density.

pairs is expected. In [8, 17] we have investigated the influence of many-body effects on both the chemical potentials of carriers, and the Mott transition of paraexcitons in Cu_2O [8] and of heavy-hole excitons in ZnSe [17] over a wide range of temperatures and carrier densities. In contrast to simplified approximations used in the literature we considered full dynamical screening between carriers and found an extension of the region of existence of excitons in the temperature-density plane. Therefore, a BEC may occur at higher temperatures than thought previously. In [6] we have discussed the possible transition between BEC and BCS condensate in the framework of real-time Green's functions. We found a smooth crossover, i.e., no phase boundary between both condensates.

Photon Green's Function for Bounded Media: Nonequilibrium Radiation Laws

Based on nonequilibrium photon Green's functions we have developed a quantum-kinetically exact theoretical framework to describe the propagation, emission, and scattering of light in bounded media in the context of semiconductor optics [13]. Its advantage is that the spatial inhomogeneity inherent to bounded media and, hence, to many semiconductor optics problems, is fully and exactly considered. The electromagnetic properties of the media are treated microscopically rather than in an effective approximation [14], and they may be arbitrarily dispersive and absorptive. Relations for the propagation of quantized squeezed light [25] as well as for the energy flow law which can be seen as a generalization of the Kirchhoff and Planck laws to nonequilibrium. With the help of the energy flow law, we have discussed mechanisms of emission and optical signatures of quantum condensates [15].

Investigations of Eye Structures by Spatially Resolved Brillouin Scattering

It is possible to investigate the rheological and biophysical metrics of the ocular structures in the anterior segment of the eye by using Brillouin-spectroscopy and thus explore e.g. the reasons for loss of accommodation of the eye lens (presbyobia). In order to measure the extremely weak Brillouin signals with spectral shifts of the order of a few GHz, we have developed an experimental setup using high-resolution dispersive components known as *virtually imaged phased arrays* (VIPA) and a highly sensitive camera [10, 11, 22]. To achieve a high spatial resolution of the order of 10 μm, the configuration was designed in the form of confocal imaging. Thus, our experimental setup fulfills the requirements of a save application also in human eyes. As an example, Fig. 2.14 shows the axial profile of the eye over the entire

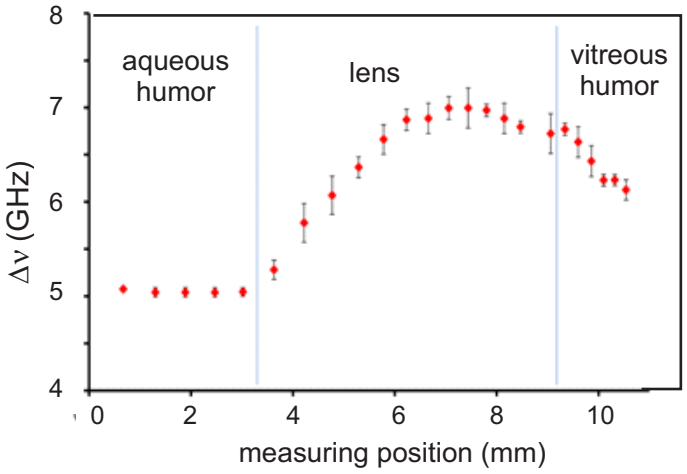

Fig. 2.14: In vivo Brillouin shift depth profile of a rabbit anterior chamber.

anterior chamber from the corneal surface to the anterior vitreous body. The graph clearly distinguishes the elements of the anterior chamber of the eye based on their Brillouin-scattering shift. Due to the high accuracy, it is possible to derive from the Brillouin-shifts the bulk modulus as a rheological measure of the eye, but also the refractive index and density for the corresponding measurement location [12].

References

[1] T. Ahrens, G. K. G. Burau, H. Stolz, S. Reitzenstein and A. Forchel. "Micro-cavity mode structure investigations with high spatial resolution". *Phys. Status Solidi C*, **8** (2011), 1239.

[2] M. Aßmann, F. Veit, J.-S. Tempel, T. Berstermann, H. Stolz, M. van der Poel,

J. M. Hvam and M. Bayer. "Measuring the dynamics of second-order photon correlation functions inside a pulse with picosecond time resolution". *Opt. Express*, **18** (2010), 20229.

[3] J. Brandt, P. Felbier, D. Fröhlich, C. Sandfort, M. Bayer and H. Stolz. "Temperature dependence of homogeneous broadening of the 1S paraexciton in Cu_2O". *Phys. Rev. B*, **81** (2010), 155214.

[4] G. K. G. Burau, G. Manzke, F. Kieseling, H. Stolz, D. Reuter and A. Wieck. "Nonlinear behaviour of the resonance fluorescence from excitons in quantum wells". *J. Phys. Conf. Ser.*, **210** (2010), 012017.

[5] D. Fröhlich, J. Brandt, C. Sandfort, M. Bayer and H. Stolz. "Anisotropic effective mass of orthoexcitons in Cu_2O". *Phys. Rev. B*, **84** (2011), 193205.

[6] D. Kremp, D. Semkat and K. Henneberger. "BEC-BCS transition in excitonic systems". *J. Phys. Conf. Ser.*, **220** (2010), 012004.

[7] G. Manzke, F. Richter, D. Semkat, G. K. G. Burau, F. Kieseling and H. Stolz. "Transition from excitonic to plasma emission from localized electron-hole pair states in GaAs-AlGaAs quantum wells". *Phys. Status Solidi C*, **8** (2011), 1161.

[8] G. Manzke, D. Semkat, F. Richter, D. Kremp and K. Henneberger. "Mott transition versus Bose-Einstein condensation of excitons". *J. Phys. Conf. Ser.*, **210** (2010), 012020.

[9] G. Manzke, D. Semkat and H. Stolz. "Mott transition of excitons in GaAs-GaAlAs quantum wells". *New J. Phys.*, **14** (2012), 095002.

[10] S. Reiss, G. Burau, O. Stachs, R. Guthoff and H. Stolz. "Spatially resolved Brillouin spectroscopy to determine the rheological properties of the eye lens". *Biomed Opt. Express*, **2** (2011), 2144.

[11] S. Reiss, K. Sperlich, M. Hovakimyan, P. Martius, R. F. Guthoff, H. Stolz and O. Stachs. "Ex vivo measurement of postmortem tissue changes in the crystalline lens by brillouin spectroscopy and confocal reflectance microscopy". *IEEE transactions on bio-medical engineering*, **59** (2012), 2348.

[12] S. Reiss, O. Stachs, R. Guthoff and H. Stolz. "Non-invasive, spatially resolved determination of tissue properties of the crystalline lens with regard to rheology, refractive index, density and protein concentration by using Brillouin spectroscopy". *Klin. Monbl. Augenheilkd.*, **228** (2011), 1079.

[13] F. Richter and K. Henneberger. "Quantum-optical radiation laws for confined semiconductors systems". *J. Phys. Conf. Ser.*, **210** (2010), 012032.

[14] F. Richter, M. Florian and K. Henneberger. "Comment on Poynting vector, heating rate, and stored energy in structured materials: A first-principles derivation". *Phys. Rev. B*, **82** (2010), 037103.

[15] F. Richter, D. Semkat and K. Henneberger. "The photon Green's function for bounded media: Splitting property and nonequilibrium radiation laws". *J. Phys. Conf. Ser.*, **220** (2010), 012006.

[16] R. Schwartz, N. Naka, F. Kieseling and H. Stolz. "Dynamics of excitons in a potential trap at ultra-low temperatures: paraexcitons in Cu_2O". *New J. Phys.*, **14** (2012), 023054.

[17] D. Semkat, F. Richter, D. Kremp, G. Manzke, W.-D. Kraeft and K. Henneberger. "Mott transition in electron-hole plasmas". *J. Phys. Conf. Ser.*, **220** (2010), 012005.

[18] D. Semkat, S. Sobkowiak, G. Manzke and H. Stolz. "Comment on "Condensation of Excitons in a Trap"". *Nano Lett.*, **12** (2012), 5055.

[19] S. Sobkowiak, D. Semkat, H. Stolz, T. Koch and H. Fehske. "Interacting multi-component exciton gases in a potential trap: Phase separation and Bose-Einstein condensation". *Phys. Rev. B*, **82** (2010), 064505.

[20] S. Sobkowiak, D. Semkat, H. Stolz, T. Koch and H. Fehske. "Phase separation of multicomponent excitonic Bose-Einstein condensates". *Phys. Status Solidi C*, **8** (2011), 1178.

[21] S. Som, F. Kieseling and H. Stolz. "Numerical simulations of exciton dynamics in Cu_2O at ultra low temperatures within a potential trap". *J. Phys.: Condens. Matter*, **24** (2012), 335803.

[22] O. Stachs, S. Reiss, R. Guthoff and H. Stolz. "Spatially resolved Brillouin spectroscopy for in vivo determination of the biomechanical properties of the crystalline lenses". *SPIE's Ophthalmic Technologies XXII*, **8209** (2012).

[23] H. Stolz, R. Schwartz, F. Kieseling, S. Som, M. Kaupsch, S. Sobkowiak, D. Semkat, N. Naka, T. Koch and H. Fehske. "Condensation of excitons in Cu_2O at ultracold temperatures: experiment and theory". *New J. Phys.*, **14** (2012), 105007.

[24] H. Stolz and D. Semkat. "Unique signatures for Bose-Einstein condensation in the decay luminescence lineshape of weakly interacting excitons in a potential trap". *Phys. Rev. B*, **81** (2010), 081302(R).

[25] D. Vasylyev, W. Vogel, K. Henneberger and F. Richter. "Propagation of quantized light through bounded dispersive and absorptive media". *Phys. Scr.*, **T 140** (2010), 014039.

2.1.6 Clusters and Nanostructures

Head: Prof. Dr. Karl-Heinz Meiwes-Broer

Staff:	PD Dr. Josef Tiggesbäumker	Prof. Dr. Vladimir Popok
	Dr. Ingo Barke	Dr. Steffen Fiedler
	Dr. Viola von Oeynhausen	Dr. Johannes Passig
	Dr. Andreas Przystawik	Dr. Kristian Sell
	Dr. Truong Xuan Nguyen	
	Dipl.-Phys. Jens Bahn	Dipl.-Phys. Stephan Bartling
	Dipl.-Phys. Sebastian Göde	Dipl.-Phys. Hannes Hartmann
	Dipl.-Phys. Robert Irsig	MSc Lev Kazak
	Dipl.-Phys. Michael Kelbg	Dipl.-Phys. Dzimitry Komar
	Dipl.-Phys. Michael Köther	Dipl.-Phys. Patrice Oelßner
	MSc Anna Oniszczuk	Dipl.-Phys. Stefan Polei
	Dipl.-Phys. Christian Schaal	Dipl.-Phys. Christian Schumann
	MSc Slawomir Skruszewicz	
	Jan Dittrich Annika Machotzek	Brigitte Schädel
Dipl.-Phys. Graduates:	Stephan Bartling	Hannes Hartmann
	Michael Kelbg	Michael Köther
	Christian Schumann	
MSc Graduates:	Anna Oniszczuk	
BSc Graduates:	Christin Baudisch	Johannes Krause
	Kevin Oldenburg	Lennart Seiffert
	Merten Siegfried	Paul Struszewski

General Outline of the Field of Research

Finite size, large surface fraction, limited capacity for heat and charge, and discrete electron states: these are characteristics of metal clusters and nanoparticles, addressed in the field of cluster physics. Our research is aimed at the remarkable consequences of nanoscale objects, many of which are accessible by spectroscopic means. Clusters in a molecular beam [1–14] allow the investigation of electronic and optical properties ranging up to the strongly nonlinear regime. For atoms and aggregates embedded in ultracold droplets [15–20] the interaction with the rare gas matrix environment becomes crucial and is a topic of intense research. If clusters and nanostructures are in contact with surfaces [21–41] a number of additional effects can be observed, ranging from structural changes to unusual transport, doping, and catalytic properties. A large part of the research has been conducted within the DFG-Sonderforschungsbereich 652, the Helmholtz Virtual Institute HICE, REMEDES, Light2Hydrogen, and other BMBF projects like Nanoscopic Systems investigated at FLASH.

Laser Spectroscopy on Molecules, Clusters, and Nanoparticles

Ultracold helium nanodroplets provide a sub-K nanolab for laser spectroscopy studies on the response of clusters within a weakly interacting and superfluid environ-

ment. The method of sequential pick-up of foreign atoms by the nanodroplets is applied to grow and prepare clusters in droplets. This technique provides a flexible tool to adjust the size of the droplets as well as that of the embedded species almost independently. The special response of the helium fluid on dopants provide a unique environment for studies on exotic species. In the linear response experiments we thus concentrate on metastable complexes exclusively formed in helium droplets. In particular, aggregates of magnesium atoms have been studied with photoelectron as well as with femtosecond pump-probe spectroscopy. Due to the van der Waals interactions between helium and the dopant atoms at ultralow temperatures, the atoms form a nm-spaced atomic network. For example, after a kick with an ultrashort laser pulse the complexes collapse which is reflected in a distinct dynamics on both the fs and ps time scales The aspect of microsolvation has been addressed in experiments on Ag-clusters in Ar droplets [18]. The line position of the octamer resonance is in good agreement with quantum-chemical calculations when taking the matrix shift into account. These studies on optical properties support our earlier work on Ag_8 in helium droplets and confirm that long-living states exist in metal clusters. In a photoelectron experiment on size-selected metal clusters we applied ultrashort wavelengths (4.7 nm) delivered by the free-electron laser FLASH to study cluster core levels. The size-dependent shift in the binding energies allows to identify the critical size in the non-metal to metal transition [12]. Moreover the spectra show electron scattering in the emission again with a characteristic size-dependence. Recently we entered the field of mass spectrometry on organic molecules produced in combustion processes as for example motor cars running with biodiesel. The aim is to analyze the toxic impact of the composition of the exhaust gases. Whereas other groups in the consortium concentrate on the cell response, the emphasis in our studies will be on the light organic molecules such as formaldehyde. First campaigns analyzing the gas exhaust of a ship diesel engine have been conducted in Rostock.

Intense ultrashort light pulses interacting with small particles open the doorway to analysis of phenomena induced by strong fields [1]. Clusters might serve as model systems to investigate multielectron dynamics relevant to other areas of intense laser-matter research, e.g. laser driven particle acceleration. The many-body aspects of the finite-sized object introduce a special behavior of the cluster response, as is reflected by the emission of ions with up to MeV energies, keV electrons and short wavelength radiation up to the X-ray regime. In contrast to atomic gas targets, the temporal laser pulse structure plays a significant role. Atomic ions in charge states as high as q=24 have been observed from laser exposed xenon clusters [16]. Indeed, the pulse intensity needed to create such high charge states is reduced by orders of magnitude when compared to free atoms. In one of the experiments the focus-scan method has been applied to monitor q-selective ionization thresholds for multiply charged ions. The comparison to molecular dynamics simulations revealed that electron recombination is strongly suppressed due to the significant increase in the nanoplasma electron temperature at the plasmon resonance. In a study on silver clusters we optimized the output of highly charged ions in a laser control ex-

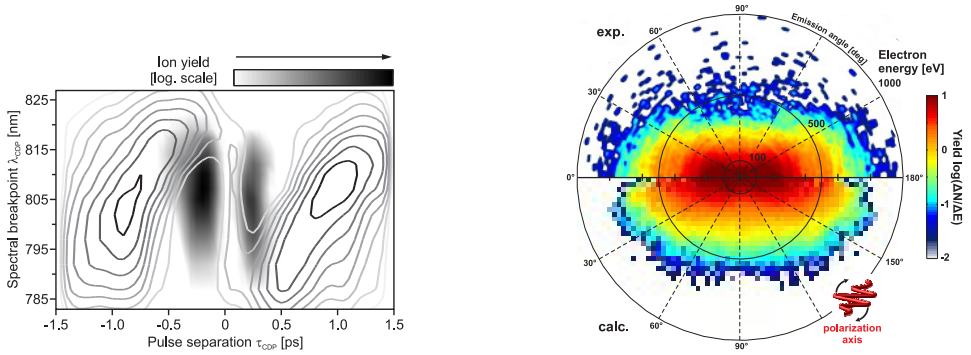

Fig. 2.15: *left:* Comparison of the colored double pulse fitness landscape spectra of Xe^{5+} (contour lines) and Xe^{23+} (grey areas) using 1.0 mJ pulses. Plasmon-induced charge state bleaching leads to a clear separation of the low-q and high-q ion features [17]. *right:* Comparison of angular-resolved electron spectra ($dN/dEd\Omega$) (top: experiment, bottom: simulation by the group of Th. Fennel) from intense laser exposed silver clusters at an optical delay of $\Delta t = 1.2$ ps delay taken at laser intensities of $0.9\times10^{14}\,\mathrm{Wcm^{-2}}$. Taken from [14].

periment [15]. The pulse envelope shows that a two pulse sequence with unbalanced intensity gives a strong signal of highly charged ions indicating the phenomenon of delayed plasmon enhanced ionization. Computer control experiments using an improved nanoplasma model support the experimental finding. A closer analysis of the optimized pulse using an SHG-FROG scheme [6] reveals that the laser frequency in the pulse adapts to the spectral evolution of the plasmon resonance. Besides these optimization studies we applied the technique of colored double pulse fitness landscapes [7, 19], thereby focusing on experiments where laser parameters such as spectral composition, ratio of pulse intensities, and optical delay are systematically varied within a single scan [17], see Fig. 2.15. With this method e.g. laser optimized conditions have been identified for selective ionization into either low or highly-charged ions [17].

In another set of experiments we investigated the strong field-induced electron emission from metal clusters. At the optimal pulse delay, that is when the subsequent pulse hits the cluster at the collective resonance, electrons gain kinetic energies dominantly within a single oscillation of the plasmon. Kinetic energies as high as 1.6 keV have been observed at already $10^{14}\,\mathrm{Wcm^{-2}}$. Whereas in atoms the maximum energy in the recollision process reaches 10 times the ponderomotive potential (U_p), a value of 300 U_p is observed in experiments on metal clusters having a size of a few nm. The angular distribution shows a characteristic pattern which proves that strong acceleration is highly directional along the axis of the collective oscillation. Molecular dynamics simulations provided by the group of Th. Fennel for the first time have achieved a quantitative agreement between experiment and theory, see Fig. 2.15, right. Stimulated by these results we conducted experiments together

with the group of Mathias Kling from the Max-Planck-Institute for Quantum Optics in Garching with bichromatic pulses which allow to control the laser field on the timescale of a single light oscillation period. Strong phase dependencies have been obtained which proves the nanoplasmonic acceleration hypothesis. In the follow-up experiments the studies were extended to carrier-envelope phase controlled excitations using the few-cycle laser system in Garching.

In the past few years a new setup was developed to produce μm-sized liquid jets of hydrogen, as well as helium and other rare gases. At the FLASH facility we use hydrogen droplets to study plasmas which are produced in the interaction with optical as well as soft-xray laser fields. The aim is to determine electron density and electron temperature of these microplasmas directly from Thomson scattering data hence without any further assumption. The results of these measurements will provide benchmark for theoretical calculations as they are performed in the group of R. Redmer in our institute. First data using soft-xray Thomson self-scattering have been collected [3] and these preliminary results suggest such an approach to be feasible. In further campaigns the time evolution of the plasma has been investigated showing e.g. a steep increase in the Rayleigh scattering signal on a ps timescale, indicating the onset of electron-ion coupling.

Clusters and Nanostructures at Surfaces

Formation of clusters in the gas phase and their deposition on crystal surfaces represent a versatile technique for the controlled production of nanosystems [35]. A number of different cluster-surface interaction regimes can be distinguished depending on the kinetic energy of the cluster during the impact with the surface. For argon clusters in graphite it was shown that the implantation depth scales linearly with cluster momentum [29]. A universal scaling law could be developed by plotting the implantation depth versus the momentum scaled with the projected surface area of the cluster.

Metal clusters soft-landed on metal oxide surfaces are intensively studied in view of potential applications in catalysis. Silver clusters on thin alumina films serve as efficient and selective model catalysts for the partial oxidation of propylene [32]. We investigated the detailed catalytic scheme and the role of cluster size and shape using a combination of methods including grazing incident X-ray scattering under realistic reaction conditions as well as electron and scanning tunneling microscopy (STM).

Access to geometric properties of supported clusters such as crystal structure, orientation, and epitaxial alignment with respect to the substrate is possible using reflection high energy electron diffraction (RHEED). For Fe clusters on W(110) we could show size-dependent spontaneous alignment and reorientation triggered by controlled annealing [23, 24], see Fig. 2.16.

Spatially resolved scanning tunneling spectroscopy (STS) allows gaining insight into the electronic coupling between metal clusters and semiconductor surfaces. Such

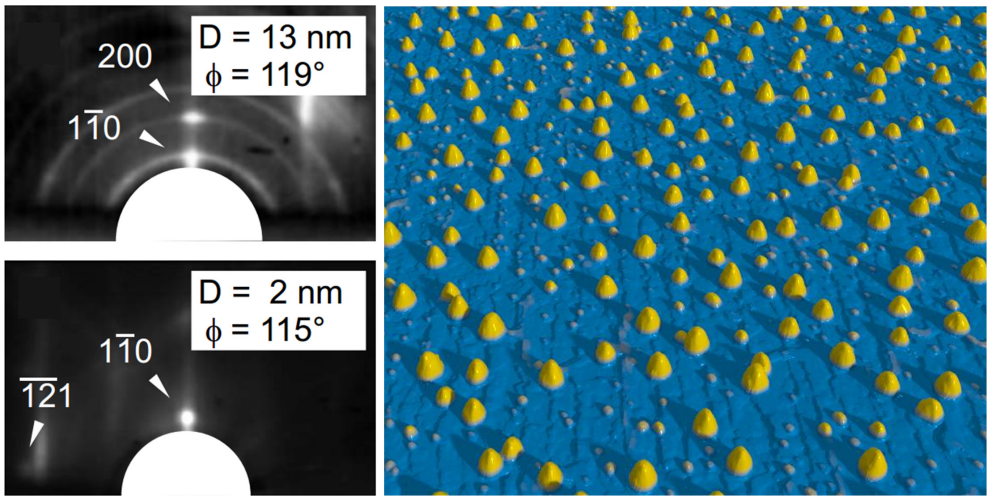

Fig. 2.16: *left:* RHEED diffraction patterns of Fe clusters on W(110) for different cluster sizes. The larger particles (top) give rise to a textured Debye-Scherrer powder pattern whereas smaller particles (bottom) show weak or no rings and an altered spot pattern, indicating the onset of spontaneous alignment relative to the substrate [24]. *right:* Pseudo-3D representation of a large-scale STM image of AuSi clusters grown on Si(111). The clusters are aligned at step edges of the substrate and exhibit epitaxial crystalline order [31].

a configuration can be viewed as a model system for a nanoscale Schottky contact. A detailed analysis of silver clusters on Si(111) based on surface photovoltage measurements revealed that the band topology is dominated by metallic surface states of the substrate [21]. Using a planar model system we could unravel the mechanism of spatially varying band bending and establish a simple model for the band topology.

To expand the range of available cluster sizes and materials and to provide highly stable cluster beams we set up a new cluster deposition system based on a commercial magnetron source [40]. The compact apparatus provides ultra-clean deposition conditions realized by several pumping stages and a cryotrap.

A promising alternate route for efficient preparation of well-ordered cluster-surface systems is the self-assembly of particles directly on a surface. For AuSi particles on Si(111) created by evaporation of Au on a silicon substrate we were able to resolve the structure by a combination of STM and RHEED [31]. The clusters exhibited pronounced facets and aligned at step edges of the underlying substrate, see Fig. 2.16, right. Perfect expitaxial alignment along with an unusual orientation of the contact facet are key findings of this study.

Finite size effects in low-dimensional systems have been the topic of research on a different class of materials, i.e. self-assembled atomic wires on semiconductor surfaces [41]. We demonstrated an interesting self-doping effect on Si(111)-(5x2)-Au that is restricted to short one-dimensional segments of atomic chains, see Fig. 2.17.

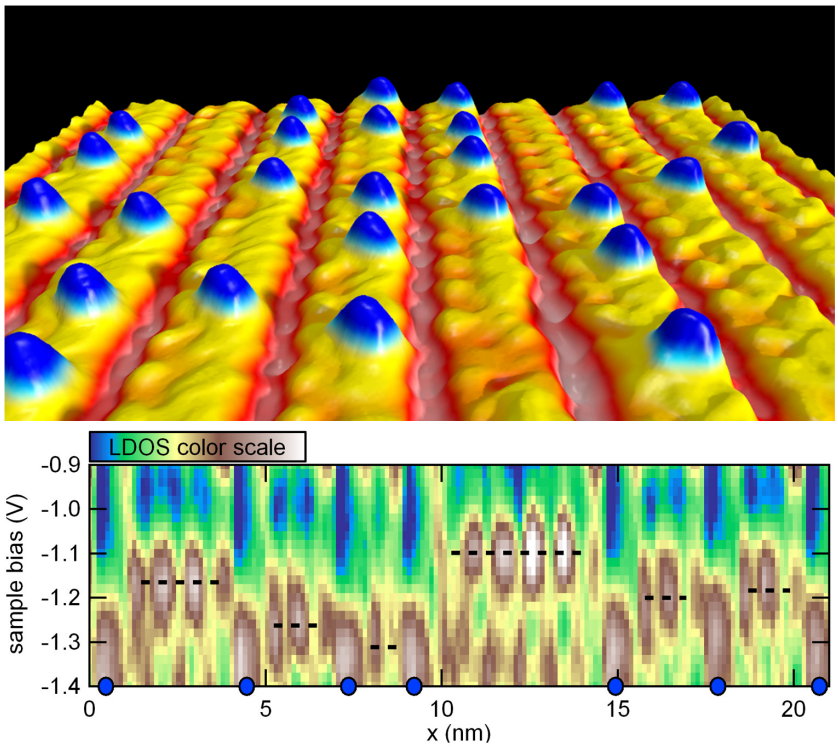

Fig. 2.17: *top:* Pseudo-3D representation of atomic chains on Si(111)-(5x2)-Au. Silicon adatoms on top of the chains appear in blue color. *bottom:* local density of states (LDOS) measured with a STM as a function of energy (vertically) and location along a chain (horizontally). The position of Si adatoms is indicated by blue circles on the abscissa. They act as electron donors resulting in a region of confined doping that affects the energy position of electron states (horizontal dashed lines) relative to the Fermi level [41].

Such confined doping is a unique property of one-dimensional systems and is not observed in higher dimensions. In addition, we mapped the detailed surface potential in direction perpendicular to the wires utilizing so-called field-emission resonances in constant-current STS [39]. We obtained exceptionally large field gradients within the surface plane, which are of potentially significant impact on catalytic, electronic, and spin properties of nanostructured surfaces.

References

[1] T. Fennel, K.-H. Meiwes-Broer, J. Tiggesbäumker, P.-G. Reinhard, P. M. Dinh and E. Suraud. "Laser-driven nonlinear cluster dynamics". *Rev. Mod. Phys.*, **82** (2010), 1793–1842.

[2] S. Toleikis, R. Fäustlin, L. Cao, T. Döppner, S. Düsterer, E. Förster, C. Fort-

mann, S. Glenzer, S. Göde, G. Gregori, R. Irsig, T. Laarmann, H. Lee, B. Li, J. Mithen, K.-H. Meiwes-Broer, A. Przystawik, P. Radcliffe, R. Redmer, F. Tavella, R. Thiele, J. Tiggesbäumker, N. Truong, I. Uschmann, U. Zastrau and T. Tschentscher. "Soft X-ray scattering using FEL radiation for probing near-solid density plasmas at few electron volt temperatures". *High Energy Density Phys.*, **6** (2010), 15–20.

[3] R. R. Fäustlin, T. Bornath, T. Döppner, S. Düsterer, E. Förster, C. Fortmann, S. H. Glenzer, S. Göde, G. Gregori, R. Irsig, T. Laarmann, H. J. Lee, B. Li, K.-H. Meiwes-Broer, J. Mithen, B. Nagler, A. Przystawik, H. Redlin, R. Redmer, H. Reinholz, G. Röpke, F. Tavella, R. Thiele, J. Tiggesbäumker, S. Toleikis, I. Uschmann, S. M. Vinko, T. Whitcher, U. Zastrau, B. Ziaja and T. Tschentscher. "Observation of Ultrafast Nonequilibrium Collective Dynamics in Warm Dense Hydrogen". *Phys. Rev. Lett.*, **104** (2010), 125002.

[4] J. Tiggesbäumker, T. Fennel, N. Truong and K.-H. Meiwes-Broer. "Resolving the Ion and Electron Dynamics in Finite Systems Exposed to Intense Optical Laser Fields". In R. Redmer, F. Hensel and B. Holst, editors, "Metal-to-Nonmetal Transitions", volume 132 of *Springer Series in Materials Science*, pages 85–113. Springer Berlin Heidelberg (2010).

[5] S. Toleikis, T. Bornath, T. Döppner, S. Düsterer, R. R. Fäustlin, E. Förster, C. Fortmann, S. H. Glenzer, S. Göde, G. Gregori, R. Irsig, T. Laarmann, H. J. Lee, B. Li, K.-H. Meiwes-Broer, J. Mithen, B. Nagler, A. Przystawik, P. Radcliffe, H. Redlin, R. Redmer, H. Reinholz, G. Röpke, F. Tavella, R. Thiele, J. Tiggesbäumker, I. Uschmann, S. M. Vinko, T. Whitcher, U. Zastrau, B. Ziaja and T. Tschentscher. "Probing near-solid density plasmas using soft x-ray scattering". *J. Phys. B*, **43** (2010), 194017.

[6] N. X. Truong, J. Tiggesbäumker and T. Döppner. "Shaper-assisted removal of the direction-of-time ambiguity in SHG-FROG". *Meas. Sci. Techn.*, **21** (2010), 085303.

[7] N. X. Truong, J. Tiggesbäumker and K.-H. Meiwes-Broer. "Intense colored pulse trains: generation, characterization, and applications". *J. Opt.*, **12** (2010), 115201.

[8] S. M. Vinko, U. Zastrau, S. Mazevet, J. Andreasson, S. Bajt, T. Burian, J. Chalupsky, H. N. Chapman, J. Cihelka, D. Doria, T. Döppner, S. Düsterer, T. Dzelzainis, R. R. Fäustlin, C. Fortmann, E. Förster, E. Galtier, S. H. Glenzer, S. Göde, G. Gregori, J. Hajdu, V. Hajkova, P. A. Heimann, R. Irsig, L. Juha, M. Jurek, J. Krzywinski, T. Laarmann, H. J. Lee, R. W. Lee, B. Li, K.-H. Meiwes-Broer, J. P. Mithen, B. Nagler, A. J. Nelson, A. Przystawik, R. Redmer, D. Riley, F. Rosmej, R. Sobierajski, F. Tavella, R. Thiele, J. Tiggesbäumker, S. Toleikis, T. Tschentscher, L. Vysin, T. J. Whitcher,

S. White and J. S. Wark. "Electronic Structure of an XUV Photogenerated Solid-Density Aluminum Plasma". *Phys. Rev. Lett.*, **104** (2010), 225001.

[9] U. Zastrau, V. Hilbert, C. Brown, T. Döppner, S. Dziarzhytski, E. Förster, S. H. Glenzer, S. Göde, G. Gregori, M. Harmand, D. Hochhaus, T. Laarmann, H. J. Lee, K.-H. Meiwes-Broer, P. Neumayer, A. Przystawik, P. Radcliffe, M. Schulz, S. Skruszewicz, F. Tavella, J. Tiggesbäumker, S. Toleikis and T. White. "In-situ determination of dispersion and resolving power in simultaneous multiple-angle XUV spectroscopy". *J. Instr.*, **6** (2011), P10001.

[10] N. Truong, J. Tiggesbäumker and K.-H. Meiwes-Broer. "Control of chirped pulse trains: a speedway for free-optimization experiments". *Appl. Phys. B*, **105** (2011), 293–300.

[11] C. Bostedt, E. Eremina, D. Rupp, M. Adolph, H. Thomas, M. Hoener, A. R. B. de Castro, J. Tiggesbäumker, K.-H. Meiwes-Broer, T. Laarmann, H. Wabnitz, E. Plönjes, R. Treusch, J. R. Schneider and T. Möller. "Ultrafast X-Ray Scattering of Xenon Nanoparticles: Imaging Transient States of Matter". *Phys. Rev. Lett.*, **108** (2012), 093401.

[12] J. Bahn, P. Oelßner, M. Köther, C. Braun, V. Senz, S. Palutke, M. Martins, E. Rühl, G. Ganteför, T. Möller, B. von Issendorff, D. Bauer, J. Tiggesbäumker and K.-H. Meiwes-Broer. "Pb 4f photoelectron spectroscopy on mass-selected anionic lead clusters at FLASH". *New J. Phys.*, **14** (2012), 075008.

[13] M. Harmand, C. D. Murphy, C. R. D. Brown, M. Cammarata, T. Döppner, S. Düsterer, D. Fritz, E. Förster, E. Galtier, J. Gaudin, S. H. Glenzer, S. Göde, G. Gregori, V. Hilbert, D. Hochhaus, T. Laarmann, H. J. Lee, H. Lemke, K.-H. Meiwes-Broer, A. Moinard, P. Neumayer, A. Przystawik, H. Redlin, M. Schulz, S. Skruszewicz, F. Tavella, T. Tschentscher, T. White, U. Zastrau and S. Toleikis. "Plasma switch as a temporal overlap tool for pump-probe experiments at FEL facilities". *J. Instr.*, **7** (2012), P08007.

[14] J. Passig, R. Irsig, N. X. Truong, T. Fennel, J. Tiggesbäumker and K.-H. Meiwes-Broer. "Nanoplasmonic electron acceleration in silver clusters studied by angular-resolved electron spectroscopy". *New J. Phys.*, **14** (2012), 085020.

[15] N. X. Truong, P. Hilse, S. Göde, A. Przystawik, T. Döppner, T. Fennel, T. Bornath, J. Tiggesbäumker, M. Schlanges, G. Gerber and K. H. Meiwes-Broer. "Optimal control of the strong-field ionization of silver clusters in helium droplets". *Phys. Rev. A*, **81** (2010), 013201.

[16] T. Döppner, J. Müller, A. Przystawik, S. Göde, J. Tiggesbäumker, K.-H. Meiwes-Broer, C. Varin, L. Ramunno, T. Brabec and T. Fennel. "Steplike intensity threshold behavior of extreme ionization in laser-driven Xe clusters". *Phys. Rev. Lett.*, **105** (2010), 053401.

[17] N. Truong, S. Göde, J. Tiggesbäumker and K.-H. Meiwes-Broer. "A study of the global chirp dependence on the interaction of intense colored double pulses with clusters". *Eur. Phys. J. D*, **63** (2011), 275–280.

[18] W. Christen, P. Radcliffe, A. Przystawik, T. Diederich and J. Tiggesbäumker. "Argon Solvent Effects on Optical Properties of Silver Metal Clusters". *J. Phys. Chem. A*, **115** (2011), 8779–8782.

[19] N. X. Truong, S. Göde, J. Tiggesbäumker and K.-H. Meiwes-Broer. "Systematically Shaped Laser Pulses for Intense Laser-Cluster Studies". *J. Phys. B*, **44** (2011), 225601.

[20] P. Hilse, T. Bornath, M. Moll, M. Schlanges, N. X. Truong, S. Göde, J. Tiggesbäumker and K.-H. Meiwes-Broer. "Control of Ionization in the Interaction of Strong Laser Fields with Dense Nanoplasmas". *Contr. Plas. Phys.*, **52** (2012), 28–32.

[21] K. Sell, I. Barke, S. Polei, C. Schumann, V. v. Oeynhausen and K.-H. Meiwes-Broer. "Surface photovoltage of Ag nanoparticles and Au chains on Si(111)". *Phys. Status Solidi B*, **247** (2010), 1087.

[22] J. Bansmann, A. Kleibert, M. Getzlaff, A. F. Rodríguez, F. Nolting, C. Boeglin and K.-H. Meiwes-Broer. "Magnetism of 3d transition metal nanoparticles on surfaces probed with synchrotron radiation - from ensembles towards individual objects". *Phys. Status Solidi B*, **247** (2010), 1152.

[23] A. Kleibert, A. Voitkans and K.-H. Meiwes-Broer. "Reflection high energy electron diffraction as a tool in cluster deposition experiments". *Phys. Status Solidi B*, **247** (2010), 1048.

[24] A. Kleibert, A. Voitkans and K.-H. Meiwes-Broer. "Size-dependent alignment of Fe nanoparticles upon deposition onto W(110)". *Phys. Rev. B*, **81** (2010), 073412.

[25] A. Kleibert, F. Bulut, W. Rosellen, K.-H. Meiwes-Broer, J. Bansmann and M. Getzlaff. "Supported and embedded Fe nanoparticles: Influence of the environment on shape and interface contributions to the magnetic anisotropy". *J. Phys. Conf. Ser.*, **211** (2010), 012017.

[26] K. Fauth, G. E. Ballentine, C. Praetorius, A. Kleibert, N. Wilken, A. Voitkans and K.-H. Meiwes-Broer. "Magnetic properties of Fe nanoclusters on Cu(111) studied with X-ray magnetic circular dichroism". *Phys. Status Solidi B*, **247** (2010), 1170.

[27] V. N. Popok, A. Kalabukhov, R. Gunnarsson, S. Lemeshko, T. Claeson and D. Winkler. "Kelvin Probe Force Microscopy Study of LaAlO3/SrTiO3 Heterointerfaces". *J. Adv. Microsc. Res.*, **5** (2010), 26.

[28] V. N. Popok, A. V. Gromov, V. I. Nuzhdin and A. L. Stepanov. "Optical and AFM study of ion-synthesised silver nanoparticles in thin surface layers of SiO2 glass". *J. Non-Cryst. Solids*, **356** (2010), 1258.

[29] V. N. Popok, J. Samela, K. Nordlund and E. E. B. Campbell. "Stopping of energetic argon cluster ions in graphite: Role of cluster momentum and charge". *Phys. Rev. B*, **82** (2010), 201403.

[30] V. N. Popok. *Handbook of Nanophysics: Clusters and Fullerenes (ed. K.D. Sattler)*, chapter Energetic Cluster-Surface Collisions. CRC Press, Boca Raton (2010).

[31] S. Bartling, I. Barke, K. Sell, S. Polei, V. v. Oeynhausen and K.-H. Meiwes-Broer. "Structure of AuSi nanoparticles on Si(111) from reflection high-energy electron diffraction and scanning tunneling microscopy". *Eur. Phys. J. D*, **63** (2011), 225.

[32] L. M. Molina, S. Lee, K. Sell, G. Barcaro, A. Fortunelli, B. Lee, S. Seifert, R. E. Winans, J. W. Elam, M. J. Pellin, I. Barke, V. v. Oeynhausen, Y. Lei, R. J. Meyer, J. A. Alonso, A. F. Rodríguez, A. Kleibert, S. Giorgio, C. R. Henry, K.-H. Meiwes-Broer and S. Vajda. "Size-dependent selectivity and activity of silver nanoclusters in the partial oxidation of propylene to propylene oxide and acrolein: A joint experimental and theoretical study". *Catal. Today*, **160** (2011), 116.

[33] V. N. Popok. "Energetic cluster ion beams: Modification of surfaces and shallow layers". *Mater. Sci. Eng. R*, **72** (2011), 137.

[34] A. Voitkans, L. Dimitrocenko, P. Kulis, S. Bartling, I. Barke, K.-H. Meiwes-Broer and I. Tale. "Ex situ investigations of MOCVD-grown gallium nitride nanowires using reflection high energy electron diffraction". *IOP Conf. Ser. Mat. Sci. Eng.*, **23** (2011), 012038.

[35] V. N. Popok, I. Barke, E. E. B. Campbell and K.-H. Meiwes-Broer. "Cluster-surface interaction: From soft landing to implantation". *Surf. Sci. Rep.*, **66** (2011), 347.

[36] S. Vajda, M. Pellin, J. Elam, C. Marshall, R. Winans and K.-H. Meiwes-Broer. "Subnanometer and nanometer catalyst, method for preparing size-selected catalysts" (2011). US Patent no.: US 2011/0045969 A1.

[37] S. Vajda, M. Pellin, J. Elam, C. Marshall, R. Winans and K.-H. Meiwes-Broer. "Subnanometer and nanometer catalyst, method for preparing size-selected catalysts" (2011). US Patent no.: US 8,143,189 B2.

[38] S. Vajda, M. Pellin, J. Elam, C. Marshall, R. Winans and K.-H. Meiwes-Broer. "Subnanometer and nanometer catalyst, method for preparing size-selected catalysts" (2012). US Patent no.: US 8,148,293 B2.

[39] S. Polei, I. Barke, S. C. Erwin and K.-H. Meiwes-Broer. "Periodic variations in the local surface potential of Si(111)-(5×2)-Au". *Phys. Rev. B*, **85** (2012), 165414.

[40] H. Hartmann, V. N. Popok, I. Barke, V. v. Oeynhausen and K.-H. Meiwes-Broer. "Design and capabilities of an experimental setup based on magnetron sputtering for formation and deposition of size-selected metal clusters on ultra-clean surfaces". *Rev. Sci. Instr.*, **83** (2012), 073304.

[41] I. Barke, S. Polei, V. v. Oeynhausen and K.-H. Meiwes-Broer. "Confined Doping on a Metallic Atomic Chain Structure". *Phys. Rev. Lett.*, **109** (2012), 066801.

2.1.7 Dynamics of Molecular Systems

Head: Prof. Dr. Stefan Lochbrunner

Staff:	Dr. Henning Marciniak	Dr. Antje Neubauer
	Dr. Stefanie Tschierlei	Dipl.-Phys. Franziska Fennel
	Dipl.-Phys. Matthias Lütgens	Dipl.-Phys. Frank Friedriszik
	Dipl.-Phys. Steffen Wolter	Dipl.-Biol. Susana Chatzipapadopoulos
	Dipl.-Phys. Conrad Schuster	Dipl.-Phys. Aleksej Friedrich
	Elke Prandke	Ursula Heyer
	Wolfgang Breitsprecher	
Dipl.-Phys. Graduates:	Conrad Schuster	Maik Teicher
	Marcus Seidel	Aleksej Friedrich
BSc Graduates:	Neeke Rothe	Karl Magnus Westphal
	Roland Mainz	Marcel Holtz
	Patrick Schwarzbach	Sebastian Gerke
	Sarah Schätzke	Sonia Meyer-Stender

General Outline of the Field of Research

The group "Dynamics of Molecular Systems" performs research on photoinduced processes in molecules, supramolecular structures, and organic materials. The goal is to observe and characterize the fundamental steps and to learn about the responsible mechanisms. Molecular systems exhibit a huge variety of properties and phenomena which can be explored in a broad spectrum of applications. This includes functional materials, organic electronics, as well as nanotechnology where implementing functions on a molecular scale is one of the ultimate goals. The rich behavior and variability result from the interplay of electronic and nuclear degrees of freedom. Understanding, control and optimization of the respective molecular processes call for a microscopic and quantum-mechanical notion of the underlying mechanisms. We apply time-resolved spectroscopy to achieve this goal. The focus is on ultrafast pump-probe techniques with a resolution down to 10 fs, which allow the observation of the processes in real time. In addition the evolution of the emission can be characterized from the pico- to the microsecond time scale by a streak camera. The following topics summarize the main activities in the last three years.

Energy Migration in Disordered Organic Materials

Intense research is going on to use organic materials in optoelectronic applications like e.g. solar cells. In this context the behavior of the fundamental electronic excitations, so-called Frenkel excitons, is crucial. The absorption of photons results typically in the formation of excitons and the associated energy is transported through the material if migration of the excitons takes place. The diffusion of excitons depends sensitively on the transfer mechanism between the molecular sites and the

degree of order in the material. Our femtosecond pump-probe experiments on different systems show that it is possible to discriminate between different scenarios and to provide absolute numbers for local mobilities [1, 2].

Organic materials with a low degree of order, e.g. many polymers, show energetic downhill migration within the inhomogeneous distribution of site energies resulting in a low exciton mobility. In polyfluorene based polymers we characterized this behavior by monitoring the spectral shift of the emission band [3]. Since these materials are promising for organic lasers also the behavior at high excitation levels was of particular interest. We found that exciton-exciton annihilation gains importance with increasing excitation density but at sufficiently high levels spontaneous amplification by stimulated emission results in a pronounced non-exponential decay of the exciton population and dominates the dynamics [3].

For better control of the spectral properties and energetic disorder we used instead of a neat polymer a polymer matrix doped with dye molecules as active sites. At high dye concentrations energy transfer becomes quite fast and a high mobility for electronic excitations is achieved [4]. The energetic disorder is reduced since the dye molecules have well-defined electronically excited states which are not strongly affected by the environment. The magnitude and time dependence of the observed transient spectral shifts are quantitatively modeled assuming Förster energy transfer. All parameters beside of the contribution of inhomogeneous broadening to the spectral widths are known from steady state spectroscopy. In this way it was possible to prove that Förster energy transfer is the dominant process, to calculate the mobility of the excitons, and to determine the amount of the energetic disorder [5].

Exciton Dynamics in Aggregates

In future, supramolecular organic structures will be most probably employed in a wide range of photonic devices like organic solar cells or light emitting diodes. Promising building blocks for such structures are J-aggregates of perylene bisimide dyes [6]. The excitons of these aggregates are highly mobile throughout their lifetime and might be used to transfer electronic energy over a significant distance [1]. Our pump-probe studies reveal that already at intermediate excitation densities exciton-exciton annihilation occurs and accelerates the decay kinetics with increasing excitation density, see Fig. 2.18. A rate model, that accounts for exciton diffusion and annihilation, is fitted to the data. From the fit a diffusion constant of $9 \cdot 10^{-3}\,\mathrm{cm}^2/\mathrm{s}$ is extracted and it is found that the motion of the excitons is restricted to one dimension [7, 8].

The aggregates are obviously long chains along which the excitons can move indicating that the chains might be applicable as photonic wires [8, 9]. These studies are carried out within the collaborative research center SFB 652 in close collaboration with Oliver Kühn and his coworkers. In future they will be extended to low temperatures to reduce the influence of thermal excitations and fluctuations. This should provide deeper insight into the interaction between excitons and the role of

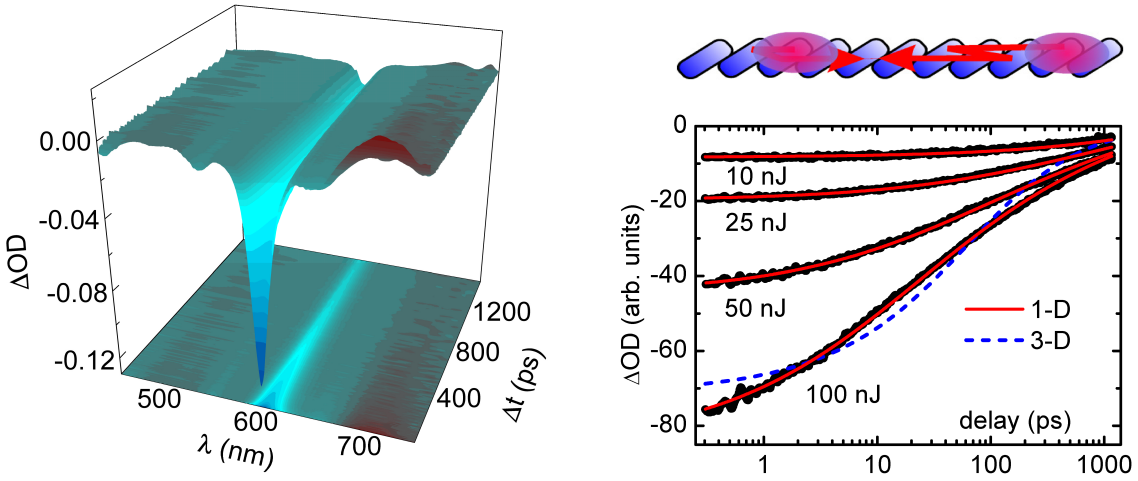

Fig. 2.18: Left: Transient absorption change after optical excitation of J-aggregates. Right: Fits of a rate model to the time-dependent absorption change for various excitation energies. Simulations based on exciton-exciton annihilation and one dimensional diffusion (1-D, red solid lines) match the data very well while assuming three dimensional diffusion (3-D, blue broken line) results in strong deviations.

two-exciton states.

Fundamental Processes in Photocatalysis

Generation of hydrogen by light-induced water splitting using catalytic systems is a promising, sun powered, alternative energy source. The Leibniz Institute for Catalysis is developing such systems and collaborating with our group within the BMBF project Light2Hydrogen (L2H), which had started at the end of 2009, to investigate the fundamental steps of the process. The results help to identify loss mechanisms and to optimize the catalytic system. The considered homogeneous systems are mixtures of solvent, water and an electron donating compound in which a photosensitizer and a catalyst are dissolved with low concentration. After photoexcitation a cascade of electron transfer processes shifts an electron from a donor molecule to a catalyst where it is used to reduce protons resulting finally in molecular hydrogen. Our transient absorption measurements on iridium complexes used as photosensitizers show that after an absorption event an extremely fast intersystem crossing occurs. Subsequent relaxation steps result within some ten picoseconds in population of the lowest triplet configuration which has a lifetime of a few hundred nanoseconds. In the presence of an electron donating compound fluorescence quenching is observed indicating that an electron transfer onto the photosensitizer occurs which is the first step in the catalytic process [10]. However, our studies show that the rate is much lower than the corresponding diffusion limit and a very high concentration of the electron donor is needed for quantitative quenching. On the

other hand the measurements indicate that the electron transfer from the sensitizer to the catalyst is highly efficient. Since the catalytic system contains a high fraction of the donor compound both electron transfer steps show a yield of almost 100 % and are no bottleneck for the process. Currently the studies are extended to other photosensitizers and to inhomogeneous systems.

Time Resolved Raman and CARS Spectroscopy of Complex Molecular Materials

In the last three years we started applying time-resolved Raman techniques to study intermolecular interactions in liquids which exhibit molecular networks. A setup for coherent anti-Stokes Raman scattering (CARS) was developed which makes use of ultrashort broadband Stokes pulses and narrowband picosecond pulses for Raman pumping and probing, see Fig. 2.19. In this way high temporal and spectral resolution is achieved simultaneously [11]. The theoretical description of CARS was adopted to our specific situation and reformulated so it can be fitted to the measured time-dependent spectra. Parameters like vibrational frequencies and dephasing times can be extracted with high accuracy even though interference effects lead in many cases to complex spectral signatures. This has been tested for several solvents with Raman spectra of varying complexity. In the case of congested Raman bands information is now accessible which is hard to reveal by linear Raman spectroscopy.

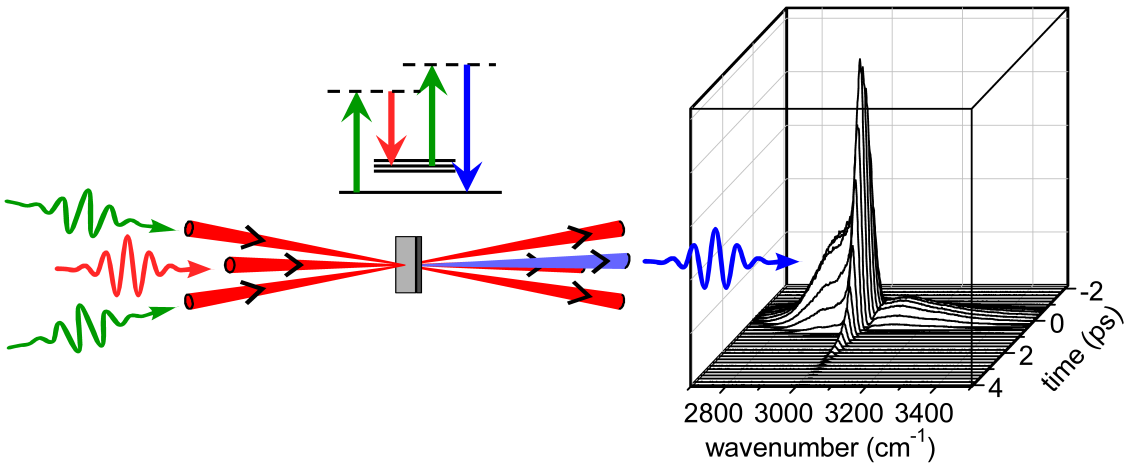

Fig. 2.19: Left: Level diagram and beam configuration of the CARS experiment. A picosecond Raman pump (green) and a femtosecond Stokes pulse (red) prepare vibrational coherences. The interaction with a picosecond Raman probe pulse (green) results in the generation of a coherent anti-Stokes signal (blue). Right: Time and spectrally resolved CARS signal of chloroform showing the interference between the nonresonant background and the signal due to a vibrational mode at 3020 cm^{-1}.

We are also setting up a pump-probe experiment in which ultrashort IR pulses from a parametric amplifier are applied to excite molecular vibrations and picosecond near infrared (NIR) pulses for Raman probing. The IR excitation will be used to disturb molecular networks. The propagation of the induced changes through the network and its subsequent reconstruction will be characterized and analyzed by time-resolved Raman spectroscopy.

The introduced techniques are applied to ionic liquids. Those can be described as molten salts at room temperature and their properties are determined by strong Coulomb forces as well as by hydrogen bonds. The latter ones lead to the formation of a molecular network which is crucial for the behavior of ionic liquids. In a joint project of the SFB 652 we investigate the network together with Ralf Ludwig from the Institute of Chemistry and Oliver Kühn. First results show that all proposed hydrogen bonds exist and that the corresponding vibrational spectra exhibit a Fermi resonance [12]. The studies are now extended to characterize the fluctuations and the dynamics of the network.

Highly Excited Dense Matter and Laser Machining

During the last three years a project was implemented that is dedicated to the interaction of intense laser radiation with condensed matter. This field attracts scientific interest for two reasons. First, femtosecond laser ablation is a promising approach for high precision machining. Second, one can generate in this way warm dense matter which is characterized by high densities in combination with high temperatures and which covers so far scarcely explored regions of the phase diagrams of most materials. To observe the time-dependent material response on the impact of intense laser pulses, we have developed a pump-probe setup utilizing transmission and diffraction of an ultraviolet probe beam. NIR pulses at 800 nm with a duration of 50 fs are manipulated by a 4f-pulse shaper based on a liquid crystal mask to provide excitation pulses with variable temporal shape. A frequency-doubled fraction of the original NIR beam is focused collinearly with the excitation pulses onto a very thin foil serving as sample and the transmitted light is monitored by a CCD camera. In first experiments a circular profile with diffraction signatures is observed which changes with time. In the next step changes of the index of refraction in the interaction region will be extracted. This should provide information about the evolution of the electron density and the dynamics of the strongly excited material. The work is performed in collaboration with the groups of Karl-Heinz Meiwes-Broer and Ronald Redmer within a collaborative BMBF project on warm dense matter.

At the same time the setup is used to test strategies for machining with shaped ultrashort pulses. The goal is to develop techniques for fabricating small implants and structuring their surfaces. This work is part of the BMBF project REMEDIS which is dedicated to the development of new implants and headed by the Institute of Biomedical Technique. Preliminary results indicate that in the case of metals the ablation process is robust with respect to the pulse shape and the precision is

independent on the pulse duration as long as it is not well above ten picoseconds. The studies are now extended to polymers which are suitable for implants.

Dynamics of Prototypical Photoreactions

Beside the main activities descirbed above several smaller projects have been persued, all in collaboration with other groups. The objective is to learn about the mechanisms of the respective photoreactions by measuring and analyzing the associated dynamics.

Together with Eberhard Riedle (Ludwig-Maximilians-Universität München) and his coworkers we investigate excited state intramolecular proton transfer processes. The reaction itself takes only about 50 fs and proceeds as a ballistic wavepacket motion. Pronounced signal oscillations are observed due to ringing of the molecule in vibrational modes which contribute significantly to the reaction path. The analysis of the coherent vibrational excitations allows reconstructing the reaction coordinate and provides direct insight into the mechanism. In the case of excited state proton transfer, coordinates contribute to the reaction path which affect strongly the distance between the hydrogen donor and the acceptor. This indicates that after optical excitation the molecular skeleton contracts till the distance is short enough for the electrons to rearrange and to bind the hydrogen atom to the acceptor. The proton plays a passive role and tunneling is not relevant. To test this notion, experiments on deuterated molecules were performed. And indeed the same transfer time and wavepacket motion were found proving the validity of the model [13].

Together with partners from Munich, Würzburg, and Basel we investigate charge transfer processes in core-substituted naphthalene diimides. For arylamino substituted compounds we demonstrated the ability to control the lifetime of the fully charge separated state via tuning the energy gap to the electronic ground state [14]. In the case of sulfanyl substituents the charge separation is accelerated if it can proceed as a two-step process. In this case an initial planarization leads first to a partial electron transfer. The transfer is then completed by a second step during which the donor moiety is twisted again [15]. If a methylene group acting as spacer is inserted, the two-step process is suppressed and the transfer time increases by one order of magnitude.

In collaboration with Udo Kragl from the Chemistry department of the University of Rostock and his group we are developing an experiment to investigate the activation dynamics of enzymes. To this end a laser pulse induces a jump of the pH-value by exciting a compound which turns into an acid by a photoreaction. The original pH-value of the solution containing the enzyme and a substrate is chosen that prior the laser pulse the enzyme is more or less inactive but becomes active after the pH-jump. The activation of the enzyme after the laser pulse is monitored by measuring the consumption of the substrate and the rise of the product concentration.

Together with Peter Langer from the Chemistry department and his coworkers we investigate the photophysical properties of newly synthesized pentaalkynylpyridines.

For some of them high fluorescence quantum yields were found which makes them interesting for photonic applications [16].

References

[1] O. Kühn and S. Lochbrunner. "Quantum dynamics and spectroscopy of excitons in molecular aggregates". In U. Würfel, M. Thorwart and E. R. Weber, editors, "Quantum efficiency in complex systems, Part II", pages 47–81. Academic Press, San Diego (2011).

[2] H. Marciniak, B. Nickel and S. Lochbrunner. "The Ultrafast Dynamics of Electronic Excitations in Pentacene Thin Films". *Mater. Res. Soc. Symp. Proc.*, **1270** (2010), 1270–II09–53.

[3] H. Marciniak, M. Teicher, U. Scherf, S. Trost, T. Riedl, M. Lehnhardt, T. Rabe, W. Kowalsky and S. Lochbrunner. "Photoexcitation dynamics in polyfluorene-based thin films: Energy transfer and amplified spontaneous emission". *Phys. Rev. B*, **85** (2012), 214204.

[4] F. Fennel and S. Lochbrunner. "Long distance energy transfer in a polymer matrix doped with a perylene dye". *Phys. Chem. Chem. Phys.*, **13** (2011), 3527–3533.

[5] F. Fennel and S. Lochbrunner. "Förster-mediated spectral diffusion in disordered organic materials". *Phys. Rev. B*, **85** (2012), 094203.

[6] D. Ambrosek, H. Marciniak, S. Lochbrunner, J. Tatchen, X.-Q. Li, F. Würthner and O. Kühn. "Photophysical and quantum chemical study on a J-aggregate forming perylene bisimide monomer". *Phys. Chem. Chem. Phys.*, **13** (2011), 17649–17657.

[7] H. Marciniak, X.-Q. Li, F. Würthners and S. Lochbrunner. "One dimensional exciton diffusion in perylene bisimide aggregates". *J. Phys. Chem. A*, **115** (2011), 648–654.

[8] S. Wolter, J. Aizezers, F. Fennel, M. Seidel, F. Würthner, O. Kühn, and S. Lochbrunner. "Size dependent exciton dynamics in one-dimensional perylene bisimide aggregates". *New J. Phys.*, **14** (2012), 105027.

[9] H. Marciniak, X.-Q. Li, F. Würthner and S. Lochbrunner. "One Dimensional Exciton Diffusion in J-Aggregates". In M. Chergui, D. M. Jonas, E. Riedle, R. W. Schoenlein and A. J. Taylor, editors, "Ultrafast Phenomena XVII", pages 439–441. Oxford University Press, New York (2011).

[10] F. Gärtner, S. Denurra, S. Losse, A. Neubauer, A. Boddien, A. Gopinathan, A. Spannenberg, H. Junge, S. Lochbrunner, M. Blug, S. Hoch, J. Busse, S. Gladiali and M. Beller. "Synthesis and Characterization of New Iridium Photosensitizers for Catalytic Hydrogen Generation from Water". *Chem. Eur. J.*, **18** (2012), 3220–3225.

[11] M. Lütgens, S. Chatzipapadopoulos and S. Lochbrunner. "Coherent anti-Stokes Raman scattering with broadband excitation and narrowband probe". *Opt. Express*, **20** (2012), 6478–6487.

[12] C. Roth, S. Chatzipapadopoulos, D. Kerlé, F. Friedriszik, M. Lütgens, S. Lochbrunner, O. Kühn, and R. Ludwig. "Hydrogen Bonding in Ionic Liquids Probed by Linear and Nonlinear Vibrational Spectroscopy". *New J. Phys.*, **14** (2012), 105026.

[13] C. Schriever, S. Lochbrunner, A. R. Ofial and E. Riedle. "The origin of ultrafast proton transfer: Multidimensional wave packet motion vs. tunneling". *Chem. Phys. Lett.*, **503** (2011), 61–65.

[14] I. Pugliesi, U. Megerle, S.-L. Suraru, F. Würthner, E. Riedle and S. Lochbrunner. "Influence of core-substitution on the ultrafast charge separation and recombination in arylamino-core-substituted naphthalene diimides". *Chem. Phys. Lett.*, **504** (2011), 24–28.

[15] I. Pugliesi, P. Krok, S. Lochbrunner, A. Błaszczyk, C. von Hänisch, M. Mayor and E. Riedle. "Variation of the ultrafast fluorescence quenching in 2,6-sulfanyl-core-substituted naphthalenediimides by electron transfer". *J. Phys. Chem. A*, **114** (2010), 12555–12560.

[16] P. Ehlers, A. Neubauer, S. Lochbrunner, A. Villinger and P. Langer. "Multiple Sonogashira reactions of polychlorinated molecules. Synthesis and photophysical properties of the first pentaalkynylpyridines". *Org. Lett.*, **13** (2011), 1618–1621.

2.1.8 Theoretical Cluster Physics

Head: Jun.-Prof. Dr. Thomas Fennel

Staff:	Dr. Jörg Köhn	Dipl.-Phys. Mathias Arbeiter
	Dipl.-Phys. Christian Peltz	Peggy Preuss
	MSc Lennart Seiffert	Merten Siegfried
	Katharina Sander	
MSc Graduates:	Alexander Breier	Lennart Seiffert
BSc Graduates:	Alexander Breier	Katharina Sander
	Semjon Köhnke	

General Outline of the Field of Research

From a fundamental viewpoint, clusters and nanoparticles embody the bridge between the atomic (or molecular) state of matter and the bulk, allowing for the bottom-up investigation of fundamental questions such as the atom-by-atom evolution of stability, structure, and chemical as well as optical properties of nanosized matter as function of size. With the advent of ultrafast and intense lasers, clusters have been found to be also a unique nanoscale laboratory for nonlinear effects and collective dynamics in many-particle systems under strong radiation fields. Our research focuses on the development and application of state-of-the-art many-particle simulation techniques to describe such ultrafast and nonlinear dynamics of clusters and nanoparticles subject to intense laser fields [1–5]. Key topics of interest are the control of the interaction process via structured or shaped laser pulses as well as the analysis of the leading response processes as function of laser frequency, e.g., from the infrared (IR) to the ultraviolet (XUV) spectral range [6–11]. Furthermore, we investigate the strong-field response of mixed nanosystems such as core-shell clusters [12–14] and analyze attosecond dynamics under phase-controlled few-cycle laser fields [15–17].

Substantial parts of the research results reported below have been conducted within the Sonderforschungsbereich SFB 652 ("strong correlations and collective effects in radiation fields: Coulomb systems, clusters and particles ") and within the DFG priority programme SPP1391 ("ultrafast nanooptics").

Clusters in Intense Short-Wavelength Pulses

One of the central topics of our work is the microscopic simulation of cluster dynamics in intense free-electron laser (FEL) radiation to study multi-photon effects and ultrafast transient response processes in finite plasmas under VUV and XUV excitations. In contrast to the multi-photon ionization in infrared fields, the high photon energy at FEL's enables direct single-photon ionization of the cluster constituent atoms. Furthermore, collisional heating, which is dominant for optical excitation, may become negligible because of the small ponderomotive energy of the light field.

For XUV excitation of rare gas clusters, sequential photoionisation ("multistep ionisation") typically leads to highly non-thermal, plateau-like electron energy spectra that can be explained by the stepwise build-up of the cluster space charge potential. With increasing laser intensity, the resulting trapping effect eventually leads to the frustration of direct photoemission and the generation of a nanoplasma. Roughly speaking, the latter process starts when the cluster potential depth exceeds the excess energy of the inner atomic photoionization such that inner photoelectrons are trapped. Experiments on Argon clusters have found indications for this transition, i.e. an additional, exponentially decaying contribution to the electron spectra which cannot be explained with direct emission.

To study the microscopic implications of frustration effects and the resulting nanoplasma dynamics under XUV excitation we employ molecular dynamics methods as well as simplified Monte-Carlo simulations (MC: frozen ionic system, only photoionization), see Fig. 2.20. Whereas both approaches yield identical results in the absence of frustration (low intensity limit), molecular dynamics (MD) shows clear signatures for (i) the quenching of direct emission, (ii) the generation of a dense, transient nanoplasma, and (iii) an additional thermal electron emission component for higher intensity, in agreement with experiments.

Figure 2.20 shows the theory results for two characteristic cases. Comparison of MC and MD results for the higher intensity shows clear deviations when the outer ionization approaches the frustration limit (q_{full}). The MD analysis (Fig. 2.20a, I=$2 \times 10^{13}\,W/cm^2$) exhibits a transient saturation of outer ionization before the frustration limit predicted in electrostatic approximation is reached (cf. MD and MC near t=0). This signature can be explained by the radial dependence of frustration (shell effect), which quenches the direct emission for core atoms first and only later also for surface atoms. Hence, already at the stage of partial frustration, electrons are trapped and affect subsequent ionization steps by their "thermal space-charge". This effectively reduces the outer ionization threshold for full frustration.

After the transient saturation, the MD results show a second phase of electron emission (Fig. 2.20a for t>0). Because of the negative "energy at birth" of electrons being photoionised in this phase, the contribution of this second emission phase can be unambiguously attributed to thermal emission. Interestingly, the thermal evaporation ceases rapidly (here after about 200 fs). This effect cannot be explained by mere evaporative cooling of the nanoplasma. Comparison of runs with frozen and free ionic motion in Fig. 2.20a (inset) shows that expansion cooling is the dominant mechanism that indirectly determines the timescale of thermal evaporation [6].

The characteristic structure of the contributions from direct and thermal emission to the electron spectra allows one to extract important information about the charge distribution in the cluster. In particular, plateau-like contributions indicate nearly homogenous cluster charging by mostly outer ionization whereas thermal spectra mark the presence of a hot and dense nanoplasma. These two scenarios are furthermore connected with characteristic types of ionic expansion, where homogenous charging (no quasifree electrons) correspond to ideal Coulomb explosion and the

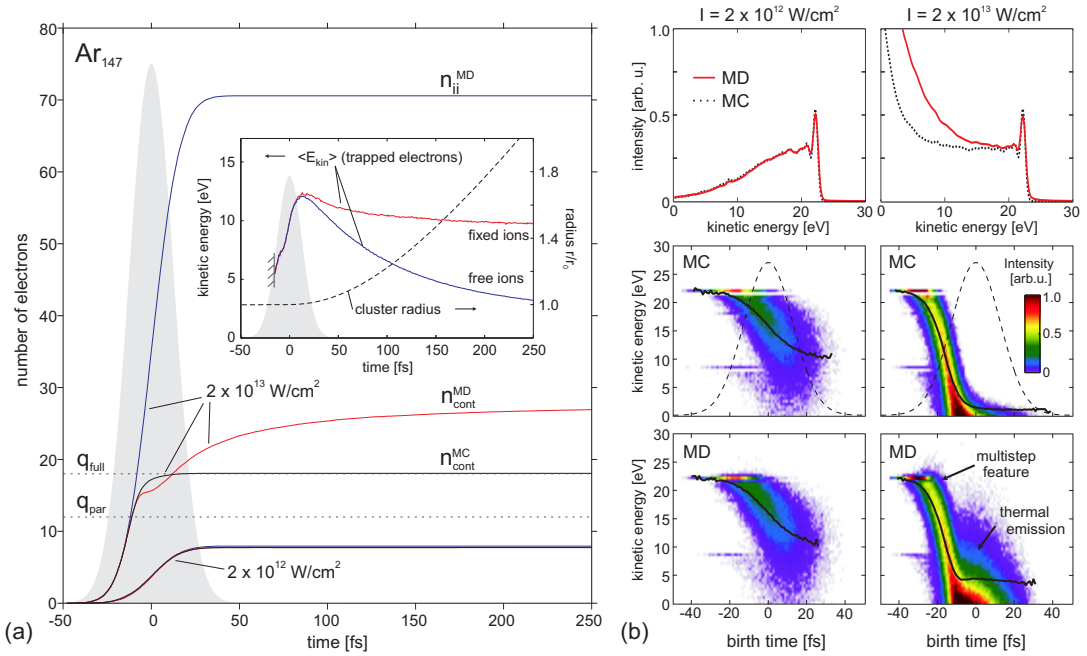

Fig. 2.20: MD and Monte-Carlo simulations (MC) of Ar_{147} under 30 fs FEL pulses at 32 nm wavelength for two selected intensities. (a) Time-evolution of inner (n_{ii}) and outer ionisation (n_{cont}), intensity envelope of the laser (gray); critical cluster charge for partial and full frustration of direct photoemission (q_{par},q_{full}); Cooling dynamics of quasifree electrons in MD for frozen vs. active ionic motion with the corresponding relative cluster expansion (inset). (b) model specific electron energy spectra and respective "energy vs. birth time" analysis. Adapted from [6].

thermal electron pressure of a hot nanoplasma drives a hydrodynamic expansion. In a comparison of excitation scenarios with VUV, XUV, and soft x-ray excitation (constant excitation energy) we could show, that the electron spectra are even more suited for characterizing the dominant expansion process than the energy spectra of the ions themselves [8].

Phase-Dependent Electron Acceleration

The second research direction we are pursuing is the study of attosecond dynamical processes that enable the control of laser-matter interaction on a sub-cycle timescale. Recently, the electron emission from large dielectric nanoparticles under phase-controlled few-cycle pulses has been investigated experimentally in collaboration with Matthias Kling (MPQ Garching) and Eckart Rühl (FU Berlin). For modeling the observed unexpectedly strong acceleration and pronounced directional control of the electron emission we developed a hybrid meanfield Monte-Carlo code that connects continuum theory for the collective response of bound electrons with microscopic kinetic methods for the description of nonlinear ionization and free car-

rier dynamics. Our theory is key to identifying the underlying near-field enhanced recollision process and has been essential for interpreting this first proof of electron acceleration via elastic backscattering at solid dielectric (nano)surfaces, see Fig. 2.21. These combined experimental and theory results [17] are relevant for sev-

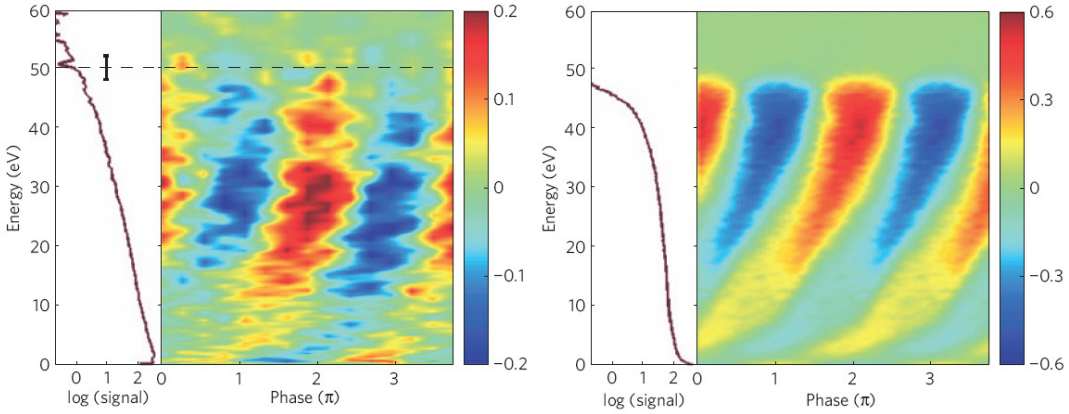

Fig. 2.21: Measured (left) and calculated (right) carrier-envelope-phase-dependent up-down asymmetry of the electron emission from $d = 100\,\mathrm{nm}$ SiO_2 nanospheres under 5 fs few-cycle pulses at 720nm wavelength and intensity $2\times10^{13}\,\mathrm{W/cm^2}$. Adapted from [16].

eral applications in light-wave attosecond control in nanoplasmonics and ultrafast nanooptics. Currently, we are developing an extended code that uses the full Mie solution to investigate the impact of propagation effects, such as nanofocusing and phase retardation of the laser field on the resulting electron and short-wavelength emission [17].

Laser-Cluster Dynamics Including Field Propagation

A solid theoretical understanding of the interplay of microscopic and collective plasma processes, including collisions and wave propagation phenomena, is important for a broad spectrum of applications ranging from short-wavelength radiation sources to the development of devices based on ultrafast strong-field nanoplasmonics. The underlying nonlinear processes take place close to or beyond the ionization threshold, where the laser-plasma dynamics is highly coupled, proceeds far from equilibrium and is strongly influenced by the plasma microfield. The full account of the many-particle plasma dynamics including surface effects requires an atomic scale resolution. However, a theoretical analysis resolving microscopic and macroscopic laser-plasma processes simultaneously remains a great challenge. Clusters range from the size of molecules to small droplets of condensed matter. This scalability makes them a valuable testing ground for exploring physical processes occurring

due to the interplay between microscopic and macroscopic processes in laser-driven matter, which is at the heart of nanoplasma science and ultrafast nanoplasmonics.

The main obstacle in modeling the dynamics of laser-driven plasmas is the enormous gap between the physical scales relevant for microscopic and macroscopic phenomena. Microscopic processes, such as the atomic scale microfield dynamics and collisions, require Ångström resolution, while the macroscopic scale of collective and wave propagation phenomena is of the order of the laser wavelength. The most common numerical tools are electrostatic molecular dynamics (MD) and the electromagnetic particle-in-cell (PIC) method. In the electrostatic limit, i.e. neglecting electromagnetic field retardation and treating the electromagnetic wave evolution explicitly, classical plasma dynamics is described exactly by MD. MD works extremely well for small nanoplasmas in few-nanometer clusters, where the dipole approximation and the neglect of field propagation are justified. Wave propagation phenomena, however, require the solution of Maxwell's equations and are commonly studied by electromagnetic PIC codes. Typically, Maxwell's equations are solved on a grid along with the relativistic equations of motion for all PIC particles. Usually, PIC particles represent an average over many microscopic particles (macroparticles). Due to averaging, all fine-grained atomic processes are lost, which is the Maxwell-Vlasov limit of light-plasma interaction. Hence, only the collective response is propagated explicitly, while higher orders of the Bogoliubov-Born-Green-Kirkwood-Yvon (BBGKY) hierarchy are dropped.

Recently, we introduced the microscopic particle-in-cell (MicPIC) method to overcome the above limitations by connecting MD and PIC in a two-level approach [4]. In MicPIC, only long-range electromagnetic interactions are treated on a coarse-grained PIC level. When two particles come close, the PIC field is replaced by the electrostatic one to fully resolve the microscopic interactions. The MicPIC dynamics can be solved efficiently (with order N) by using the particle-particle particle-mesh (P3M) concept introduced originally for electrostatic simulations by Eastwood and Hockney. By enabling a fully microscopic electromagnetic description, MicPIC is expected to open up new frontiers in the classical microscopic analysis of macroscopic laser-matter processes.

As a first application of this new approach, we study resonant Mie plasmon excitation of metal-like cluster nanoplasmas. A comparison with MD and Mie theory validates MicPIC and shows that propagation effects notably modify the absorption for cluster radii R>20 nm: i.e., an electrostatic treatment is no longer justified. The simultaneous resolution of collisions and wave propagation has made it possible, to describe the size-dependent plasmon lifetime including the experimentally known fact of a maximum for few ten nanometer particles [5]. The quenching of the lifetime for smaller/larger systems could be shown to stem from the competition of surface collisions of conduction electrons and radiation damping. A simultaneous account of these processes demonstrates the inclusion of microscopic collisions and macroscopic wave propagation in MicPIC.

For nonlinear excitations we find the excitation of plasma waves in surprisingly

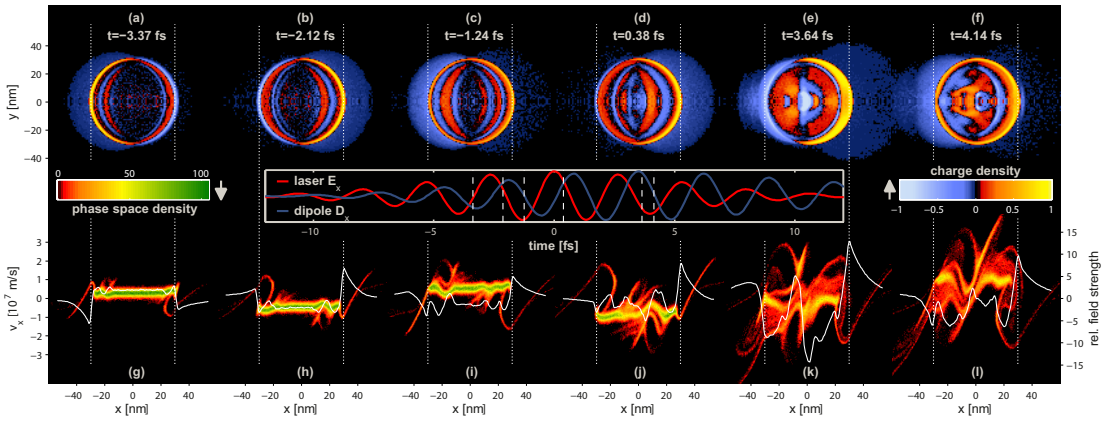

Fig. 2.22: Time evolution of a R=30nm cluster excited at resonance (800 nm) by a 7 fs laser pulse with peak intensity 6×10^{13}W/cm^2. The top panel shows the charge density (normalized to the ion density) in the x-y plane at different times indicated below the tags (a-f) and as vertical lines in the plot of the laser field and dipole moment (see inset). The lower panels (g-l) show the corresponding electron density in the phase-space f(x; v_x) evaluated on the x-axis. The x-component of the electric field (normalized to the peak laser field) is shown as a white curve on top of the phase-space graphs. Adapted from [5].

small clusters. The plasma waves are created by electrons recolliding with the cluster surface and propagate into the cluster. The spherical cluster geometry focuses the waves toward the cluster center, where they collide and break, see Fig 2.22. This results in the enhanced generation of fast electrons near the cluster center and in strong attosecond electric field fluctuations [5]. The generation and breaking of plasma waves in nanoparticles is an interesting physical process that may be probed by single-shot diffractive imaging with sub-femtosecond pulses from x-ray free electron lasers.

References

[1] Fennel Th., Meiwes-Broer K.-H., Tiggesbäumker J., Reinhard P.-G., Dinh P.M., Suraud E. “Laser-driven nonlinear cluster dynamics”. *Rev. Mod. Phys.*, **82** (2010), 1793.

[2] Tiggesbäumker J., Fennel Th., Truong N.X., Meiwes-Broer K.-H. “Resolving the Ion and Electron Dynamics in Finite Systems Exposed to Intense Optical Laser Fields”. In Redmer R., Holst B., Hensel F., editor, “Metal-To-Nonmetal Transitions”, chapter 5. Springer, Berlin (2010).

[3] Meiwes-Broer K.-H., Tiggesbäumker J., Fennel Th. "Intense Laser-Cluster Interactions". In K. Sattler, editor, "Handbook of Nanophysics: Clusters and Fullerenes", chapter 13. CRC Press, Taylor and Francis (2010).

[4] Varin C., Peltz C., Brabec T., Fennel. Th. "Attosecond plasma wave dynamics in laser-driven cluster nanoplasmas". *Phys. Rev. Lett.*, **108** (2012), 175007.

[5] Peltz C., Varin C., Brabec T., Fennel Th. "Fully microscopic analysis of laser-driven finite plasmas using the example of clusters". *New J. Phys.*, **14** (2012), 065011.

[6] Arbeiter M., Fennel Th. "Ionization heating in rare-gas clusters under intense XUV laser pulses". *Phys. Rev. A*, **82** (2010), 013201.

[7] Truong N.X., Hilse P., Göde S., Przystawik A., Döppner T., Fennel Th., Bornath Th., Tiggesbäumker J., Schlanges M., Gerber G., Meiwes-Broer K.-H. "Optimal control of the strong-field ionization of silver clusters in helium droplets". *Phys. Rev. A*, **81** (2010), 013201.

[8] Arbeiter M., Fennel Th. "Rare-gas clusters in intense VUV, XUV and soft x-ray pulses: Signatures of the transition from nanoplasma-driven cluster expansion to Coulomb explosion in ion and electron spectra". *New J. Phys.*, **13** (2011), 053022.

[9] Radcliffe P., Arbeiter M., Li W.B., Düsterer S., Redlin H., Hayden P., Hough P., Richardson V., Costello J.T., Fennel Th., Meyer M. "Atomic photoionization in combined intense XUV free-electron and infrared laser fields". *New J. Phys.*, **14** (2012), 043008.

[10] Köhn J., Redmer R., Fennel Th. "Collision-enhanced plasmonic electron acceleration in small metal clusters". *New J. Phys.*, **14** (2012), 055011.

[11] Passig J. and Irsig R., Truong N.X., Fennel Th., Tiggesbäumker J., Meiwes-Broer K.-H. "Nanoplasmonic electron acceleration in silver clusters studied by angular-resolved electron spectroscopy". *New J. Phys.*, **14** (2012), 085020.

[12] Döppner T., Müller J.P., Przystawik A., Göde S., Tiggesbäumker J., Meiwes-Broer K.-H., Varin C., Ramunno L., Brabec T., Fennel Th. "Steplike intensity threshold behavior of extreme ionization in laser-driven Xe clusters". *Phys. Rev. Lett.*, **105** (2010), 053401.

[13] Peltz C., Fennel Th. "Resonant charging of Xe clusters in Helium nanodroplets under intense laser fields". *Eur. Phys. J. D*, **63** (2011), 281.

[14] Krishnan S.R., Peltz C., Fechner, L., Sharma V., Kremer M., Fischer B., Camus N., Pfeiffer T., Jha J., Krishnamurthy M., Schröter C.D., Ullrich J., Stienkemeier F., Moshammer R., Fennel Th., Mudrich M. "Evolution of dopant-induced helium nanoplasmas". *New J. Phys.*, **14** (2012), 075016.

[15] Köhn J., Fennel Th. "Time-resolved analysis of strong-field induced plasmon oscillations in metal clusters by spectral interferometry with few-cycle laser fields". *Phys. Chem. Chem. Phys.*, **13** (2011), 8747–8754.

[16] Zherebtsov S., Fennel Th., Plenge J., Antonsson E., Znakovskaya I., Wirth A., Herrwerth O., Süßmann F., Peltz C., Ahmad I., Trushin S.A., Pervak V., Karsch S., Vrakking M.J.J., Langer B., Graf C., Stockman M.I., Krausz F., Rühl E., Kling M. "Controlled near-field enhanced electron acceleration from dielectric nanospheres with intense few-cycle laser fields". *Nat. Phys.*, **7** (2011), 656.

[17] Zherebtsov S., Süßmann F., Peltz C., Plenge J., Betsch K.J., Znakovskaya I., Alnaser A.S., Johnson N.G., Kübel M., Horn A., Mondes V., Graf C., Trushin S.A., Azzeer A., Vrakking M.J.J., Paulus G.G., Krausz F., Rühl E., Fennel Th., Kling M. "Carrier-envelope phase tagged imaging of the controlled electron acceleration from SiO2 nanospheres in intense few-cycle laser fields". *New J. Phys.*, **14** (2012), 075010.

2.2 Physics of Nanomaterials

2.2.1 Physics of New Materials

Head: Prof. Dr. Eberhard Burkel

Staff:	Dr. Faming Zhang	Dr. Wiktor Bodnar
	Dipl.-Phys. Kerstin Witte	MSc. Dieter Skroblin
	MSc. Rico Schnierer	MSc. Qingqing Xu
	MSc. Wenwei Gu	MSc. Yujie Quan
	MSc. Lijun Jing	BSc. Lars Assmus
	BSc. Martin Hantusch	BSc. Frank Eisenhut
	Stephan Flor	Bärbel Przybill
	Ulrike Schöder	
MSc Graduates:	Rico Schnierer	Dieter Skroblin
Dipl.-Phys. Graduates:	Jörg Krause	Lennart Forck
	Kerstin Witte	Peter Sänger
	Josefin Schlichting	Finn Fock
BSc Graduates:	Dieter Skroblin	Rico Schnierer
	Lars Assmus	Thomas Orlowski
	Martin Hantusch	Christopher Jacob
	Frank Eisenhut	Susanne Kuhrau
	Wolf Zabka	

General Outline of the Field of Research

The main interests of the group "Physics of New Materials" are in the synthesis and the study of the static and dynamic structure as well as properties of novel advanced functional materials. Most of the investigations are performed using different scattering techniques with X-rays, synchrotron radiation or neutrons. The methods used for obtaining such novel materials are eclectic: from a simple sol-gel method, over mechanical alloying to non-equilibrium hybrid synthesis methods like field-assisted sintering (FAST) or microwave sintering. The main research areas of the past few years will be introduced shortly in the next four paragraphs.

I. Novel Material Systems for Environmental Protection

The concern about environmental protection has increased over the years from a global view point. Today, rapidly changing technologies, industrial products and practices generate waste that could threaten public health and the environment, therefore the investigation of new materials, e.g. for CO_2 capture or waste water detoxification are of great interest.

New Materials for CO_2 capturing. Increase in the atmospheric concentrations of gases such as methane (CH_4), nitrous oxide (N_2O) and, especially, carbon dioxide (CO_2) has enhanced the heat trapping capability of the Earth's atmosphere

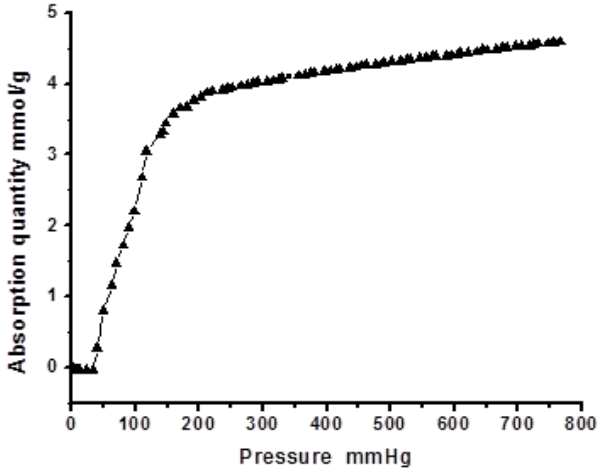

Fig. 2.23: The chemisorption behavior of $Ca_3Ti_2O_7$ annealed at 1000°C for 2 h with pure CO_2.

via the greenhouse effect. CO_2 capture technology is growing fast because of the global climate warming. There are two main branches for CO_2 capture and storage, namely chemisorption and physisorption, both having their advantages and disadvantages. The physisorption already occurs at relatively low temperatures and can release CO_2 with temperature and pressure changing. Chemisorption is more stable, because the CO_2 is chemically bound to the material at higher operation temperature and pressure. Important factors for the adsorption behavior of possible material systems besides the adsorption itself are the surface area, the micropore volume, as well as the size. Nanoparticles or porous materials offer these characteristics. Chemical methods, traditional annealing of nanoparticles or novel technologies like field-assisted sintering are used to produce systems, e.g. of calcium titanate ($Ca_3Ti_2O_7$) or lithium orthosilicate (Li_4SiO_4) for possible CO_2 capture applicants.

New Material Systems for Waste Water Detoxification. Despite the reduction of the number of people without access to clean potable water, the chemical recovery of polluted water is still of major interest. Thus, this research focuses on photocatlytic properties of suitable materials, e.g. titanium dioxide TiO_2 for waste water detoxification by sun light [1].

TiO_2, appearing in different phases like anatase and rutile, with its wide range of applications is also a promising photocatalyst. Pure anatase and rutile powders as well as the reference material *P*25 degussa which is a mixture of these two phases, have been used for the investigations. One main factor influencing the photocatalytic behavior is the physisorption of organic pollutants which are studied through the adsorption behavior of the polar molecule CO_2. Huge differences in the adsorption

behavior of anatase, rutile and $P25$ were noticed. An additional photodiode in the energy range of the band gaps of anatase and rutile showed a drastic change of the CO_2 adsorption by these materials.

II. Novel Material Systems for Bone Implants

Possible bone implant materials can be divided into three classes i.e. metals, ceramics and polymers. Each class has of course advantages for the usage in particular parts of the bone. Investigations on metals and ceramics, as well as on combinations of these materials for bone implants are intensively performed and shall be illustrated with a few examples. Biomaterials need a co-work of many adjacent sciences like biology, chemistry, engineering, medicine or physics since the knowledge of each offers different points of view for the understanding of a subject. This research is supported by DFG GRK 1505/1 (Welisa).

Titanium based implant materials. Porous titanium and its alloys are widely used in the biomedical field due to their outstanding mechanical properties, low density, chemical resistance and biocompatibility [2–7]. Unfortunately, the fabrication of porous Ti and its alloys with standard techniques is difficult due to the high melting point and the extreme chemical affinity to atmospheric gases. Still porous structures are expected to provide good interaction with bones. New hybrid techniques like the field-assisted sintering technology open the possibilities to fabricate Ti_6Al_4V foams using a blend of Ti_6Al_4V and sodium chloride powders.

First results showed that the foam walls cannot be densified within a single FAST process. Therefore, a pressureless post-heat treatment was developed to reduce the microporosity in the foam walls and to densify them. The Young's moduli of the foams with different porosities are in the range of (9.5 ± 1.0) GPa to (33.0 ± 3.2) GPa and the yield strengthes range from (43.0 ± 2.8) MPa to (110.2 ± 8.0) MPa. The results prove the validity of the Gibson-Ashby model.

Calcium Titanate based Implant Material. Ceramics as $CaSiO_3$ or $CaTiO_3$ are the main candidates for novel bone implant materials. Especially, $CaTiO_3$ offers better mechanical properties and higher osteoblast adhesion rates than commonly used hydroxylapatite. Calcium titanate produced by the sol-gel method and sintered by FAST or conventional methods is proven to have comparable impedance to bone tissue. Another important property of this material is the piezoelectrical behavior which is also observed for the bone tissue. The origin of such behaviour is still a topic of debate. The piezoelectrical and the impedance characteristics of $CaTiO_3$ are expected to improve the acceptance of the implant by the surrounding tissue and support its possible usage as a bone implant material. By changing the porosity and also by doping $CaTiO_3$ with, e.g. Fe, Mg or Ba these properties can be influenced and optimized for the application as a possible bone implant material [8].

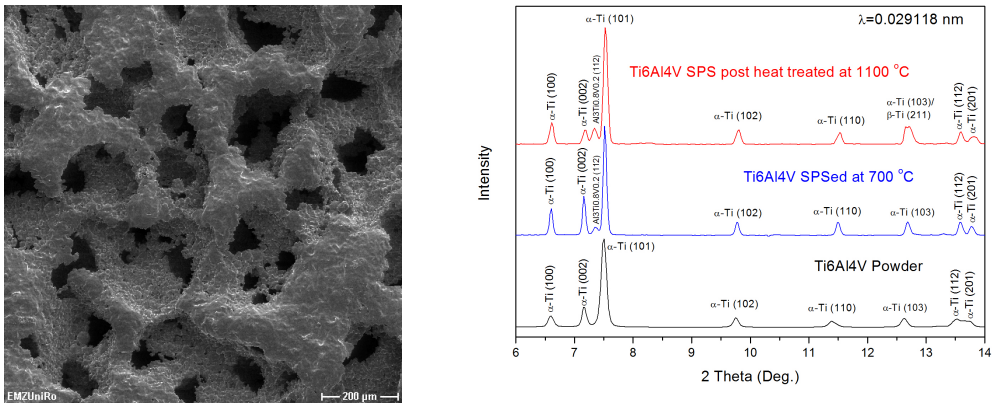

Fig. 2.24: SEM image of the Ti_6Al_4V foams prepared by FAST with 70.0 % porosity (left), and synchrotron radiation high energy X-ray diffraction patterns of the Ti_6Al_4V powder and field-assisted sintered Ti_6Al_4V foams (right).

Gradient Materials - Metall-Ceramic Interfaces. New sintering techniques like microwave sintering [2, 9, 10] or FAST also offer the possibility of consolidating metals with ceramics and combining the advantages of both materials. A crucial point in this research is the interface of the gradient material. The lattice parameters of both sides change and material from one side diffuses into the other part. Still, this simple two-layer gradient is not always stable due to different lattice parameters or thermal expansions coefficients.

Gradient samples such as Ti-$CaTiO_3$, Ti-HA, Ti-TCP and Ti-$CaSiO_3$ are investigated. Because of the comparable to Ti thermal expansion coefficient, $CaTi_3$ is the most promising candidate for further applications. Hardness and Young's modulus do not drop abruptly at the interface. Still, some decomposition of $CaTiO_3$ takes place in the sintering procedure.

III. Zero-, Two- and Three-Dimensional Magnetic Materials

Various scientifically interesting and technologically important magnetic properties resulting from nanoscale confinements have been reported [11–13]. Examples are superparamagnetism, incresed energy products in small-scale nanocomposites and exchange bias in thin films. The majority of the investigated materials have been powders and thin films. Also here, FAST offers new possibilities through three-dimensional nanostructured magnetic composites. In the last few years attempts were made to understand the magnetic behavior and relaxation phenomena in these materials.

Zero-dimensional Magnetic Materials. Magnetic nanoparticles consisting of magnetite offer great opportunities in biomedicine because of their sophisticated coatings

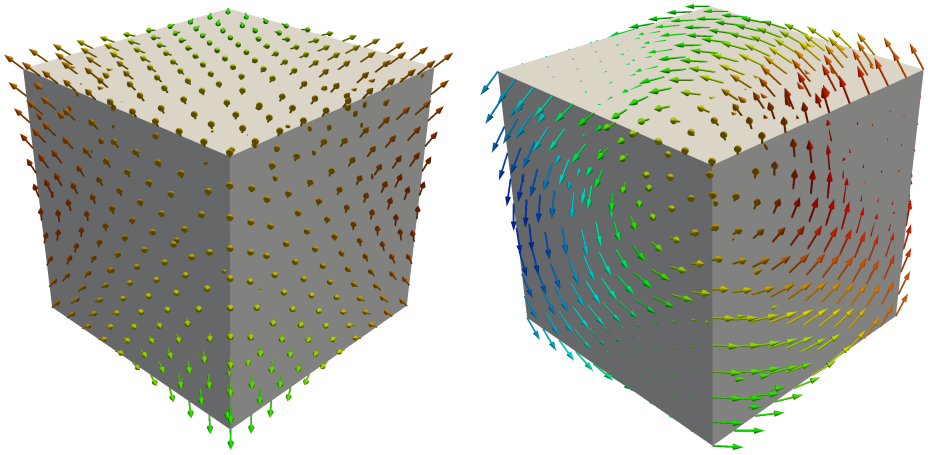

Fig. 2.25: Cubic magnetite model with flowerstate (left) and vortexstate (right).

which lead to nontoxicity. They can be used for magnetic separation, for therapeutic drug, gene or radionuclide delivery, for cancer hyperthermia treatment or, especially, magnetic resonance imaging contrast enhancement.

The particles have been prepared by the co-precipitation method in combination with FAST. In the co-precipitation method the application of different ratios of $FeCl_2$ and $FeCl_3$ together with sodium hydroxide as precursors results in iron oxides nanoparticles with sizes from 4 nm to 20 nm. The size of the crystallites after sintering rises to about 150 nm, therefore a multidomain state of the particles appears. In addition, micromagnetic simulations using finite element method have been performed on single spheres and cubes to get a deeper understanding of the behavior of nanostructured materials, see Fig. 2.25. Frequency dependent simulations offer the unique possibility to analyze the particles in high frequency fields and determine their resonance behavior [14].

Two-dimensional Magnetic Materials. The magnetization of permanent magnetic materials tends to orientate in special crystallographic directions. These preferred directions refer to the magnetic anisotropy. Considering thin films, a large form anisotropy in plane of the thin film appears, which forces the magnetization into this plane. The orientation of the magnetisation in plane leads to large domains. An attempt to overcome this large form anisotropy to obtain a magnetisation out of plane with smaller domains are coupling effects between different layers. These anisotropy phenomena are studied in a cobalt-palladium multilayer system.

The samples are prepared by physical vapor deposition in a 20-layer system, where each layer consists of one cobalt monolayer and four palladium monolayers on a substrate. The structure of the substrate is of great importance in such thin layer systems, which is proven by the use of a glass subtrate and a glass substrate sputtered with carbon. The carbon underlayer leads to a higher roughness of the surface which

increases the crystalline anisotropy of the cobalt structures. It is proven that the hysteresis changes and the domain sizes in these systems are smaller which refers to a perpendicular arrangement of the magnetic moments in the systems.

Three-dimensional Magnetic Materials. The vast majority of the investigated magnetic materials are nanoparticles and thin films. Three-dimensional nanostructured materials also offer interesting phenomena. Novel sintering technologies like FAST offer the possibility to consolidate such materials. The ideal material systems are iron oxides because of their metastable nature and the huge single domain of magnetite [15].

Iron oxides, like magnetite, hematite or a mixture of hematite and iron in the nanometer regime are the precursor materials for FAST processes. The densified samples show much higher coercivity, as well as, higher hyperfine fields which can result from two differnet origins that need further investigations, the ferrimagnetic - antiferromagnetic interactions and the grain size of the composite. As an example Fig. 2.26 shows the composition of a sample sintered in FAST and the transmission Mössbauer spectra of the same sample with the contributing subspectra.

IV. Synthesis Optimization

The development of new technologies always demands the need for the optimization of synthesis methods for various materials, which are presented with two examples.

Field-Assisted Sintering Technology for the Synthesis of Diamonds. This research is supported by DFG BU 547/10-1 and BU 547/10-2, as well as Venture Cup MV UR11007VC-2011. Diamond is a material with superlative physical qualities. In this research, the diamond synthesis by FAST has been first studied through the selection of the appropriate carbon modifications, the incorporation of suitable catalysts and the optimization of the technological processes. The thermal stabilities of carbon nanotubes, fullerene as C_{60} and graphite are investigated under FAST conditions compared to conventional methods [16–21].

It is shown that nanotubes and fullerene partly transformed into diamond (particle sizes from 10 μm to 40 μm) in FAST, see Fig. 2.27 left. However, there is no diamond conversion in the *in-situ* X-ray experiments, Fig. 2.27 right. At the minimum FAST pressure (9.55 MPa), high quality diamond crystals are obtained only in the argon atmosphere. Their phase transitional mechanism leads to the assumption that a plasma existed during the FAST processing.

Optimization of Tungsten Carbide Synthesis by Field-Assisted Sintering. This research is supported by the BMBF Wachstumkerns Centrifluidic Technologies in the frame of the Project 8.3. Cemented carbides are a wide group of dense sintered materials consisting of mainly transition metal carbides with a metal sintering aid.

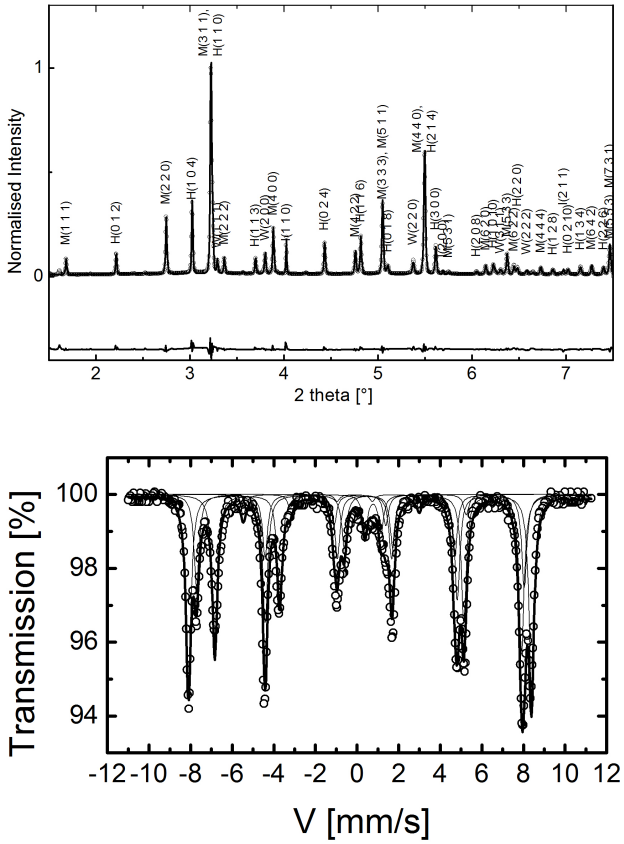

Fig. 2.26: Top: High energy diffractogramm ($\lambda = 0.1424\mathring{A}$) of a sintered sample from hematite and iron. Fitted differential pattern is added below. The labels indicate the Miller indices of the constituent phases (M - magnetite, H - hematite, W - wustite, I - iron). Bottom: Mössbauer spectra of the same sample with the contributing subspectra.

They are characterized by high hardness and wear resistance resulting from the high carbide content. The sintering of tungsten carbide (WC) without metal sintering aids is very difficult due to the low atomic self-diffusion coefficients. In order to achieve acceptable densification of the sintered powder, high temperature and long heating time are required. These on the other hand lead to abnormal grain growth and result in undesirable microstructures consisting of large grains. Other transition metals (e.g. Fe, Co, Ni) are often used in combination with WC in order to improve sintering conditions and to alter the overall physical and mechanical properties such as hardness and Young's modulus.

It is shown that WC doped with cobalt can be densified at 1200°C and 1300°C to nearly 100 % while maintaining nanostructured grain, which increases hardness and Young's modulus. For higher sintering temperatures abnormal grain growth occurs

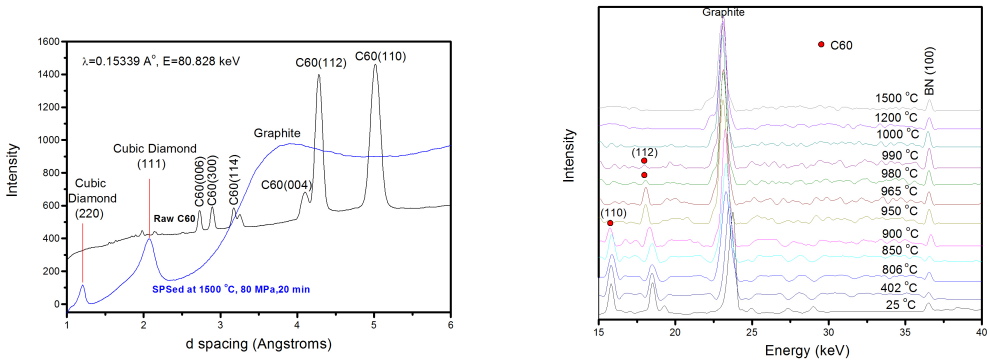

Fig. 2.27: Left: High energy X-ray diffraction patterns of the pure C_{60} and the field-assisted sintered C_{60} at 1500°C, 80 MPa showing the diamond phase. Right: The F2.1 Max 80 *in-situ* X-ray diffraction patterns of the pure C_{60} at 80 MPa under different temperatures without diamond phase formation.

which has a negative influence on the mechanical properties of WC.

References

[1] V. Bessergenev, M. Mateus, D. Vasconcelos, J. Mariano, A. B. D. Rego, R. Lange and E. Burkel. "TiO_2:(Fe,S) thin films prepared from complex precursors by CVD, physical chemical properties, and photocatalysis". *Int. J. Photoenergy*, **2012** (2012), 767054.

[2] T. Galek, K. Porath, E. Burkel and U. van Rienen. "Extraction of effective permittivity and permeability of metallic powders in the microwave range". *Model. Simul. Mater. Sci.*, **18** (2010), 025015.

[3] A. Ibrahim, F. Zhang, E. Otterstein and E. Burkel. "Processing of porous Ti and Ti_5Mn foams by spark plasma sintering". *Mater. Design*, **32** (2011), 146–153.

[4] F. Zhang and E. Burkel. *Novel titanium manganese alloys and their macroporous foams for biomedical applications prepared by field assisted sintering, in Biomedical Engineering, Trends, Researches and Technologies.* InTech. (2011).

[5] F. Zhang, A. W. B. Nebe, U. Beck and E. Burkel. "Preparation, microstructures, mechanical properties, and cytocompatibility of TiMn alloys for biomedical applications". *J. Biomed. Mater. Res. A*, **94** (2010), 406–413.

[6] F. Zhang, E. Otterstein and E. Burkel. "Spark plasma sintering, microstructures, and mechanical properties of macroporous titanium foams". *Adv. Eng. Mater.*, **12** (2010), 863–872.

[7] F. Zhang, Y. Quan, M. Reich, O. Kessler and E. Burkel. *Sintering and heat treatment of titanium alloys by pulsed electric current sintering, in Sintering.* InTech. (2013).

[8] G. Rott, F. Zhang, Y. Haba, W. Kruger and E. Burkel. *Dielectric Properties of Porous Calcium Titanate ($CaTiO_3$), in Biomaterials Science-Processing, Properties, and Applications.* John Wiley and Sons, Inc., Hoboken, NJ, USA (2011 Volume 228).

[9] C. Mihoc, E. Burkel and J.Bednarcik. "Hard X-ray diffraction studies on the quasicrystal phase formation in Al-Cu-Fe alloys by field activated sintering". (2010).

[10] C. Mihoc, D. Schick, M. Lüttgens, C. Lathe and E. Burkel. "Formation of $Al_6Cu_{23}Fe_{10}$ quasicrystals by microwave heating". *Int. J. Mater. Res.*, **103** (2012), 1340.

[11] V. Cojocaru, R. Nicula, M. Stir and E. Burkel. "Compression behaviour of nanostructured NANOPERM alloy at 500°C". **5** (2011), 1093–1096.

[12] V. Cojocaru, R. Nicula, M. Stir and E. Burkel. "Synthesis and microstructural observations during ball milling in $Fe_{88}Zr_7B_4CU_1$ nanostructured alloys". *Politeh. Univ. Buchar. Sci. Bull. Ser. B Chem. Mater. Sci.*, **72** (2010), 207–214.

[13] V. Cojocaru, F. Turquier, R. Nicula, M. Stir and E. Burkel. "Ball milling synthesis and BCC to FCC phase transition under pressure in nanostructured NANOPERM alloys". *J. Optoelectron. Adv. Mat.*, **12** (2010), 397–401.

[14] K. Witte, K. Porath and E. Burkel. "Magnetic Nanoparticles and Their Potential for Contrast Enhancement in Magnetic Resonance Imaging". *J. Spintron. Mag. Nanomater.*, **1** (2012), 40–46.

[15] K. Witte, D. Skroblin, N. Schell and E. Burkel. "Hard X-ray diffraction studies on the composition of ball milled Fe_2O_3 Fe mixtures". *An. Rep. HASYLAB DESY*, (2011).

[16] F. Zhang, M. Adam, F. Ahmed, E. Otterstein and E. Burkel. "Pulsed electric field induced diamond synthesis from carbon nanotubes with solvent catalysts". *Diamond Relat. Mater.*, **20** (2011), 853–858.

[17] F. Zhang, F. Ahmed, J. Bednarcik and E. Burkel. "Diamond synthesis through the generation of plasma during spark plasma sintering". *Phys. Stat. Sol. A*, **209** (2012), 2241–2246.

[18] F. Zhang, F. Ahmed, G. Holzhüter and E. Burkel. "Growth of diamond from fullerene C_{60} by spark plasma sintering". *J. Cryst. Growth*, **340** (2012), 1–5.

[19] F. Zhang, J. Chang and E. Burkel. "Dissolution of poly(vinyl alcohol)-modified carbon nanotubes in a buffer solution". *New Carbon Mater.*, **25** (2010), 241–247.

[20] F. Zhang and E. Burkel. *Synthesis of diamond using spark plasma sintering, in Sintering of ceramics-new emerging techniques.* InTech. (2012).

[21] F. Zhang, C. Mihoc, F. A. adn C. Lathe and E. Burkel. "Thermal stability of carbon nanotubes, fullerene and graphite under spark plasma sintering". *Chem. Phys. Lett.*, **510** (2011), 109–114.

2.2.2 Polymer Physics

Head: Prof. Dr. Christoph Schick

Staff:	Dr. Heiko Huth	Dr. Andreas Wurm
	Dr. Jürn W.P. Schmelzer	Dr. Evgeny Zhuravlev
	Dr. Benjamin Milkereit	Dr. Ricardas Ralys (until 2011)
	Dr. Uladzimir Yemelyanenka	Dr. Xavier Tardif
	Dipl.-Phys. Gunnar Schulz	Dipl.-Phys. Mathias Ahrenberg
	Dipl.-Phys. Daniela Arbeiter (until 2010)	
	M.Sc. Evgeni Shoifet	M.Sc. David Zohrabyan
	M.Sc. Bin Yang	M.Sc. Andrei Yermalayeu
	M.Sc. Yeong Zen Chua	M.Sc. Payam Pakmehr
	B.Sc. Julia Heller	
	Cand.-Phys. Arian-Christoph Pfahl (until 2012)	Renate Nareyka
MSc Graduates:	Chua Yeong Zen	Daniela Arbeiter
BSc Graduates:	Anja Herrmann	

General Outline of the Field of Research

For engineering materials, solidification during processing is a very important step. It proceeds either by crystallization or by a glass transition. Both routes show a characteristic energetic signature, which can be followed by calorimetry. Solidification kinetically depends on many parameters – material properties as well as processing conditions. Calorimeters covering a dynamic range from 10^{-4} K/s up to 10^{6} K/s in cooling and heating are available in the Polymer Physics Group and are used in combination with theoretical analysis to study solidification of different materials.

Experimental and Theoretical Studies on Nucleation-Growth Processes

Experimental studies of nucleation-growth processes and their theoretical interpretation are one of the main directions of research of our group. In the previous years, here the following topics have been in the center of interest.

Size-Dependent Nucleation of Single Tin Particles by Differential Fast Scanning Calorimetry

The undercooling of single micro-sized tin particles has been studied via differential fast scanning calorimetry, employing cooling rates from 100 K/s to 14000 K/s. The diameter of the investigated particles varied from 7.5 μm to 40 μm. Owing to the nearly spherical shape of a single particle upon heating and cooling and the resultant geometric stability, the influence of the particle size on the solidification process could be eliminated. As a result, the issue of how to separate the mutual effects of particle size and cooling rate in the field of rapid solidification has been primarily solved. Two different heterogeneous nucleation mechanisms act for the nucleation

of the single pure Sn particle, indicated by a shelf-like dependence of undercooling. A particle-size dependent nucleation was detected and is discussed by advancing an appropriate theoretical model.

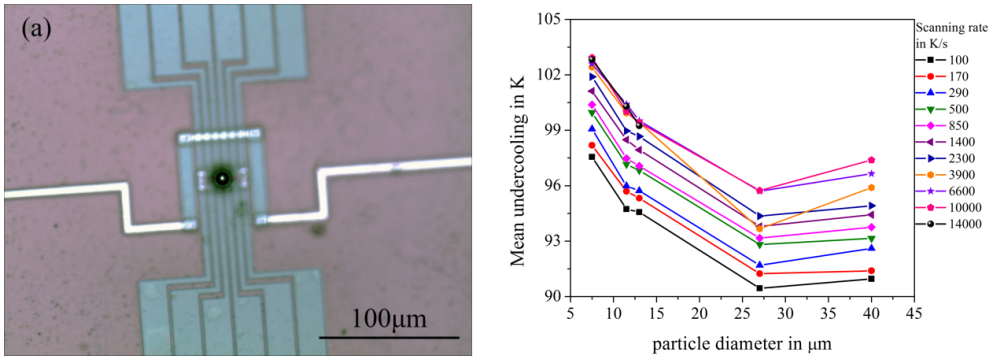

Fig. 2.28: Microphotograph of the 11.5 μm diameter drop of pure Sn (left) and relation between mean undercooling and drop diameter for the single Sn drops at different cooling rates (right).

Continuous Cooling Precipitation (CCP) Diagrams of Al-Mg-Si Alloys

The temperature- and time-dependent precipitation behaviour of Al-based 6060, 6063, 6005A and 6082 alloys at different cooling rates after solution annealing has been investigated. The continuous cooling precipitation diagrams of these alloys were recorded by differential scanning calorimetry. The cooling rate was varied over more than five orders of magnitude ($0.05 - 20000\,\mathrm{K/min}$). Cooling–rate-dependent precipitate formation was analysed by light microscopy, scanning and transmission electron microscopy. Cooling rate-dependent hardness was tested after artificial ageing. Over an appropriate range of cooling rates all alloys show similar precipitation behaviour. At least two precipitation reactions were observed in different temperature ranges. The high-temperature reactions correspond to the precipitation of the equilibrium phase Mg_2Si, and the low-temperature reactions correspond to the precipitation of precursor phases such as β' and B'. The precipitation kinetics depends on the alloy composition. Maximum hardness values are to find as long as the materials were cooled faster than alloy specific critical cooling rate, which increases with increasing alloy content.

Investigation of Extraordinarily Stable Glasses

Low molecular glass formers were used to investigate the stability of physical vapor deposited glasses under certain deposition conditions by in-situ differential AC-chip calorimetry in a ultra high vacuum (UHV). Recent investigations revealed that a mobile surface layer exists on the sample during deposition which allows the molecules

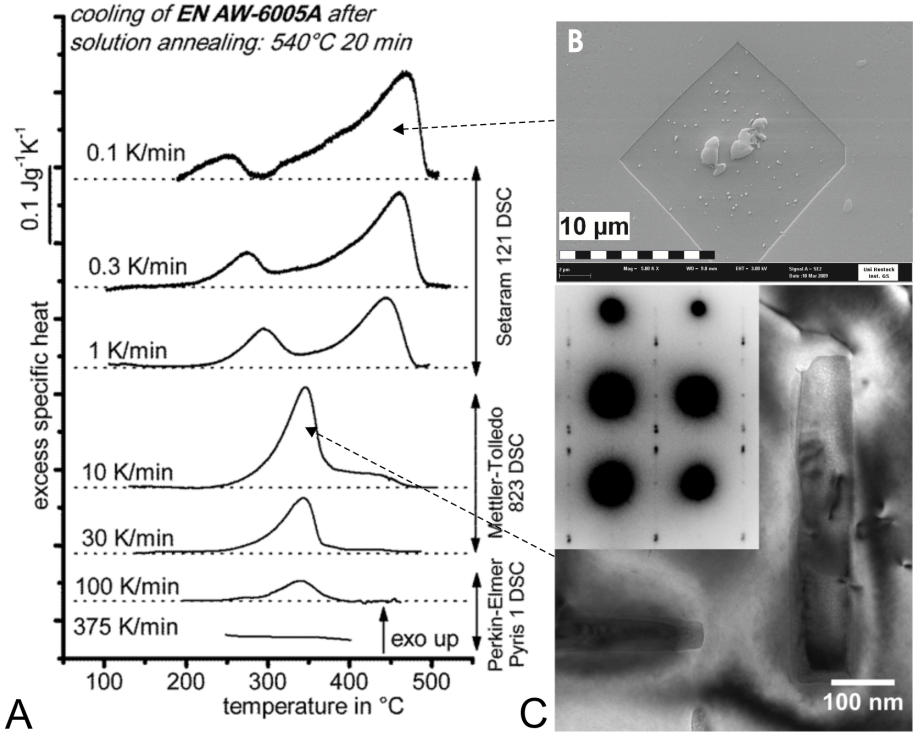

Fig. 2.29: (A) Selected cooling curves of the investigated composition of 6005A alloy after solution annealing; curves were obtained from three different types of DSC devices corresponding to different cooling rates from 0.1 to 375 K/min. (B) Typical equilibrium phase (Mg_2Si) precipitate in 6005A corresponding to high temperature reaction at slow cooling rates. Mg_2Si seem to nucleate mostly heterogeneously at primary precipitates. (C) Metastable precursor precipitate in 6005A corresponding to low temperature reactions at 10 K/min. The corresponding diffraction pattern is given in the insert.

coming from the vapor phase and hitting the surface to sample different configurations on the energy landscape before they get buried by the next layer of molecules from the vapor phase. This yields denser glasses as commonly obtained by liquid quenching. A denser packing can be linked to the vibrational degrees of freedom and thus to a lower heat capacity. This denser packing remains up to temperatures higher than the conventional glass transition.

We observe that vapor-deposited glasses of toluene and ethylbenzene have up to 4 % lower heat capacities than the ordinary glass. The largest heat capacity decrease and the most kinetically stable glasses of toluene and ethylbenzene are observed in a range of deposition temperatures between $0.75T_g$ and $0.96T_g$, see Fig. 2.30a. Compared to larger molecules, the deposition rate has a minor influence on the kinetic stability of these glasses.

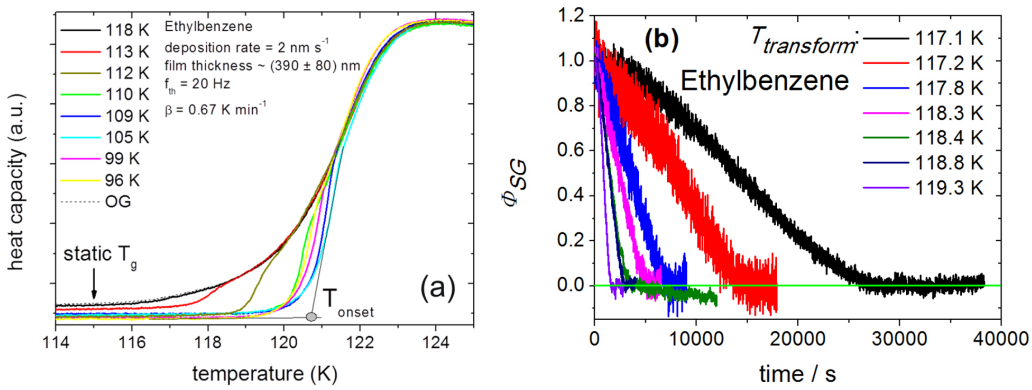

Fig. 2.30: (a) Heat capacity of as-deposited glasses of ethylbenzene deposited at different substrate temperatures ranging from 96 K to 118 K. For comparison, a heating curve corresponding to an ordinary glass (OG) is shown. Except for the highest deposition temperatures, all of the vapor-deposited glasses show lower heat capacity, in comparison to the ordinary glasses. (b) Isothermal transformation kinetics of stable glasses ($\Phi_{SG} = 1$) of ethylbenzene to the supercooled liquid ($\Phi_{SG} = 0$) for different transformation temperatures. All samples were deposited at a substrate temperature of 105 K and a deposition rate of 2 nm/s. Film thickness is 390 nm.

For both toluene and ethylbenzene, the kinetic stability is strongly correlated with the heat capacity decrease for deposition temperatures above $0.8T_g$. In addition, AC-chip calorimetry was used to follow the isothermal transformation of the stable glasses into the supercooled liquid at temperatures slightly above T_g as shown in Fig. 2.30b. Toluene and ethylbenzene stable glasses exhibit a constant transformation rate which is consistent with the growth front mechanism recently demonstrated for tris-naphthylbenzene and indomethacin. The kinetic stability of the most stable toluene and ethylbenzene glasses is comparable to that observed for other stable glasses formed by vapor deposition.

References

[1] C. Schick, D. Lexa and L. Leibowitz. *Differential Scanning Calorimetry and Differential Thermal Analysis*, volume 1, pages 483–495. John Wiley & Sons, Inc. (2012).

[2] D. Seehase, H. Huth, F. Bremerkamp and M. Nowottnick. "Energetic analysis of solder paste deposits as reference for soldering with selective heat". In "35th International Spring Seminar on Electronics Technology (ISSE) 2012", pages 31–36.

[3] I. S. Gutzow and J. W. P. Schmelzer. *The Vitreous State Thermodynamics, Structure, Rheology, and Crystallization*. Springer (2012).

[4] K. R. Whitaker, M. Ahrenberg, C. Schick and M. D. Ediger. "Vapor-deposited α,α,β-tris-naphthylbenzene glasses with low heat capacity and high kinetic stability". *J. Chem. Phys.*, **137** (2012), 154502/1–7.

[5] S. Verevkin, R. Ralys, V. Emel'yanenko, D. Zaitsau and C. Schick. "Thermochemistry of the pyridinium- and pyrrolidinium-based ionic liquids". *J. Therm. Anal. Calorim.*, (2012), 1–6.

[6] A. S. Abyzov, J. W. P. Schmelzer and V. M. Fokin. "Elastic stresses in crystallization processes in finite domains". *J. Non-Cryst. Solids*, **356** (2010), 1670–1678.

[7] A. S. Abyzov, J. W. P. Schmelzer, A. A. Kovalchuk and V. V. Slezov. "Evolution of Cluster Size-Distributions in Nucleation-Growth and Spinodal Decomposition Processes in a Regular Solution". *J. Non-Cryst. Solids*, **356** (2010), 2915–2922.

[8] R. Androsch, M. L. D. Lorenzo, C. Schick and B. Wunderlich. "Mesophases in polyethylene, polypropylene, and poly(1-butene)". *Polymer*, **51** (2010), 4639–4662.

[9] G. S. Boltachev and J. W. P. Schmelzer. "On the definition of temperature and its fluctuations in small systems". *J. Chem. Phys.*, **133** (2010), 134509/1–11.

[10] V. N. Emel'yanenko, S. P. Verevkin, C. Schick, E. N. Stepurko, G. N. Roganov and M. K. Georgieva. "The thermodynamic properties of S-lactic acid". *Russ. J. Phys. Chem. A*, **84** (2010), 1491–1497.

[11] V. M. Fokin, E. D. Zanotto and J. W. P. Schmelzer. "On the thermodynamic driving force for interpretation of nucleation experiments". *J. Non-Cryst. Solids*, **356** (2010), 2185–2191.

[12] N.-A. Gotzen, H. Huth, C. Schick, G. van Assche, C. Neus and B. van Mele. "Phase separation in polymer blend thin films studied by differential AC Chip Calorimetry". *Polymer*, **51** (2010), 647–654.

[13] S. Guns, P. Kayaert, J. A. Martens, J. Van Humbeeck, V. Mathot, T. Pijpers, E. Zhuravlev, C. Schick and V. d. M. Guy. "Characterization of the copolymer poly(ethyleneglycol-g-vinylalcohol) as a potential carrier in the formulation of solid dispersions". *Eur. J. Pharm. Biopharm.*, **74** (2010), 239–247.

[14] I. Gutzow, R. Pascova and J. W. P. Schmelzer. "Glass Transition Behavior: A Generic Phenomenological Approach". *Int. J. Appl. Glass Sci.*, **1** (2010), 221–236.

[15] W. Jiang, M. Du, Q. Gu, J. Jiang, H. Huth, D. Zhou, G. Xue and C. Schick. "Calorimetric study of blend miscibility of polymers confined in ultra-thin films". *Eur. Phys. J. Special Topics*, **189** (2010), 187–195.

[16] K. L. Kearns, M. D. Ediger, H. Huth and C. Schick. "One Micrometer Length Scale Controls Kinetic Stability of Low-Energy Glasses". *J. Phys. Chem. Lett.*, **1** (2010), 388–392.

[17] K. L. Kearns, K. R. Whitaker, M. D. Ediger, H. Huth and C. Schick. "Observation of low heat capacities for vapor-deposited glasses of indomethacin as determined by AC nanocalorimetry". *J. Chem. Phys.*, **133** (2010), 014702/1–10.

[18] B. Milkereit, L. Jonas, C. Schick and O. Keßler. "Das kontinuierliche Zeit-Temperatur- Ausscheidungs- Diagramm einer Aluminiumlegierung EN AW-6005A". *HTM J. Heat Treatm. Mat.*, **65** (2010), 159–171.

[19] B. Milkereit, C. Schick and O. Kessler. "Continuous Cooling Precipitation Diagrams Depending on the Composition of Aluminum-Magnesium-Silicon Alloys". In "12th International Conference on Aluminium Alloys", pages 407–412.

[20] C. Schick. "Glass transition under confinement-what can be learned from calorimetry". *Eur. Phys. J. Special Topics*, **189** (2010), 3–36.

[21] J. W. P. Schmelzer. "On the determination of the kinetic pre-factor in classical nucleation theory". *J. Non-Cryst. Solids*, **133** (2010), 134509.

[22] J. W. P. Schmelzer, V. M. Fokin, A. S. Abyzov, E. D. Zanotto and I. Gutzow. "How Do Crystals Form and Grow in Glass-Forming Liquids: Ostwald's Rule of Stages and Beyond". *Int. J. Appl. Glass Sci.*, **1** (2010), 16–26.

[23] M. Tress, M. Erber, E. U. Mapesa, H. Huth, J. Müller, A. Serghei, C. Schick, K.-J. Eichhorn, B. Voit and F. Kremer. "Glassy Dynamics and Glass Transition in Nanometric Thin Layers of Polystyrene". *Macromolecules*, **43** (2010), 9937–9944.

[24] S. Vyazovkin, V. Rives and C. Schick. "Making Impact in Thermal Sciences: Overview of Highly Cited Papers Published in Thermochimica Acta". *Thermochim. Acta*, **500** (2010), 1–5.

[25] A. Wurm, M. Ismail, B. Kretzschmar, D. Pospiech and C. Schick. "Retarded Crystallization in Polyamide/Layered Silicates Nanocomposites caused by an Immobilized Interphase". *Macromolecules*, **43** (2010), 1480–1487.

[26] B. Yang, Y. Gao, C. Zou, Q. Zhai, E. Zhuravlev and C. Schick. "Size-dependent undercooling of pure Sn by single particle DSC measurements". *Chinese Science Bulletin*, **55** (2010), 2063–2065.

[27] E. Zhuravlev and C. Schick. "Fast scanning power compensated differential scanning nano-calorimeter: 1. The device". *Thermochim. Acta*, **505** (2010), 1–13.

[28] E. Zhuravlev and C. Schick. "Fast scanning power compensated differential scanning nano-calorimeter: 2. Heat capacity analysis". *Thermochim. Acta*, **505** (2010), 14–21.

[29] E. Zhuravlev and C. Schick. "Calorimeter and methods of using it and control systems therefor" (2010). US patent US 2010/0046573 Al, 12/479,105.

[30] A. S. Abyzov, J. W. P. Schmelzer and V. M. Fokin. "Theory of pore formation in glass under tensile stress: Generalized Gibbs approach". *J. Non-Cryst. Solids*, **357** (2011), 3474–3479.

[31] M. Chen, M. Du, J. Jiang, D. Li, W. Jiang, E. Zhuravlev, D. Zhou, C. Schick and G. Xue. "Verifying the symmetry of ultra-fast scanning calorimeters using liquid crystal secondary temperature standards". *Thermochim. Acta*, **526** (2011), 58–64.

[32] S. Davtyan, C. Schick, A. Tonoyan and D. Zohrabyan. "SiO2 Nanofiller impact on crystallization kinetics during adiabatic anionic polymerization of epsilon-caprolactam". *e-polymers*, **040** (2011), 1–10.

[33] S. H. El-Taweel, B. Stoll and C. Schick. "Crystallization kinetics and miscibility of blends of polyhydroxybutyrate (PHB) with ethylene vinyl acetate copolymers (EVA)". *e-polymers*, **018** (2011), 1–16.

[34] I. Gutzow, R. Pascova, N. Jordanov, S. Gutzov, I. Penkov, I. Markovska, J. W. P. Schmelzer and F.-P. Ludwig. *Structure, Thermodynamic Properties, Solubility and Synthesis of the Different Modifications of Silica*, chapter 6, pages 95–143. Dubna (2011).

[35] O. Hellmuth, V. I. Khvorostyanov, J. A. Curry, A. K. Shchekin, J. W. P. Schmelzer and V. G. Baidakov. *Review on the Phenomenology and Mechanism of Atmospheric Ice Formation: Selected Questions of Interest*, chapter 25, pages 441–475. Joint Institute for Nuclear Research, Dubna (2011).

[36] G. W. H. Höhne and C. Schick. "Preface". *Thermochim. Acta*, **522** (2011), 1.

[37] A. R. Imre, A. S. Abyzov, I. F. Barna and J. W. P. Schmelzer. "Homogeneous bubble nucleation limit of mercury under the normal working conditions of the planned European spallation neutron source". *Eur. Phys. J. B*, **79** (2011), 107–113.

[38] I. Kolesov, D. Mileva, R. Androsch and C. Schick. "Structure formation of polyamide 6 from the glassy state by fast scanning chip calorimetry". *Polymer*, **52** (2011), 5156–5165.

[39] D. Mileva, R. Androsch, E. Zhuravlev, C. Schick and B. Wunderlich. "Formation and reorganization of the mesophase of random copolymers of propylene and 1-butene". *Polymer*, **52** (2011), 1107–1115.

[40] D. Mileva, R. Androsch, E. Zhuravlev, C. Schick and B. Wunderlich. "Isotropization, perfection and reorganization of the mesophase of isotactic polypropylene". *Thermochim. Acta*, **522** (2011), 100–109.

[41] B. Milkereit, M. Beck, M. Reich, O. Kessler and C. Schick. "Precipitation kinetics of an aluminium alloy during Newtonian cooling simulated in a differential scanning calorimeter". *Thermochim. Acta*, **522** (2011), 86–95.

[42] R. Nicula, M. Stir, A. Wurm, J. M. Catalá-Civera, K. Ishizaki, S. Vaucher, E. Zhuravlev and C. Schick. "Microwave calorimetry using X-rays". *Thermochim. Acta*, **526** (2011), 137–142.

[43] M. Pasichny, A. Shirinyan and J. Schmelzer. "Evolution of new phase clusters at the initial stages of binary alloy decomposition described in terms of a modified theory of nucleation". *Ukr. J. Phys.*, **56** (2011), 192–199.

[44] G. V. Poel, A. Sargsyan, V. Mathot, G. V. Assche, A. Wurm, C. Schick, A. Krumme and D. Zhou. *Recommendation for Temperature Calibration of Fast Scanning Calorimeters (FsCs) for Sample Mass and Scan Rate.* Beuth Verlag GmbH, Berlin (2011).

[45] V. Rives, C. Schick and S. Vyazovkin. "New procedures for articles reporting thermophysical properties". *Thermochim. Acta*, **521** (2011), 1.

[46] J. W. P. Schmelzer. *Structural Order Parameters, Relaxation and Crystallization*, volume 3. Joint Institute for Nuclear Research, Dubna (2011).

[47] J. W. P. Schmelzer and A. S. Abyzov. "Thermodynamic analysis of nucleation in confined space: Generalized Gibbs approach". *J. Chem. Phys.*, **134** (2011), 054511/1–11.

[48] J. W. P. Schmelzer and A. S. Abyzov. "On the theoretical description of nucleation in confined space". *AIP Advances*, **1** (2011), 042160/1–9.

[49] J. W. P. Schmelzer and I. S. Gutzow. *Glasses and the Glass Transition.* WILEY-VCH Verlag, Berlin (2011).

[50] J. W. P. Schmelzer, G. Röpke and V. B. Priezzhev. *Nucleation Theory and Applications.* Joint Institute for Nuclear Research, Dubna (2011).

[51] J. W. P. Schmelzer, T. V. Tropin and C. Schick. *On the Dependence of the Properties of Glasses on Cooling and Heating Rates: What is the Right Deborah Number?*, chapter 24, pages 355–428. Dubna (2011).

[52] A. S. Shirinyan, Y. S. Bilogorodskyy, G. Wilde and J. W. P. Schmelzer. "Size-dependent hysteresis and phase formation kinetics during temperature cycling of metal nanopowders". *J. Phys.: Condens. Matter*, **23** (2011), 245301.

[53] X. Si, C. Jiao, F. Li, J. Zhang, S. Wang, S. Liu, Z. Li, L. Sun, F. Xu, Z. Gabelica and C. Schick. "High and selective CO_2 uptake, H2 storage and methanol sensing on the amine-decorated 12-connected MOF CAU-1". *Energy Environ. Sci.*, **4** (2011), 4522–4527.

[54] T. V. Tropin, J. W. P. Schmelzer and C. Schick. "On the dependence of the properties of glasses on cooling and heating rates: I. Entropy, entropy production, and glass transition temperature". *J. Non-Cryst. Solids*, **357** (2011), 1291–1302.

[55] T. V. Tropin, J. W. P. Schmelzer and C. Schick. "On the dependence of the properties of glasses on cooling and heating rates II: Prigogine-Defay ratio, fictive temperature and fictive pressure". *J. Non-Cryst. Solids*, **357** (2011), 1303–1309.

[56] A. L. Tseskis, N. M. Kortsensteyn and J. W. P. Schmelzer. *On "Smoothing" of First Order Phase Transition in Small Systems*, chapter 20, pages 313–317. Joint Institute for Nuclear Research, Dubna (2011).

[57] B. Yang, Y. Gao, C. Zou, Q. Zhai, A. Abyzov, E. Zhuravlev, J. Schmelzer and C. Schick. "Cooling rate dependence of undercooling of pure Sn single drop by fast scanning calorimetry". *Appl. Phys. A*, **104** (2011), 189–196.

[58] W. Yave, H. Huth, A. Car and C. Schick. "Peculiarity of a CO_2-philic block copolymer confined in thin films with constrained thickness: "a super membrane for CO_2-capture"". *Energy Environ. Sci.*, **4** (2011), 4656–4661.

[59] E. Zhuravlev, J. W. Schmelzer, B. Wunderlich and C. Schick. "Kinetics of nucleation and crystallization in poly(epsilon caprolactone) (PCL)". *Polymer*, **52** (2011), 1983–1997.

[60] A. Abyzov, J. Schmelzer, L. Davydov and V. Slezov. "Homogeneous bubble nucleation limit of lead". *Problems of Atomic Science and Technology, Series: Nuclear Physics Investigations*, **1** (2012), 283–287.

[61] M. Ahrenberg, E. Shoifet, K. R. Whitaker, H. Huth, M. D. Ediger and C. Schick. "Differential alternating current chip calorimeter for in situ investigation of vapor-deposited thin films". *Rev. Sci. Instrum.*, **83** (2012), 033902/1–12.

[62] B. Milkereit, J. Osten, C. Schick and O. Kessler. "Continuous Heating Dissolution Diagrams of Aluminium Alloys". In W. A. C. Hasso Weiland, Anthony D. Rollett, editor, "13th International Conference on Aluminum Alloys (ICAA13)", pages 1095–1100. TMS (The Minerals, Metals & Materials Society).

[63] S. Bulut and C. Schick. "Devitrification of the amorphous fractions of starch during gelatinisation". *Chem. Phys.*, **90** (2012), 140–146.

[64] C. Krause, H. Yin, C. Cerclier, D. Morineau, A. Wurm, C. Schick, F. Emmerling and A. Schonhals. "Molecular dynamics of a discotic liquid crystal investigated by a combination of dielectric relaxation and specific heat spectroscopy". *Soft Matter*, **8** (2012), 11115–11122.

[65] D. Mileva, R. Androsch, E. Zhuravlev and C. Schick. "Morphology of mesophase and crystals of polyamide 6 prepared in a fast scanning chip calorimeter". *Polymer*, **53** (2012), 3994–4001.

[66] D. Mileva, R. Androsch, E. Zhuravlev, C. Schick and B. Wunderlich. "Formation and Reorganization of the Mesophase of Isotactic Polypropylene". *Mol. Cryst. Liq. Cryst.*, **556** (2012), 74–83.

[67] D. Mileva, R. Androsch, E. Zhuravlev, C. Schick and B. Wunderlich. "Homogeneous nucleation and mesophase formation in glassy isotactic polypropylene". *Polymer*, **53** (2012), 277–282.

[68] B. Milkereit, N. Wanderka, C. Schick and O. Kessler. "Continuous cooling precipitation diagrams of Al-Mg-Si alloys". *Mater. Sci. Eng. A*, **550** (2012), 87–96.

[69] O. Kessler, D. Zohrabyan, B. Milkereit and C. Schick. "Monitoring Precipitation during Rapid Quenching of Aluminium Alloys by Calorimetric Reheating Experiments". In W. A. C. Hasso Weiland, Anthony D. Rollett, editor, "13th International Conference on Aluminum Alloys (ICAA13)", pages 43–48. TMS (The Minerals, Metals & Materials Society).

[70] R. Pascova, G. Avdeev, I. Gutzow, I. Penkov, F.-P. Ludwig and J. W. P. Schmelzer. "Refractory Alkali-Free Cristobalite Glass-Ceramics: Activated Reaction Sinter-Crystallization Synthesis and Properties". *Int. J. Appl. Glass Sci.*, **3** (2012), 75–87.

[71] C. Schick. *Calorimetry*, volume 2, chapter 2.31, pages 793–823. Elsevier B.V., Amsterdam (2012).

[72] J. W. P. Schmelzer and C. Schick. "Dependence of crystallization processes of glass-forming melts on melt history: a theoretical approach to a quantitative

treatment". *Phys. Chem. Glasses Eur. J. Glass Sci. Technol. B*, **53** (2012), 99–106.

[73] J. W. P. Schmelzer. "Kinetic criteria of glass formation and the pressure dependence of the glass transition temperature". *J. Chem. Phys.*, **136** (2012), 074512/1–11.

[74] J. W. P. Schmelzer and A. S. Abyzov. "Comment on "Minimum free-energy pathway of nucleation" [J. Chem. Phys. **135**, 134508 (2011)]". *J. Chem. Phys.*, **136** (2012), 107101/1–2.

[75] T. P. Selvin, S. Thomas, N. E. Zafeiropoulos, S. Bandyopadhyay, A. Wurm and C. Schick. "Polystyrene/calcium phosphate nanocomposites: Morphology, mechanical, and dielectric properties". *Polym. Eng. Sci.*, **52** (2012), 689–699.

[76] A. V. Svanidze, H. Huth, S. G. Lushnikov and C. Schick. "Study of phase transition in tetragonal lysozyme crystals by AC-nanocalorimetry". *Thermochim. Acta*, **544** (2012), 33–37.

[77] T. V. Tropin, J. W. P. Schmelzer, I. Gutzow and C. Schick. "On the theoretical determination of the Prigogine-Defay ratio in glass transition". *J. Chem. Phys.*, **136** (2012), 124502/1–14.

[78] S. P. Verevkin, V. N. Emel'yanenko, D. H. Zaitsau, R. V. Ralys and C. Schick. "Ionic liquids: Differential scanning calorimetry as a new indirect method for determination of vaporization enthalpies". *J. Phys. Chem. B*, **116** (2012), 4276–4285.

[79] S. P. Verevkin, R. V. Ralys, D. H. Zaitsau, V. N. Emel'yanenko and C. Schick. "Express thermo-gravimetric method for the vaporization enthalpies appraisal for very low volatile molecular and ionic compounds". *Thermochim. Acta*, **538** (2012), 55–62.

[80] S. P. Verevkin, D. H. Zaitsau, V. N. Emel'yanenko, R. V. Ralys, A. V. Yermalayeu and C. Schick. "Vaporization enthalpies of imidazolium based ionic liquids. A thermogravimetric study of the alkyl chain length dependence". *J. Chem. Thermodyn.*, **54** (2012), 433–437.

[81] S. P. Verevkin, D. H. Zaitsau, V. N. Emel'yanenko, C. Schick, S. Jayaraman and E. J. Maginn. "An elegant access to formation and vaporization enthalpies of ionic liquids by indirect DSC experiment and "in silico" calculations". *Chem. Commun.*, **48** (2012), 6915–6917.

[82] A. Wurm, E. Zhuravlev, K. Eckstein, D. Jehnichen, D. Pospiech, R. Androsch, B. Wunderlich and C. Schick. "Crystallization and Homogeneous Nucleation Kinetics of Poly(epsilon-caprolactone) (PCL) with Different Molar Masses". *Macromolecules*, **45** (2012), 3816–3828.

[83] J. Zhang, L. Sun, F. Xu, F. Li, H.-Y. Zhou, F.-L. Huang, Z. Gabelica and C. Schick. "Hydrogen storage and selective carbon dioxide capture in a new chromium(iii)-based infinite coordination polymer". *RSC Advances*, **2** (2012), 2939–2945.

[84] J. Zhang, L. Sun, F. Xu, F. Li, H.-Y. Zhou, Y.-L. Liu, Z. Gabelica and C. Schick. "H_2 storage and CO_2 capture on a nanoscale metal organic framework with high thermal stability". *Chem. Commun.*, **48** (2012), 759–761.

[85] D. Zohrabyan, B. Milkereit, O. Kessler and C. Schick. "Precipitation Enthalpy during Cooling of Aluminum Alloys Obtained from Calorimetric Reheating Experiments". *Thermochim. Acta*, **529** (2012), 51–58.

2.2.3 Physics of Nanomaterials

Head: Prof. Dr. Thomas Gerber

Staff:	Dr. Gerd Holzhüter	Dr. Cornelia Ganz	
	Dr. Weiguo Xu	Dipl.-Phys. Sven Radefeld	
	Dipl.-Chem. Ulf Weber	Dipl.-Phys. Martin Adam	
	Dipl.-Phys. Holger Keuer	Dipl.-Phys. Richard Dietrich	
	Anja Clasen	Dorothea Gütschow	
BSc Graduates:	Jörg Jeschke	Christian Seidel	Peter Vogel

Nanostructure Processing of Advanced Biomaterials

The main topic of our research is the structure analysis and development of nanoscaled materials. The investigations are performed using X-ray tomography, X-ray diffraction, small- and wide-angle X-ray scattering (SAXS and WAXS), scanning and transmission electron microscopy (SEM and TEM) including energy-dispersive X-ray (EDX) and electron energy loss spectroscopy (EELS) and electron diffraction.

The sol-gel-process is the key technique for manufacturing nanostructured materials. The improvement of the acceptance of a synthetic material in living tissue is of great importance. Therefore we developed a synthetic nanostructured biomaterial with special properties. The interaction between the synthetic material and autological proteins is achieved by using a synthetic matrix of defined porosity. The special properties of the matrix are the reason for a high bioactivity. This activity stimulates the differentiation of adult stem cells and the formation of various tissues.

The interdisciplinary research projects are cross-disciplinary efforts that draw together working groups of our faculty and the faculty of medicine, including physicists, chemists, biologists and physicians [1–17].

Nanostructured Coating of Dental Implants

A new nanostructured coating material was invented and investigated *in vitro* and *in vivo*. The coating consists of a high porous silica matrix with embedded nanocrystalline hydroxyapatite (ncHA). The nanostructure of the coating material is shown in Fig. 2.31 (A-C). The TEM micrograph (A) demonstrates the silica gel with the embedded HA crystals. The silica gel is a xerogel network and is visible as very small granular structures, about $0.5 - 1\,\mathrm{nm}$, on and between the HA crystals and is represented by a scanning TEM micrograph in Fig. 2.31(C). For a higher magnification see Fig. 2.31(B). To investigate the improvement on osseointegration, coated (NB-C) and uncoated (Ctrl) implants were inserted in the femora of New Zealand White Rabbits and after 2, 4 and 6 weeks the bone-to-implant-contact (BIC) was determined. The results of the BIC-measurement are demonstrated in Fig. 2.31(F). The BIC of the control group (Ctrl) is increasing within 6 weeks from 42 % at 2 weeks up to 50 % at 6 weeks. The BIC of the coated implants is significantly higher

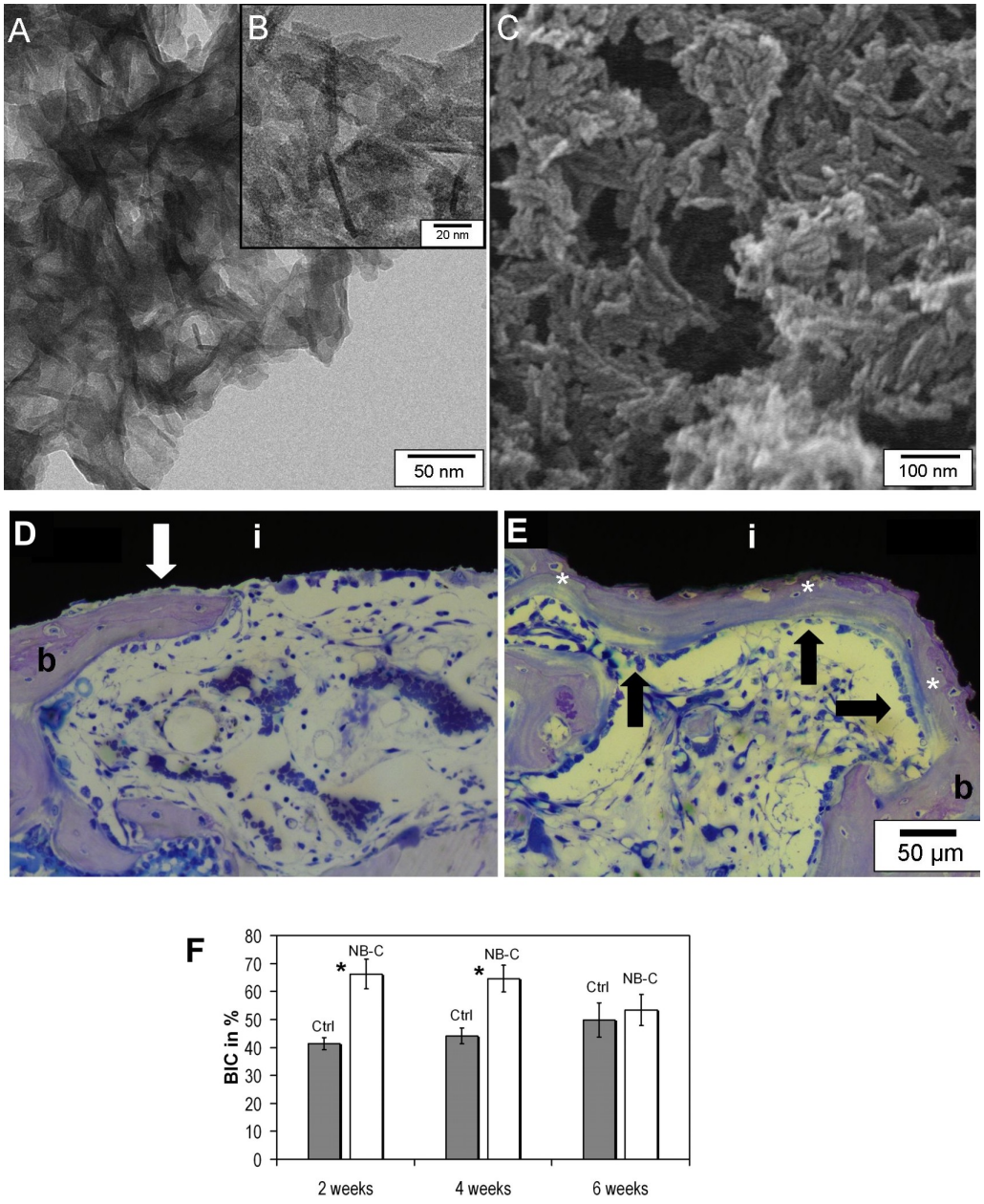

Fig. 2.31: (A-C) The coating consists of a silica matrix with embedded nanocrystalline hydroxyapatite. The coating material is characterized by a high porosity on the nanometer scale. (D-E) Images of histological, polished cross sections after 2 weeks in the femora of rabbits. (F) Bone-to-Implant-Contact of uncoated and coated implants.

than the one of the control group at 2 (66 %) and 4 weeks (65 %) with $p < 0.005$ (if the null hypothesis is true, the p-value is a probability for the obtaining test

statistic). After 6 weeks the BIC of NB-C is decreasing to the level of the Ctrl group.

Two histological images after 2 weeks *in vivo* are shown in Fig. 2.31. For the control group (D), bone formation occurred in direction to the implant surface. In many cases there is still connective tissue between new formed bone and implant surface (white arrow). In contrast to that, in the coated group bone formation occurred directly on the implant surface. In Fig. 2.31 (B) an osteoblastic border has formed osteoid on the coating interface (black arrows). Osteocytes are included in the new formed bone on the coating material (asterisks). A close connection of new bone and coating has developed.

Osseointegration of 3-Dimensional Porous Implants

A new effective implant design does the implant fixation without the use of bone cement. Therefore, it is necessary to produce an implant structure that allows the bone ingrowth for the anchoring. A porous titanium pin was designed as a model for orthopaedic implants by the place-holder technique. The titanium implants were inserted into New Zealand Rabbit femora for 4 and 12 weeks. Two groups were implanted: a control and a NanoBone®coated group. For the evaluation of the ingrowth behaviour, the implant was separated into an edge (thickness 0.5 mm) and a core zone. In both zones, groups and dwell times the BIC and the bone-area

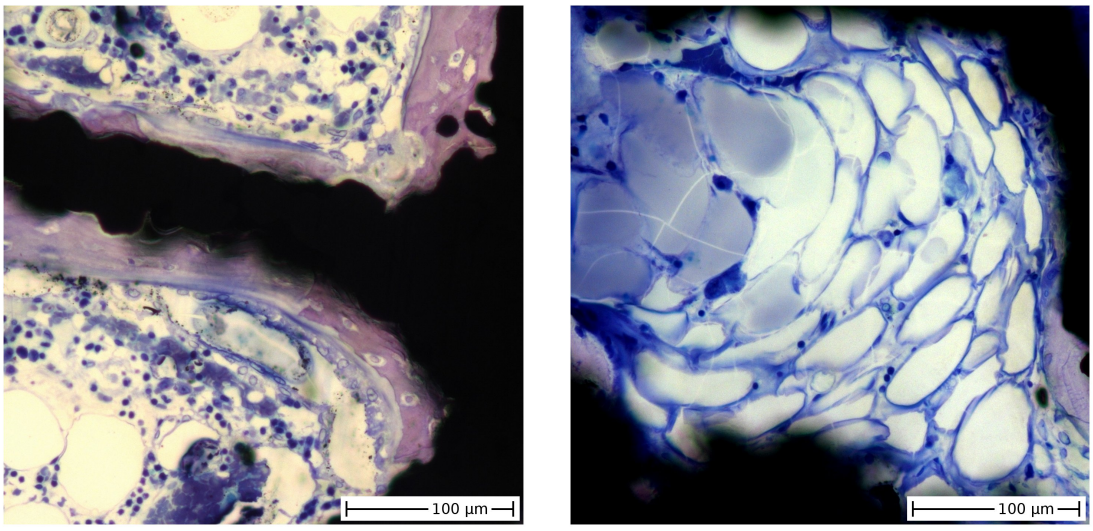

(a) (b)

Fig. 2.32: Histomorphometric cross section from the *in vivo* experiment. (a) Thin bone layer in the core zone of the coated group. (b) High amount of adipocytes in the pores of the core zone of the coated group.

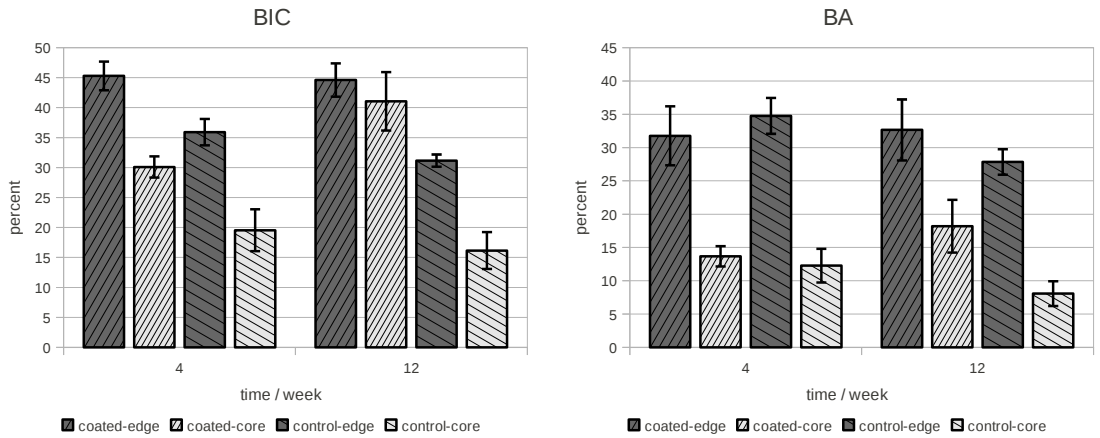

(a) (b)

Fig. 2.33: The evaluation of the *in vivo* experiment. (a) The result of the BIC measurement. (b) The result of the BA measurement.

(BA) were measured.

The evaluation offers a better ossification of the coated group, see Fig. 2.33(a) and (b). In Fig. 2.32(a) is shown on a histomorphometric cross section of the coated group, that the bone was grown on the pores surfaces as thin bone layers at the core zone. This effect was not measurable for the control group. Furthermore, the amount of adipocytes at the core zone was increased, see Fig. 2.32(b).

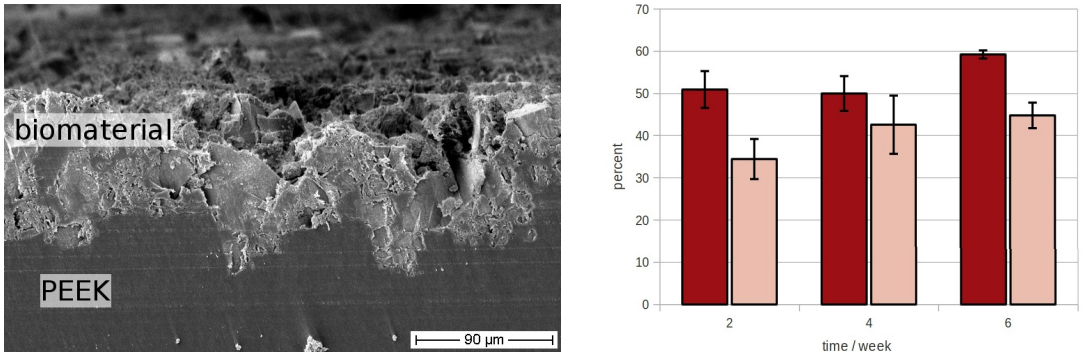

(a) (b)

Fig. 2.34: The results of the osseoinductive PEEK coating. (a) A cross section of the coated polymer. (b) The result of the BIC measurement of the *in vivo* test offers a better osseointegration for the coated group.

Osseoinductive Coating on PEEK Surfaces

The polymer polyether ether ketone (PEEK) has a high potential as implant material. It is biocompatible and has very good mechanical properties compared with metals, that are used as implant material (e.g. Ti, Ti-6Al-4V, CoCrMo). But the cell adhesion on the polymer surface is very bad. To avoid this negativ effect, an osseoinductive coating, based on the NanoBone®technique, was developed. During the coating process, the molten polymer created a new composite with the biomaterial on the surface (Fig. 2.34(a)). This implant prototype was tested *in vivo* in femora of New Zealand White Rabbits. The evaluation of the harvested implants offered improved osseointegration by the osseoinductive coating (Fig. 2.34(b)).

Polymer-silica Nanocomposites for Wound Dressing

In Germany alone, about three million – mostly elderly – patients suffer from poorly healing large-area wounds caused by complaints such as diabetes, burns or bedsores. The wounds can be treated with conventional wound dressings, but the success rate is not as good as it should be. We believe that a new type of dressing made of silica nanoparticles, developed in our group, will solve the problem. This novel dressing works as a drug delivery for nano-silica which supports the tissue regeneration, it is pH-neutral and 100 percent bioresorbable.

Silica has been successfully used therapeutically for many conditions. Remarkable healing properties associated with silica are well known and documented. The physiological activity of silica depends on the degree of cross-linking of the silica

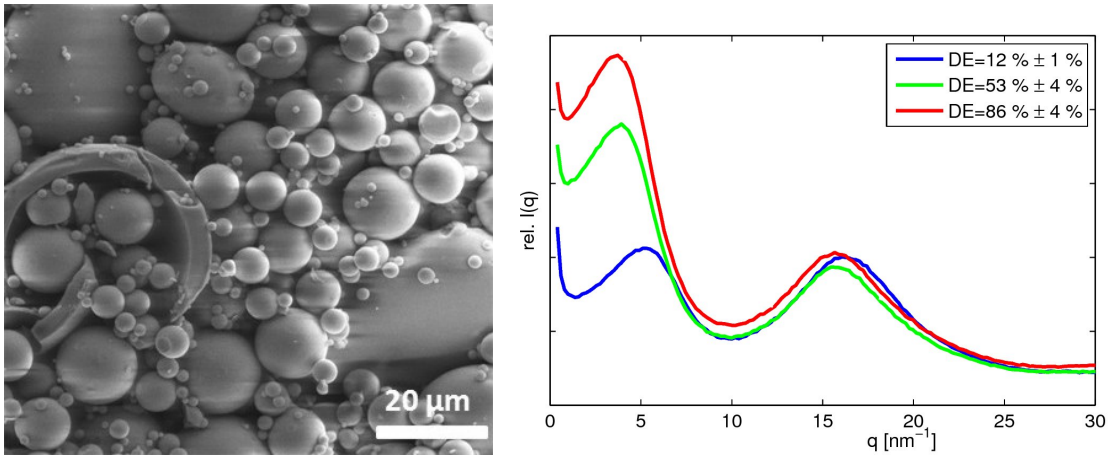

(a) (b)

Fig. 2.35: (a) SEM micrograph of silica micro particles. The hollow micro particles exist out of nano particles with a diameter of 0.5 nm. (b) The peak in the WAXS curves at 4 nm^{-1} documents the packing of the nano particles.

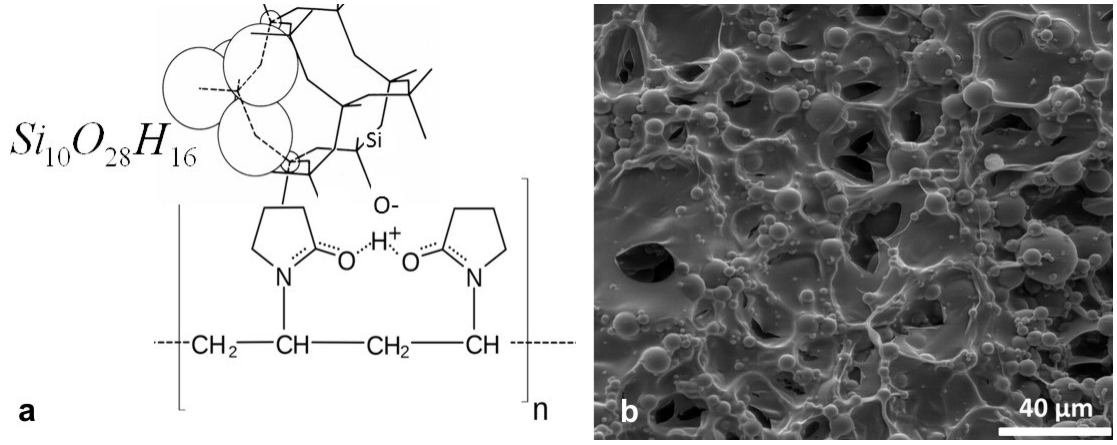

Fig. 2.36: (a) Chemical structure of the nano composite which is the carrier material. (b) Scanning electron micrograph of the wound dressing. The carrier material forms a sponge containing the silica micro particles.

network. Crystalline compounds and silica glass networks show a low activity. A silica polyhedron with a $Si_{10}O_{28}H_{16}$ structure shows the lowest cross-linking of a three dimensional network and the highest physiological activity.

It is possible to produce and stabilize such polyhedrons by sol-gel processes. SAXS and WAXS are used to control the procedures. The silica polyhedron has a size of 0.5 nm. It is used to produce secondary structures. The Fig. 2.35(a) shows the SEM micrograph of silica micro particles. The WAXS measurements (Fig. 2.35(b)) demonstrate the degree of cross-linking of the silica network which is depending on the degree of esterification (DE) of the primary polyhedron. The first peak at $4\,\mathrm{nm}^{-1}$ contains information about the packing of the polyhedrons. A high degree of esterification causes a low degree of cross-linking of the silica network.

A polymer-silica nanocomposite is used as a carrier material for the micro particles for the application as wound dressing. The polymer is polyvinylpyrrolidone (PVP). It is a water-soluble polymer made from the monomer N-vinylpyrrolidone. PVP and negative charged silica nanoparticles form at pH 7 a hydrogel. A sponge-like structure is obtained by freeze-drying this gel including the silica micro particles. The Fig. 2.36 (a) shows the main structure element of the carrier material and Fig. 2.36 (b) documents the structure of the final wound dressing by SEM microscopy.

References

[1] M. Adam, C. Ganz, W. Xu, B. Frerich and T. Gerber. “Controlled self-coating of implant surfaces with autologous molecules”. *KEM*, **529-530** (2012), 207–212.

[2] M. Adam, C. Ganz, W. Xu, H. R. Sarajian, B. Frerich and T. Gerber. “How to

Enhance Osseointegration – Roughness, Hydrophilicity or Bioactive Coating?" *KEM*, **493-494** (2012), 467–472.

[3] C. Ganz, W. Xu, G. Holzhüter, W. Götz, B. Vollmar and T. Gerber. "Comparison of bone substitutes in a tibia defect model in Wistar-rats". *KEM*, **493-494** (2012), 732–738.

[4] T. Gerber. "Low cross-linking structures of silica". *International Patent*, **PCT/EP2012/051603** (2012).

[5] T. Gerber. "Silica/polymer composite". *International Patent*, **PCT/EP2012/051581** (2012).

[6] T. Gerber. "Kieselsäurekondensate in einer Polymermatrix für therapeutische Zwecke in der Medizin und Verfahren zur Herstellung". *German Patent*, **DE 102011 009 838.9** (2011).

[7] T. Gerber. "Kieselsäurekondensate für therapeutische Zwecke in der Medizin und Verfahren zur Herstellung". *German Patent*, **DE 102011 009 838.0** (2011).

[8] T. Gerber, C. Ganz, W. Xu, F. Maier, B. Frerich and S. Lenz. "Bone Grafting Putty - Animal Experiments and Clinical Applications". *KEM*, **529-530** (2012), 285–290.

[9] T. Gerber and H. Keuer. "Osteokonduktive Beschichtung von Kunststoffimplantaten". *German Patent*, **DE 10 2012 020 603.8** (2012).

[10] T. Gerber, S. Lenz, G. Holzhüter, W. Götz, K. Helms, C. Harms and T. Mittlmeier. "Nanostructured Bone Grafting Substitute - A Pathway to Osteoinductivity". *KEM*, **493-494** (2012), 147–152.

[11] W. Götz, S. Lenz, C. Reichert, K.-O. Henkel, V. Bienengräber, L. Pernicka, K. Gundlach, T. Gredes, T. Gerber, T. Gedrange and F. Heinemann. "A preliminary study in osteoinduction by a nano-crystalline hydroxyapatite in the mini pig". *Folia Histochem. Cytobiol.*, **48** (2010), 589–596.

[12] C. Harms, K. Helms, T. Taschner, I. Stratos, A. Ignatius, T. Gerber, S. Lenz, S. Rammelt, B. Vollmar and T. Mittlmeier. "Osteogenic capacity of nanocrystalline bone cement in a weight-bearing defect at the ovine tibial metaphysis". *Int. J. of Nanomed.*, **7** (2012), 2883 – 2889.

[13] H. Keuer, C. Ganz, W. Xu, B. Frerich and T. Gerber. "Bioactive Coating on Porous Materials with an Interconnected Pore System to Improve Osseointegration". *KEM*, **493-494** (2012), 499–503.

[14] H. Keuer, C. Ganz, W. Xu, A. Schubert, B. Frerich and T. Gerber. "Osteoinductive coating on PEEK surfaces by using nanocrystalline biomaterial and in vivo test". *KEM*, **529-530** (2012), 345–349.

[15] M. Kirchhoff, S. Lenz, K.-O. Henkel, B. Frerich, G. Holzhüter, S. Radefeldt and T. Gerber. "Lateral augmentation of the mandible in minipigs with a synthetic nanostructured hydroxyapatite block". *J. Biomed. Mater. Res. Part B: Appl. Biomater.*, **96B** (2011), 342–350.

[16] C. Punke, T. Zehlicke, T. Just, G. Holzhüter, T. Gerber and H. W. Pau. "Matrix change of bone grafting substitute after implantation into guinea pig bulla". *Folia Morphologica*, **71** (2012), 109–114.

[17] W. Xu, C. Ganz, U. Weber, M. Adam, G. Holzhüter, D. Wolter, B. Frerich, B. Vollmar and T. Gerber. "Evaluation of injectable silica-embedded nanohydroxyapatite bone substitute in a rat tibia defect model". *Int. J. of Nanomed.*, **6** (2011), 1543–1552.

2.2.4 Physics of Surfaces and Interfaces

Head: Prof. Dr. Sylvia Speller

Staff: Theresa Kopplow

General Outline of the Field of Research

The research group Physics of Surface and Interfaces has been installed at the Institute of Physics of the University of Rostock in March 2012. The output described below partly originates from the research activities of the group leader at the Radboud University Nijmegen, prior to her change to Rostock in 2012. The research program of the group is dedicated to unravel mechanisms and processes relevant in the coupling of solid, organic, and biologic structures on the nanometer scale. Respective investigations require scanning probe microscopy (SPM) based approaches, interdisciplinary linked projects and a well-established network including chemists, biologists, and life scientists. On the one hand the research questions directly address the nanoscopic phenomena in the hybrid systems under study. On the other hand the studies also make contributions to the development of novel methods for the characterization and manipulation on the nanometer scale. In this connection the influence of electronic states due to transfer of charge carriers on SPM signatures and the local spectroscopy methods receive special attention. The research program comprises three components, i.e. nanoelectronic transitions in individual clusters and nanostructures, the influence of the local environment on chemical reaction, and biophysical interactions in protein complexes and at surfaces of living cells [1–13].

Electronic Properties of Solid State Nanostructures

In the group we study the electronic properties of materials being characterized by peculiarities of either geometry or their electronic structure. The system may be made up of aggregates of quantum dots or clusters, surface structures of oxides, or nano-contacts. The scientific questions behind these studies concern nanoelectronic or magnetic structure, the nature of the electron transport through individual quantum structures and their aggregates, tunneling through atomic and molecular nanocontacts, and their stability in the quantum regime.

Conductivity Switching in Polyoxometalate Clusters

In a collaboration with Prof. Lee Cronin, University of Glasgow, we investigate the nanoelectronic properties of polyoxometalate clusters by scanning probe microscopy methods. Special feature of this material class is the abundance of oxidation states and the coincidence of different types of chromism, such as thermochromism and electrochromism. In particular anion dimers contained in the metal oxide cages can

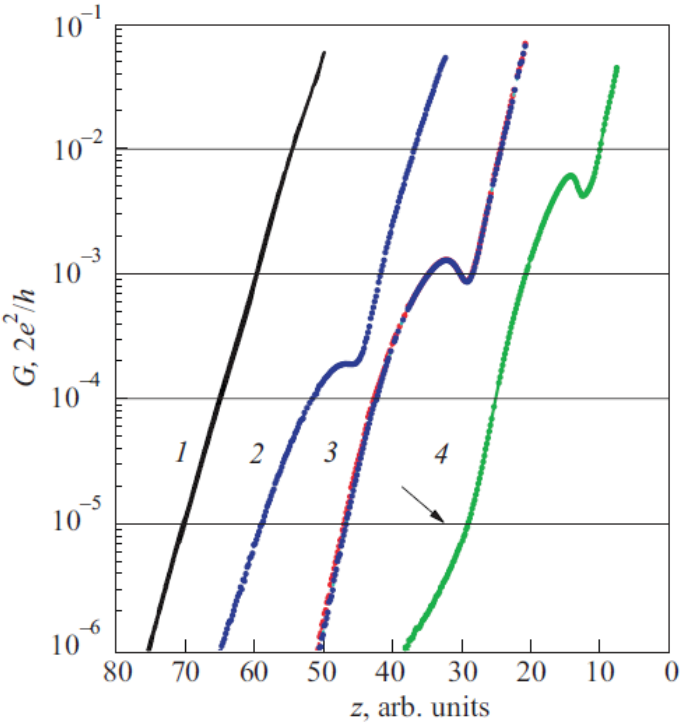

Fig. 2.37: Conductance G versus electrode separation z for a Au nanocontact at 22 K in vacuum (curve 1), and with physisorbed H_2 (curves 2–4). Curve 4 shows the possible presence of a second layer of adsorbed hydrogen molecules at G dependence around $10^{-5}G_0$ (indicated by the black arrow). The deviation from the exponential behavior is attributed to electron scattering at the H_2 layer [2].

take on distinct states upon electron transfer reaction, which can be addressed in Scanning Tunneling Microscopy (STM) via the tunnel voltage. The clusters can be attached to the tip and spontaneous and induced changes in configuration can be studied in the time domain. We developed a preparation protocol for monolayer aggregates of molecule clusters and explored the layers by atomic force microscopy (AFM) and STM.

Molecular Aggregates Studied by Tunneling Microscopy

Two-dimensional aggregates of tetracyclic organic molecules are quite versatile and can be prepared with favorable intermolecular spacing as to electronic, catalytic, and energy transfer properties. In the past few years we developed instruments and corresponding protocols for tunneling microscopy and spectroscopy experiments for the characterization and manipulation of molecules on surfaces in liquids. Our liquid cell STM allows us to study the dynamics in the aggregates and reactions in organic layers in equilibrium with the solvent. We achieved the monitoring of reaction steps at solid-liquid interfaces in real time and space, on the scale of individual molecules.

To a certain extent, the observed SPM signatures can be attributed not only to the molecular species but also the respective oxidation states.

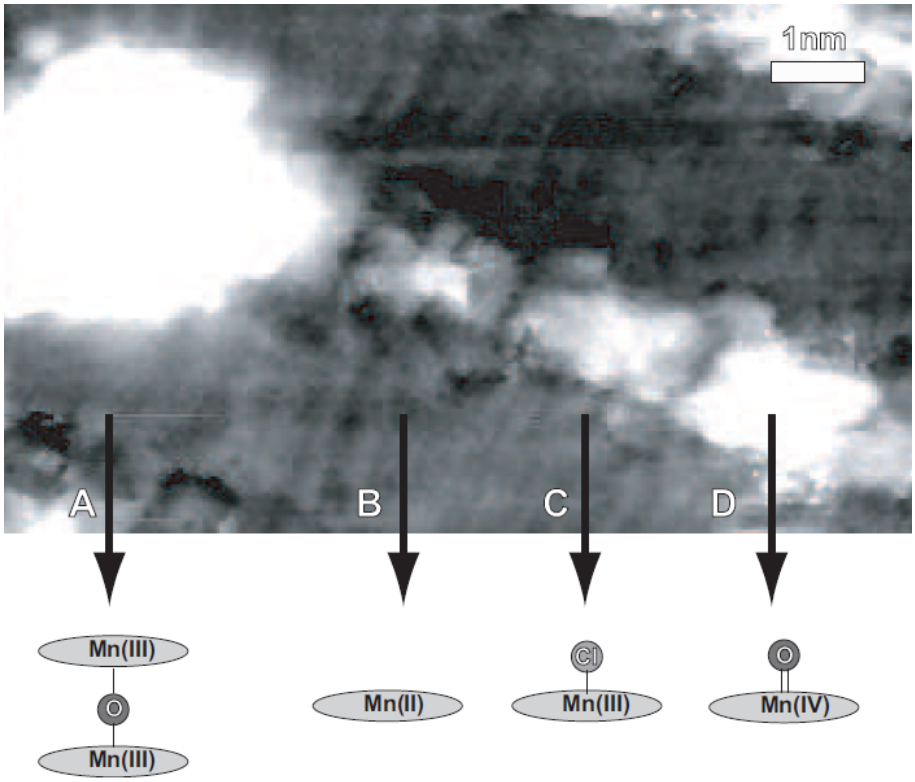

Fig. 2.38: Scanning Tunneling Microscopy topography of Mn porphyrins at the HOPG/octanoic acid interface showing the four distinct states in close vicinity. (D. den Boer, Reactivity of single molecules at a solid/liquid interface , thesis RU Nijmegen, 2012).

Nanoelectronic and -chemical Properties of Porphyrin Layers

In terms of molecular nanoelectronics, understanding of the origin of conductivity changes, stability and controlled switchability of states is desirable. Also in terms of catalytic applications knowledge about the nature of molecular excitations and their dynamics is sought. Our aim is to structure molecular layers, e.g. by command layers or by means of AFM based nanostructuration. These aggregates are characterized in terms of surface potential and electronic transitions. Taking Mn as a metal center, leads to a maximum number of redox states being accessible while with Cu porphyrin electron transfer reactions rather involve the organic parts and require high electric fields.

Biophysical Interactions on the Nanoscale

Morphology of nucleic acids and protein adsorbed to surfaces is accessible via AFM. The observed configurations depend on a number of factors such as the interaction with the medium and the surface modification. In the AFM liquid cell viral bonds in individual complexes can be exposed to pharmacologic agents at different concentrations. Effectiveness in blocking high affinity binding sites to prevent specific binding can be assessed on the basis of force spectroscopy. We studied be binding and blocking of RNA protein complexe of HI virus [1]. Also cell adhesion phenomena can be addressed by force spectrosocpy. The nanoprobe can be functionalized by living cells, while on the sample side molecules can be nanografted (J. te Riet, Force spectroscopy to understand cell surface receptor interactions in the immune system, thesis RU Nijmegen, 2010)

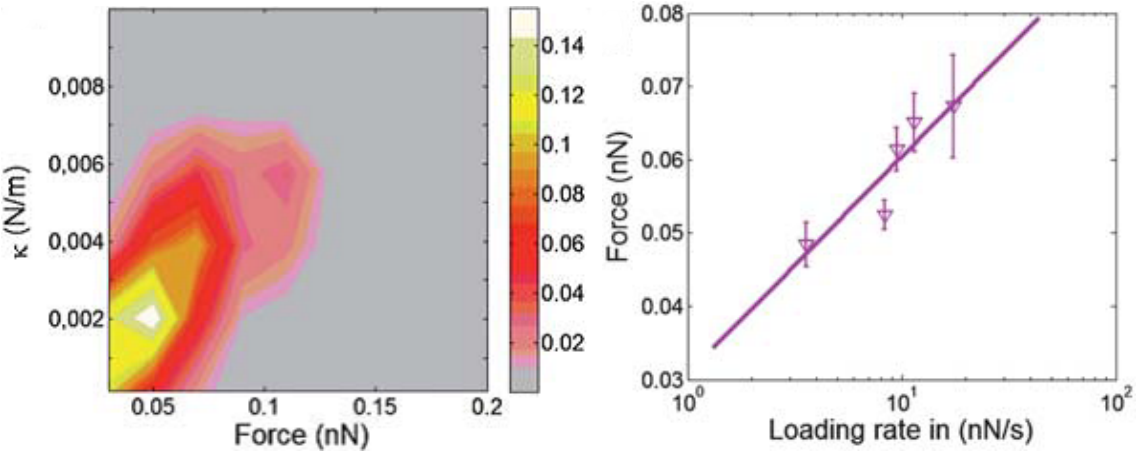

Fig. 2.39: Contour plot with the histogram of rupture forces plotted against the histogram of effective spring constants for wild type RNA protein complexes (RRE–Rev peptide). The graph shows one strong peak at kappa $\approx 0.0026\,\mathrm{N/m}$, indicating the existence of a single binding mode. The dynamic force plot obtained from the most probable forces and loading rates yields the dissociation rate and a barrier width[1].

Studies by AFM and magnetic force microscopy, in combination with electron microscopy and fluorescence microscopy allow one to correlate the different information channels. Correlative microscopy can contribute to elucidate the transduction mechanism in magneto reception involving magnetite nanoparticles. Our studies of salmon nasal epithelium revealed the distribution of magnetic material among the cells.

Scanning Ion Conductance Microscopy to Elucidate Synaptogenesis

Recently we started to study processes at surfaces of living cells. Interaction in scanning probe microscopy can be accompanied by undesired manipulation of the sample. This is especially delicate as it comes to extremely soft and vulnerable samples such as live cells with their dynamic involved surfaces. It is important to find strategies to further minimize the interaction between the nanoprobe with the sample. In that respect, recent developments have unfolded the huge potential of Scanning Ion Conductance Microscopy (SICM). This type of SPM is extremely gentle because the ion flow through a nanopipette opening is employed. It enables the acquisition of topographies on cell surfaces of living neurons with nanoscopic resolution. The nanoprobe can also be used to deliver and uptake minute volumes of messengers and individual nanoparticles such as vesicles, and serve as a local electrode. In collaboration with Dr. WJJM Scheenen (Donders Centre for NeuroScience, RU Nijmegen) and Dr. NN Kasri (Donders Centre for Brain, Cognition, and behavior, Nijmegen) we investigate rat embryonic hippocampal neurons. These neurons are on the verge of neurite outgrowth initially, will successively couple and form networks within a few weeks. In our experiments we combine SICM with more established methods such as fluorescence microscopy and patch-clamp electrophysiology. The correlation of morphologic, optical, and electrophysiological results allows us to elucidate mechanisms that control neuroplasticity, especially at the level of synapses, where interneuronal communication and integration of information take place.

References

[1] J. Zivkovic, L. Janssen, F. Alvarado, H. Heus and S. Speller. "Force spectroscopy of Rev-peptide-RRE interaction from HIV-1". *Soft Matter*, **8** (2012), 2103.

[2] M. van der Maas, S. Vasnyov, B. Hendriksen, O. Shklyarevskii and S. Speller. "Electron scattering effects at physisorbed hydrogen molecules on break-junction electrodes and nanowires formation in hydrogen environment". *Low Temp. Phys.*, **38** (2012), 517.

[3] G. Salassa, M. Coenen, S. Wezenberg, B. Hendriksen, S. Speller, J. Elemans and A. Kleij. "Extremely Strong Self-Assembly of a Bimetallic Salen Complex Visualized at the Single-Molecule Level". *J. Am. Chem. Soc.*, **134** (2012), 7186.

[4] M. Coenen, M. Cremers, D. den Boer, F. van den Bruele, T. Khoury, M. Sintic, M. Crossley, W. van Enckevort, B. Hendriksen, J. Elemans and S. Speller. "Little exchange at the liquid/solid interface: defect-mediated equilibration of physisorbed porphyrin monolayers". *Chem. Commun.*, **47** (2011), 9666.

[5] D. den Boer, O. Shklyarevski, M. Coenen, M. van der Maas, T. Peters, J. Elemans and S. Speller. "Mechano-Catalysis. Cyclohexane Oxidation in a Silver Nanowire Break Junction". *J. Phys. Chem.*, **115** (2011), 8295.

[6] D. den Boer, T. Habets, M. Coenen, M. van der Maas, T. Peters, M. Crossley, T. Khoury, A. Rowan, R. Nolte, S. Speller and J. Elemans. "Controlled Templating of Porphyrins by a Molecular Command Layer". *Langmuir*, **27** (2011), 2644.

[7] J. te Riet, A. Katan, C. Rankl, S. Stahl, A. van Buul, I. Phang, A. Gomez-Casado, J. Gerritsen, A. Cambi, A. Rowan, G. Vancso, P. Jonkheijm, J. Huskens, T. Oosterkamp, H. Gaub, P. Hinterdorfer, C. Figdor and S. Speller. "Interlaboratory round robin on cantilever calibration for AFM force spectroscopy". *Ultramicroscopy*, **111** (2011), 1659.

[8] J. te Riet, T. Smit, M. Coenen, J. Gerritsen, A. Cambi, J. Elemans, C. Figdor and S. Speller. "AFM topography and friction studies of hydrogen-bonded bilayers of functionalized alkanethiols". *Soft Matter*, **6** (2010), 3450.

[9] J. Elemans, S. Wezenberg, M. Coenen, E. Escudero-Adan, J. Benet-Buchholz, D. den Boer, S. Speller, A. Kleij and S. De Feyter. "Axial ligand control over monolayer and bilayer formation of metal-salophens at the liquid.solid interface". *Chem. Commun.*, **46** (2010), 2548.

[10] J. Zivkovic, L. Janssen, H. Heus, M. Mitrovic, B. Tadic and S. Speller. "Network theory approach for data evaluation in the dynamic force spectroscopy of biomolecular interactions". *Europhys. Lett.*, **89** (2010), 68004.

[11] J. te Riet, T. Smit, J. Gerritsen, A. Cambi, J. Elemans, C. Figdor and S. Speller. "Molecular Friction as a Tool to Identify Functionalized Alkanethiols". *Langmuir*, **26** (2010), 6357.

[12] E. Dubrovin, J. Gerritsen, J. Zivkovic, I. Yaminsky and S. Speller. "The effect of underlying octadecylamine monolayer on the DNA conformation on the graphite surface". *Colloids Surf., B*, **76** (2010), 63.

[13] D. den Boer, M. Coenen, J. Elemans and S. Speller. *Scanning Probe Microscopy of Chemistry at solid-liquid interfaces*, chapter 22, page 411. Encyclopedia of Nanoscience and Nanotechnology, 2nd edition, H. S. Nalwa (Editor). American Scientific Publishers (2011).

2.2.5 Electron Scattering – Insulator Physics

Head: Prof. Dr. Hans-Joachim Fitting

Bis 2010 bestehende Arbeitsgruppe: **"Elektronenstreuung und Isolatorphysik"**

The research group is dealing with electron scattering, spectroscopy, and microscopy mainly in wide-gap dielectrics and insulators. Therefore, the electron energies cover the wide range from meV to MeV. Consequently, eleastic and ineleastic interactions of electrons with atoms, with core and valence band electrons as well as collective interactions with plasmons and phonons are taken into account and have been transformed to Monte-Carlo (MC) simulations associated to our experiments of electron emission, spectroscopy, and microscopy in thin layers and structured solids as well as of hot and ballistic electron transport in semiconductors and dielectric layers. During the last period of research, 2010-12, scanning transmission electron microscopy (STEM) and energy filtered transmission electron microscopy (EFTEM) in combination with electron energy loss spectroscopy (EELS), and cathodoluminescence (CL) have been used to investigate Si^+ ion beam mixing and Si nanocluster formation at the interface SiO_2/Si of amorphous silicon dioxide layers to crystalline Si substrate. After high fluence Si^+ ion implantation near to the interface an ion-beam mixed SiO_x buffer layer in this region is detected by means of EFTEM and EELS, demonstrated in Fig. 2.40. towards and into the Si substrate. This structure is due to atomic knock-on and knock-off effects and respective ion beam mixing processes during the Si^+ ion implantation near and into the SiO_2/Si interface region. Thus the interface layer is smeared out and extended over 20 nm, even 10 nm into the previous Si substrate and consists mainly of an understoichiometric SiO_x matrix $2 < x < 0$ with gradually decreasing of x

The respective CL spectra in the near infrared (NIR) region indicate such structural changes by appearance of an additional side-band shifting with thermal annealing from the red band R towards lower energies, very probably caused by Si nanocluster growth and respective quantum confinement effects as we have published in several articles [1–24].

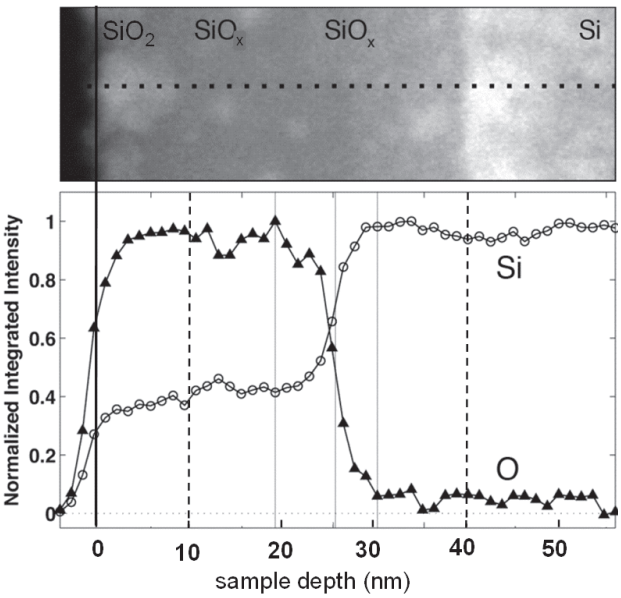

Fig. 2.40: STEM micrograph and EELS profile over the gradual SiO_x interface.

References

[1] D. Zatsepin, S. Kaschieva, M. Zier, B. Schmidt and H.-J. Fitting. "X-ray Emission Spectroscopy of a SiO_2/Si Interface after Si^+ ion Implantation and Ion Beam Mixing". *Phys. Stat. Sol. A*, **207** (2010), 743 – 747.

[2] A. Matoussi, F. Ben Nasr, T. Boufaden, R. Salh, Z. Fakhfakh, S. Guermazi, B. Eljani and H.-J. Fitting. "Luminescente Properties of GaN Films Grown on Porous Silicon Substrate". *J. of Luminescence*, **130** (2010), 399 – 403.

[3] A. Shakhmin, I. Sedova, S. Sorokin, H.-J. Fitting and M. Zamoryanskaya. "ZnSe Based Films Characterization by Cathodoluminescence". *Physica B*, **404** (2010), 5016 – 5018.

[4] A. Shakhmin, I. Sedova, S. Sorokin, H.-J. Fitting and M. Zamoryanskaya. "Cathodoluminescence of Wide-Band-Gap II-VI Quaternary Alloys". *Phys. Stat. Sol. C*, **7** (2010), 1457 – 1459.

[5] H.-J. Fitting, L. Fitting Kourkoutis, R. Salh, M. Zamoryanskaya and B. Schmidt. "Silicon Nanocluster Aggregation in SiO_2:Si Layers". *Phys. Stat. Sol. A*, **207** (2010), 117 – 123.

[6] H.-J. Fitting, L. Fitting Kourkoutis, R. Salh, E. Kolesnikova, M. Zamoryanskaya, A. v. Czarnowski and B. Schmidt. "Silicon Cluster Aggregation in Silica Layers". *Solid State Phenomena*, **156 - 158** (2010), 529 – 533.

[7] M. Touzin, D. Goeriot, C. Guerret-Piécourt, D. Juvé and H.-J. Fitting. "Alumina Based Ceramics for High-Voltage Insulation". *J. European Ceramic Society*, **30** (2010), 805 – 817.

[8] A. Zatsepin, V. Pustovarov, E. Buntov and H.-J. Fitting. "Low Temperature Photoluminescence of SiO_2 Films Implanted with Sulfur Ions". *HASYLAB Annual Report 2009, Hamburg, March 2010*, (2010).

[9] H.-J. Fitting. "Ultrafast Relaxation of Electrons and Selfconsistent Electrical Charging of Insulators". *Radiation Measurements*, **45** (2010), 530 – 532.

[10] H.-J. Fitting and M. Touzin. "Time-dependent Start-up and Decay of Secondary Electron Emission in Dielectricse". *J. Appl. Phys.*, **108** (2010), 033711.

[11] H.-J. Fitting and M. Touzin. "Fast Electron Beam Switching in Dielectric Samples". *Microscopy & Microanalysis USA*, **16** (2010), 264 – 265.

[12] H.-J. Fitting and D. Zatsepin. "Si^+ Implantation into SiO_2 Layers and Ion Beam Mixing in SiO_2/Si Interfaces". *Microscopy & Microanalysis USA*, **16** (2010), 1532 – 1533.

[13] A. F. Zatsepin, E. Buntov, V. Kortov, H.-J. Fitting and Y. S. Posonov. "Photoelectron Emission from Implanted SiO_2:Se^+ Films". *Bulletin of the Russian Academy of Science (RAS) Physics*, **74** (2010), 201 – 205.

[14] H.-J. Fitting, D. Zatsepin, L. Fitting Kourkoutis and B. Schmidt. "Si^+ Ion Implantation in Silica and Ion Beam Mixing in SiO_2/Si Interfaces". *Phys. Stat. Sol. C*, **8** (2011), 1398 – 1402.

[15] H.-J. Fitting, M. Touzin and E. Schreiber. "Fast Electron Beam Charge Injection and Switching in Dielectrics". *Phys. Stat. Sol. C*, **8** (2011), 1282 – 1286.

[16] D. Zatsepin, P. Mack, A. Wright, B. Schmidt and H.-J. Fitting. "XPS Analysis and Valence Band Structure of a Low-dimensional SiO_2/Si System after Si^+ Ion Implantation". *Phys. Stat. Sol. A*, **208** (2011), 1658 – 1661.

[17] H.-J. Fitting and M. Touzin. "Secondary Electron Emission and Self-consistent Charge Transport in Semi-insulating Samples". *J. Appl. Phys.*, **110** (2011), 044111.

[18] H.-J. Fitting and M. Touzin. "SEM Charge Contrast of Semi-insulating Samples". In "Microscopy Conference MC", Kiel, Germany (2011). Rep. IM7_P 185.

[19] H.-J. Fitting, L. Fitting Kourkoutis and B. Schmidt. "EFTEM and STEM Imaging of an Ion-beam Mixed SiO_2/Si Interface". In "Microscopy Conference MC", Kiel, Germany (2011). Rep. IM7_P 112.

[20] W. Li, H.-J. Fitting and W. Bauhofer. "SEM Imaging of Carbon Nanotubes on Glass, Au Layers, and in Epoxy". In "Microscopy Conference MC", Kiel, Germany (2011). Rep. IM7_P 187.

[21] E. Buntov, A. Zatsepin, V. Kortov, V. Pustovarov and H.-J. Fitting. "Electronic and Vibrational States of Oxygen and Sulfur Molecular Ions inside Implanted SiO_2 Films". *J. Non-Chrys. Sol.*, **357** (2011), 1977 – 1980.

[22] W. Li, Y. Zhou, H.-J. Fitting and W. Bauhofer. "Imaging Mechanism of Carbon Nanotubes on Insulating and Conductive Substrates Using a Scanning Electron Microscope". *J. Material Science*, **46** (2011), 7626–7632.

[23] H.-J. Fitting, L. Fitting Kourkoutis, B. Schmidt, B. Liedke, E. V. Ivanova, M. Zamoryanskaya, V. Pustovarov and A. Zatsepin. "Electron Microscopic Imaging of an Ion Beam Mixed SiO_2/Si Interface Correlated with Photo- and Cathodoluminescence". *Phys. Stat. Sol. A*, **1 - 8** (2012), 1101 – 1108.

[24] A. Zatsepin, E. Buntov, H.-J. Fitting, B. Schmidt, V. Pustovarov and N. Gavrilov. "Low Temperature Photoluminescence of Ion-Implanted SiO_2:Sn^+ Films and Glasses". *Journal of Surface Investigation, X-ray Spectroscopy, Synchrotron and Neutron Techniques*, **6** (2012), 668 – 672.

2.3 Physics of Particles and Fields

2.3.1 Quantum Theory and Many-Particle Systems

Head: Prof. Dr. Dieter Bauer

Staff:	Prof. Dr. Gerd Röpke (emeritus)	
	PD Dr. Reinhard Mahnke	PD Dr. Heidi Reinholz
	Dr. Tatyana Liseykina	Dr. Yaroslav Lutsyshyn
	Dr. Christof Liebe	Dr. Banaz Omar
	Dr. Yultuz Omarbakiyeva	Dr. Thomas Raitza
	Dr. Michael Ruggenthaler	Dr. Andrea Sengebusch
	Dr. Takaaki Sogo	Dr. August Wierling
	Dipl.-Phys. Niels-Uwe Bastian	MSc Martins Brics
	MSc Yiling Chen	MSc Varun Kapoor
	Dipl.-Phys. Thomas Keil	Dipl.-Phys. Sonja Lorenzen
	Dipl.-Phys. Volker Mosert	Dipl.-Phys. Norbert Weinkauf
	Tian-Min Yan	
	Mohammad Adel-Almajid	Nils Fahrenkamp
	Julius Rapp	Franziska Reimann
	Marina Hertzfeldt	
Dipl.-Phys. Graduates:	Niels-Uwe Bastian Thomas Keil Norbert Weinkauf	
MSc Graduates:	Martins Brics	
BSc Graduates:	Nils Fahrenkamp Julius Rapp Franziska Reimann	
	Konstantin Schaar	Sebastian Rosmej

Photoelectron Holography and Quantum Orbits

Photoelectron spectra contain a wealth of information about both the target and the laser pulse and thus can be potentially used for time-resolved imaging. However, the interaction of the outgoing photoelectron with the residual target needs to be understood before the richly structured photoelectron spectra can be interpreted. This interaction is usually neglected in the strong field approximation. We continued with the further development of our semi-classical quantum-trajectory based strong field approximation with Coulomb correction, which is capable of interpreting strong laser-field matter interaction phenomena in terms of interfering quantum orbits. In particular, we investigated the origin of holographic side-lobes in photoelectron spectra [1, 2] that might be useful for imaging atomic and molecular structure in a time-resolved manner, and the experimentally observed so-called "low energy structure" (LES), see Fig. 2.41 [3], i.e., an unexpectedly high yield of photoelectrons at low energy. We were also able to account for the sub-barrier Coulomb correction, which leads to a shift of interference fringes in photoelectron spectra [4].

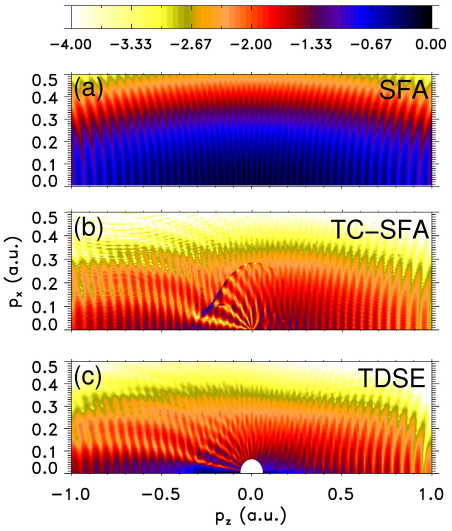

Fig. 2.41: Logarithmically scaled photoelectron momentum distributions in the $p_z p_x$-plane for argon in an intense laser pulse (polarization direction $p_{\parallel} = p_z$) calculated using (a) plain strong field approximation (SFA), (b) our semi-classical quantum trajectory-based approach (TC-SFA), and (c) numerical solution of the time-dependent Schrödinger equation (TDSE). Laser parameters: $I = 100\,\mathrm{TW/cm^2}$, $\lambda = 2\,\mu\mathrm{m}$, 3-cycle $\sin^2$ pulse. The overemphasized caustic feature in (b) helped identifying the mechanism underlying the LES. From Ref. [3].

Time-Dependent Density Functional Theory

Time-dependent density functional theory (TDDFT) is a central topic for the group and also is at the heart of subproject A9 within the SFB 652. As TDDFT has many practical limitations when it comes to phenomena beyond linear response theory, we focus both on fundamental issues and improvements of TDDFT, and applications where possible. In particular, we applied TDDFT to the study of core-hole relaxation in clusters [5]. In the experimental subproject A1 of the SFB 652, metal clusters were exposed to free electron laser (FEL) radiation at FLASH, DESY, Hamburg [6]. From the photoelectron peak positions core-electron binding energies were determined as a function of the cluster size. Deviations from the metal-sphere behavior indicate a changing screening capability in the system and thus point towards structural changes. Other activities in the TDDFT domain concerned fundamental issues such as the generalization of the Runge-Gross theorem [7], the applicability of TDDFT to quantum electrodynamics [8], and the possibility to combine TDDFT with Floquet theory [9].

Radiation Reaction Effects in Super-Intense Laser-Plasma Interaction

Polarization and radiation reaction effects in the interaction of a superintense laser pulse ($I > 10^{23}\,\mathrm{W/cm^2}$) with a thin plasma foil were investigated with particle-in-cell (PIC) simulations [10–12]. It was found that the radiation reaction force leads to a significant electron cooling and to an increased spatial bunching of both electrons and ions. For a linearly polarized laser pulse, strong anisotropies such as the formation of two high-energy clumps in the plane perpendicular to the propagation direction and significant radiation reactions effects were observed. As opposed to this, neither anisotropies nor significant radiation reaction effects were observed using circularly polarized laser pulses, for which the maximum ion energy exceeded

the value obtained in simulations of lower dimensionality. The dynamical bending of the initially flat plasma foil leads to the self-formation of a quasiparabolic shell that focuses the impinging laser pulse, strongly increasing its energy and momentum densities.

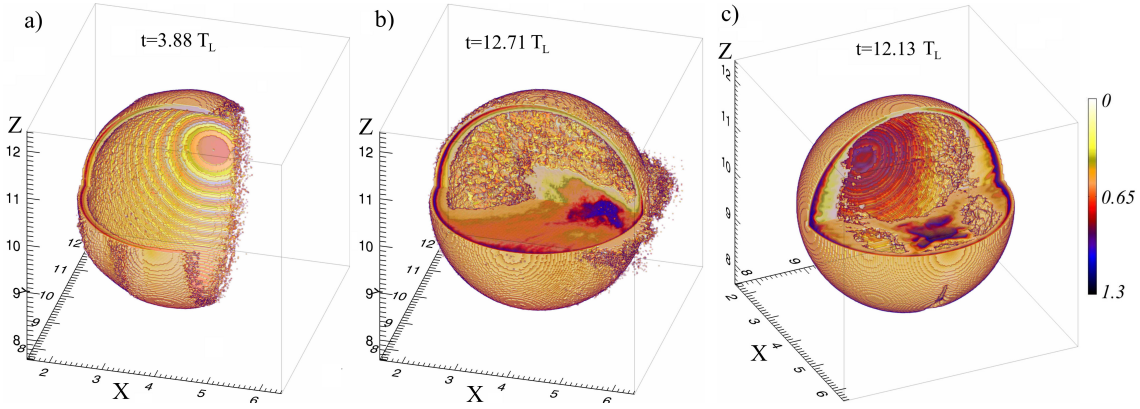

Fig. 2.42: Ionization dynamics of a He droplet. Electron density in the beginning (a) and the end (b) of the interaction with a laser pulse. He^{2+} density (c) at the end of the interaction. For better visualization of the droplet interior a quarter of it was cut-out. Laser and droplet parameters: $5.2 \times 10^{17}\,\mathrm{W/cm^2}$, $\lambda = 800\,\mathrm{nm}$, radius $R = 2\lambda = 3.2\,\mu\mathrm{m}$, density $\rho = 0.14\,\mathrm{g/cm^{-3}}$.

Intense Laser-Droplet Interaction

The interaction of high-intensity femtosecond laser pulses with He droplets was studied with PIC simulations. It was found that multi-MeV electron bunches of attosecond duration are produced when intense laser fields interact with overdense droplets of diameters comparable to the laser wavelength [13]. These bunches are emitted each half-laser cycle alternatingly under plus and minus a certain angle with respect to the wave vector of the incoming plane wave in the polarization plane. The preferred electron emission angles and the high kinetic energies arise due to local field enhancements at the droplet surface that can be calculated using Mie theory.

Using PIC simulations with ionization included we find that, despite the fact that the plasma created at the droplet surface is overdense, oscillating electric fields may penetrate into the droplet under a certain angle, ionize and propagate in the just generated plasma. Again, this effect is due to the local field enhancement at the droplet surface. The penetration of the fields into the droplet leads to the formation of a highly inhomogeneous charge density distribution in the droplet interior, see Fig. 2.42, which may be probed via Thomson scattering at FEL facilities (collaboration with the Redmer group, see also A2 within the SFB 652).

Proton Acceleration with Intense Chirped Laser Pulses

The interaction of a frequency-chirped laser pulse with single protons and a hydrogen gas target was studied analytically and by means of PIC simulations [14]. The feasibility of generating ultraintense (10^7 particles per bunch) and phase-space collimated beams of protons (energy spread of about 1 %) was demonstrated. Phase synchronization of the protons and the laser field, guaranteed by the appropriate chirping of the laser pulse, allows the particles to gain sufficient kinetic energy (around 250 MeV) required for applications such as hadron cancer therapy.

Mega-Gauss Magnetic Field Generation at Laser-Irradiated Foils

We provided numerical support to an experimental study at the Vulcan laser system, Rutherford Appleton Laboratory, of the dynamics of intense magnetic fields (amplitudes on the order of 50 MGauss) at the surfaces of solid targets, irradiated with high intensity ($I \simeq 10^{19}\,\mathrm{W/cm^2}$), short ($\sim 1\,\mathrm{ps}$) laser pulses [15]. Temporally and spatially resolved proton imaging indicates the generation of toroidal magnetic fields having tens of megagauss strength on both sides of a foil. The magnetic fields are strong enough to effectively confine the radial expansion of the plasma, thus possibly affecting the ion acceleration in the expanding sheath. The presence of megagauss magnetic fields of opposite polarity at both sides of the target is also supported by two-dimensional (2D) PIC simulations. see Fig. 2.43.

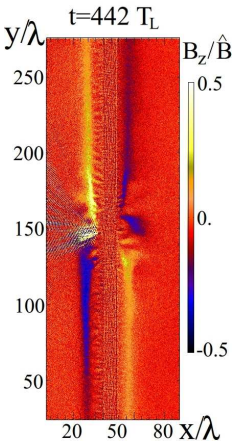

Fig. 2.43: Transverse magnetic field distribution at $t \simeq 1.5\,\mathrm{ps}$ in units of $B_0 = 107\,\mathrm{MG}$, generated at the front and rear surfaces of a thin foil, irradiated by a high-intensity laser pulse of duration 0.8 ps, intensity $10^{19}\,\mathrm{W/cm^2}$, incidence angle 20°. The initial density profile of the target was composed of an exponential ramp, followed by a plasma bulk with electron density $n_e = 44 \times 10^{21}\,\mathrm{cm^{-3}}$. A charge-to-mass ratio $Z/A = 9/26$ is assumed. From [15].

Properties of Quantum Point Defects in Supersolids

Point defects in bosonic solids may lead to Andreev–Lifshitz supersolidity. We investigated a range of properties of vacancy defects in solid ^{4}He at zero and very low temperatures [16]. A detailed calculation allowed us to describe the thermodynamic properties of quantum defects as a function of pressure, thus permitting comparison with experimental results.

Both perfect and defected ^{4}He solids were studied with first-principles numerical methods to determine the entire set of elastic constants of hexagonal close-packed (hcp) ^{4}He [17], following recent findings that the elastic properties of ^{4}He crystals change along with what appears to be a non-classical rotation of solid helium.

Ordered Phases of Model Rydberg Systems

Clouds of up to several thousand Rydberg atoms are routinely created in the laboratory to study the Rydberg blockade. We have numerically studied the equilibrium phase diagram of atoms with model repulsive van der Waals interaction, a common case in the blockade experiments. A universal phase diagram was calculated, mapping the conditions according to the interaction strength, atomic mass, temperature and density [18].

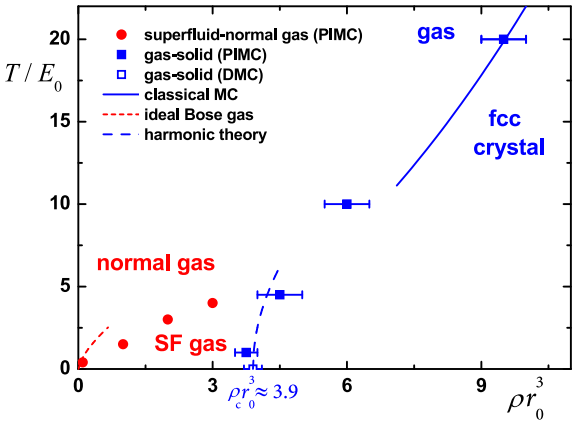

Fig. 2.44: Phase diagram of particles interacting with repulsive r^{-6} interaction. Phase transitions were determined numerically with diffusion, classical, and path-integral Monte Carlo methods. Density and temperatures are scaled to universal units determined by the interaction strength, particle density and mass, and system temperature, as described in Ref. [18].

Transport Properties of Dense Plasmas

Using linear response theory, quantum statistical approaches were worked out to relate the dynamical conductivity to equilibrium correlation functions. Comparisons with kinetic theory and the relaxation time approximation were performed. Interpolation formulae valid for a wide range of frequencies were discussed [19–22].

We investigated the wave-vector dependence of dynamical correlations in dense plasmas using different methods. In particular, a new interpolation scheme that accounts for dynamic collisions and electron correlations (local field corrections) was established. Consequences for plasmon dispersion and Thomson scattering were studied and used to explain recent experiments (FLASH) [23–25].

Dynamical Structure Factor and Optical Properties of Finite Dense Plasmas

We investigated the bi-local frequency-dependent structure factor for nanoplasmas (metallic clusters excited by ultra-short intense laser pulses) at various temperatures,

densities, particle numbers and ionization degree. Restricted MD simulations (classical, fixed ion configuration) were compared with quantum statistical approaches (density functional theory). Resonance structures were investigated, the relation between current density and particle density correlation functions was shown. Different collective excitations were identified and characterized by the spatial distribution of the current auto-correlation function [26], see Fig. 2.45. To compare with bulk properties, size effects of the Mie mode and the bulk plasmon-like excitation were considered. Furthermore, the dependence of damping rates on the cluster size was studied [27–29].

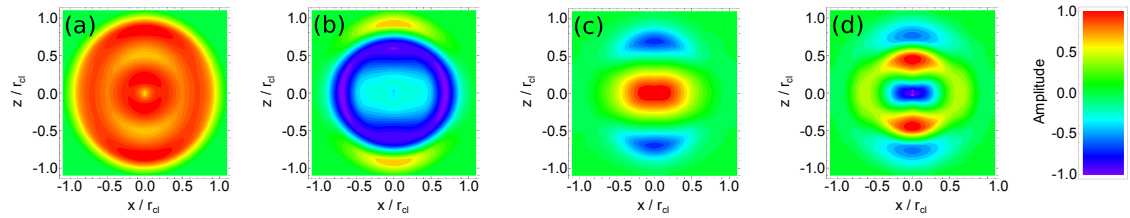

Fig. 2.45: Resonances of dipole-like modes of laser excited Na_{1000}-clusters for temperature $T = 1\,\mathrm{eV}$, ion density $n = 2.8 \cdot 10^{22}\,\mathrm{cm}^{-3}$, cluster charge state $Z = 16$ [26]. Resonances occur at frequencies $4.80\,\mathrm{fs}^{-1}$ (a), $6.18\,\mathrm{fs}^{-1}$ (b), $9.15\,\mathrm{fs}^{-1}$ (c), $8.23\,\mathrm{fs}^{-1}$ (d); for comparison, the plasmon frequency at the same density is $\omega_\mathrm{p} = 9.4\,\mathrm{fs}^{-1}$, the Mie frequency $5.5\,\mathrm{fs}^{-1}$.

Spectral Line Profiles in Dense Plasmas

Interactions with surrounding particles alter the states of an emitter emerged in a dense plasma. Thus, spectral lines are strongly broadened and shifted compared to their isolated, atomic counterparts. Our quantum statistical approach was modified, with a focus on strong electron-emitter collisions, and applied to hydrogen [30–33] and helium. Furthermore, the role of ion-dynamics for spectral line shapes was analyzed employing different approaches to ion-dynamics (frequency fluctuation model and model microfield method).

X-ray spectroscopy is an important tool for diagnostics of dense plasmas. K_α spectra of mid-Z atoms such as Si, Cl, and Ti, produced by strong laser irradiation or ion collisions, were analyzed. A blue-shift due to ionization/excitation satellites and a red shift due to screening by free electrons in the plasma compete to form the K_α line profile. Silicon spectra obtained at GSI Darmstadt were analyzed. The temperature and density profile of the laser excited plasma was inferred from measured titanium spectra, see Fig. 2.46 and Refs. [34, 35]. This was accomplished within a GIF-project (I-880-135.7/2005) that ended successfully in 2010.

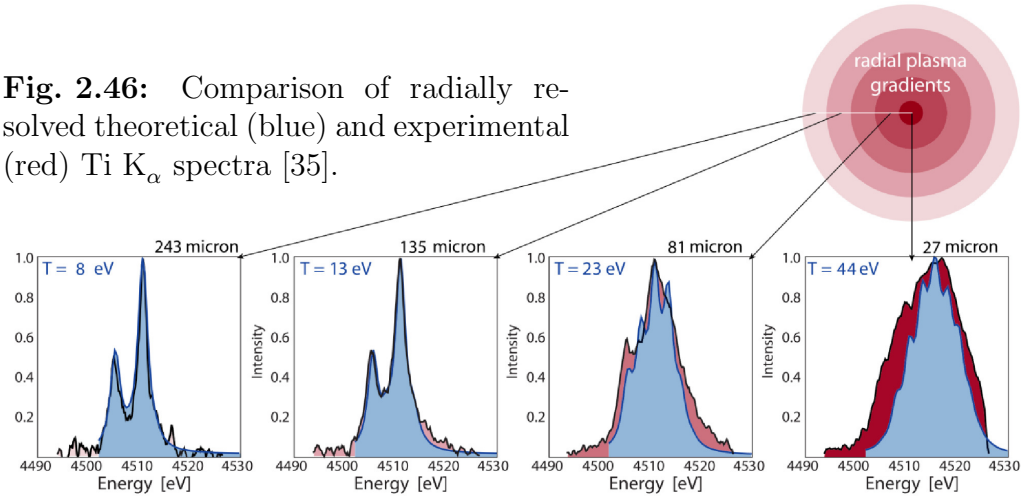

Fig. 2.46: Comparison of radially resolved theoretical (blue) and experimental (red) Ti K_α spectra [35].

Thermodynamics and Cluster Virial Expansions in Dense Quantum Systems

The Beth-Uhlenbeck formula for the second virial coefficient was extended to a chemical model where bound states are considered as elementary constituents [36–38]. A quasiparticle concept was introduced where double counting had to be avoided. Within a generalized Beth-Uhlenbeck approach to a partially ionized plasma, electron-atom and electron-molecule scattering were included [39]. Cluster virial expansions were considered also for nuclear matter.

Clusters and Quantum Condensates in Nuclear Matter

The equation of state of nuclear matter at finite temperature and density with various proton fractions was further worked out [40–44], in particular the region of medium excitation energy given by the temperature range $T \leq 30\,\mathrm{MeV}$ and the baryon density range $\rho_B \leq 10^{14.2}\,\mathrm{g/cm^3}$. In addition to mean-field effects, the formation of few-body correlations, in particular light bound clusters up to the α-particle ($1 \leq A \leq 4$), and their in-medium shift (Pauli blocking) have to be considered. The shift data are reproduced by fit formulae in good approximation.

New results were obtained for quantum correlations in hot dense matter (alpha condensates, alpha-like correlations in excited light nuclei). A mean-field approach similar to BCS theory was established. Applications are heavy-ion collisions [45–48] and, in astrophysics, supernova explosions [49]. In particular, the influence of cluster formation on the symmetry energy was investigated [50, 51].

An interesting phenomenon is the Bose-Einstein condensation of alpha clusters. New results were elaborated for nuclear matter [52–57]. Intense investigations were performed with respect to the cluster structure of low-density excited states of ^{12}C (Hoyle state) and ^{16}O, see also [58–61].

Kinetic Theory and Decoherence in Quantum Systems

Kinetic theory including strong laser fields was worked out within a quantum-statistical approach [62–64]. Exactly solvable model systems that contain the coupling to a bath were investigated. A solution of the Unruh model with initial correlations was found [65, 66]. The time-evolution of the entropy was considered.

Soliton Transport in Nonlinear Systems

Within an European project (SPARK-FP6-004690, EXPLORA FIS2009-06585), solitonic excitations and transport properties (solectron) in nonlinear systems (Davydov excitons) were investigated. The formation of pairs (bisolectron) and possible Bose condensation were discussed in relation to high-temperature superconductivity [67–70].

Stochastic Theory and Power Laws

Traffic flow theory taking into account randomness was investigated. Based on our understanding of the stochastic nature of traffic breakdown the energy flow balance in driven systems was analyzed [71].

The emergence of power-law distributions in evolving systems is presented in [72, 73] using a master-equation approach. Recent research was focused on how to solve the Fokker-Planck equation treating mixed eigenvalue spectra correctly, see Fig. 2.47.

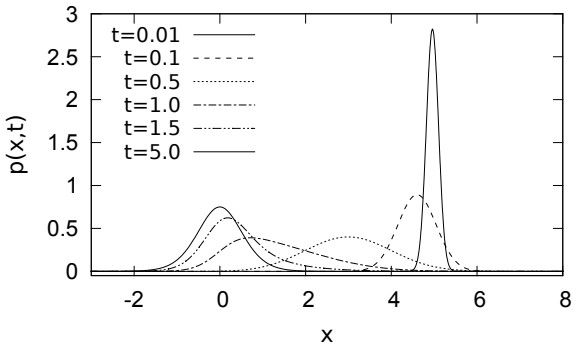

Fig. 2.47: Solution of the Fokker-Planck equation treating a mixed eigenvalue spectrum for the Pöschl-Teller potential. Probability distribution $p(x,t)$ at various time instants.

References

[1] Y. Huismans, A. Rouzée, A. Gijsbertsen, J. H. Jungmann, A. S. Smolkowska, P. S. W. M. Logman, F. Lépine, C. Cauchy, S. Zamith, T. Marchenko, J. M. Bakker, G. Berden, B. Redlich, A. F. G. van der Meer, H. G. Muller, W. Vermin, K. J. Schafer, M. Spanner, M. Y. Ivanov, O. Smirnova, D. Bauer, S. V. Popruzhenko and M. J. J. Vrakking. "Time-Resolved Holography with Photoelectrons". *Science*, **331** (2011), 61–64.

[2] Y. Huismans, A. Gijsbertsen, A. S. Smolkowska, J. H. Jungmann, A. Rouzée, P. S. W. M. Logman, F. Lépine, C. Cauchy, S. Zamith, T. Marchenko, J. M. Bakker, G. Berden, B. Redlich, A. F. G. van der Meer, M. Y. Ivanov, T.-M. Yan, D. Bauer, O. Smirnova and M. J. J. Vrakking. "Scaling Laws for Photoelectron Holography in the Midinfrared Wavelength Regime". *Phys. Rev. Lett.*, **109** (2012), 013002.

[3] T.-M. Yan, S. V. Popruzhenko, M. J. J. Vrakking and D. Bauer. "Low-Energy Structures in Strong Field Ionization Revealed by Quantum Orbits". *Phys. Rev. Lett.*, **105** (2010), 253002.

[4] T.-M. Yan and D. Bauer. "Sub-barrier Coulomb effects on the interference pattern in tunneling-ionization photoelectron spectra". *Phys. Rev. A*, **86** (2012), 053403.

[5] D. Bauer. "Modeling the core-hole screening in jellium clusters using density functional theory". *New J. Phys.*, **14** (2012), 055012.

[6] J. Bahn, P. Oelßner, M. Köther, C. Braun, V. Senz, S. Palutke, M. Martins, E. Rühl, G. Ganteför, T. Möller, B. von Issendorff, D. Bauer, J. Tiggesbäumker and K.-H. Meiwes-Broer. "Pb 4f photoelectron spectroscopy on mass-selected anionic lead clusters at FLASH". *New J. Phys.*, **14** (2012), 075008.

[7] M. Ruggenthaler, M. Penz and D. Bauer. "General Runge-Gross-type theorem for dipole laser-matter interaction". *Phys. Rev. A*, **81** (2010), 062108.

[8] M. Ruggenthaler, F. Mackenroth and D. Bauer. "Time-dependent Kohn-Sham approach to quantum electrodynamics". *Phys. Rev. A*, **84** (2011), 042107.

[9] V. Kapoor and D. Bauer. "Floquet analysis of real-time wave functions without solving the Floquet equation". *Phys. Rev. A*, **85** (2012), 023407.

[10] A. Macchi, M. Tamburini, F. Pegoraro and T. V. Liseykina. "Radiation friction modeling in superintense laser-plasma interactions". *Proc. SPIE*, **8075** (2011), 807509.

[11] M. Tamburini, T. V. Liseykina, F. Pegoraro and A. Macchi. "Radiation-pressure-dominant acceleration: Polarization and radiation reaction effects and energy increase in three-dimensional simulations". *Phys. Rev. E*, **85** (2012), 016407.

[12] M. Tamburini, F. Pegoraro, A. D. Piazza, C. Keitel, T. Liseykina and A. Macchi. "Radiation reaction effects on electron nonlinear dynamics and ion acceleration in laser–solid interaction". *Nucl. Inst. Meth. Phys. Res. A*, **653** (2011), 181 – 185.

[13] T. V. Liseykina, S. Pirner and D. Bauer. "Relativistic Attosecond Electron Bunches from Laser-Illuminated Droplets". *Phys. Rev. Lett.*, **104** (2010), 095002.

[14] B. J. Galow, Y. I. Salamin, T. V. Liseykina, Z. Harman and C. H. Keitel. "Dense Monoenergetic Proton Beams from Chirped Laser-Plasma Interaction". *Phys. Rev. Lett.*, **107** (2011), 185002.

[15] G. Sarri, A. Macchi, C. A. Cecchetti, S. Kar, T. V. Liseykina, X. H. Yang, M. E. Dieckmann, J. Fuchs, M. Galimberti, L. A. Gizzi, R. Jung, I. Kourakis, J. Osterholz, F. Pegoraro, A. P. L. Robinson, L. Romagnani, O. Willi and M. Borghesi. "Dynamics of Self-Generated, Large Amplitude Magnetic Fields Following High-Intensity Laser Matter Interaction". *Phys. Rev. Lett.*, **109** (2012), 205002.

[16] R. Rota, Y. Lutsyshyn, C. Cazorla and J. Boronat. "A Microscopic Description of Vacancies in Solid ^{4}He". *J. Low Temp. Phys.*, **168** (2012), 150.

[17] C. Cazorla, Y. Lutsyshyn and J. Boronat. "Elastic constants of solid ^{4}He under pressure: Diffusion Monte Carlo study". *Phys. Rev. B*, **85** (2012), 024101.

[18] O. N. Osychenko, G. E. Astrakharchik, Y. Lutsyshyn, Y. E. Lozovik and J. Boronat. "Phase diagram of Rydberg atoms with repulsive van der Waals interaction". *Phys. Rev. A*, **84** (2011), 063621.

[19] J. R. Adams, H. Reinholz and R. Redmer. "Application of linear response theory to magnetotransport properties of dense plasmas". *Phys. Rev. E*, **81** (2010), 036409.

[20] V. S. Karakhtanov, R. Redmer, H. Reinholz and G. Röpke. "Transport Coefficients in Dense Plasmas Including Ion-Ion Structure Factor". *Contrib. Plasma Phys.*, **51** (2011), 355–360.

[21] H. Reinholz and G. Röpke. "Dielectric function beyond the random-phase approximation: Kinetic theory versus linear response theory". *Phys. Rev. E*, **85** (2012), 036401.

[22] Y. B. Zaporozhets, V. Mintsev, V. Gryaznov, V. E. Fortov, H. Reinholz and G. Röpke. "The Investigation of s- and p-Polarized Reflectivities of Nonideal Plasma". *Contrib. Plasma Phys.*, **50** (2010), 60–63.

[23] C. Fortmann, A. Wierling and G. Röpke. "Influence of local-field corrections on Thomson scattering in collision-dominated two-component plasmas". *Phys. Rev. E*, **81** (2010), 026405.

[24] R. R. Fäustlin, T. Bornath, T. Döppner, S. Düsterer, E. Förster, C. Fortmann, S. H. Glenzer, S. Göde, G. Gregori, R. Irsig, T. Laarmann, H. J. Lee,

B. Li, K. . H. Meiwes-Broer, J. Mithen, B. Nagler, A. Przystawik, H. Redlin, R. Redmer, H. Reinholz, G. Röpke, F. Tavella, R. Thiele, J. Tiggesbäumker, S. Toleikis, I. Uschmann, S. M. Vinko, T. Whitcher, U. Zastrau, B. Ziaja and T. Tschentscher. "Observation of Ultrafast Nonequilibrium Collective Dynamics in Warm Dense Hydrogen". *Phys. Rev. Lett.*, **104** (2010), 125002.

[25] S. Toleikis, T. Bornath, T. Döppner, S. Düsterer, R. R. Fäustlin, E. Förster, C. Fortmann, S. H. Glenzer, S. Göde, G. Gregori, R. Irsig, T. Laarmann, H. J. Lee, B. Li, K. . H. Meiwes-Broer, J. Mithen, B. Nagler, A. Przystawik, P. Radcliffe, H. Redlin, R. Redmer, H. Reinholz, G. Röpke, F. Tavella, R. Thiele, J. Tiggesbäumker, I. Uschmann, S. M. Vinko, T. Whitcher, U. Zastrau, B. Ziaja and T. Tschentscher. "Probing near-solid density plasmas using soft x-ray scattering". *J. Phys. B*, **43** (2010), 194017.

[26] T. Raitza, H. Reinholz, P. Reinhard, G. Röpke and I. Broda. "Spatially resolved collective excitations of nano-plasmas via molecular dynamics simulations and fluid dynamics". *New J. Phys.*, **14** (2012), 115016.

[27] T. Raitza, I. Broda, H. Reinholz and G. Röpke. "Collective Excitations of Finite-Temperature Nano Plasmas". *Contrib. Plasma Phys.*, **52** (2012), 118–121.

[28] T. Raitza, G. Röpke, H. Reinholz and I. Morozov. "Spatially resolved dynamic structure factor of finite systems from molecular dynamics simulations". *Phys. Rev. E*, **84** (2011), 036406.

[29] T. Raitza, H. Reinholz and G. Röpke. "Dynamical Spatially Resolved Response Function of Finite 1-d Nano Plasmas". *Int. J. Mod. Phys. B*, **24** (2010), 4961.

[30] S. Lorenzen, A. Wierling, H. Reinholz and G. Röpke. "Improved Self-Energy Calculations for Pressure Broadening of Spectral Lines in Dense Plasmas". *Contrib. Plasma Phys.*, **51** (2011), 349–354.

[31] S. Lorenzen, A. Wierling, H. Reinholz, G. Röpke, M. C. Zammit, D. V. Fursa and I. Bray. "Quantum-statistical T-matrix approach to line broadening of hydrogen in dense plasmas". *AIP Conference Proceedings*, **1290** (2010), 99–103.

[32] S. Lorenzen, A. Wierling, H. Reinholz, G. Röpke, M. C. Zammit, D. V. Fursa and I. Bray. "Quantum-statistical line shape calculation for Lyman-α lines in dense H plasmas". *J. Phys. Conf. Ser.*, **397** (2012), 012021.

[33] B. Omar, A. Wierling and G. Röpke. "Diagnostics of High-Pressure Arc Plasmas by Hydrogen Balmer Spectra". *Contrib. Plasma Phys.*, **51** (2011), 22–33.

[34] U. Zastrau, P. Audebert, V. Bernshtam, E. Brambrink, T. Kaempfer, E. Kroupp, R. Loetzsch, Y. Maron, Y. Ralchenko, H. Reinholz, G. Röpke, A. Sengebusch, E. Stambulchik, I. Uschmann, L. Weingarten and E. Förster. "Temperature and K α-yield radial distributions in laser-produced solid-density plasmas imaged with ultrahigh-resolution x-ray spectroscopy". *Phys. Rev. E*, **81** (2010), 026406.

[35] U. Zastrau, A. Sengebusch, P. Audebert, E. Brambrink, R. R. Faeustlin, T. Kaempfer, E. Kroupp, R. Loetzsch, Y. Maron, H. Reinholz, G. Röpke, E. Stambulchik, I. Uschmann and E. Förster. "High-resolution radial K α spectra obtained from a multi-keV electron distribution in solid-density titanium foils generated by relativistic laser-matter interaction". *High Energy Density Phys.*, **7** (2011), 47–53.

[36] W. Ebeling, W. D. Kraeft and G. Röpke. "Bound States in Coulomb Systems — Old Problems and New Solutions". *Contrib. Plasma Phys.*, **52** (2012), 7–16.

[37] W. Ebeling, W.-D. Kraeft and G. Röpke. "On the quantum statistics of bound states within the Rutherford model of matter". *Ann. Phys. (Berlin)*, **524** (2012), 311–326.

[38] R. Redmer and G. Röpke. "Progress in the Theory of Dense Strongly Coupled Plasmas". *Contrib. Plasma Phys.*, **50** (2010), 970–985.

[39] Y. A. Omarbakiyeva, C. Fortmann, T. S. Ramazanov and G. Röpke. "Cluster virial expansion for the equation of state of partially ionized hydrogen plasma". *Phys. Rev. E*, **82** (2010), 026407.

[40] M. Hempel, J. Schaffner-Bielich, S. Typel and G. Röpke. "Light clusters in nuclear matter: Excluded volume versus quantum many-body approaches". *Phys. Rev. C*, **84** (2011), 055804.

[41] G. Röpke. "Parametrization of light nuclei quasiparticle energy shifts and composition of warm and dense nuclear matter". *Nucl. Phys. A*, **867** (2011), 66–80.

[42] G. Röpke. "Light Clusters In Nuclear Matter". *Int. J. Mod. Phys. E*, **20** (2011), 897–901.

[43] G. Röpke. "Light Clusters In Nuclear Matter". *Int. J. Mod. Phys. B*, **24** (2010), 4993.

[44] S. Typel, G. Röpke, T. Klaehn, D. Blaschke and H. H. Wolter. "Composition and thermodynamics of nuclear matter with light clusters". *Phys. Rev. C*, **81** (2010), 015803.

[45] K. Hagel, R. Wada, L. Qin, J. B. Natowitz, S. Shlomo, A. Bonasera, G. Röpke, S. Typel, Z. Chen, M. Huang, J. Wang, H. Zheng, S. Kowalski, C. Bottosso, M. Barbui, M. R. D. Rodrigues, K. Schmidt, D. Fabris, M. Lunardon, S. Moretto, G. Nebbia, S. Pesente, V. Rizzi, G. Viesti, M. Cinausero, G. Prete, T. Keutgen, Y. El Masri and Z. Majka. "Experimental Determination of In-Medium Cluster Binding Energies and Mott Points in Nuclear Matter". *Phys. Rev. Lett.*, **108** (2012), 062702.

[46] J. B. Natowitz, K. Hagel, R. Wada, L. Qin, Z. Chen, P. Sahu, G. Röpke, S. Kowalski, C. Bottosso, S. Shlomo, M. Barbui, D. Fabris, M. Lunardon, S. Moretto, G. Nebbia, S. Pesente, V. Rizzi, G. Viesti, M. Cinausero, G. Prete, T. Keutgen, Y. El Masri and Z. Majka. "Clustered Low Density Nuclear Matter In Near Fermi Energy Collisions". *Int. J. Mod. Phys. E*, **20** (2011), 987–992.

[47] L. Qin, K. Hagel, R. Wada, Z. Chen, M. Huang, S. Kowalski, C. Bottosso, S. Shlomo, M. Barbui, A. Bonasera, M. Rodrigues, J. B. Natowitz, G. Röpke, D. Fabris, M. Lunardon, S. Moretto, G. Nebbia, S. Pesente, G. Viesti, M. Cinausero, G. Prete, V. Rizzi, T. Keutgen, Y. El Masri and Z. Majka. "Low Density Nuclear Matter In Fermi Energy Collisions". *Int. J. Mod. Phys. E*, **19** (2010), 1513–1522.

[48] L. Qin, J. B. Natowitz, G. Röpke, K. Hagel, R. Wada, Z. Chen, M. Huang, S. Kowalski, C. Bottosso, S. Shlomo, M. Barbui, A. Bonasera, M. Rodrigues, D. Fabris, M. Lunardon, S. Moretto, G. Nebbia, S. Pesente, V. Rizzi, G. Viesti, M. Cinausero, G. Prete, T. Keutgen, Y. El Masri and Z. Majka. "Laboratory Studies of low density matter". *Nucl. Phys. A*, **834** (2010), 521c.

[49] L. Qin, K. Hagel, R. Wada, J. B. Natowitz, S. Shlomo, A. Bonasera, G. Röpke, S. Typel, Z. Chen, M. Huang, J. Wang, H. Zheng, S. Kowalski, M. Barbui, M. R. D. Rodrigues, K. Schmidt, D. Fabris, M. Lunardon, S. Moretto, G. Nebbia, S. Pesente, V. Rizzi, G. Viesti, M. Cinausero, G. Prete, T. Keutgen, Y. El Masri, Z. Majka and Y. G. Ma. "Laboratory Tests of Low Density Astrophysical Nuclear Equations of State". *Phys. Rev. Lett.*, **108** (2012), 172701.

[50] J. B. Natowitz, G. Röpke, S. Typel, D. Blaschke, A. Bonasera, K. Hagel, T. Klaehn, S. Kowalski, L. Qin, S. Shlomo, R. Wada and H. H. Wolter. "Symmetry Energy of Dilute Warm Nuclear Matter". *Phys. Rev. Lett.*, **104** (2010), 202501.

[51] R. Wada, K. Hagel, L. Qin, J. B. Natowitz, Y. G. Ma, G. Röpke, S. Shlomo, A. Bonasera, S. Typel, Z. Chen, M. Huang, J. Wang, H. Zheng, S. Kowalski, C. Bottosso, M. Barbui, M. R. D. Rodrigues, K. Schmidt, D. Fabris, M. Lunardon, S. Moretto, G. Nebbia, S. Pesente, V. Rizzi, G. Viesti, M. Cinausero, G. Prete, T. Keutgen, Y. El Masri and Z. Majka. "Nuclear matter symmetry energy at $0.03 \leq \rho/\rho(0) \leq 0.2$". *Phys. Rev. C*, **85** (2012), 064618.

[52] Y. Funaki, M. Girod, H. Horiuchi, G. Röpke, P. Schuck, A. Tohsaki and T. Yamada. "Open problems in α particle condensation". *J. Phys. G*, **37** (2010), 064012.

[53] Y. Funaki, T. Yamada, A. Tohsaki, H. Horiuchi, G. Röpke and P. Schuck. "Microscopic study of 4α-particle condensation with inclusion of resonances". *Phys. Rev. C*, **82** (2010), 024312.

[54] P. Schuck, T. Sogo and G. Röpke. "Quartetting in Nuclear Matter". *Progr. Theor. Phys. Suppl.*, (2012), 56–71.

[55] P. Schuck, T. Sogo and G. Röpke. "Critical temperature for α-condensation in asymmetric nuclear matter. The astrophysical context". *Int. J. Mod. Phys. E*, **20** (2011), 889–892.

[56] T. Sogo, G. Röpke and P. Schuck. "Critical temperature for α-particle condensation in asymmetric nuclear matter". *Phys. Rev. C*, **82** (2010), 034322.

[57] T. Sogo, G. Röpke and P. Schuck. "Many-body approach for quartet condensation in strong coupling". *Phys. Rev. C*, **81** (2010), 064310.

[58] Y. Funaki, T. Yamada, H. Horiuchi, G. Röpke, P. Schuck and A. Tohsaki. "α Cluster States and Condensation in O-16". *Progr. Theor. Phys. Suppl.*, (2012), 439.

[59] Y. Funaki, T. Yamada, H. Horiuchi, G. Röpke, P. Schuck and A. Tohsaki. "α Clustering and Condensation In O-16". *Mod. Physics Lett. A*, **25** (2010), 1939–1942.

[60] T. Yamada, Y. Funaki, T. Myo, H. Horiuchi, K. Ikeda, G. Röpke, P. Schuck and A. Tohsaki. "Isoscalar monopole excitations in O-16: α-cluster states at low energy and mean-field-type states at higher energy". *Phys. Rev. C*, **85** (2012), 034315.

[61] B. Zhou, Z. Ren, C. Xu, Y. Funaki, T. Yamada, A. Tohsaki, H. Horiuchi, P. Schuck and G. Röpke. "New concept for the ground-state band in Ne-20 within a microscopic cluster model". *Phys. Rev. C*, **86** (2012), 014301.

[62] D. B. Blaschke, V. V. Dmitriev, G. Röpke and S. A. Smolyansky. "BBGKY kinetic approach for an $e^-e^+\gamma$ plasma created from the vacuum in a strong laser-generated electric field: The one-photon annihilation channel". *Phys. Rev. D*, **84** (2011), 085028.

[63] D. B. Blaschke, G. Röpke, S. M. Schmidt, S. A. Smolyansky and A. V. Tarakanov. "Kinetics of Photon Radiation off an e^-e^+- Plasma Created from the Vacuum in a Strong Laser Field". *Contrib. Plasma Phys.*, **51** (2011), 451.

[64] G. Gregori, D. B. Blaschke, P. P. Rajeev, H. Chen, R. J. Clarke, T. Huffman, C. D. Murphy, A. V. Prozorkevich, C. D. Roberts, G. Röpke, S. M. Schmidt, S. A. Smolyansky, S. Wilks and R. Bingham. "A proposal for testing subcritical vacuum pair production with high power lasers". *High Energy Density Phys.*, **6** (2010), 166–170.

[65] V. G. Morozov, S. Mathey and G. Röpke. "Decoherence in an exactly solvable qubit model with initial qubit-environment correlations". *Phys. Rev. A*, **85** (2012), 022101.

[66] V. G. Morozov and G. Röpke. "Two-time correlation functions in an exactly solvable spin-boson model". *Theor. Math. Phys.*, **168** (2011), 1271–1277.

[67] L. Brizhik, A. P. Chetverikov, W. Ebeling, G. Röpke and M. G. Velarde. "Electron pairing and Coulomb repulsion in one-dimensional anharmonic lattices". *Phys. Rev. B*, **85** (2012), 245105.

[68] A. P. Chetverikov, W. Ebeling, G. Röpke and M. G. Velarde. "Hopping Transport and Stochastic Dynamics of Electrons in Plasma Layers". *Contrib. Plasma Phys.*, **51** (2011), 814–829.

[69] M. G. Velarde, L. Brizhik, A. P. Chetverikov, L. Cruzeiro, W. Ebeling and G. Röpke. "Electron pairing in one-dimensional anharmonic crystal lattices". *Int. J. Quantum Chem.*, **112** (2012), 551–565.

[70] M. G. Velarde, L. Brizhik, A. P. Chetverikov, L. Cruzeiro, W. Ebeling and G. Röpke. "Quartic lattice interactions, soliton-like excitations, and electron pairing in one-dimensional anharmonic crystals". *Int. J. Quantum Chem.*, **112** (2012), 2591–2598.

[71] C. Liebe, R. Mahnke and R. Kühne. "From traffic breakdown to energy flow analysis". *Trans. Res. C*, **19** (2011), 172–181.

[72] R. Mahnke, J. Kaupuzs and M. Brics. "Power laws and skew distributions". *Commun. Comput. Phys. (CiCP)*, **12** (2012), 721–731.

[73] J. Kaupuzs, R. Mahnke and H. Weber. "Comment on "How skew distributions emerge in evolving systems" by Choi M. Y. et al." *Europhys. Lett.*, **91** (2010), 30004–1–2.

[74] H. M. C. Cortés, S. V. Popruzhenko, D. Bauer and A. Pálffy. "Laser-assisted decay of quasistationary states". *New J. Phys.*, **13** (2011), 063007.

[75] P. A. Korneev, S. V. Popruzhenko, S. P. Goreslavski, T.-M. Yan, D. Bauer, W. Becker, M. Kübel, M. F. Kling, C. Rödel, M. Wünsche and G. G. Paulus. "Interference Carpets in Above-Threshold Ionization: From the Coulomb-Free to the Coulomb-Dominated Regime". *Phys. Rev. Lett.*, **108** (2012), 223601.

[76] M. Kundu, P. K. Kaw and D. Bauer. "Laser-cluster interaction with subcycle pulses". *Phys. Rev. A*, **85** (2012), 023202.

[77] P. Mulser and D. Bauer. "Anharmonic resonance in intense laser-matter interaction: Key to collisionless absorption". *AIP Conf. Proc.*, **1209** (2010), 75.

[78] P. Mulser and D. Bauer. *High-Power Laser-Matter Interaction*. Springer, Heidelberg (2010).

[79] T.-M. Yan, S. Popruzhenko, M. Vrakking and D. Bauer. "Trajectory-Based Coulomb-Corrected Strong Field Approximation". In K. Yamanouchi and M. Katsumi, editors, "Multiphoton Processes and Attosecond Physics", volume 125 of *Springer Proceedings in Physics*, pages 221–230. Springer Berlin Heidelberg (2012).

[80] W. Lubashevsky, I. Lubashevsky and R. Mahnke. "Distributed self-regulation of living tissue: Beyond the ideal limit". *Phys. Rev. E*, **81** (2010), 021922–1–14.

[81] A. Macchi, S. Veghini, T. V. Liseykina and F. Pegoraro. "Radiation pressure acceleration of ultrathin foils". *New J. Phys.*, **12** (2010), 045013.

[82] P. Mulser, S. M. Weng and T. Liseykina. "Analysis of the Brunel model and resulting hot electron spectra". *Phys. Plasmas*, **19** (2012), 043301.

[83] L. Romagnani, A. Bigongiari, S. Kar, S. V. Bulanov, C. A. Cecchetti, T. Z. Esirkepov, M. Galimberti, R. Jung, T. V. Liseykina, A. Macchi, J. Osterholz, F. Pegoraro, O. Willi and M. Borghesi. "Observation of Magnetized Soliton Remnants in the Wake of Intense Laser Pulse Propagation through Plasmas". *Phys. Rev. Lett.*, **105** (2010), 175002.

2.3.2 Statistical Physics

Head: Prof. Dr. Ronald Redmer

Staff:	PD Dr. Thomas Bornath	
	Andreas Becker	Dipl.-Phys. Mandy Bethkenhagen
	Dipl.-Phys. Richard Bredow	MSc. Daniel Cebulla
	Dr. Martin French	Dr. Bastian Holst
	Dipl.-Phys. Ulrike Kramm	Dr. Winfried Lorenzen
	Dr. Nadine Nettelmann	Dipl.-Phys. Kai-Uwe Plagemann
	Dipl.-Phys. Robert Püstow	Dipl.-Phys. Phillip Sperling
	Dr. Robert Thiele	Prof. em. Wolf-Dietrich Kraeft
Dipl.-Phys. Graduates:	Kai-Uwe Plagemann	Robert Püstow
	Richard Bredow	Mandy Bethkenhagen
	Kai Jakob Brunner	Robin Schmidt
MSc Graduates:	Daniel Cebulla	
BSc Graduates:	Daniel Cebulla	Caspar Haverkamp
	Chris Lappe	Carsten Schult
	Erik Jeglorz	Manuel Schöttler
	Laura Villardel	Nils Arbeiter

General Outline of the Research

The research activities in the group *Statistical Physics* are focused to strongly correlated many-particle systems. We are interested in matter under extreme conditions and in the dynamics of the light-matter interaction on ultra-short time scales. We develop and apply methods of many-particle physics in order to treat quantum effects and strong correlations adequately. Our research is funded by the German Science Foundation (DFG) within the SFB 652 *Strong Correlations in Radiation Fields*, the SPP 1385 *The first 10 Million Years of the Solar System* and the SPP 1488 *Planetary Magnetism*, and the BMBF within the FSP 301 FLASH. We use computing resources at the HLRN (mvp0001), on JUROPA at the FZ Jülich (HRO02), and on the compute clusters Merkur and Venus at the RZ of the Universität Rostock.

Warm Dense Matter and ab initio Molecular Dynamics Simulations

The behavior of the light elements H and He (including H-He mixtures) and of C, N, O and their hydrides under extreme conditions is of great importance for interior models of giant planets and brown dwarfs as well as for inertial confinement fusion experiments. A precise knowledge of thermodynamic, transport, and optical properties is needed for a large domain of densities and temperatures, especially for high densities as typical for condensed matter and for temperatures of several eV, i.e. for *warm dense matter (WDM)*; for a review, see [1].

We have determined thermophysical properties of H [2–4], H-He mixtures [5], and water [6–9] via *ab initio* molecular dynamics simulations (AIMD) which combine a

classical treatment (molecular dynamics) for the ions with a full quantum description for the electrons using density functional theory. Besides the equation of state (EOS), transport coefficients such as the electrical conductivity and the diffusion coefficient, the pair correlation functions [10], and the opacity can be gained. A major goal is the calculation of the widely unknown high-pressure phase diagram of WDM, especially with respect to nonmetal-to-metal transitions [11, 12] and demixing phenomena. The predictive power of such AIMD simulations has recently been proven by shock-wave experiments for water – excellent agreement has been found [9].

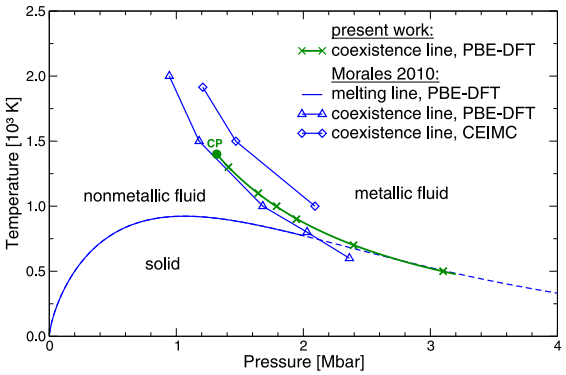

Fig. 2.48: High-pressure phase diagram of H with a first-order liquid-liquid phase transition (PBE-DFT, green line) which ends in a critical point at about 1400 K and 1.4 Mbar; for details, see [2]. Blue lines (PBE-DFT and CEIMC): see M. Morales et al., Proc. Natl. Acad. Sci. U.S.A., **107**, 12799 (2010).

As an outstanding example we show in Fig. 2.48 the high-pressure phase diagram of H. Interestingly, this simplest element undergoes a liquid-liquid phase transition at high pressures with a critical point at about 1400 K and 1.4 Mbar. Analysis of the EOS data, the pair correlation functions and the electrical conductivity confirms that the transition between a molecular nonconducting and an atomic conducting liquid is of the first order [2] as has been predicted long ago. Earlier estimates for this *plasma phase transition* based on chemical models locate this transition in a different region of the phase diagram.

Planetary Physics

Planets are perfect laboratories to study WDM states. Gas giants such as Jupiter and Saturn contain mainly H and He, while ice giants like Uranus and Neptune are composed of C-N-O-H-He mixtures. For Super Earths like COROT-7b which might represent a substantial fraction of extrasolar planets in the Galaxy, the high-pressure behavior of MgO-Si alloys is perhaps most important. Interior, evolution, and dynamo models for solar and extrasolar planets require accurate EOS data in order to narrow down the diversity of possible solutions. An important and so far not solved problem in this context is the size of Jupiter's core [13].

We have used our AIMD EOS data for H, He and water in order to construct interior models for Uranus and Neptune [14], see Fig. 2.49, Jupiter [15], and for extrasolar planets such as GJ 436b [16, 17], GJ 1214b [18], and HAT-P-13b [19]. Furthermore, we have calculated for the first time all material properties along

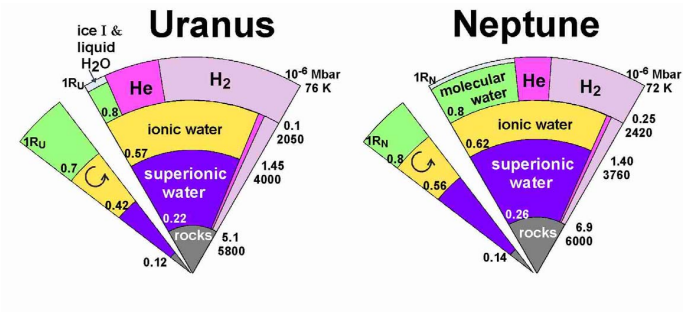

Fig. 2.49: The interiors of Uranus and Neptune displayed in the right panels were calculated using AIMD EOS data for water [14]. The smaller charts shown in the left panels stem from dynamo models that reproduce their unusal magnetic fields [S. Stanley and J. Bloxham, Icarus **184**, 556].

Jupiter's isentrope which are needed as input in dynamo simulations for its magnetic field structure [20]. Proposals for experiments at the future heavy ion beam accelerator FAIR in Darmstadt [21–23] were made in order to probe conditions deep in planetary interiors. We are members of the Young Exoplanet Transit Initiative (YETI) [24] that makes a coordinated effort to detect and subsequently model young exoplanets in order to unravel details of planetary formation and evolution processes.

Interaction of Plasmas with Electromagnetic Fields

X-ray Thomson scattering (XRTS) has demonstrated its capacity as a reliable and versatile tool for the diagnostics of dense plasmas , see e.g. [28–34]. X-rays emitted from laser-produced plasmas or from free electron lasers (FELs) can probe WDM states with temperatures of several eV and densities close to solid density up to compressed matter. For instance, collective XRTS experiments yield information on the density and temperature of dense plasmas via the plasmon peaks. Their frequency position is directly related to the free electron density, and the temperature is derived from the detailed balance relation.

We have performed particle-in-cell as well as hydrodynamic simulations in order to characterize the target state during and shortly after illumation with intense optical lasers or FELs [35, 36]. The ultra-short time dynamics (fs – ps) in the plasma is dominated by strong inhomogeneities imposed by intense pump pulses. The XRTS spectrum is calculated for inhomogeneous targets based on the Chihara decomposition where the Born-Mermin approximation is used for the free electron contribution. By varying the time delay between (optical) pump and X-ray probe pulse, the relaxation behavior into an equilibrium state can be studied. We have also performed AIMD simulations for the dynamic structure factor $S(\omega)$ of compressed and uncompressed Be [37] for which a simple Drude model perfectly applies.

Interaction of Clusters with Laser Fields

In the interaction of atomic clusters with femtosecond laser pulses, nanoplasmas with high density and high temperature are created [41–43]. Here, inverse bremsstrahlung (IB) heating is one of the most important heating processes [44]. In dense plasmas that are produced by a laser excitation, the free electrons exchange photons with the laser field permanently. When the electrons are accelerated in the Coulomb field of the ions, they emit photons, a phenomenon commonly known as bremsstrahlung. In the presence of the external field, the electrons absorb laser photons as well. In the time average, the absorption exceeds the emission, and the plasma is heated due to inverse bremsstrahlung.

IB heating involves two different kinds of interaction – the interaction of the electrons with the external laser field and the electron-ion interaction. This makes analytical approaches very difficult. In a quantum perturbative approach to the IB heating rate in strong laser fields, usually the first Born approximation with respect to the electron-ion potential is considered, whereas the influence of the electric field is taken exactly in the Volkov wave functions. In [45] the momentum-dependent, angle-averaged heating rate was calculated adopting a screened electron-ion interaction potential. Going a step further in the perturbation series, we considered the transition amplitude in the second Born approximation as well.

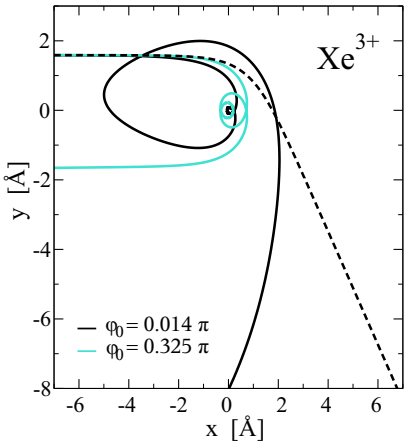

Fig. 2.50: Electron trajectories for the scattering on a xenon ion with charge Z=3 in the x-y plane for the initial velocity parallel to the electric field F and different values of the initial laser field phase φ_0. The ion is located in the origin, the electron is approaching from the left with energy $E = 50\,\mathrm{eV}$ and the laser field strength $F = 2.6 \cdot 10^8\,\mathrm{V/cm}$ at a wavelength $\lambda = 825\,\mathrm{nm}$. The dashed line indicates the trajectory without external field ($F = 0$).

In many approaches for the calculation of the IB heating rate such as the Born approximation, large-angle scattering events are underestimated. However, rescattering events of an electron on the same atomic ion play an important role because they increase the amount of energy exchanged between the electrons and the laser field. For typical noble gas clusters studied in experiments, one is advised to take into account not only the screening by the surrounding plasma medium but also the inner structure of the ions what can be accomplished by the use of appropriate model potentials. In [46] the IB heating rate has been calculated from the classical simulation of individual electron trajectories. Especially for higher energies, the

consideration of the ionic structure increases the heating rate compared with the scattering on point-like particles.

References

[1] R. Redmer and G. Röpke. "Progress in the Theory of Dense Strongly Coupled Plasmas". *Contrib. Plasma Phys.*, **50** (2010), 970–985.

[2] W. Lorenzen, B. Holst and R. Redmer. "First-order liquid-liquid phase transition in dense hydrogen". *Phys. Rev. B*, **82** (2010), 195107.

[3] B. Holst, M. French and R. Redmer. "Electronic transport coefficients from *ab initio* simulations and application to dense liquid hydrogen". *Phys. Rev. B*, **83** (2011), 235120.

[4] B. Holst, R. Redmer, V. K. Gryaznov, V. E. Fortov and I. L. Iosilevskiy. "Hydrogen and deuterium in shock wave experiments, ab initio simulations and chemical picture modeling". *Eur. Phys. J. D*, **66** (2012), 104.

[5] W. Lorenzen, B. Holst and R. Redmer. "Metallization in hydrogen-helium mixtures". *Phys. Rev. B*, **84** (2011), 235109.

[6] M. French, T. R. Mattsson and R. Redmer. "Diffusion and electrical conductivity in water at ultrahigh pressures". *Phys. Rev. B*, **82** (2010), 174108.

[7] M. French and R. Redmer. "Optical properties of water at high temperature". *Phys. Plasmas*, **18** (2011), 043301.

[8] M. French, S. Hamel and R. Redmer. "Dynamical Screening and Ionic Conductivity in Water from *Ab Initio* Simulations". *Phys. Rev. Lett.*, **107** (2011), 185901.

[9] M. D. Knudson, M. P. Desjarlais, R. W. Lemke, T. R. Mattsson, M. French, N. Nettelmann and R. Redmer. "Probing the Interiors of the Ice Giants: Shock Compression of Water to 700 GPa and 3.8 g/cm^3". *Phys. Rev. Lett.*, **108** (2012), 091102.

[10] V. Schwarz, B. Holst, T. Bornath, C. Fortmann, W.-D. Kraeft, R. Thiele, R. Redmer, G. Gregori, H. J. Lee, T. Döppner and S. H. Glenzer. "Static ion structure factor for dense plasmas: Semi-classical and ab initio calculations". *High Energy Density Phys.*, **6** (2010), 305–310.

[11] P. P. Edwards, M. T. J. Lodge, F. Hensel and R. Redmer. "... a metal conducts and a non-metal doesn't". *Phil. Trans. R. Soc. Lond. A*, **368** (2010), 941–965.

[12] R. Redmer, B. Holst and F. Hensel, editors. *Metal-to-Nonmetal Transitions, In: Springer Series in Material Sciences, Vol. 132*. Springer (2010).

[13] N. Nettelmann. "Predictions on the core mass of Jupiter and of giant planets in general". *Astrophys. Space Sci.*, **336** (2011), 47–51.

[14] R. Redmer, T. R. Mattsson, N. Nettelmann and M. French. "The phase diagram of water and the magnetic fields of Uranus and Neptune". *Icarus*, **211** (2011), 798–803.

[15] N. Nettelmann, A. Becker, B. Holst and R. Redmer. "Jupiter Models with Improved Ab Initio Hydrogen Equation of State (H-REOS.2)". *Astrophys. J.*, **750** (2012), 52.

[16] N. Nettelmann, U. Kramm, R. Redmer and R. Neuhäuser. "Interior structure models of GJ 436b". *Astron. Astrophys.*, **523** (2010), A26.

[17] U. Kramm, N. Nettelmann, R. Redmer and D. J. Stevenson. "On the degeneracy of the tidal Love number k2 in multi-layer planetary models: application to Saturn and GJ 436b". *Astron. Astrophys.*, **528** (2011), A18.

[18] N. Nettelmann, J. J. Fortney, U. Kramm and R. Redmer. "Thermal Evolution and Structure Models of the Transiting Super-Earth GJ 1214b". *Astrophys. J.*, **733** (2011), 2.

[19] U. Kramm, N. Nettelmann, J. J. Fortney, R. Neuhäuser and R. Redmer. "Constraining the interior of extrasolar giant planets with the tidal Love number k2 using the example of HAT-P-13b". *Astron. Astrophys.*, **538** (2012), A146.

[20] M. French, A. Becker, W. Lorenzen, N. Nettelmann, M. Bethkenhagen, J. Wicht and R. Redmer. "Ab Initio Simulations for Material Properties along the Jupiter Adiabat". *Astrophys. J. Suppl. Ser.*, **202** (2012), 5.

[21] N. A. Tahir, T. Stöhlker, A. Shutov, I. V. Lomonosov, V. E. Fortov, M. French, N. Nettelmann, R. Redmer, A. R. Piriz, C. Deutsch, Y. Zhao, P. Zhang, H. Xu, G. Xiao and W. Zhan. "Ultrahigh compression of water using intense heavy ion beams: laboratory planetary physics". *New J. Phys.*, **12** (2010), 073022.

[22] N. A. Tahir et al. "High Energy Density Physics Studies at the Facility for Antiprotons and Ion Research: the HEDgeHOB Collaboration". *Contrib. Plasma Phys.*, **51** (2011), 309–321. (incl. R. Redmer).

[23] N. Tahir et al. "Laboratory planetary physics using intense heavy ion beams at the Facility for Antiprotons and Ion Research at Darmstadt: the HEDgeHOB collaboration". *Astrophys. Space Sci.*, **336** (2011), 61–65. (incl. M. French, N. Nettelmann, R. Redmer).

[24] R. Neuhäuser et al. "The Young Exoplanet Transit Initiative (YETI)". *Astron. Nachr.*, **332** (2011), 547–561. (incl. R. Redmer, U. Kramm, N. Nettelmann).

[25] J. R. Adams, H. Reinholz and R. Redmer. "Application of linear response theory to magnetotransport properties of dense plasmas". *Phys. Rev. E*, **81** (2010), 036409.

[26] V. S. Karakhtanov, R. Redmer, H. Reinholz and G. Röpke. "Transport Coefficients in Dense Plasmas Including Ion-Ion Structure Factor". *Contrib. Plasma Phys.*, **51** (2011), 355–360.

[27] T. S. Ramazanov, M. T. Gabdullin, K. N. Dzhumagulova and R. Redmer. "Ionization Equiibrium and Composition of a Dense Partially Ionized Metal Plasma". *Contrib. Plasma Phys.*, **51** (2011), 391–394.

[28] S. Toleikis et al. "Soft X-ray scattering using FEL radiation for probing near-solid density plasmas at few electron volt temperatures". *High Energy Density Phys.*, **6** (2010), 15–20. (incl. R. Redmer, R. Thiele).

[29] S. Glenzer, H. Lee, P. Davis, T. Döppner, R. Falcone, C. Fortmann, B. Hammel, A. Kritcher, O. Landen, R. Lee, D. Munro, R. Redmer and S. Weber. "Dense plasma X-ray scattering: Methods and applications". *High Energy Density Phys.*, **6** (2010), 1–8.

[30] R. R. Fäustlin et al. "Observation of Ultrafast Nonequilibrium Collective Dynamics in Warm Dense Hydrogen". *Phys. Rev. Lett.*, **104** (2010), 125002. (incl. Th. Bornath, R. Redmer, R. Thiele).

[31] S. Toleikis et al. "Probing near-solid density plasmas using soft x-ray scattering". *J. Phys. B*, **43** (2010), 194017. (incl. Th. Bornath, R. Redmer, R. Thiele).

[32] T. Döppner, C. Fortmann, P. F. Davis, A. L. Kritcher, O. L. Landen, H. J. Lee, R. Redmer, S. P. Regan and S. H. Glenzer. "X-ray Thomson scattering for measuring dense beryllium plasma collisionality". *J. Phys. Conf. Ser.*, **244** (2010), 032044.

[33] H. J. Lee et al. "X-ray Thomson scattering measurement in shock-compressed beryllium". *J. Phys. Conf. Ser.*, **244** (2010), 042015. (incl. R. Redmer).

[34] S. M. Vinko et al. "Electronic Structure of an XUV Photogenerated Solid-Density Aluminum Plasma". *Phys. Rev. Lett.*, **104** (2010), 225001. (incl. R. Redmer, R. Thiele).

[35] R. Thiele, P. Sperling, M. Chen, T. Bornath, R. R. Fäustlin, C. Fortmann, S. H. Glenzer, W.-D. Kraeft, A. Pukhov, S. Toleikis, T. Tschentscher and R. Redmer.

"Thomson scattering on inhomogeneous targets". *Phys. Rev. E*, **82** (2010), 056404.

[36] P. Sperling, R. Thiele, B. Holst, C. Fortmann, S. H. Glenzer, S. Toleikis, T. Tschentscher and R. Redmer. "Two-color Thomson scattering at FLASH". *High Energy Density Phys.*, **7** (2011), 145–149.

[37] K.-U. Plagemann, P. Sperling, R. Thiele, M. P. Desjarlais, C. Fortmann, T. Döppner, H. J. Lee, S. H. Glenzer and R. Redmer. "Dynamic structure factor in warm dense beryllium". *New J. Phys.*, **14** (2012), 055020.

[38] M. Schlanges, T. Bornath, J. Vorberger and D. O. Gericke. "Energy Relaxation Study for Warm Dense Matter Experiments". *Contrib. Plasma Phys.*, **50** (2010), 64–68.

[39] J. Vorberger, D. O. Gericke, T. Bornath and M. Schlanges. "Energy relaxation in dense, strongly coupled two-temperature plasmas". *Phys. Rev. E*, **81** (2010), 046404.

[40] J. Vorberger, D. O. Gericke, T. Bornath and M. Schlanges. "Energy and temperature relaxation described by nonequilibrium Green's functions". *J. Phys. Conf. Ser.*, **220** (2010), 012002.

[41] N. X. Truong, P. Hilse, S. Göde, A. Przystawik, T. Döppner, T. Fennel, T. Bornath, J. Tiggesbäumker, M. Schlanges, G. Gerber and K.-H. Meiwes-Broer. "Optimal control of the strong-field ionization of silver clusters in helium droplets". *Phys. Rev. A*, **81** (2010), 013201.

[42] P. Hilse, T. Bornath, M. Moll, M. Schlanges, N. X. Truong, S. Göde, J. Tiggesbäumker and K.-H. Meiwes-Broer. "Control of Ionization in the Interaction of Strong Laser Fields with Dense Nanoplasmas". *Contrib. Plasma Phys.*, **52** (2012), 28–32.

[43] J. Köhn, R. Redmer and T. Fennel. "Collision-enhanced plasmonic electron acceleration in small metal clusters". *New J. Phys.*, **14** (2012), 055011.

[44] M. Moll, P. Hilse, M. Schlanges, T. Bornath and V. P. Krainov. "Electron-ion collision rates in atomic clusters irradiated by femtosecond laser pulses". *J. Phys. B*, **43** (2010), 135103.

[45] M. Moll, M. Schlanges, T. Bornath and V. P. Krainov. "Inverse bremsstrahlung heating beyond the first Born approximation for dense plasmas in laser fields". *New J. Phys.*, **14** (2012), 065010.

[46] M. Moll, T. Bornath, M. Schlanges and V. P. Krainov. "Inverse bremsstrahlung heating rate in atomic clusters irradiated by femtosecond laser pulses". *Phys. Plasmas*, **19** (2012), 033303.

2.3.3 Physics of Elementary Particles

Head: Priv.-Doz. Dr. Roland Waldi
Head (until 2010): Prof. Dr. Henning Schröder

Staff:	Dipl.-Phys. Chris Bünger	Yanjun Cong
	Dipl.-Phys. Sebastian Dittrich	Dr. Marcus Ebert
	Dipl.-Phys. Oliver Grünberg	Dr. Thomas Hartmann
	MSc Miriam Heß	Dipl.-Phys. Torsten Leddig
	Dipl.-Phys. Oliver Schäfer	Dipl.-Phys. Erik Schmidt
	Dr. Stefan Strauß	Dipl.-Phys. Christian Voß
Dipl.-Phys. Graduates:	Karsten Dittrich	Sebastian Dittrich
	Christian Voss	
MSc Graduates:	Yanjun Cong	Miriam Hess
BSc Graduates:	Julia Heller	Martin Jessen

The BABAR Experiment

Since summer 2000 the group participates in the BABAR-experiment at the SLAC National Accelerator Laboratory in California (USA), supported by the BMBF. This experiment studies multi-particle final states produced in the electron-positron annihilation at a centre-of-mass energy of 10.58 GeV. At this energy, the $\Upsilon(4S)$-resonance is produced, an excited bound state of a b- and an anti-b-quark. It decays exclusively into a pair of B mesons, massive particles heavier than a helium nucleus. Data were taken between 1999 and 2008, and are analysed since 2000, with many analyses still ongoing and a continuous output of interesting results.

The main aim of the experiment is the investigation of a time-dependent CP asymmetry (particle-antiparticle asymmetry) in the decay of neutral B mesons. The main achievement of BABAR was the first observation of this CP asymmetry in 2001. In the following years, subsequent studies have revealed CP asymmetries in more B decay channels, and improved the precision of the parameters of the Cabibbo-Kobayashi-Maskawa matrix which are responsible for this effect.

In addition to these key questions, the BABAR experiment offers an almost unlimited potential for studying charmed mesons, charmed baryons, tau leptons, and exclusive final states from radiative e^+e^- annihilation. Also, the 480 million $B\overline{B}$ pairs collected are used to study much more details than CP asymmetries. The focus of our group's investigations is the production of baryons in B meson decays. Since B mesons are the heaviest weakly decaying mesons, they offer a unique possibility to study baryon production in meson decays. Our group has investigated the features of new and established baryonic final states. One of the new decay channels found at Rostock is shown in Fig. 2.51. Many of those decays exhibit an enhancement of the decay rate at the threshold of the baryon-antibaryon mass. We have found a common pattern for this effect, which still puzzles the theorists working in this field.

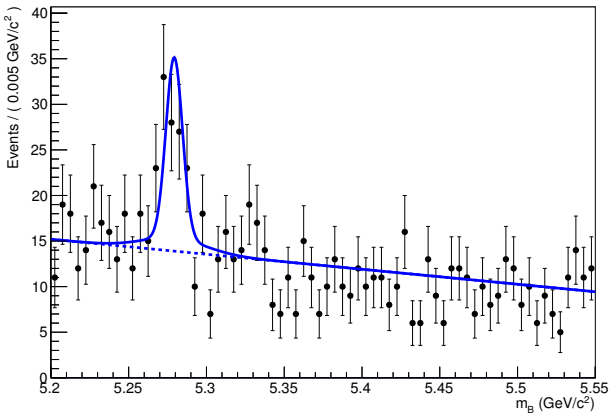

Fig. 2.51: A signal of a very rare B meson decay to final states with baryons: $\overline{B}^0 \to \Lambda_c^+ \overline{p} K^+ K^-$ seen in the invariant mass distribution of the final state from the BABAR experiment.

Monte Carlo Studies for an International Linear Collider

The next generation of particle accelerators will operate at 1000 GeV scattering energy and above (Terascale). A collider for electrons and positrons is under exploratory studies and could be realized as the ILC (International Linear Collider). Our group participated in the past in detector development and in the physics program for this machine.

High precision analyses of physics questions such as the electroweak symmetry breaking require a close collaboration of experimentalists and theorists. This is realized by simulating theoretical models and the complex experimental set-up in depth, starting from an effective Lagrangian quantum field theory that includes alternatives to the Standard Model approach for mass generation. Using this theory, a Monte Carlo event generator simulates intermediate states with three vector bosons produced in e^+e^- collisions, their decay, the hadronisation of six quark final states and gluons, and the detector response. New physics is expected to manifest itself in the interaction of the vector bosons. The most prominent example is a non-standard Higgs boson. The simulated events are reconstructed to determine the sensitivity of an ILC experiment to new physics encoded in the effective Lagrangian, and the regions in the parameter space of the non-standard Higgs boson where the real experiment could make a discovery or exclude the existence of such a particle. This study is supported by the Helmholtz Alliance “Physics at the Terascale”.

The LHCb Experiment

In July 2011 our group joined the LHCb collaboration, an international group of physicists who operate the LHCb detector at the CERN Large Hadron Collider

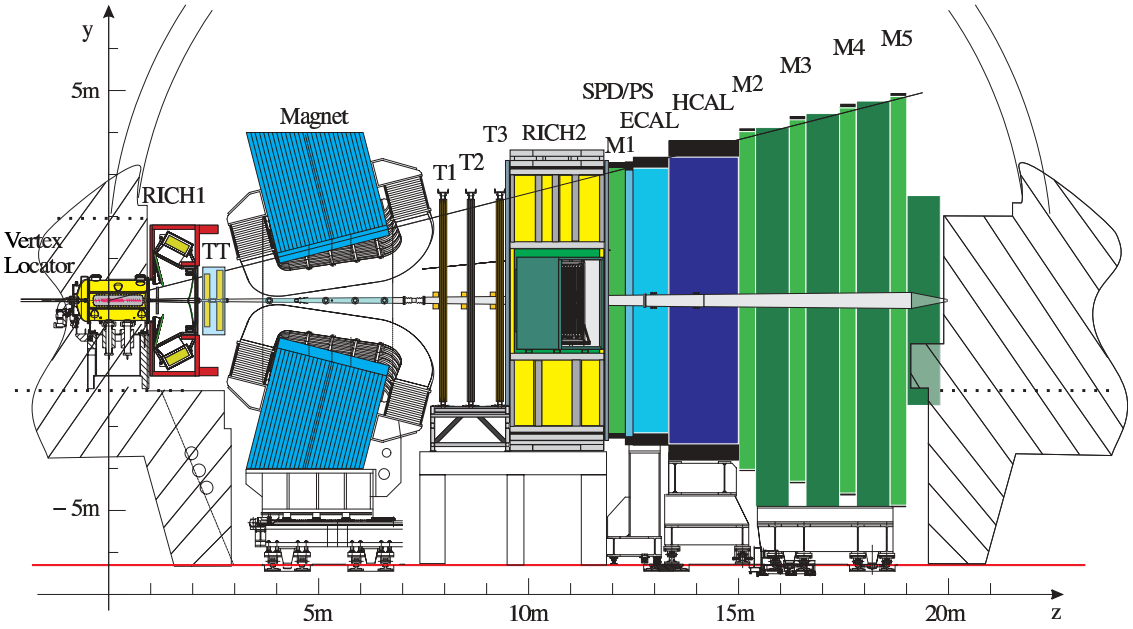

Fig. 2.52: The LHCb experiment. Shown is the schematic of the detector cut along the beam pipe. The *pp* collision point is at the left, in the coordinate system origin.

(LHC) near Geneva. This project is also funded by the BMBF. The LHC at the European Research Laboratory CERN is providing proton proton collisions since March 2010, at centre-of-mass energies of 7 TeV and since 2012 of 8 TeV. The heavy b and $\bar{b}$ quarks are preferentially emitted at small angles to the beams, where the LHCb detector is positioned. In contrast to the experiments ATLAS and CMS which operate in the central region, the LHCb experiment is therefore ideally suited to study B mesons and baryons with b quarks, and can ideally supplement the CP violation studies at BABAR.

The experimental environment is quite different from BABAR, with higher particle multiplicity and jets focused in forward direction, but a high precision vertex reconstruction makes good for the increased combinatorial backgrounds. Our group is investigating B meson decays into baryons. These studies can supplement our results obtained with the BABAR detector, but the higher B production rate allows us also to study CP and T (time reversal) symmetries and their violation. We have just started analyses to measure these effects. We also look for decays that violate the conservation of baryon and lepton number, but conserve the difference of these numbers, e.g., $B^0 \to p\mu^-$. Such processes are predicted to be extremely rare (with probabilities around 10^{-30}) by the Standard Model but could explain the baryon-antibaryon asymmetry in our universe as proposed for the first time by the Russian physicist Andrei Sakharov. Astrophysical measurements (WMAP) set the upper limit for such decays to 10^{-10}, a scale that is accessible by LHCb due to its unique production rate of $\sim 10^{11}$ B and D mesons per year. The observation of

such processes would prove physics beyond the Standard Model and would provide the missing link to understand the matter-antimatter asymmetry of our universe.

References

[1] B. Aubert et al. "Measurement of $|V(cb)|$ and the form-factor slope in $\overline{B} \to Dl^-\overline{\nu}$ decays in events tagged by a fully reconstructed B meson". *Phys. Rev. Lett.*, **104** (2010), 011802. (incl. M. Ebert, T. Hartmann, H. Schröder, R. Waldi).

[2] B. Aubert et al. "Searches for lepton flavor violation in the decays $\tau^\pm \to e^\pm\gamma$ and $\tau^\pm \to \mu^\pm\gamma$". *Phys. Rev. Lett.*, **104** (2010), 021802. (incl. M. Ebert, T. Hartmann, H. Schröder, R. Waldi).

[3] J. Lees et al. "Search for charged lepton flavor violation in narrow Υ decays". *Phys. Rev. Lett.*, **104** (2010), 151802. (incl. M. Ebert, T. Hartmann, H. Schröder, R. Waldi).

[4] P. del Amo Sanchez et al. "Test of lepton universality in Υ(1S) decays at BABAR". *Phys. Rev. Lett.*, **104** (2010), 191801. (incl. M. Ebert, T. Hartmann, T. Leddig, H. Schröder, R. Waldi).

[5] B. Aubert et al. "Measurements of charged current lepton universality and $|V_{us}|$ using tau lepton decays to $e^-\overline{\nu}_e\nu_\tau$, $\mu^-\overline{\nu}_\mu\nu_\tau$, $\pi^-\nu_\tau$ and $K^-\nu_\tau$". *Phys. Rev. Lett.*, **105** (2010), 051602. (incl. M. Ebert, T. Hartmann, H. Schröder, R. Waldi).

[6] P. del Amo Sanchez et al. "Measurement of D^0-$\overline{D}^0$ mixing parameters using $D^0 \to K^0_S\pi^+\pi^-$ and $D^0 \to K^0_S K^+K^-$ decays". *Phys. Rev. Lett.*, **105** (2010), 081803. (incl. M. Ebert, T. Hartmann, T. Leddig, H. Schröder, R. Waldi).

[7] P. del Amo Sanchez et al. "Evidence for direct CP violation in the measurement of the Cabibbo-Kobayashi-Maskawa angle γ with $B^\mp \to D^{(*)}K^{(*)\mp}$ decays". *Phys. Rev. Lett.*, **105** (2010), 121801. (incl. M. Ebert, T. Hartmann, T. Leddig, H. Schröder, R. Waldi).

[8] P. del Amo Sanchez et al. "Search for $f_J(2220)$ in radiative J/ψ decays". *Phys. Rev. Lett.*, **105** (2010), 172001. (incl. T. Hartmann, T. Leddig, H. Schröder, R. Waldi).

[9] B. Aubert et al. "Observation of inclusive $D^{*\pm}$ production in the decay of Υ(1S)". *Phys. Rev. D*, **81** (2010), 011102. (incl. M. Ebert, T. Hartmann, H. Schröder, R. Waldi).

[10] B. Aubert et al. "Measurement and interpretation of moments in inclusive semileptonic decays $\overline{B} \to X_c l^- \overline{\nu}$". *Phys. Rev. D*, **81** (2010), 032003. (incl. M. Ebert, T. Hartmann, H. Schröder, R. Waldi).

[11] B. Aubert et al. "A search for $B^+ \to \ell^+ \nu_\ell$ recoiling against $B^- \to D^0 \ell^- \overline{\nu} X$". *Phys. Rev. D*, **81** (2010), 051101. (incl. M. Ebert, T. Hartmann, H. Schröder, R. Waldi).

[12] B. Aubert et al. "Measurement of branching fractions of B decays to $K_1(1270)\pi$ and $K_1(1400)\pi$ and determination of the CKM angle α from $B^0 \to a_1(1260)^{\pm}\pi^{\mp}$". *Phys. Rev. D*, **81** (2010), 052009. (incl. M. Ebert, T. Hartmann, H. Schröder, R. Waldi).

[13] J. Lees et al. "Measurement of the $\gamma\gamma^* \to \eta_c$ transition form factor". *Phys. Rev. D*, **81** (2010), 052010. (incl. M. Ebert, T. Hartmann, T. Leddig, H. Schröder, R. Waldi).

[14] B. Aubert et al. "Observation of the $\chi_{c2}(2P)$ meson in the reaction $\gamma\gamma \to D\overline{D}$ at BABAR". *Phys. Rev. D*, **81** (2010), 092003. (incl. M. Ebert, T. Hartmann, H. Schröder, R. Waldi).

[15] J. Lees et al. "Limits on tau lepton-flavor violating decays in three charged leptons". *Phys. Rev. D*, **81** (2010), 111101. (incl. M. Ebert, T. Hartmann, T. Leddig, H. Schröder, R. Waldi).

[16] P. del Amo Sanchez et al. "Search for CP violation using T-odd correlations in $D^0 \to K^+K^-\pi^+\pi^-$ decays". *Phys. Rev. D*, **81** (2010), 111103. (incl. M. Ebert, T. Hartmann, T. Leddig, H. Schröder, R. Waldi).

[17] P. del Amo Sanchez et al. "Evidence for the decay $X(3872) \to J/\psi\,\omega$". *Phys. Rev. D*, **82** (2010), 011101. (incl. T. Hartmann, T. Leddig, H. Schröder, R. Waldi).

[18] P. del Amo Sanchez et al. "B-meson decays to $\eta'\rho$, $\eta' f_0$, and $\eta' K^*$". *Phys. Rev. D*, **82** (2010), 011502. (incl. M. Ebert, T. Hartmann, T. Leddig, H. Schröder, R. Waldi).

[19] P. del Amo Sanchez et al. "Observation of the rare decay $B^0 \to K^0_S K^{\pm}\pi^{\mp}$". *Phys. Rev. D*, **82** (2010), 031101. (incl. M. Ebert, T. Hartmann, T. Leddig, H. Schröder, R. Waldi).

[20] B. Aubert et al. "Observation of the decay $\overline{B}^0 \to \Lambda_c^+ \overline{p}\pi^0$". *Phys. Rev. D*, **82** (2010), 031102. (incl. M. Ebert, T. Hartmann, H. Schröder, R. Waldi).

[21] P. del Amo Sanchez et al. "Study of $B \to X\gamma$ decays and determination of $|V_{td}/V_{ts}|$". *Phys. Rev. D*, **82** (2010), 051101. (incl. T. Hartmann, T. Leddig, H. Schröder, R. Waldi).

[22] P. del Amo Sanchez et al. "Exclusive production of $D_s^+ D_s^-$, $D_s^{*+} D_s^-$, and $D_s^{*+} D_s^{*-}$ via e^+e^- annihilation with initial-state-radiation". *Phys. Rev. D*, **82** (2010), 052004. (incl. T. Hartmann, T. Leddig, H. Schröder, R. Waldi).

[23] P. del Amo Sanchez et al. "Measurement of CP observables in $B^\pm \to D_{\rm CP} K^\pm$ decays and constraints on the CKM angle γ". *Phys. Rev. D*, **82** (2010), 072004. (incl. T. Hartmann, T. Leddig, H. Schröder, R. Waldi).

[24] P. del Amo Sanchez et al. "Search for $b \to u$ transitions in $B^- \to DK^-$ and D^*K^- decays". *Phys. Rev. D*, **82** (2010), 072006. (incl. T. Hartmann, T. Leddig, H. Schröder, R. Waldi).

[25] P. del Amo Sanchez et al. "Search for B^+ meson decay to $a_1^+(1260)K^{*0}(892)$". *Phys. Rev. D*, **82** (2010), 091101. (incl. T. Hartmann, T. Leddig, H. Schröder, R. Waldi).

[26] B. Aubert et al. "Correlated leading baryon-antibaryon production in $e^+e^- \to c\bar{c} \to \Lambda_c^+ \overline{\Lambda}_c^- X$". *Phys. Rev. D*, **82** (2010), 091102. (incl. M. Ebert, T. Hartmann, H. Schröder, R. Waldi).

[27] P. del Amo Sanchez et al. "Measurement of the absolute branching fractions for $D_s^- \to \ell^- \overline{\nu}_\ell$ and extraction of the decay constant f_{D_s}". *Phys. Rev. D*, **82** (2010), 091103. (incl. T. Hartmann, T. Leddig, H. Schröder, R. Waldi).

[28] P. del Amo Sanchez et al. "Search for $B^+ \to D^+ K^0$ and $B^+ \to D^+ K^{*0}$ decays". *Phys. Rev. D*, **82** (2010), 092006. (incl. M. Ebert, T. Hartmann, T. Leddig, H. Schröder, R. Waldi).

[29] P. del Amo Sanchez et al. "Observation of new resonances decaying to $D\pi$ and $D^*\pi$ in inclusive e^+e^- collisions near $\sqrt{s} = 10.58\,\text{GeV}$". *Phys. Rev. D*, **82** (2010), 111101. (incl. T. Hartmann, T. Leddig, H. Schröder, R. Waldi).

[30] P. del Amo Sanchez et al. "Observation of the $\Upsilon(1^3\mathrm{D_J})$ bottomonium state through decays to $\pi^+\pi^-\Upsilon(1\mathrm{S})$". *Phys. Rev. D*, **82** (2010), 111102. (incl. M. Ebert, T. Hartmann, T. Leddig, H. Schröder, R. Waldi).

[31] P. del Amo Sanchez et al. "Search for the rare decay $B \to K\nu\overline{\nu}$". *Phys. Rev. D*, **82** (2010), 112002. (incl. T. Hartmann, T. Leddig, H. Schröder, R. Waldi).

[32] P. del Amo Sanchez et al. "Dalitz-plot analysis of $B^0 \to \overline{D}^0\pi^+\pi^-$". *PoS*, **ICHEP2010** (2010), 250. (incl. T. Hartmann, T. Leddig, H. Schröder, R. Waldi).

[33] T. Hartmann. "Observation and study of B meson decays with Λ_c baryons with the BABAR detector". *PoS*, **ICHEP2010** (2010), 204.

[34] N. Agafonova et al. "Observation of a first ν_τ candidate in the OPERA experiment in the CNGS beam". *Phys. Lett. B*, **691** (2010), 138–145. (incl. H. Schröder).

[35] N. Agafonova et al. "Measurement of the atmospheric muon charge ratio with the OPERA detector". *Eur. Phys. J. C*, **67** (2010), 25–37. (incl. H. Schröder).

[36] S. Strauß and M. Beyer. "Low-dimensional light front gauge theory at finite temperature". *Nucl. Phys. Proc. Suppl.*, **199** (2010), 160–165.

[37] P. del Amo Sanchez et al. "Search for production of invisible final states in single-photon decays of $\Upsilon(1S)$". *Phys. Rev. Lett.*, **107** (2011), 021804. (incl. T. Hartmann, T. Leddig, H. Schröder, R. Waldi).

[38] P. del Amo Sanchez et al. "Observation of the decay $B^- \to D_s^{(*)+} K^- \ell^- \overline{\nu}_\ell$". *Phys. Rev. Lett.*, **107** (2011), 041804. (incl. T. Hartmann, T. Leddig, H. Schröder, R. Waldi).

[39] J. Lees et al. "Search for hadronic decays of a light Higgs boson in the radiative decay $\Upsilon \to \gamma A^0$". *Phys. Rev. Lett.*, **107** (2011), 221803. (incl. C. Bünger, O. Grünberg, T. Hartmann, T. Leddig, H. Schröder, R. Waldi).

[40] P. del Amo Sanchez et al. "Measurement of partial branching fractions of inclusive charmless B meson decays to K^+, K^0, and π^+". *Phys. Rev. D*, **83** (2011), 031103. (incl. C. Bünger, T. Hartmann, T. Leddig, H. Schröder, R. Waldi).

[41] P. del Amo Sanchez et al. "Studies of $\tau^- \to \eta K^- \nu_\tau$ and $\tau^- \to \eta \pi^- \nu_\tau$ at BABAR and a search for a second-class current". *Phys. Rev. D*, **83** (2011), 032002. (incl. T. Hartmann, T. Leddig, H. Schröder, R. Waldi).

[42] P. del Amo Sanchez et al. "Measurement of the $B \to \overline{D}^{(*)} D(*) K$ branching fractions". *Phys. Rev. D*, **83** (2011), 032004. (incl. T. Hartmann, T. Leddig, H. Schröder, R. Waldi).

[43] P. del Amo Sanchez et al. "Search for the decay $B^0 \to \gamma\gamma$". *Phys. Rev. D*, **83** (2011), 032006. (incl. T. Hartmann, T. Leddig, H. Schröder, R. Waldi).

[44] P. del Amo Sanchez et al. "Study of $B \to \pi \ell \nu$ and $B \to \rho \ell \nu$ decays and determination of $|V_{ub}|$". *Phys. Rev. D*, **83** (2011), 032007. (incl. M. Ebert, T. Hartmann, T. Leddig, H. Schröder, R. Waldi).

[45] P. del Amo Sanchez et al. "Measurements of branching fractions, polarizations, and direct CP-violation asymmetries in $B^+ \to \rho^0 K^{*+}$ and $B^+ \to f_0(980) K^{*+}$ decays". *Phys. Rev. D*, **83** (2011), 051101. (incl. T. Hartmann, T. Leddig, H. Schröder, R. Waldi).

[46] P. del Amo Sanchez et al. "Dalitz plot analysis of $D_s^+ \to K^+K^-\pi^+$". *Phys. Rev. D*, **83** (2011), 052001. (incl. T. Hartmann, T. Leddig, H. Schröder, R. Waldi).

[47] P. del Amo Sanchez et al. "Measurement of the $B^0 \to \pi^-\ell^+\nu$ and $B^+ \to \eta^{(\prime)}\ell^+\nu$ branching fractions, the $B^0 \to \pi^-\ell^+\nu$ and $B^+ \to \eta\ell^+\nu$ form-factor shapes, and determination of $|V_{ub}|$". *Phys. Rev. D*, **83** (2011), 052011. (incl. T. Hartmann, T. Leddig, H. Schröder, R. Waldi).

[48] P. del Amo Sanchez et al. "Search for CP violation in the decay $D^\pm \to K_S^0\pi^\pm$". *Phys. Rev. D*, **83** (2011), 071103. (incl. C. Bünger, T. Hartmann, T. Leddig, H. Schröder, R. Waldi).

[49] P. del Amo Sanchez et al. "Analysis of the $D^+ \to K^-\pi^+e^+\nu_e$ decay channel". *Phys. Rev. D*, **83** (2011), 072001. (incl. T. Hartmann, T. Leddig, H. Schröder, R. Waldi).

[50] J. Lees et al. "Measurement of the mass and width of the $D_{s1}(2536)^+$ meson". *Phys. Rev. D*, **83** (2011), 072003. (incl. C. Bünger, T. Hartmann, T. Leddig, H. Schröder, R. Waldi).

[51] P. del Amo Sanchez et al. "Searches for the baryon- and lepton-number violating decays $B^0 \to \Lambda_c^+\ell^-$, $B^- \to \Lambda\ell^-$, and $B^- \to \overline{\Lambda}\ell^-$". *Phys. Rev. D*, **83** (2011), 091101. (incl. C. Bünger, T. Hartmann, T. Leddig, H. Schröder, R. Waldi).

[52] J. Lees et al. "Amplitude analysis of $B^0 \to K^+\pi^-\pi^0$ and evidence of direct CP violation in $B \to K^*\pi$ decays". *Phys. Rev. D*, **83** (2011), 112010. (incl. C. Bünger, T. Hartmann, T. Leddig, H. Schröder, R. Waldi).

[53] J. Lees et al. "Study of di-pion bottomonium transitions and search for the $h_b(1P)$ state". *Phys. Rev. D*, **84** (2011), 011104. (incl. C. Bünger, O. Grünberg, T. Hartmann, T. Leddig, H. Schröder, R. Waldi).

[54] J. Lees et al. "Measurements of branching fractions and CP asymmetries and studies of angular distributions for $B \to \phi\phi K$ decays". *Phys. Rev. D*, **84** (2011), 012001. (incl. C. Bünger, T. Hartmann, T. Leddig, H. Schröder, R. Waldi).

[55] J. Lees et al. "Search for $b \to u$ transitions in $B^\pm \to [K^\mp\pi^\pm\pi^0]_D K^\pm$ decays". *Phys. Rev. D*, **84** (2011), 012002. (incl. C. Bünger, T. Hartmann, T. Leddig, H. Schröder, R. Waldi).

[56] P. del Amo Sanchez et al. "Observation of $\eta_c(1S)$ and $\eta_c(2S)$ decays to $K^+K^-\pi^+\pi^-\pi^0$ in two-photon interactions". *Phys. Rev. D*, **84** (2011), 012004. (incl. T. Hartmann, T. Leddig, H. Schröder, R. Waldi).

[57] J. Lees et al. "Search for CP violation using T-odd correlations in $D^+ \to K^+K^0_S\pi^+\pi^-$ and $D^+_s \to K^+K^0_S\pi^+\pi^-$ decays". *Phys. Rev. D*, **84** (2011), 031103. (incl. C. Bünger, O. Grünberg, T. Hartmann, T. Leddig, H. Schröder, R. Waldi).

[58] P. del Amo Sanchez et al. "Measurement of the $\gamma\gamma^* \to \eta$ and $\gamma\gamma^* \to \eta'$ transition form factors". *Phys. Rev. D*, **84** (2011), 052001. (incl. C. Bünger, T. Hartmann, T. Leddig, H. Schröder, R. Waldi).

[59] J. Lees et al. "Observation of the baryonic B decay $\overline{B}^0 \to \Lambda^+_c\overline{\Lambda}K^-$". *Phys. Rev. D*, **84** (2011), 071102. (incl. C. Bünger, T. Hartmann, T. Leddig, H. Schröder, R. Waldi).

[60] J. Lees et al. "Study of radiative bottomonium transitions using converted photons". *Phys. Rev. D*, **84** (2011), 072002. (incl. C. Bünger, T. Hartmann, T. Leddig, H. Schröder, R. Waldi).

[61] J. Lees et al. "Searches for rare or forbidden semileptonic charm decays". *Phys. Rev. D*, **84** (2011), 072006. (incl. C. Bünger, O. Grünberg, T. Hartmann, T. Leddig, H. Schröder, R. Waldi).

[62] J. Lees et al. "Evidence for the $h_b(1P)$ meson in the decay $\Upsilon(3S) \to \pi^0 h_b(1P)$". *Phys. Rev. D*, **84** (2011), 091101. (incl. C. Bünger, T. Hartmann, T. Leddig, H. Schröder, R. Waldi).

[63] J. Lees et al. "Study of $\Upsilon(3S, 2S) \to \eta\Upsilon(1S)$ and $\Upsilon(3S, 2S) \to \pi^+\pi^-\Upsilon(1S)$ hadronic transitions". *Phys. Rev. D*, **84** (2011), 092003. (incl. C. Bünger, O. Grünberg, T. Hartmann, T. Leddig, H. Schröder, R. Waldi).

[64] J. Lees et al. "Observation of the rare decay $B^+ \to K^+\pi^0\pi^0$ and measurement of the quasi-two body contributions $B^+ \to K^*(892)^+\pi^0$, $B^+ \to f_0(980)K^+$ and $B^+ \to \chi_{c0}K^+$". *Phys. Rev. D*, **84** (2011), 092007. (incl. C. Bünger, O. Grünberg, T. Hartmann, T. Leddig, H. Schröder, R. Waldi).

[65] J. Lees et al. "Branching fraction measurements of the color-suppressed decays $\overline{B}^0 \to D^{(*)0}\pi^0$, $D^{(*)0}\eta$, $D^{(*)0}\omega$, and $D^{(*)0}\eta'$ and measurement of the polarization in the decay $\overline{B}^0 \to D^{*0}\omega$". *Phys. Rev. D*, **84** (2011), 112007. (incl. C. Bünger, O. Grünberg, T. Hartmann, T. Leddig, H. Schröder, R. Waldi).

[66] T. Leddig. "Investigation of B-meson decays into baryons with the BABAR detector". *Int. J. Mod. Phys. A*, **26** (2011), 545–548.

[67] N. Agafonova et al. "Study of neutrino interactions with the electronic detectors of the OPERA experiment". *New J. Phys.*, **13** (2011), 053051. (incl. H. Schröder).

[68] J. Lees et al. "Search for low-mass dark-sector Higgs bosons". *Phys. Rev. Lett.*, **108** (2012), 211801. (incl. C. Bünger, O. Grünberg, T. Hartmann, T. Leddig, H. Schröder, C. Voß, R. Waldi).

[69] J. Lees et al. "Evidence for an excess of $\overline{B} \to D^{(*)}\tau^-\bar{\nu}_\tau$ decays". *Phys. Rev. Lett.*, **109** (2012), 101802. (incl. C. Bünger, O. Grünberg, T. Hartmann, T. Leddig, H. Schröder, C. Voß, R. Waldi).

[70] J. Lees et al. "Precision measurement of the $B \to X_s\gamma$ photon energy spectrum, branching fraction, and direct CP asymmetry $A_{CP}(B \to X_{s+d}\gamma)$". *Phys. Rev. Lett.*, **109** (2012), 191801. (incl. C. Bünger, O. Grünberg, T. Hartmann, T. Leddig, C. Voß, R. Waldi).

[71] J. Lees et al. "Observation of time reversal violation in the B^0 meson system". *Phys. Rev. Lett.*, **109** (2012), 211801. (incl. C. Bünger, O. Grünberg, T. Hartmann, T. Leddig, C. Voß, R. Waldi).

[72] J. Lees et al. "A measurement of the semileptonic branching fraction of the B_s meson". *Phys. Rev. D*, **85** (2012), 011101. (incl. C. Bünger, O. Grünberg, T. Hartmann, T. Leddig, H. Schröder, R. Waldi).

[73] J. Lees et al. "Search for $\overline{B} \to \Lambda_c^+ X l^- n u_l$ decays in events with a fully reconstructed B meson". *Phys. Rev. D*, **85** (2012), 011102. (incl. C. Bünger, O. Grünberg, T. Hartmann, T. Leddig, H. Schröder, R. Waldi).

[74] J. Lees et al. "Search for CP violation in the decay $\tau^- \to \pi^- K_S^0(\geq 0\pi^0)\nu_\tau$". *Phys. Rev. D*, **85** (2012), 031102. (incl. C. Bünger, O. Grünberg, T. Hartmann, T. Leddig, H. Schröder, R. Waldi).

[75] J. Lees et al. "Search for the $Z_1(4050)^+$ and $Z_2(4250)^+$ states in $\overline{B}^0 \to \chi_{c1}K^-\pi^+$ and $B^+ \to \chi_{c1}K_S^0\pi^+$". *Phys. Rev. D*, **85** (2012), 052003. (incl. C. Bünger, O. Grünberg, T. Hartmann, T. Leddig, H. Schröder, C. Voß, R. Waldi).

[76] J. Lees et al. "Amplitude analysis and measurement of the time-dependent CP asymmetry of $B^0 \to K_S^0 K_S^0 K_S^0$ decays". *Phys. Rev. D*, **85** (2012), 054023. (incl. C. Bünger, O. Grünberg, T. Hartmann, T. Leddig, H. Schröder, R. Waldi).

[77] J. Lees et al. "Search for lepton-number violating processes in $B^+ \to h^- l^+ l^+$ decays". *Phys. Rev. D*, **85** (2012), 071103. (incl. C. Bünger, O. Grünberg, T. Hartmann, T. Leddig, H. Schröder, C. Voß, R. Waldi).

[78] J. Lees et al. "B^0 meson decays to $\rho^0 K^{*0}$, $f_0 K^{*0}$, and $\rho^- K^{*+}$, including higher K^* resonances". *Phys. Rev. D*, **85** (2012), 072005. (incl. C. Bünger, O. Grünberg, T. Hartmann, T. Leddig, H. Schröder, R. Waldi).

[79] J. Lees et al. "Search for the decay $D^0 \to \gamma\gamma$ and measurement of the branching fraction for $D^0 \to \pi^0\pi^0$". *Phys. Rev. D*, **85** (2012), 091107. (incl. C. Bünger, O. Grünberg, T. Hartmann, T. Leddig, H. Schröder, R. Waldi).

[80] P. del Amo Sanchez et al. "Observation and study of the baryonic B-meson decays $B \to D^{(*)}p\overline{p}(\pi)(\pi)$". *Phys. Rev. D*, **85** (2012), 092017. (incl. C. Bünger, O. Grünberg, T. Hartmann, T. Leddig, H. Schröder, R. Waldi).

[81] J. Lees et al. "Initial-state radiation measurement of the $e^+e^- \to \pi^+\pi^-\pi^+\pi^-$ cross section". *Phys. Rev. D*, **85** (2012), 112009. (incl. C. Bünger, O. Grünberg, T. Hartmann, T. Leddig, H. Schröder, R. Waldi).

[82] J. Lees et al. "Study of CP violation in Dalitz-plot analyses of $B^0 \to K^+K^-K^0_S$, $B^+ \to K^+K^-K^+$, and $B^+ \to K^0_SK^0_SK^+$". *Phys. Rev. D*, **85** (2012), 112010. (incl. C. Bünger, O. Grünberg, T. Hartmann, T. Leddig, H. Schröder, C. Voß, R. Waldi).

[83] J. Lees et al. "A search for the decay modes $B^\pm \to h^\pm\tau\ell$". *Phys. Rev. D*, **86** (2012), 012004. (incl. C. Bünger, O. Grünberg, T. Hartmann, T. Leddig, H. Schröder, C. Voß, R. Waldi).

[84] J. Lees et al. "Cross sections for the reactions $e^+e^- \to K^+K^-\pi^+\pi^-$, $K^+K^-\pi^0\pi^0$, and $K^+K^-K^+K^-$ measured using initial-state radiation events". *Phys. Rev. D*, **86** (2012), 012008. (incl. C. Bünger, O. Grünberg, T. Hartmann, T. Leddig, H. Schröder, R. Waldi).

[85] J. Lees et al. "Search for the decay modes $D^0 \to e^+e^-$, $D^0 \to \mu^+\mu^-$, and $D^0 \to e\mu$". *Phys. Rev. D*, **86** (2012), 032001. (incl. C. Bünger, O. Grünberg, T. Hartmann, T. Leddig, H. Schröder, C. Voß, R. Waldi).

[86] J. Lees et al. "Study of $\overline{B} \to X_u\ell\bar{\nu}$ decays in $B\overline{B}$ events tagged by a fully reconstructed B-meson decay and determination of $|V_{ub}|$". *Phys. Rev. D*, **86** (2012), 032004. (incl. C. Bünger, O. Grünberg, T. Hartmann, T. Leddig, H. Schröder, R. Waldi).

[87] J. Lees et al. "Measurement of branching fractions and rate asymmetries in the rare decays $B \to K^{(*)}l^+l^-$". *Phys. Rev. D*, **86** (2012), 032012. (incl. C. Bünger, O. Grünberg, T. Hartmann, T. Leddig, H. Schröder, C. Voß, R. Waldi).

[88] J. Lees et al. "Precise measurement of the $e^+e^- \to \pi^+\pi^-(\gamma)$ cross section with the initial-state radiation method at BABAR". *Phys. Rev. D*, **86** (2012), 032013. (incl. C. Bünger, O. Grünberg, T. Hartmann, T. Leddig, H. Schröder, C. Voß, R. Waldi).

[89] J. Lees et al. "Study of the reaction $e^+e^- \to J/\psi\pi^+\pi^-$ via initial-state radiation at BABAR". *Phys. Rev. D*, **86** (2012), 051102. (incl. C. Bünger, O. Grünberg, T. Hartmann, T. Leddig, H. Schröder, C. Voß, R. Waldi).

[90] J. Lees et al. "Improved limits on B^0 decays to invisible final states and to $\nu\bar{\nu}\gamma$". *Phys. Rev. D*, **86** (2012), 051105. (incl. C. Bünger, O. Grünberg, T. Hartmann, T. Leddig, H. Schröder, C. Voß, R. Waldi).

[91] J. Lees et al. "Exclusive measurements of $b \to s\gamma$ transition rate and photon energy spectrum". *Phys. Rev. D*, **86** (2012), 052012. (incl. C. Bünger, O. Grünberg, T. Hartmann, T. Leddig, H. Schröder, C. Voß, R. Waldi).

[92] J. Lees et al. "Study of $X(3915) \to J/\psi\omega$ in two-photon collisions". *Phys. Rev. D*, **86** (2012), 072002. (incl. C. Bünger, O. Grünberg, T. Hartmann, T. Leddig, C. Voß, R. Waldi).

[93] J. Lees et al. "Study of the baryonic B decay $B^- \to \Sigma_c^{++}\bar{p}\pi^-\pi^-$". *Phys. Rev. D*, **86** (2012), 091102. (incl. C. Bünger, O. Grünberg, T. Hartmann, T. Leddig, C. Voß, R. Waldi).

[94] J. Lees et al. "Branching fraction and form-factor shape measurements of exclusive charmless semileptonic B decays, and determination of $|V_{ub}|$". *Phys. Rev. D*, **86** (2012), 092004. (incl. C. Bünger, O. Grünberg, T. Hartmann, T. Leddig, C. Voß, R. Waldi).

[95] J. Lees et al. "Search for resonances decaying to $\eta_c\pi^+\pi^-$ in two-photon interactions". *Phys. Rev. D*, **86** (2012), 092005. (incl. C. Bünger, O. Grünberg, T. Hartmann, T. Leddig, C. Voß, R. Waldi).

[96] J. Lees et al. "Study of high-multiplicity 3-prong and 5-prong tau decays at BABAR". *Phys. Rev. D*, **86** (2012), 092010. (incl. C. Bünger, O. Grünberg, T. Hartmann, T. Leddig, C. Voß, R. Waldi).

[97] J. Lees et al. "The branching fraction of $\tau^- \to \pi^- K_S^0 K_S^0(\pi^0)\nu_\tau$ decays". *Phys. Rev. D*, **86** (2012), 092013. (incl. C. Bünger, O. Grünberg, T. Hartmann, T. Leddig, C. Voß, R. Waldi).

[98] J. Lees et al. "Measurement of the Time-Dependent CP Asymmetry of Partially Reconstructed $B^0 \to D^{*+}D^{*-}$ Decays". *Phys. Rev. D*, **86** (2012), 112006. (incl. C. Bünger, O. Grünberg, T. Hartmann, T. Leddig, C. Voß, R. Waldi).

[99] J. Lees et al. "Measurement of $\mathcal{B}(B \to X_s\gamma)$, the $B \to X_s\gamma$ photon energy spectrum, and the direct CP asymmetry in $B \to X_{s+d}\gamma$ decays". *Phys. Rev. D*, **86** (2012), 112008. (incl. C. Bünger, O. Grünberg, T. Hartmann, T. Leddig, C. Voß, R. Waldi).

[100] O. Grünberg. "Baryonic B decays at BABAR (in Proc. Moriond 2012, QCD and High Energy Interactions)". *arXiv*, **1211.0212** (2012), 1.

[101] R. Aaij et al. "Measurement of the CP-violating phase ϕ_s in the decay $B_s^0 \to J/\psi\,\phi$". *Phys. Rev. Lett.*, **108** (2012), 101803. (incl. T. Hartmann).

[102] R. Aaij et al. "Evidence for CP violation in time-integrated $D^0 \to h^-h^+$ decay rates". *Phys. Rev. Lett.*, **108** (2012), 111602. (incl. T. Hartmann).

[103] R. Aaij et al. "Observation of $B_s \to J/\psi\, f_2'(1525)$ in $J/\psi\, K^+K^-$ final states". *Phys. Rev. Lett.*, **108** (2012), 151801. (incl. T. Hartmann).

[104] R. Aaij et al. "First observation of the decays $\overline{B}^0 \to D^+K^-\pi^+\pi^-$ and $B^- \to D^0K^-\pi^+\pi^-$". *Phys. Rev. Lett.*, **108** (2012), 161801. (incl. T. Hartmann).

[105] R. Aaij et al. "Differential branching fraction and angular analysis of the decay $B^0 \to K^{*0}\mu^+\mu^-$". *Phys. Rev. Lett.*, **108** (2012), 181806. (incl. T. Hartmann).

[106] R. Aaij et al. "First evidence of direct CP violation in charmless two-body decays of B_s mesons". *Phys. Rev. Lett.*, **108** (2012), 201601. (incl. T. Hartmann, R. Waldi).

[107] R. Aaij et al. "Strong constraints on the rare decays $B_s \to \mu^+\mu^-$ and $B^0 \to \mu^+\mu^-$". *Phys. Rev. Lett.*, **108** (2012), 231801. (incl. O. Grünberg, T. Hartmann, C. Voß, R. Waldi).

[108] R. Aaij et al. "Determination of the sign of the decay width difference in the B_s system". *Phys. Rev. Lett.*, **108** (2012), 241801. (incl. T. Hartmann).

[109] R. Aaij et al. "First observation of the decay $B_c^+ \to J/\psi\pi^+\pi^-\pi^+$". *Phys. Rev. Lett.*, **108** (2012), 251802. (incl. T. Hartmann, R. Waldi).

[110] R. Aaij et al. "Observation of the decay $B^0 \to \overline{D}^0K^+K^-$ and evidence for $B_s \to \overline{D}^0K^+K^-$". *Phys. Rev. Lett.*, **109** (2012), 131801. (incl. O. Grünberg, T. Hartmann, C. Voß, R. Waldi).

[111] R. Aaij et al. "Measurement of the B_s effective lifetime in the $J/\psi\, f_0(980)$ final state". *Phys. Rev. Lett.*, **109** (2012), 152002. (incl. O. Grünberg, T. Hartmann, C. Voß, R. Waldi).

[112] R. Aaij et al. "Observation of excited Λ_b^0 baryons". *Phys. Rev. Lett.*, **109** (2012), 172003. (incl. O. Grünberg, T. Hartmann, C. Voß, R. Waldi).

[113] R. Aaij et al. "Measurement of the $B^\pm$ production cross-section in pp collisions at $\sqrt{s} = 7\,\text{TeV}$". *JHEP*, **1204** (2012), 093. (incl. T. Hartmann).

[114] R. Aaij et al. "Measurement of mixing and CP violation parameters in two-body charm decays". *JHEP*, **1204** (2012), 129. (incl. T. Hartmann).

[115] R. Aaij et al. "Inclusive W and Z production in the forward region at $\sqrt{s} = 7\,\text{TeV}$". *JHEP*, **1206** (2012), 058. (incl. O. Grünberg, T. Hartmann, C. Voß, R. Waldi).

[116] R. Aaij et al. "Measurements of the branching fractions of the decays $B_s^0 \to D_s^{\mp} K^{\pm}$ and $B_s^0 \to D_s^- \pi^+$". *JHEP*, **1206** (2012), 115. (incl. T. Hartmann, R. Waldi).

[117] R. Aaij et al. "Observation of double charm production involving open charm in pp collisions at $\sqrt{s} = 7\,\text{TeV}$". *JHEP*, **1206** (2012), 141. (incl. T. Hartmann, R. Waldi).

[118] R. Aaij et al. "Measurement of the isospin asymmetry in $B \to K^{(*)}\mu^+\mu^-$ decays". *JHEP*, **1207** (2012), 133. (incl. O. Grünberg, T. Hartmann, C. Voß, R. Waldi).

[119] R. Aaij et al. "Measurement of b-hadron branching fractions for two-body decays into charmless charged hadrons". *JHEP*, **1210** (2012), 037. (incl. T. Hartmann, R. Waldi).

[120] R. Aaij et al. "Study of D_{sJ} decays to $D^+K_S^0$ and D^0K^+ final states in pp collisions". *JHEP*, **1210** (2012), 151. (incl. O. Grünberg, T. Hartmann, C. Voß, R. Waldi).

[121] R. Aaij et al. "Measurement of the fraction of $\Upsilon(1S)$ originating from $\chi_b(1P)$ decays in pp collisions at $\sqrt{s} = 7\,\text{TeV}$". *JHEP*, **1211** (2012), 031. (incl. O. Grünberg, T. Hartmann, C. Voß, R. Waldi).

[122] R. Aaij et al. "Measurement of the CP violating phase ϕ_s in $\overline{B}_s^0 \to J/\psi\, f_0(980)$". *Phys. Lett. B*, **707** (2012), 497–505. (incl. T. Hartmann).

[123] R. Aaij et al. "Measurement of b-hadron masses". *Phys. Lett. B*, **708** (2012), 241–248. (incl. T. Hartmann).

[124] R. Aaij et al. "Observation of CP violation in $B^+ \to DK^+$ decays". *Phys. Lett. B*, **712** (2012), 203–212 and erratum 713, 351. (incl. T. Hartmann, R. Waldi).

[125] R. Aaij et al. "Measurement of the $B_s^0 \to J/\psi\, K_S^0$ branching fraction". *Phys. Lett. B*, **713** (2012), 172–179. (incl. T. Hartmann, R. Waldi).

[126] R. Aaij et al. "Measurement of the D_s^+-D_s^- production asymmetry in 7 TeV pp collisions". *Phys. Lett. B*, **713** (2012), 186–195. (incl. O. Grünberg, T. Hartmann, C. Voß, R. Waldi).

[127] R. Aaij et al. "Measurement of the polarization amplitudes and triple product asymmetries in the $B_s^0 \to \phi\phi$ decay". *Phys. Lett. B*, **713** (2012), 369–377. (incl. T. Hartmann, R. Waldi).

[128] R. Aaij et al. "Measurement of the CP-violating phase ϕ_s in $B_s \to J/\psi\,\pi^+\pi^-$ decays". *Phys. Lett. B*, **713** (2012), 378–386. (incl. T. Hartmann, R. Waldi).

[129] R. Aaij et al. "Measurement of the effective $B_s^0 \to K^+K^-$ lifetime". *Phys. Lett. B*, **716** (2012), 393–400. (incl. O. Grünberg, T. Hartmann, C. Voß, R. Waldi).

[130] R. Aaij et al. "A model-independent Dalitz plot analysis of $B^\pm \to DK^\pm$ with $D \to K^0_S h^+h^-$ ($h = \pi, K$) decays and constraints on the CKM angle γ". *Phys. Lett. B*, **718** (2012), 43–55. (incl. O. Grünberg, T. Hartmann, C. Voß, R. Waldi).

[131] R. Aaij et al. "Measurement of the ratio of prompt χ_c to J/ψ production in pp collisions at $\sqrt{s} = 7$ TeV". *Phys. Lett. B*, **718** (2012), 431–440. (incl. O. Grünberg, T. Hartmann, C. Voß, R. Waldi).

[132] R. Aaij et al. "Observation of $X(3872)$ production in pp collisions at $\sqrt{s} = 7\,\text{TeV}$". *Eur. Phys. J. C*, **72** (2012), 1972. (incl. T. Hartmann, R. Waldi).

[133] R. Aaij et al. "Opposite-side flavour tagging of B mesons at the LHCb experiment". *Eur. Phys. J. C*, **72** (2012), 2022. (incl. T. Hartmann).

[134] R. Aaij et al. "Measurement of Upsilon production in pp collisions at $\sqrt{s} = 7\,\text{TeV}$". *Eur. Phys. J. C*, **72** (2012), 2025. (incl. T. Hartmann).

[135] R. Aaij et al. "Measurement of $\psi(2S)$ meson production in pp collisions at $\sqrt{s} = 7\,\text{TeV}$". *Eur. Phys. J. C*, **72** (2012), 2100. (incl. T. Hartmann, R. Waldi).

[136] R. Aaij et al. "Measurement of relative branching fractions of B decays to $\psi(2S)$ and J/ψ mesons". *Eur. Phys. J. C*, **72** (2012), 2118. (incl. O. Grünberg, T. Hartmann, C. Voß, R. Waldi).

[137] R. Aaij et al. "Measurement of prompt hadron production ratios in pp collisions at $\sqrt{s} = 0.9$ and 7 TeV". *Eur. Phys. J. C*, **72** (2012), 2168. (incl. O. Grünberg, T. Hartmann, C. Voß, R. Waldi).

[138] R. Aaij et al. "Search for the $X(4140)$ state in $B^+ \to J/\psi\,\phi K^+$ decays". *Phys. Rev. D*, **85** (2012), 091103. (incl. T. Hartmann).

[139] R. Aaij et al. "Measurements of the branching fractions and CP asymmetries of $B^+ \to J/\psi\,\pi^+$ and $B^+ \to \psi(2S)\pi^+$ decays". *Phys. Rev. D*, **85** (2012), 091105. (incl. T. Hartmann, R. Waldi).

[140] R. Aaij et al. "Searches for Majorana neutrinos in B^- decays". *Phys. Rev. D*, **85** (2012), 112004. (incl. T. Hartmann, R. Waldi).

[141] R. Aaij et al. "Measurement of the ratio of branching fractions $\mathcal{B}(B^0 \to K^{*0}\gamma)/\,\mathcal{B}(B_s^0 \to \phi\gamma)$". *Phys. Rev. D*, **85** (2012), 112013. (incl. T. Hartmann).

[142] R. Aaij et al. "Analysis of the resonant components in $B_s \to J/\psi\,\pi^+\pi^-$". *Phys. Rev. D*, **86** (2012), 052006. (incl. T. Hartmann, R. Waldi).

[143] R. Aaij et al. "Measurement of the $B_s^0 \to J/\psi\,K^{*0}$ branching fraction and angular amplitudes". *Phys. Rev. D*, **86** (2012), 071102. (incl. O. Grünberg, T. Hartmann, C. Voß, R. Waldi).

[144] N. Agafonova et al. "Momentum measurement by the Multiple Coulomb Scattering method in the OPERA lead emulsion target". *New J. Phys.*, **14** (2012), 013026. (incl. H. Schröder).

2.3.4 Molecular Quantum Dynamics

Head: Prof. Dr. Oliver Kühn

Staff:	Dr. David Ambrosek	Dr. Olga Bokareva	
	Dr. Sergey Bokarev	Dr. Sergei D. Ivanov	
	Dr. Guennaddi Paramonov	Dr. Sergey Polyutov	
	Dr. Yunan Yan		
	MSc Mahmud Abdel-Latif	MSc Ashour Ahmed	
	MSc Mateusz Lisaj	MSc Mahdi Taghikhani	
	MSc Tobias Zentel	Per-Arno Plötz	
	Marco Schröter	Jan Schulze	
	Marina Hertzfeldt		
MSc Graduates:	Janis Aizezers	Tobias Zentel	
BSc Graduates:	Fabian Gottwald	Gilbert Grell	Sven Karsten
	Robert Kemsies	Per-Arno Plötz	Marco Schröter
	Jan Schulze	Laura Tropf	

General Outline of the Field of Research

The focus of the Molecular Quantum Dynamics group is on computer simulations of the dynamics, spectroscopy, and laser control of molecular systems in gas and solution phase. Here, dynamics comprises reactive and nonreactive processes of the nuclear degrees of freedom (adiabatic dynamics in the electronic ground state) as well as coupled (non-adiabatic) electron-nuclear dynamics as it occurs in Photophysics and Photochemistry. Spectroscopic methods range from electron paramagnetic resonance to stationary as well as ultrafast infrared and optical spectroscopy. The range of applications encompasses small model systems like H_2^+ or HCOOH, metal-organic compounds and their complexes with small metal clusters, extended molecular aggregates formed by organic dye molecules, ionic liquids, biologically relevant molecules in solution and soil organic matter [1–29].

The spectrum of available methods includes first principles electronic structure theory and classical force fields for the determination of interaction potentials and various means to solve the time-dependent Schrödinger or Liouville-von Neumann equation in gas and condensed phase, respectively. The complexity of the considered systems often requires to use hybrid methods where different parts of the system are treated at different levels of approximation. This includes the quantum mechanics/molecular mechanics (QM/MM) method for determination of interaction potentials or quantum-classical dynamical approaches combining trajectory simulations with quantisation of certain degrees of freedom.

Quantum-Classical Dynamics for Spectroscopy

The response of a material system to an external field can be expressed in terms of (multi-time) correlation functions. Infrared (IR) spectroscopy thus requires the cal-

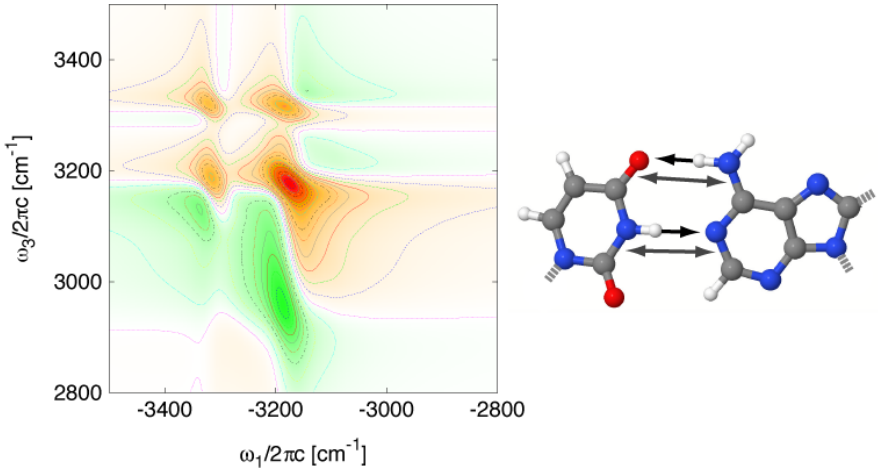

Fig. 2.53: Two-dimensional IR spectrum (left) in rephasing phase matching direction calculated for an adenine-uracil base pair (right) in $CDCl_3$. The elongation of the peaks around $(\omega_1, \omega_3) \approx (-3200, 3320)\,\mathrm{cm}^{-1}$ along the figure diagonal gives evidence for in-phase fluctuations of the two hydrogen bonds. (adapted from Ref. [25])

culation of dipole autocorrelation functions. Note that a general procedure to assign spectral features to molecular motions has been developed not only for single- but for the multi-reference cases, that is the cases when the system under investigation undergoes conformation transitions [29]. Focusing on hydrogen bonds one faces the challenge that the quantisation of hydrogen stretching motions in general cannot be neglected. Here a hybrid treatment is required, in which, for instance, the N-H vibration is quantised whereas the remaining intramolecular and intermolecular degrees of freedom are treated in the classical approximation. The effect of their interaction with the quantum degree(s) of freedom can be expressed in terms of energy gap fluctuations and their correlation functions. Using this strategy IR spectra have been calculated in particular for DNA base pairs in solution [14, 23–25] and also for other systems [27].

The considered DNA base pair (adenine-uracil, see right panel in Fig. 2.53) has two hydrogen bonds and the question we have addressed concerned their type of fluctuation, i.e. whether it is in-phase or out-of-phase. Notice that compression/elongation of a hydrogen bond leads to a red-/blue-shifted absorption due to increased/decreased bonding strength. The dynamical aspects of this behaviour for two hydrogen bonds cannot be obtained from the linear IR absorption profile, but from nonlinear two-dimensional IR spectroscopy. In the left panel of Fig. 2.53 simulated 2D IR spectra are presented for such a base pair solvated in $CDCl_3$. From the shape of the so-called off-diagonal peaks one can infer that the two hydrogen bonds fluctuate in-phase [25].

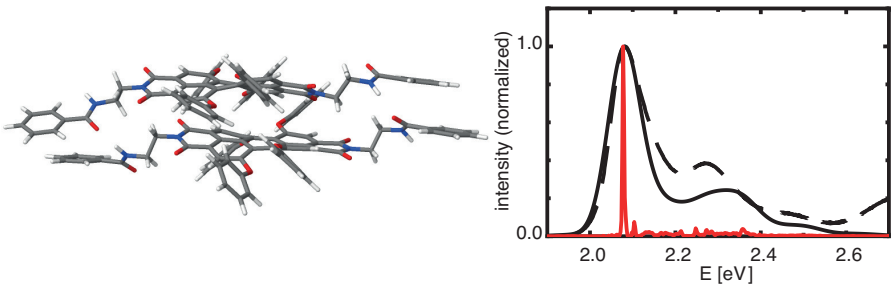

Fig. 2.54: PBI dimer taken from a hexameric aggregate (left) and its absorption spectrum (right). The spectrum is shown at different resolutions (solid) and compared to the experimental result of the Lochbrunner group (dashed). (adapted from Ref. [6])

Exciton Dynamics in Molecular Aggregates

Frenkel exciton dynamics and spectroscopy is the focus of our project B10, which is conducted in collaboration with the group of Prof. S. Lochbrunner in the SFB 652 [12]. Apart from general aspects of non-perturbative exciton-vibrational coupling [20, 26] specific effort is devoted to obtain a detailed understanding of perylene bisimide aggregates based on first principles simulations. The developed simulation protocol starts with the monomeric building blocks including ground and excited state absorption [7]. Aggregate structures are obtained by employing self-consistent charge tight-binding density functional theory (DFTB). As an example a dimer cut out of a hexameric aggregate is shown in Fig. 2.54. Coulomb interactions between electronic transitions can be calculated using time-dependent DFT (TDDFT) in the linear response formulation [6]. Supplementing the electronic Hamiltonian with the coupling to the vibrational degrees of freedom, here taken in harmonic approximation, absorption spectra and exciton transfer dynamics can be determined. If the exciton-vibrational coupling is taken into account explicitly within the Schrödinger equation, a high-dimensional state vector has to be propagated. This is achieved by means of the Multiconfiguration Time-dependent Hartree (MCTDH) method.

The absorption spectrum shows the typical features of so-called J-aggregates, i.e. a concentration of oscillator strength at the lower edge of the one-exciton band [15]. This can be explained as a collective response of monomeric excitations triggered by the Coulomb interaction. Another interesting feature concerns the effect of coupled vibrations. Judged on the basis of the experimental absorption one would have assigned the higher energetic side band to a one-quantum vibronic transition. However, from the high-resolution spectrum it becomes clear that it is in fact the effect of many small-amplitude transitions which shape this side band. This is important for understanding exciton transfer, which - depending on the exciton-vibrational coupling strength - can change from the coherent to the incoherent regime. In fact the incoherent transfer in long one- and two-dimensional PBI aggregates has been

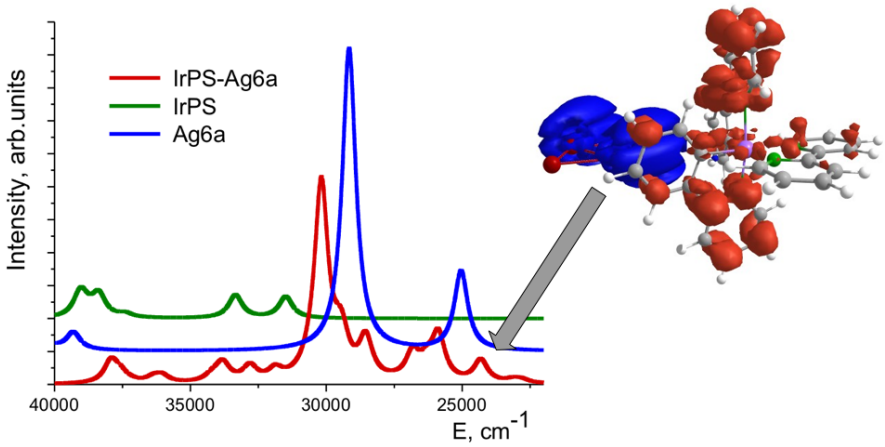

Fig. 2.55: Electronic absorption spectra of $[Ir(ppy)_2(bpy)]^+$, Ag_6, and their complex as obtained using long-range corrected TDDFT (LC-BLYP). Also shown is the difference density for the transition leading to the indicated peak. (adapted from Ref. [9])

treated using the kinetic Monte Carlo method, which revealed a high directionality of the transport over several tens of nanometers [22].

Elementary Processes in Photocatalytic Water Splitting

Photocatalytic water splitting is the central theme of two collaborative research projects combining efforts of the Institutes of Physics and Chemistry and the Leibniz Institute of Catalysis (LIKAT). Light2Hydrogen (L2H) is funded by the BMBF and focuses on homogeneous catalysis with participation of several research groups from Berlin and Potsdam. Our goal is to understand the initial photophysical and photochemical processes after light absorption of an Iridium based photosensitizer. The latter is a part of a catalytic cycle, which has been shown by the LIKAT group to be successful in producing H_2. First principles electronic structure theory methods have been validated and used for this complex to assign the excitation spectrum [8]. Essential for the function is a singlet-triplet transition occurring within a few hundreds of femtoseconds and leading to a charge separated state. Upon complexation with a sacrificial reductant an electron transfer process takes place, which is important for subsequent water splitting. The obtained understanding of the electronic states and pathways of the electron transfer allows us to judge different chemically modified systems with respect to their efficiency, thus giving a theoretical foundation for design optimisation.

Nano4Hydrogen (N4H) is a related ESF project, which places emphasis on heterogeneous photocatalysis. Specifically, we have addressed the question how the electronic properties of the Ir-photosensitizer are modified upon complexation with

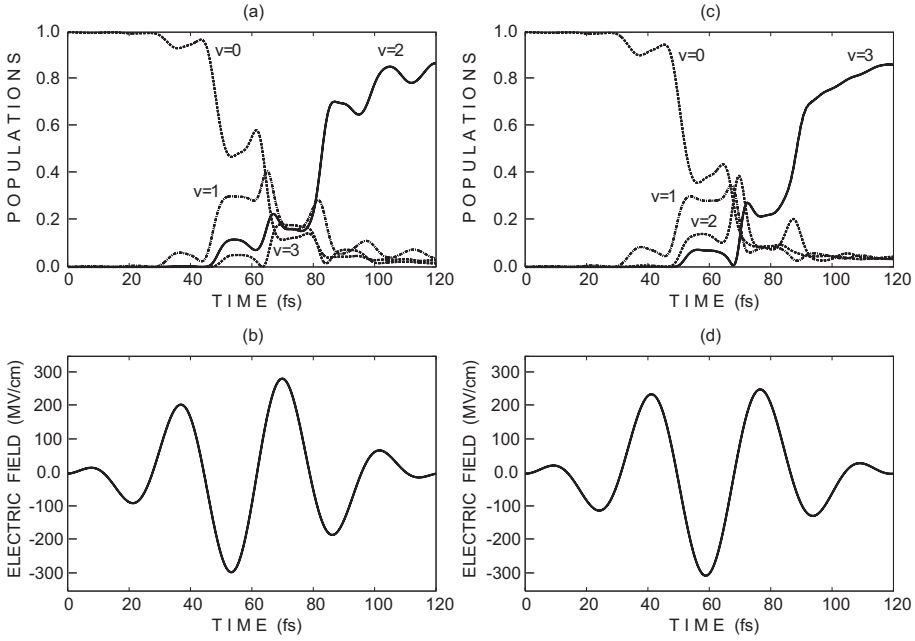

Fig. 2.56: Optimal below-resonant state-selective excitation of $|v = 2\rangle$ (a and b) and $|v = 3\rangle$ (c and d) in H_2^+. Upper panels: time-dependent populations of the vibrational levels v =0, 1, 2 and 3. The respective optimal below-resonant IR laser fields are shown in the bottom panels. (adapted from Ref. [18])

small silver clusters in a regime where every cluster atom counts. In Fig. 2.55 absorption spectra are plotted for the photosensitizer, Ag_6, and their complex. Clearly the effect of complexation on the spectrum is not additive and enhances the range of absorption of the photosensitizer. Furthermore, it is found that electronic excitation directly leads to a charge transfer transition, whose direction depends on whether the number of cluster atoms is even or odd.

Laser Control of Molecular Dynamics

During the last two decades the control of molecular dynamics using shaped laser fields has developed from an exotic theoretical consideration into a regular experimental tool. Our recent focus has been on vibrational [1–3, 10] and coupled electron-vibrational processes [18, 26]. The latter also include exciton dynamics, which has been investigated in the regime where two excitons are present on an aggregate [26]. Usually the two-exciton state will be rapidly quenched by local internal conversion processes. Laser optimisation has been performed to find the conditions for transient suppression of the internal conversion, which is indeed possible depending on the electronic level structure of the aggregate. Furthermore, a non-Born-Oppenheimer quantum dynamics study has been performed for H_2^+ employing a three-dimensional model with cylindrical symmetry [18]. Here a genuine non-Born-Oppenheimer ef-

fect was found, namely that vibrational states can be prepared with high-selectivity in this homonuclear molecule; see Fig. 2.56. The underlying mechanism involves electron field following and simultaneous coupling of electronic and nuclear degrees of freedom.

References

[1] M. K. Abdel-Latif and O. Kühn. "Infrared laser driven double proton transfer. An optimal control theory study". *Chem. Phys.*, **368** (2010), 76–82.

[2] M. K. Abdel-Latif and O. Kühn. "Carbonyl vibrational wave packet circulation in $Mn_2(CO)_{10}$ driven by ultrashort polarized laser pulses". *J. Chem. Phys.*, **135** (2011), 084314.

[3] M. K. Abdel-Latif and O. Kühn. "Laser control of double proton transfer in porphycenes: Towards an ultrafast switch for photonic molecular wires". *Theor. Chem. Acc.*, **128** (2011), 307.

[4] A. Accardi, I. Barth, O. Kühn and J. Manz. "From synchronous to sequential double proton transfer: Quantum dynamics simulations for the model porphine". *J. Phys. Chem. A*, **114** (2010), 11252–11262.

[5] A. A. Ahmed, O. Kühn and P. Leinweber. "Controlled experimental soil organic matter modification for study of organic pollutant interactions in soil". *Science Total Environ.*, **441** (2012), 151–158.

[6] D. Ambrosek, A. Köhn, J. Schulze and O. Kühn. "Quantum chemical parametrization and spectroscopic characterization of the Frenkel exciton hamiltonian for a J-aggregate forming perylene bisimide dye". *J. Phys. Chem. A*, **116** (2012), 11451–11458.

[7] D. Ambrosek, H. Marciniak, S. Lochbrunner, J. Tatchen, X.-Q. Li, F. Würthner and O. Kühn. "Photophysical and quantum chemical study on a J-aggregate forming perylene bisimide monomer". *Phys. Chem. Chem. Phys.*, **13** (2011), 17649.

[8] S. I. Bokarev, O. S. Bokareva and O. Kühn. "Electronic excitation spectrum of the photosensitizer $[Ir(ppy)_2(bpy)]^+$". *J. Chem. Phys.*, **136** (2012), 214305.

[9] O. S. Bokareva, S. I. Bokarev and O. Kühn. "Electronic excitation spectra of the $[Ir(ppy)_2(bpy)]^+$ photosensitizer bound to small silver clusters Ag_n (n = 1–6)". *Phys. Chem. Chem. Phys.*, **14** (2012), 4977.

[10] N. Došlić, M. K. Abdel-Latif and O. Kühn. "Laser control of single and double proton transfer reactions". *Acta Chim. Slov.*, **58** (2011), 411–424.

[11] O. Kühn. "Moleküle in Bewegung". *traditio et innovatio*, (2010), 10–14.

[12] O. Kühn and S. Lochbrunner. "Quantum dynamics and spectroscopy of excitons in molecular aggregates". In U. Würfel, M. Thorwart and E. R. Weber, editors, "Quantum efficiency in complex systems, Part II", pages 47–81. Academic Press, San Diego (2011).

[13] O. Kühn, J. Manz and A. Schild. "Quantum effects of translational motions in solid para-hydrogen and ortho-deuterium: Anharmonic extension of the Einstein model". *J. Phys.: Condens. Matter*, **22** (2010), 135401.

[14] O. Kühn and Y. Yan. "Simulation of nonlinear infrared spectroscopy of hydrogen-bonded systems using classical trajectories". *Bunsenmagazin*, **13** (2011), 198.

[15] V. May and O. Kühn. *Charge and Energy Transfer Dynamics in Molecular Systems, 3rd revised and enlarged edition*. Wiley-VCH, Weinheim (2011).

[16] J. Novak, M. Mališ, A. Prlj, I. Ljubić, O. Kühn and N. Došlić. "Photoinduced dynamics of formic acid monomers and dimers: The role of the double hydrogen bond". *J. Phys. Chem. A*, **116** (2012), 11467–11475.

[17] G. K. Paramonov, A. D. Bandrauk and O. Kühn. "Long-range energy transfer and ionization in extended quantum systems driven by ultrashort spatially shaped laser pulses". *Phys. Chem. Chem. Phys.*, **13** (2011), 8637.

[18] G. K. Paramonov and O. Kühn. "State-selective vibrational excitation and dissociation of H_2^+ by strong infrared laser pulses: Below-resonant versus resonant laser fields and electron–field following". *J. Phys. Chem. A*, **116** (2012), 11388–11397.

[19] G. K. Paramonov, O. Kühn and A. D. Bandrauk. "Energy transfer among distant quantum systems in spatially shaped laser fields: Two H atoms with an internuclear separation of 5.29 nm (100 a.u.)". *Phys. Rev. A*, **83** (2011), 013418.

[20] S. Polyutov, O. Kühn and T. Pullerits. "Exciton-vibrational coupling in molecular aggregates: Electronic versus vibronic dimer". *Chem. Phys.*, **394** (2012), 21–28.

[21] C. Roth, S. Chatzipapadopoulos, D. Kerlé, F. Friedriszik, M. Lütgens, S. Lochbrunner, O. Kühn and R. Ludwig. "Hydrogen bonding in ionic liquids probed by linear and nonlinear vibrational spectroscopy". *New J. Phys.*, **14** (2012), 105026.

[22] S. Wolter, J. Aizezers, F. Fennel, M. Seidel, F. Würthner, O. Kühn and S. Lochbrunner. "Size-dependent exciton dynamics in one-dimensional perylene bisimide aggregates". *New J. Phys.*, **14** (2012), 105027.

[23] Y. Yan and O. Kühn. "Geometric correlations and infrared spectrum of adenine-uracil hydrogen bonds in $CDCl_3$ solution". *Phys. Chem. Chem. Phys.*, **12** (2010), 15695–15703.

[24] Y. Yan and O. Kühn. "Vibrational dynamics of the double hydrogen bonds in nucleic acid base pairs". In K.-L. Han and G.-J. Zhao, editors, "Hydrogen bonding and transfer in the excited state", page 1. Wiley and Sons, Chichester (2010).

[25] Y. Yan and O. Kühn. "Unraveling the correlated dynamics of the double hydrogen bonds of nucleic acid base pairs in solution". *J. Phys. Chem. B*, **115** (2011), 5254.

[26] Y. Yan and O. Kühn. "Laser control of dissipative two-exciton dynamics in molecular aggregates". *New J. Phys.*, **14** (2012), 105004.

[27] Y. Yan, M. Petković, G. M. Krishnan and O. Kühn. "IR spectrum of the O-H·O hydrogen bond of phthalic acid monomethylester in gas phase and in CCl_4 solution". *J. Mol. Struct.*, **972** (2010), 68–74.

[28] Y. Yang and O. Kühn. "H/D isotope effects on the geometry and infrared spectrum of the protonated ammonia dimer". *Chem. Phys. Lett.*, **505** (2011), 1–4.

[29] G. Mathias, S. D. Ivanov, A. Witt, M. Baer and D. Marx. "Infrared Spectroscopy of Fluxional Molecules from (ab Initio) Molecular Dynamics: Resolving Large-Amplitude Motion, Multiple Conformations, and Permutational Symmetries". *J. Chem. Theory Comput.*, **8** (2012), 224–234.

2.4 Institute of Atmospheric Physics Kühlungsborn

Name of the facility:	Leibniz-Institut für Atmosphärenphysik e. V. (IAP) an der Universität Rostock
Address:	Schlossstr. 6, 18225 Ostseebad Kühlungsborn, Germany
Director:	Prof. Dr. Franz-Josef Lübken
Telephone:	+49-38293-68-0
Fax:	+49-38293-68-50
Web:	www.iap-kborn.de
Source for more information:	Institute report (every two years)
Other locations:	Außenstelle Juliusruh, Drewoldke 13 18556 Juliusruh, Germany

2.4.1 Main Areas of Research

The main task of the Institute of Atmospheric Physics (IAP) at the Rostock University is to conduct research in the field of atmospheric physics. The atmosphere is a multi-faceted and often quite variable medium of complex behavior. Its great complexity gives us the opportunity to seek niches in international research activity where even comparatively small investments can yield distinctive and interesting contributions to a deeper understanding of the atmosphere. The IAP emphasizes research in the areas of (a) the mesosphere, in particular at Arctic latitudes, (b) the dynamical coupling between the troposphere, stratosphere, and mesosphere, and (c) long-term changes of the thermal and dynamical structure in the middle atmosphere (∼10–120 km).

The main building of IAP being located in Kühlungsborn provides modern offices, laboratories, high speed computer facilities, and administrative and technical infrastructure. Field measurements are performed primarily here and at the institute's field station in Juliusruh (on the island Rügen) as well as at the ALOMAR observatory in Northern Norway. ALOMAR hosts instruments from several international institutes and is located close to the Andøya Rocket Range (69°N,16°E), poleward of the Arctic circle. The IAP also operates a mobile lidar (laser induced detection and ranging) in a container which was stationed at various locations and is currently located in Davis (69°S, Antarctica). The instrumentation at IAP mainly consists of lidars at various frequencies from the infrared to the ultraviolet range of the electromagnetic spectrum and several radars with frequencies between 100 kHz and 1 GHz. Furthermore, instruments are installed on sounding rockets to measure dust, and neutral and plasma number densities in the mesosphere and lower thermosphere. Balloon borne measurements of turbulence in the stratosphere are performed at various field stations. Since 2009 a new microwave spectrometer is installed at Kühlungsborn to measure water vapor profiles up to ∼85 km. The IAP performs model calculations and theoretical studies for better physical understanding in the aforementioned areas of research, with emphasis on the interpretation of local phenomena in a global context. This includes the development of specially

designed numerical models and cooperation with the experimental investigations. The scientists at IAP cooperate with several international research institutes and universities both on experimental and theoretical aspects of atmospheric physics.

Supplemental Information

Typically 79 individuals were employed at the IAP, amongst them 25 scientists and 25–30 students. In the period 2010–2012 the following staff members of the IAP gave courses and seminars at the Rostock University in the field of physics of the atmosphere: Prof. Dr. F.-J. Lübken, Prof. Dr. E. Becker, Prof. Dr. M. Rapp (now professor at the University in Munich), and Dr. habil. D. Peters. They also provided opportunities for students to work at the IAP for their bachelor, master, diploma, and Ph. D. thesis.

In the following we provide some examples of typical research results in the three departments of the IAP. More details can be found in 122 scientific papers published by IAP scientists in the period 2010–2012. The list is provided in the appendix of this report.

2.4.2 Optical Sounding of the Atmosphere

Head: Prof. Dr. Franz-Josef Lübken

Staff: Dr. Gerd Baumgarten, Dr. Uwe Berger, Dr. Ronald Eixmann, Dr. Jens Fiedler, Dr. Michael Gerding, Dr. Josef Höffner, Dr. Jens Lautenbach
9 PhD students and 6 master/diploma/bachelor students

The main areas of research are the exploration of (a) the Arctic middle atmosphere at approximately 10 to 120 km altitude, (b) the thermal structure of the mesopause region at various latitudes (mesopause = pronounced temperature minimum near 90–100 km altitude), (c) ice clouds in the mesopause region known as "noctilucent clouds" (NLC), and (d) turbulence in the lower stratosphere. Field measurements are performed by a number of lidars and by instruments mounted on balloons. A global scale model called LIMA (Leibniz Institute Model of the Atmosphere) is used to interpret ice cloud measurements, their connection to background conditions, and long term trends.

In the following we present an example of results from our mobile iron-lidar which was transported via Australia to Antarctica, where it arrived at Davis Station (69°S, 78°E) in November 2010. The iron lidar measures temperatures in the iron layer (appr. 80 to 120 km) by probing the Doppler width of the Fe resonance line. Furthermore, Fe densities and neutral winds (from Doppler shift) are derived. Temperatures at lower altitudes are inferred from Rayleigh scattering. The instrument is capable of performing measurements during full daylight with high precision which is unprecedented worldwide. In the first 15 months more than 2700 hours of data were

collected which represents a unique and very valuable data set.

In Fig. 2.57 temperature deviations from the mean are shown. A total of 171 hours of observations within 12 days in January 2011 contribute to this plot. Below approximately 90 km the diurnal component of tides with a period of 24 hours is dominant and leads to generally higher temperatures in the morning hours (∼6–12 LST) and lower ones 12 hours later. The magnitude of the modulation is approximately ∼4–7 K. Above ∼92 km a semi-diurnal variation is clearly visible. Tidal modulations of such large magnitude were not expected at polar latitudes during summer solstice since sunshine is present practically permanently which minimizes excitation of tides. We will investigate other potential explanations such as the propagation of tides from lower latitudes. Large tidal variations were also observed in Fe densities practically all year round. There are many more interesting and unique results derived from our Davis lidar, for example mesopause temperatures being linked to stratospheric circulation. It is planned to bring our lidar back to IAP in early 2013. Except from observations by lidars we also study the creation

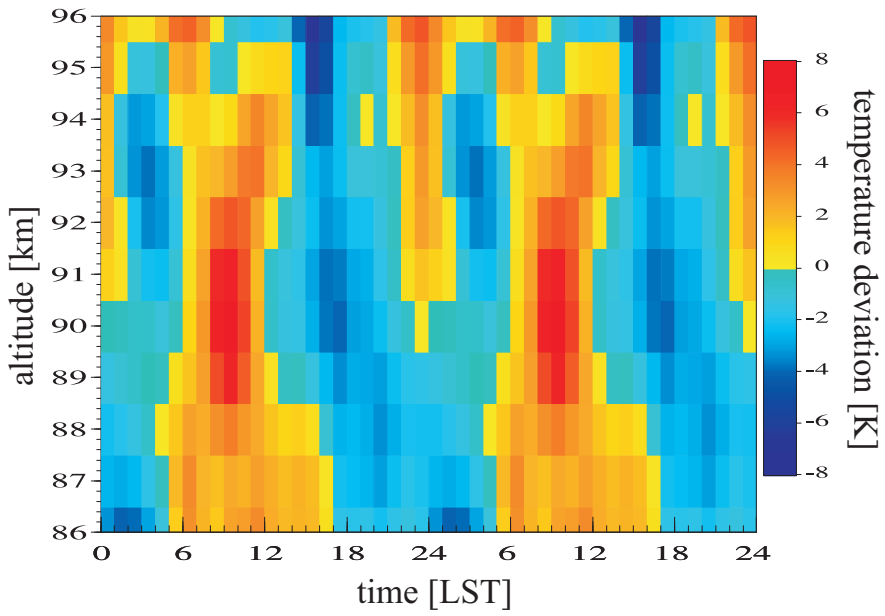

Fig. 2.57: Temperature deviations from the mean in Kelvin (LST = local solar time). To highlight the phase progression with altitude, the deviations are shown for a period of two days (from *Lübken et al., Geophys. Res. Lett., 2011*).

of ice clouds and their morphology by the LIMA model dealing with microphysical processes of ice particles in an atmospheric background with spatial and temporal variability. With LIMA we have been able to reproduce long term variations of ice clouds as observed by satellite instruments and also long term temperature trends in the middle atmosphere. In some altitudes these trends are much larger (and

negative) compared to tropospheric trends.

2.4.3 Radar and Rocket Borne Soundings of the Atmosphere

Head: Prof. Dr. Markus Rapp

Staff: Dr. Kishore Grandhi, Dieter Keuer, Dr. Ralph Latteck, Dr. Qiang Li, Jens Mielich, Dr. Gunter Stober, Dr. Boris Strelnikov, Dr. Irina Strelnikova, Dr. Marius Zecha
8 PhD students, 11 master/diploma/bachelor students

Main areas of research are the dynamical structure of the mesosphere and lower thermosphere (MLT, 60–120 km altitude) and of the troposphere and lower stratosphere (0–20 km altitude), the coupling of the MLT to the troposphere and vice versa, the composition of the MLT, and finally the detection and interpretation of its long term variability (forced by both natural and anthropogenic effects). All these areas are addressed using radar systems at various frequencies (∼100 kHz to ∼1 GHz) as well as sounding rockets for *in situ* observations. Radar observations are both made at mid-latitudes (Kühlungsborn and Juliusruh) and polar regions in Northern Norway. The latter is important since many atmospheric effects are most pronounced at the poles like, e.g., the seasonal cycle of temperatures leading for instance to the unique phenomenon of mesospheric ice clouds. In addition, the nearby location of the Andøya Rocket Range offers the opportunity to launch sounding rockets and hence to combine state-of-the-art radar and lidar remote sensing with high resolution *in situ* measurements.

In 2011 the IAP completed the installation of a new powerful very high frequency (VHF) radar at ALOMAR. The Middle Atmosphere Alomar Radar System (MAARSY) is designed for atmospheric studies from the troposphere to the lower thermosphere with high spatial and temporal resolution. Special focus is directed to the investigation of horizontal structures of Polar Mesosphere Summer Echoes (PMSE) caused by mesospheric ice clouds. This is motivated by the desire to study their 3D morphology, and also to infer information on 3D structures of the background atmosphere owing to, e.g., gravity waves and turbulence. MAARSY is composed of an active phased antenna consisting of 433 array elements and an identical number of transceiver modules individually controllable in frequency, phase, and output power on a pulse-to-pulse basis. This arrangement allows high flexibility of beam forming and beam steering with a narrow radar beam and arbitrary beam pointing directions. The major objective for building MAARSY, namely the investigation of horizontal structures of Polar Mesosphere Echoes, was successfully tested during several campaigns in summer and winter of 2011 and 2012. 3D resolved structures of Polar Mesosphere Summer and Winter Echoes were observed using multi-beam experiments with up to 97 beams quasi-simultaneously. An example of horizontal and vertical slices of signal-to-noise ratio of a PMSE as shown in Fig. 2.58 indicates that mesospheric echoes (or the underlying structures and processes) reveal

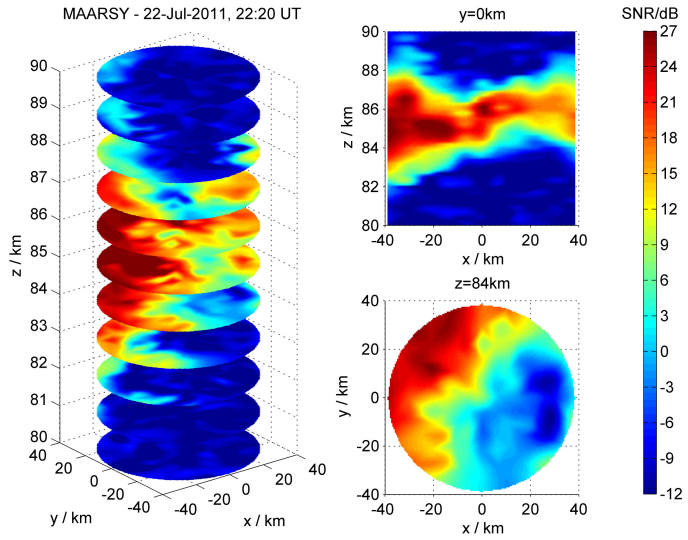

Fig. 2.58: 3D structure of a PMSE quasi-simultaneously observed with MAARSY using 97 beam direction on July 22, 2011.

a pronounced spatial variability that asks for in-depth studies. Sophisticated wind analysis methods such as an extended velocity azimuth display have been applied to retrieve additional parameters from the wind field, e.g., horizontal divergence, vertical velocity, stretching and shearing deformation. The obtained results resolve the classical space time ambiguity of single beam observations and provide a first insight into the strong horizontal variability of scattering structures occurring in the polar mesosphere over Andøya during summer and winter time. The implementation of interferometric radar imaging methods offers further improvement of the horizontal and the vertical resolution.

Investigations with sounding rockets are typically complementary to ground based observations with radars in the sense that some quantities cannot be measured remotely, for example tiny nanoparticles of meteoric origin which are presumably the key players in the microphysics of the above mentioned mesospheric ice clouds. Another benefit of *in situ* measurements is the accessibility of quantities that can not be measured remotely with sufficient spatial resolution. A corresponding subject under consideration at the IAP is the characterization of turbulent heat production following the breakdown of waves which are excited in the troposphere and propagate into the MLT. This heat production occurs on spatial scales of meters and less and is hence inaccessible for any state-of-the-art remote sensing technique. Our *in situ* measurements confirm that corresponding heating rates are significant contributions to the heat budget of the MLT with values in excess of the direct radiative input.

2.4.4 Theory and Modeling

Head: Prof. Dr. Erich Becker

Staff: Dr. Oliver Bothe, Dr. Axel Gabriel, Dr. Almut Gaßmann, Dr. Mykhaylo Grygalashvyly, Dr. Rahel Knöpfel, PD Dr. Dieter Peters, Dr. Urs-Schaefer-Rolffs, Dr. Andrea Schneidereit, Dr. Christoph Zülicke, 6 PhD students, 3 master/diploma/bachelor students

The main field of research is the coupling between the lower atmosphere (troposphere, 0–10 km) and the middle atmosphere (stratosphere, 10–50 km, and mesosphere, 50–100 km) with emphasis on long-term variability and small-scale dynamical processes. Coupling of atmospheric layers is controlled by radiative transfer, transport of chemically and radiatively active minor constituents, and atmospheric waves on vastly different temporal and spatial scales. The latter predominantly originate in the troposphere; they propagate upward and dissipate at higher altitudes, giving rise to dynamical control of the middle atmosphere and feedbacks on the troposphere. During the last decade, processes in the middle atmosphere and interactions across atmospheric scales have been recognized as important aspects of climate change. In the following we describe two contributions by IAP in this context.

In weather or climate models, unresolved small-scale or diabatic processes need to be parameterized in order to drive the temporal evolution of the explicitly resolved meteorological fields. For a consistent coupling of the lower and middle atmosphere with regard to the radiation budget it is important to compute the radiative energy fluxes from the surface to the *top of the atmosphere* (TOA). This is particularly challenging because of different physical regimes for long-wave radiation: Local thermodynamic equilibrium (LTE) and broad lines in the lower atmosphere as opposed to non-LTE and narrow lines in the mesosphere. Comprehensive climate models use different schemes for the different regimes, thereby lacking a consistent calculation of the complete radiation budget. We have developed a new, though idealized, method that yields the complete radiation budget up to 100 km in an uniform fashion. Since we also take the surface budget consistently into account, our global circulation model yields an equilibrated radiation budget at the TOA in the climatological mean, see Fig. 2.59a. Moreover, the net incoming radiation (RTOA) shows a systematic annual variation that is largely caused by a deviation of the global-mean surface temperature from its long-term mean (panel b): The Earth's surface is coldest in late northern hemispheric winter due to cooling of the land masses. This behavior can also be found in observational meteorological data (not shown).

Large-scale atmospheric waves induce strong interactions across all scales of motion. An issue in this context is the interpretation of the so-called Nastrom-Gage spectrum, i.e., the -5/3 exponential spectral slope of the atmospheric kinetic energy spectrum for horizontal wavelengths smaller than a few 100 km. We have analyzed

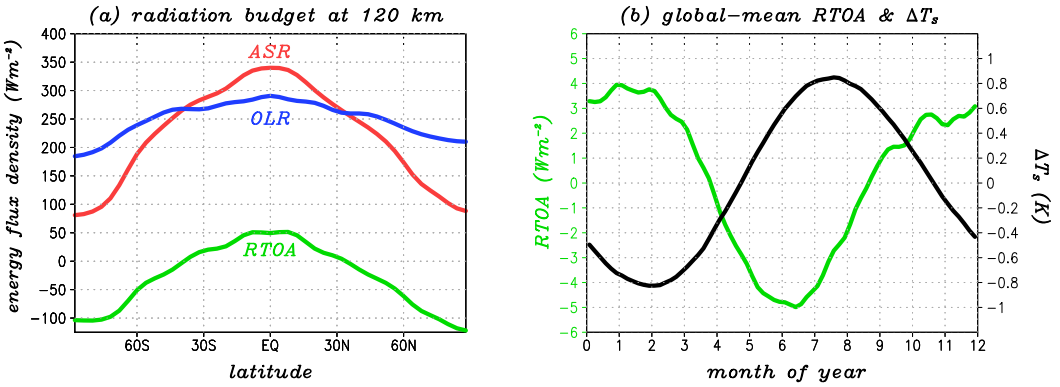

Fig. 2.59: (a) Simulated radiation budget at the top of the atmosphere (TOA) as a function of latitude: absorbed (incoming minus reflected) solar radiation (red, ASR); outgoing long-wave radiation (OLR, blue); net downward radiation (RTOA=ASR-OLR, green). Integration over all latitudes yields an error of about $0.2\,\mathrm{W\,m^{-2}}$. (b) Annual cycle of the global-mean RTOA (green) and of the global-mean surface temperature deviation (black, ΔT_s).

the global kinetic energy spectrum in the upper troposphere from a global simulation of the atmospheric circulation with very high spatial resolution. It is widely accepted that the -5/3 regime can neither be explained by 2-dimensional nor by isotropic 3-dimensional turbulence. Rather, according to simple forced-dissipative models, the scaling laws of stratified turbulence (ST) should apply. Our analysis confirms this interpretation on the basis of a global circulation model. In addition we find that ST in the upper troposphere is maintained through vertical exchange of kinetic energy with the mid troposphere by the small scales. As a result, the forward spectral fluxes of kinetic energy associated with horizontal advection and buoyancy forces have the same order of magnitude in the upper troposphere in the regime of ST. These dynamical exchanges are an essential part of the global energy cycle. They strongly control the middle atmosphere through the generation of internal gravity waves.

References

[1] U. Achatz, R. Klein and F. Senf. "Gravity waves, scale asymptotics, and the pseudo-incompressible equations". *J. Fluid Mech.*, **663** (2010), 120–147.

[2] G. Baumgarten, J. Fiedler and M. Rapp. "On microphysical processes of Noctilucent Clouds (NLC): Observations and modeling of mean and width of the particle size-distribution". *Atmos. Chem. Phys.*, **10** (2010), 6661–6668.

[3] G. Baumgarten. "Doppler Rayleigh/Mie/Raman lidar for wind and temper-

ature measurements in the middle atmosphere up to 80 km". *Atmos. Meas. Tech.*, **3** (2010), 1509–1518.

[4] E. Becker and C. von Savigny. "Dynamical heating of the polar summer mesopause induced by solar proton events". *J. Geophys. Res.*, **115** (2010), D00I18.

[5] R. Büttner, M. Brede, A. Leder and F.-J. Lübken. "Experimental investigation on the characteristics of propagating internal waves in laboratory environment". In "Fachtagung 'Lasermethoden in der Strömungsmesstechnik"', Cottbus (2010).

[6] R. Eixmann, D. Peters, C. Zülicke, M. Gerding and A. Dörnbrack. "On the upper tropospheric formation and occurence of high and thin cirrus clouds during anticyclonic poleward Rossby wave breaking events". *Tellus*, **62 A** (2010), 228–242.

[7] M. Gerding, J. Höffner, M. Kopp, R. Eixmann and F.-J. Lübken. "Mesospheric temperature and aerosol soundings during day and Night: Spectral and spatial filtering Techniques". In "Reviewed and revised papers at the 25th International Laser Radar Conference", pages 67–70. St. Petersburg, Russia (2010).

[8] M. Grygalashvyly, P. Hartogh, G. Sonnemann and A. S. Medvedev. "The Doppler-Sonnemann Effect (DSE) on the Photochemistry on Mars". *Adv. Geoscience*, **19** (2010), 163–176.

[9] P. Hartogh, G. R. Sonnemann, Song Li, M. Grygalashvyly, U. Berger and F.-J. Lübken. "Water vapor measurements at ALOMAR over a solar cycle compared with model calculations by LIMA". *J. Geophys. Res.*, **115** (2010), D00I17.

[10] P. Hoffmann, E. Becker, W. Singer and M. Placke. "Seasonal variation of mesospheric waves at northern middle and high latitudes". *J. Atmos. Solar-Terr. Phys.*, **72** (2010), 1068–1079.

[11] H. Körnich and E. Becker. "A simple model for the interhemispheric coupling of the middle atmosphere circulation". *Adv. Space Res.*, **45** (2010), 661–668.

[12] G. Kishore Kumar and W. K. Hocking. "Climatology of northern polar latitude MLT dynamics: mean winds and tides". *Ann. Geophys.*, **28** (2010), 1859–1876.

[13] R. Latteck, W. Singer, M. Rapp and T. Renkwitz. "MAARSY - The new MST Radar on Andøya/ Norway". *Adv. Radio Sci.*, **8** (2010), 219–224.

[14] Q. Li, M. Rapp, J. Röttger, R. Latteck, M. Zecha, I. Strelnikova, G. Baumgarten, M. Hervig, C. Hall and M. Tsutsumi. "Microphysical parameters of mesospheric ice clouds derived from calibrated observations of polar mesosphere summer echoes at Bragg wavelengths of 2.8 m and 30 cm". *J. Geophys. Res.*, **115** (2010), D00I13.

[15] Q. Li and M. Rapp. "PMSE studied with the EISCAT IS Radars: Results on microphysics, neutral dynamics, and electron densities". In "Proceedings of 2010 Asia-Pacific Radio Science Confernce (AP-RASC')10", Toyana, Japan (2010).

[16] R. Q. Liu, C. Jacobi, P. Hoffmann, G. Stober and E. G. Merzlyakov. "A piecewise linear model for detecting climatic trends and their structural changes with application to mesosphere/lower thermosphere winds over Collm, Germany". *J. Geophys. Res.*, **115** (2010), D22105.

[17] F.-J. Lübken, J. Austin, U. Langematz and J. Oberheide. "Introduction to special section on Climate and Weather of the Sun Earth System". *J. Geophys. Res.*, **115** (2010), D00I19.

[18] J. Mielich and J. Bremer. "A modified index for the description of the ionospheric short- and long-term activity". *Ann. Geophys.*, **28** (2010), 2227–2236.

[19] D. Offermann, P. Hoffmann, P. Knieling, R. Koppmann, J. Oberheide and W. Steinbrecht. "Long-term trends and solar cycle variations of mesospheric temperature and dynamics". *J. Geophys. Res.*, **115** (2010), D18127.

[20] O. Otto, F. Czerwinski, J. L. Gornall, G. Stober, L. B. Oddershede, R. Seidel and U. F. Keyser. "Real-time particle tracking at 10,000 fps using optical fiber illumination". *Optics Express*, **18** (2010).

[21] D. Peters, P. Vargin, A. Gabriel, N. Tsvetkova and V. Yushkov. "Tropospheric forcing of the boreal polar vortex splitting in January 2003". *Ann. Geophys.*, **28** (2010), 2133–2148.

[22] M. Rapp, I. Strelnikova, B. Strelnikov, P. Hoffmann, M. Friedrich, J. Gumbel, L. Megner, U.-P. Hoppe, S. Robertson, S. Knappmiller, M. Wolff and D. R. Marsh. "Rocket-borne in situ measurements of meteor smoke: Charging properties and implications for seasonal variation". *J. Geophys. Res.*, **115** (2010), D00I16.

[23] M. Rapp and F.-J. Lübken. "Reply to comment by P. M. Bellan on 'Comment on 'Ice iron/sodium film as cause for high noctilucent cloud radar reflectivity"'. *J. Geophys. Res.*, **115** (2010), D13207.

[24] J. Schmale, J. Schneider, T. Jurkat, C. Voigt, H. Kalesse, M. Rautenhaus, M. Lichtenstern, H. Schlager, G. Ancellet, F. Arnold, M. Gerding, I. Mattis, M. Wendisch and S. Borrmann. "Aerosol layers from the 2008 eruptions of Mount Okmok and Mount Kasatochi: In situ upper troposphere and lower stratosphere measurements of sulfate and organics over Europe". *J. Geophys. Res.*, (2010), D00L07.

[25] I. Semenov, P. Papadopoulos, G. Stober and F. Kremer. "Ionic concentration- and pH-dependent electrophoretic mobility as studied by single colloid electrophoresis". *J. Phys.: Condens. Matter*, **22** (2010).

[26] A. Senior, M. T. Rietveld, M. J. Kosch and W. Singer. "Diagnostic radio plasma heating in the polar summer mesosphere using cross modulation: Theory and observations". *J. Geophys. Res.*, (2010), A09318.

[27] G. Sonnemann, P. Hartogh, M. Grygalashvyly and A. S. Medvedev. "A new coupled 3d-model of the dynamics and chemistry of the martian atmosphere". *Adv. Geoscience*, **19** (2010), 177–194.

[28] M.-H. Stevens, D. E. Siskind, S. D. Eckermann, L. Coy, J. P. McCormack, C. R. Englert, K. W. Hoppel, K. Nielsen, A. J. Kochenash, M. E. Hervig, C. E. Randall, J. Lumpe, S. M. Bailey, M. Rapp and P. Hoffmann. "Tidally induced variations of polar mesospheric cloud altitudes and ice water content using a data assimilation system". *J. Geophys. Res.*, **115** (2010), D18209.

[29] G. Stober, C. Jacobi and D. Keuer. "Distortion of meteor count rates due to cosmic radio noise and atmospheric particularities". *Adv. Radio Sci.*, **8** (2010), 1–5.

[30] I. Strelnikova and M. Rapp. "Studies of polar mesosphere summer echoes with the EISCAT VHF and UHF Radars: Information contained in the spectral shape." *Adv. Space Res.*, (2010), 247–259.

[31] B. Thurairajah, R. L. Collins, V. L. Harvey, R. S. Liebermann, M. Gerding, K. Mizutani and J. M. Livingston. "Gravity Wave Activity in the Arctic Stratosphere and Mesosphere during the 2007–2008 and 2008–2009 stratospheric sudden warming events". *J. Geophys. Res.*, (2010), D00N06.

[32] W. E. Ward, J. Oberheide, L. P. Goncharenko, T. Nakamura, P. Hoffmann, W. Singer, L. C. Chang, J. Du, D.-Y. Wang, P. Batista, B. Clemesha, A. H. Manson, D. M. Riggin, C.-Y. She, T. Tsuda and T. Yuan. "On the consistency of model, ground-based, and satellite observations of tidal signatures: Initial results from the CAWSES tidal campaigns". *J. Geophys. Res.*, **115** (2010), D07107.

[33] C. Zülicke and D. Peters. "On the estimation of persistence in geophysical time series". *European Phys. J.*, (2010), 101–108.

[34] E. Becker. "Dynamical control of the middle atmosphere". *Space Sci. Rev.*, (2011).

[35] U. Berger and F.-J. Lübken. "Mesospheric temperature trends at mid-latitudes in summer". *Geophys. Res. Lett.*, (2011), L22804.

[36] M. Brede, R. Büttner, F.-J. Lübken and A. Leder. "Quantification of turbulence and mixing in breaking internal waves in laboratory experiments". In "Fachtagung 'Lasermethoden in der Strömungstechnik"', Ilmenau (2011).

[37] C.-F. Enell, J. Hedin, J. Stegman, G. Witt, M. Friedrich, W. Singer, G. Baumgarten, B. Kaifler, U.-P. Hoppe, B. Gustavsson, U. Brändström, M. Khaplanov, A. Kero, T. Ulich and E. Turunen. "The Hotel Payload 2 campaign: Overview of NO, O and electron density measurements in the upper mesosphere and lower thermosphere". *J. Atmos. Solar-Terr. Phys.*, (2011), 2228–2236.

[38] S. M. Ernst, S. Skruszewicz, B. Strelnikov and M. Rapp. "Absolute calibration of vacuum ultraviolet Xenon flash lamps used for photoionization of meteor smoke particles". In "Proceedings of the 20^{th} ESA Symposium on European Rocket and Balloon Programmes and Related Research, 22-26 May 2011, Hyeres, France (ESA SP-700)", (2011).

[39] J. Fiedler, G. Baumgarten, U. Berger, P. Hoffmann, N. Kaifler and F.-J. Lübken. "NLC and the background atmosphere above ALOMAR". *Atmos. Chem. Phys.*, (2011), 5701–5717.

[40] M. Friedrich, M. Rapp, J. M. C. Plane and K. M. Torkar. "Bite-outs and other depletions of mesospheric electrons". *J. Atmos. Solar-Terr. Phys.*, (2011), 2201–2211.

[41] M. Friedrich, M. Rapp, T. Blix, U.-P. Hoppe and K. Torkar. "Electron loss and meteoric dust in the mesosphere". In "Proceedings of the 20^{th} ESA Symposium on European Rocket and Balloon Programmes and Related Research, 22-26 May 2011, Hyeres, France (ESA SP-700)", (2011).

[42] A. Gabriel, H. Schmidt and D. Peters. "Effects of the 11 year solar cycle on middle atmospheric stationary wave patterns in temperature, ozone, and water vapor". *J. Geophys. Res.*, (2011), D23301.

[43] A. Gabriel, H. Körnich, S. Lossow, D. Peters, J. Urban and D. Murtagh. "Zonal asymmetries in middle atmospheric ozone and water vapour derived from Odin satellite data 2001-2010". *Atmos. Chem. Phys.*, **11** (2011), 9865–9885.

[44] I. Glatt, A. Dörnbrack, S. Jones, J. Keller, O. Martius, A. Müller, D. Peters and V. Wirth. "Utility of Hovmöller diagrams to diagnose Rossby wave trains". *Tellus*, (2011), 991–1006.

[45] C. Gritzner and M. Rapp. "ECOMA Unravelling the Riddles of the Middle Atmosphere". In "DLR newsletter", pages 12–15 (2011).

[46] M. Grygalashvyly, E. Becker and G. R. Sonnemann. "Wave mixing effects on minor chemical constituents in the MLT-region: Results from a global CTM driven by high-resolution dynamics". *J. Geophys. Res.*, (2011).

[47] J. Gumbel, H. Körnich, S. M. Bailey, F.-J. Lübken and R. Morris. "Foreword: Special issue on layered phenomena in the mesopause region". *J. Atmos. Solar-Terr. Phys.*, (2011).

[48] P. Hartogh, G. R. Sonnemann, M. Grygalashvyly and C. Jarchow. "Ozone trends in mid-latitude stratopause region based on microwave measurements at Lindau (51.66° N, 10.13° E), the ozone reference model, and model calculations". *Adv. Space Res.*, **47** (2011).

[49] P. Hartogh, C. Jarchow, G. R. Sonnemann and M. Grygalashvyly. "Ozone distribution in the middle latitude mesosphere as derived from microwave measurements at Lindau (51.66° N, 10.13° E)". *J. Geophys. Res.*, **116** (2011), D04305.

[50] M. E. Hervig, M. Rapp, R. Latteck and L. L. Gordley. "Observations of mesospheric ice particles from the ALWIN radar and SOFIE". *J. Atmos. Solar-Terr. Phys.*, (2011), 2176–2183.

[51] W. K. Hocking and G. Kishore Kumar. "Long term behaviour of the MLT quasi-7-day wave at two radar-sites at Northern Polar Latitudes". *J. Atmos. Solar-Terr. Phys.*, (2011).

[52] P. Hoffmann, M. Rapp, W. Singer and D. Keuer. "Trends of mesospheric gravity waves at northern middle latitudes during summer". *J. Geophys. Res.*, (2011).

[53] U.-P. Hoppe, M. Friedrich, T. Blix, J. I. Moen, T. A. Bekkeng, K. R. Svenes, Å. Svendsen, M. Rapp and K. Torkar. "The charge balance in the presence of meteoric smoke in the upper mesosphere under winter conditions - preliminary results". In "Proceedings of the 20^{th} ESA Symposium on European Rocket and Balloon Programmes and Related Research, 22-26 May 2011, Hyeres, France (ESA SP-700)", (2011).

[54] K. Hultgren, H. Körnich, J. Gumbel, M. Gerding, P. Hoffmann, S. Lossow and L. Megner. "What caused the exceptional mid-latitudinal noctilucent cloud event in July 2009". *J. Atmos. Solar-Terr. Phys.*, (2011), 2125–2131.

[55] H. Iimura, D. C. Fritts, M. Tsutsumi, T. Nakamura, P. Hoffmann and W. Singer. "Long-term observations of the wind field in the Antarctic and Arctic mesosphere and lower thermosphere at conjugate latitudes". *J. Geophys. Res.*, **116** (2011), D20112.

[56] C. Jacobi, P. Hoffmann, M. Placke and G. Stober. "Some anomalies of mesosphere/lower thermosphere parameters during the recent solar minimum". *Adv. Radio Sci.*, **9** (2011).

[57] N. Kaifler, G. Baumgarten, J. Fiedler, R. Latteck, F.-J. Lübken and M. Rapp. "Coincident measurements of PMSE and NLC above ALOMAR (69° N, 16° E) by Radar and Lidar from 1999-2008". *Atmos. Chem. Phys.*, (2011).

[58] P. Keckhut, W. J. Randel, C. Claud, T. Leblanc, W. Steinbrecht, B. M. Funatsu, H. Bencherif, I. S. McDermid, A. Hauchecorne, C. Long, R. Lin and G. Baumgarten. "An evaluation of uncertainties in monitoring middle atmosphere temperatures with the ground-based Lidar network in support of space observations". *J. Atmos. Solar-Terr. Phys.*, (2011).

[59] S. Knappmiller, M. Rapp, S. Robertson and J. Gumbel. "Charging of meteoric smoke and ice particles in the mesosphere including photoemission and photodetachment rates". *J. Atmos. Solar-Terr. Phys.*, (2011), 2212–2220.

[60] R. Knöpfel and E. Becker. "An Idealized Radiative Transfer Scheme for Use in a Mechanistic General Circulation Model From the Surface up to the Mesopause Region". *J. Quant. Spectrosc. Radiat. Transfer*, **112** (2011), 1460–1478.

[61] M. Kopp, M. Gerding, J. Höffner, M. Zecha and F.-J. Lübken. "Lidar soundings of noctilucent clouds and temperatures during day and night in the summer mid-latitude middle atmosphere". In "Proceedings of the 20^{th} ESA Symposium on European Rocket and Balloon Programmes and Related Research, 22-26 May 2011, Hyeres, France (ESA SP-700)", (2011).

[62] G. A. Lehmacher, T. D. Scott, M. F. Larsen, S. Bilén, C. L. Croskey, J. D. Mitchell, M. Rapp, F.-J. Lübken and R. L. Collins. "The Turbopause Experiment: Atmospheric stability and turbulent structure spanning the turbopause altitude". *Ann. Geophys.*, **29** (2011), 2327–2339.

[63] Q. Li and M. Rapp. "PMSE-observations with the EISCAT VHF and UHF-Radars: Statistical properties". *J. Atmos. Solar-Terr. Phys.*, **73** (2011), 944–956.

[64] F.-J. Lübken and U. Berger. "Latitudinal and interhemispheric variation of stratospheric effects on mesospheric ice layer trends". *J. Geophys. Res.*, **116** (2011), D00P03.

[65] F.-J. Lübken, J. Höffner, T. P. Viehl, B. Kaifler and R. J. Morris. "First measurements of thermal tides in the summer mesopause region at Antarctic latitudes". *Geophys. Res. Lett.*, **38** (2011).

[66] A. S. Medvedev, E. Yiğit, P. Hartogh and E. Becker. "Influence of gravity waves on the Martian atmosphere: General circulation modeling". *J. Geophys. Res.*, **116** (2011).

[67] D. Offermann, P. Hoffmann, P. Knieling, R. Koppmann, J. Oberheide, D. Riggin, V. M. Tunbridge and W. Steinbrecht. "Quasi 2 Day Waves in the summer mesosphere: Triple structure of amplitudes and long-term development". *J. Geophys. Res.*, **116** (2011), D00P02.

[68] O. Otto, J. L. Gornall, G. Stober, F. Czerwinski, R. Seidel and U. F. Keyser. "High-Speed Video-Based Tracking of Optically trapped colloids". *J. Opt.*, **13** (2011).

[69] M. Placke, G. Stober and C. Jacobi. "Gravity wave momentum fluxes in the MLT–Part I: Seasonal variation at Collm (51.3° N, 13.0° E)". *J. Atmos. Solar-Terr. Phys.*, **73** (2011), 904–910.

[70] M. Placke, P. Hoffmann, E. Becker, C. Jacobi, W. Singer and M. Rapp. "Gravity wave momentum fluxes in the MLT–Part II: Meteor radar investigations at high and midlatitudes in comparison with modeling studies". *J. Atmos. Solar-Terr. Phys.*, **73** (2011), 911–920.

[71] M. Rapp, L. Leitert, R. Latteck, M. Zecha, P. Hoffmann, J. Höffner, U.-P. Hoppe, C. La Hoz and E. V. Thrane. "Localized mesosphere-stratosphere-troposphere radar echoes from the E-region at 69° N: Properties and physical mechanism". *J. Geophys. Res.*, **116** (2011), A02320.

[72] M. Rapp, R. Latteck, G. Stober, P. Hoffmann, W. Singer and M. Zecha. "First three-dimensional observations of polar mesosphere winter echoes: Resolving space-time ambiguity". *J. Geophys. Res.*, **116** (2011), A11307.

[73] M. Rapp, I. Strelnikova, B. Strelnikov, M. Friedrich, J. Gumbel, U.-P. Hoppe, T. Blix, O. Havnes, P. Bracikowski, K. Lynch and S. Knappmiller. "Microphysical properties of mesospheric aerosols: An overview of in situ-results from the ECOMA-project". In M. A. Abdu, D. Pancheva and A. Bhattacharyya, editors, "Aeronomy of the Earth's Atmosphere and Ionosphere", pages 67–74. Springer Science+Business Media B. V. (2011). IAGA Special Sopron Book Series.

[74] J. D. Reimuller, J. P. Thayer, G. Baumgarten, A. Chandran, B. Hulley, D. Rusch, K. Nielsen and J. Lumpe. "Synchronized imagery of noctilucent

clouds at the day-night terminator using airborne and spaceborne platforms". *J. Atmos. Solar-Terr. Phys.*, (2011), 2091–2096.

[75] T. Renkwitz, W. Singer, R. Latteck and M. Rapp. "Multi beam observations of cosmic radio noise using a VHF radar with beam forming by a Butler matrix". *Adv. Radio Sci.*, (2011).

[76] F. Senf and U. Achatz. "On the impact of middle-atmosphere thermal tides on the propagation and dissipation of gravity waves". *J. Geophys. Res.*, **116** (2011), D24110.

[77] A. Senior, M. T. Rietveld, F. Honary, W. Singer and M. J. Kosch. "Measurements and modeling of Cosmic Noise absorption changes due to radio heating of the D-region ionosphere". *J. Geophys. Res.*, (2011), A04310.

[78] T. A. Shaw and E. Becker. "Comments on 'A Spectral Parameterization of Drag, Eddy Diffusion and Wave Heating for a Three-Dimensional Flow Induced by Breaking Gravity Waves"'. *J. Atmos. Sci.*, (2011), 2465–2469.

[79] W. Singer, R. Latteck, M. Friedrich, M. Wakabayashi and M. Rapp. "Seasonal and solar activity variability of D-region electron density at 69° N". *J. Atmos. Solar-Terr. Phys.*, (2011).

[80] G. Stober, W. Singer and C. Jacobi. "Cosmic Radio Noise Observations using a mid-latitude Meteor Radar". *J. Atmos. Solar-Terr. Phys.*, **73** (2011), 1069–1076.

[81] G. Stober, C. Jacobi and W. Singer. "Meteoroid mass determination from underdense trails". *J. Atmos. Solar-Terr. Phys.*, **73** (2011), 895–900.

[82] B. Strelnikov and M. Rapp. "In situ measurements of small-scale structures in neutrals and charged aerosols". In M. A. Abdu, D. Pancheva and A. Bhattacharyya, editors, "Aeronomy of the Earth's Atmosphere and Ionosphere", pages 83–91. Springer Science+Business Media B. V. (2011). IAGA Special Sopron Book Series.

[83] I. Strelnikova and M. Rapp. "Majority of PMSE spectral widths at UHF and VHF are compatible with a single scattering mechanism". *J. Atmos. Solar-Terr. Phys.*, (2011), 2142–2152.

[84] A. Szewczyk, B. Strelnikov, G. Baumgarten and M. Rapp. "In situ density, temperature, and turbulence measurements in the middle atmosphere during ECOMA 2010". In "Proceedings of the 20^{th} ESA Symposium on European Rocket and Balloon Programmes and Related Research, 22-26 May 2011, Hyeres, France (ESA SP-700)", (2011).

[85] A. Theuerkauf, M. Gerding and F.-J. Lübken. "LITOS – a new balloon-borne instrument for fine-scale turbulence soundings in the stratosphere". *Atmos. Meas. Tech.*, (2011).

[86] U. von Zahn and U. Berger. "Langfristige "Anderungen in Eigenschaften der oberen Atmosphäre". In "Nordrhein-Westf'alische Akademie der Wissenschaften und der K"unste", Verlag Ferdinand Sch"oningh, Paderborn (2011). Vorträge, NM 478, 87 S.

[87] U. Achatz, F. Senf and N. Grieger. "Solar tides in the middle atmosphere: Interactions with the zonal- mean flow, planetary waves and gravity waves". In F.-J. Lübken, editor, "Climate And Weather of the Sun-Earth System (CAWSES): Highlights from a priority program", Springer, Dordrecht, The Netherlands (2012).

[88] G. Baumgarten, A. Chandran, J. Fiedler, P. Hoffmann, N. Kaifler, J. Lumpe, A. Merkel, C. E. Randall, D. Rusch and G. Thomas. "On the horizontal and temporal structure of noctilucent clouds as observed by satellite and lidar at ALOMAR (69N)". *Geophys. Res. Lett.*, **39** (2012).

[89] E. Becker and M. Rycroft. "Preface to the Special Issue on Crucial Processes Acting in the Mesosphere/Lower Thermosphere". *Surv. Geophys.*, (2012), 1173–1176.

[90] J. Bremer, T. Damboldt, J. Mielich and P. Suessmann. "Comparing long-term trends in the ionospheric F2-region with two different methods". *J. Atmos. Solar-Terr. Phys.*, (2012).

[91] R. Büttner, M. Brede, F.-J. Lübken and A. Leder. "Experimentelle Untersuchungen zur Ausbreitung und Transition interner Wellen". In "Fachtagung 'Lasermethoden in der Strömungsmesstechnik"', Rostock (2012).

[92] R. Büttner, A. Leder and F.-J. Lübken. "Experimentelle Untersuchungen zur Ausbreitung und Transition interner Wellen". In "Fachtagung 'Schall und Schwingungen, Wellen und Turbulenz in sensibler Umgebung"', Kiel (2012).

[93] L. C. Chang, W. E. Ward, S. E. Palo, J. Du, D.-Y. Wang, H.-L. Liu, M. E. Hagan, Y. Portnyagin, J. Oberheide, L. P. Goncharenko, T. Nakamura, P. Hoffmann, W. Singer, P. Batista, B. Clemesha, A. H. Manson, D. M. Riggin, C.-Y. She, T. Tsuda and T. Yuan. "Comparison of diurnal tide in models and ground-based observations during the 2005 Equinox CAWSES Tidal Campaign". *J. Atmos. Solar-Terr. Phys.*, **78–79** (2012), 19–30.

[94] J. T. Fentzke, V. Hsu, C. G. M. Brum, I. Strelnikova, M. Rapp and M. Nicolls. "D region meteoric smoke and neutral temperature retrieval using the poker flat incoherent scatter radar". *Geophys. Res. Lett.*, **39** (2012), L21102.

[95] J. Fiedler and G. Baumgarten. "On the relationship between lidar sensitivity and tendencies of geophysical time series". In "Reviewed and Revised Papers at the 26th International Laser Radar Conference", pages 63–66. Porto Heli, Greece (2012).

[96] J. S. Friedman, D. Maldonado-Nieves, I. González, J. Lautenbach, X. Chu, J. A. Smith and W. Huang. "High spectral resolution test and calibration of an ultra-narrowband Faraday anomalous dispersion optical filter for use in daytime mesospheric resonance Doppler lidar". *J. Atmos. Solar-Terr. Phys.*, (2012), 187–194.

[97] M. Friedrich, M. Rapp, T. Blix, U.-P. Hoppe, K. Torkar, S. Robertson, S. Dickson and K. Lynch. "Electron loss and meteoric dust in the mesosphere". *Ann. Geophys.*, (2012), 1495–1501.

[98] D. C. Fritts, H. Iimura, R. Lieberman, D. Janches and W. Singer. "A conjugate study of mean winds and planetary waves employing enhanced meteor radars at Rio Grande, Argentina (53.8°S) and Juliusruh, Germany (54.6°N)". *J. Geophys. Res.*, **117** (2012), D05117.

[99] A. Gabriel, I. Höschel, D. Peters, I. Kirchner and H.-F. Graf. "The influence of zonally asymmetric stratospheric ozone on the coupling of atmospheric layers". In F.-J. Lübken, editor, "Climate And Weather of the Sun-Earth System (CAWSES): Highlights from a priority program", Springer, Dordrecht, The Netherlands (2012).

[100] A. Gaßmann. "A global hexagonal C-grid non-hydrostatic dynamical core (ICON-IAP) designed for energetic consistency". *Quart. J. R. Met. Soc.*, (2012).

[101] M. Grygalashvyly, E. Becker and G. R. Sonnemann. "Gravity wave mixing and effective diffusivity for Minor chemical constituents in the mesosphere/lower thermosphere". *Space Sci. Rev.*, **168** (2012), 333–362.

[102] J. Hedin, M. Rapp, M. Khaplanov, J. Stegman and G. Witt. "Observations of NO in the upper mesosphere and lower thermosphere during ECOMA 2010". *Ann. Geophys.*, **30** (2012), 1611–1621.

[103] J. Hildebrand, G. Baumgarten, J. Fiedler, U.-P. Hoppe, B. Kaifler, F.-J. Lübken and B. P. Williams. "Combined wind measurements by two different lidar instruments in the Arctic middle atmosphere". *Atmos. Meas. Tech.*, **5** (2012), 2433–2445.

[104] M. Kassa, M. Rapp, T. W. Hartquist and O. Havnes. "Secondary charging effects due to icy dust particle impacts on rocket payloads". *Ann. Geophys.*, **30** (2012), 433–439.

[105] A. A. Kutepov, A. G. Feofilov, A. S. Medvedev, U. Berger, M. Kaufmann and A. W. A. Pauldrach. "Infra-red radiative cooling/heating of mesosphere and lower thermosphere due to the small-scale temperature fluctuations associated with gravity waves". In F.-J. Lübken, editor, "Climate And Weather of the Sun-Earth System (CAWSES): Highlights from a priority program", Springer, Dordrecht, The Netherlands (2012).

[106] R. Latteck, W. Singer, M. Rapp, B. Vandepeer, T. Renkwitz, M. Zecha and G. Stober. "MAARSY - The new MST radar on Andøya–System description and first results". *Radio Sci.*, (2012).

[107] R. Latteck, W. Singer, M. Rapp, T. Renkwitz and G. Stober. "Horizontally resolved structures of radar backscatter from polar mesospheric layers". *Adv. Radio Sci.*, **10** (2012), 1–6.

[108] F.-J. Lübken, U. Berger, J. Kiliani, G. Baumgarten and J. Fiedler. "Solar variability and trend effects in mesospheric ice layers". In F.-J. Lübken, editor, "Climate And Weather of the Sun-Earth System (CAWSES): Highlights from a priority program", Springer, Dordrecht, The Netherlands (2012).

[109] F.-J. Lübken. "Scientific summary of the German CAWSES priority program". In F.-J. Lübken, editor, "Climate And Weather of the Sun-Earth System (CAWSES): Highlights from a priority program", Springer, Dordrecht, The Netherlands (2012).

[110] V. Matthias, P. Hoffmann, M. Rapp and G. Baumgarten. "Composite analysis of the temporal development of waves in the polar MLT region during stratospheric warmings". *J. Atmos. Solar-Terr. Phys.*, **90-91** (2012), 86–96.

[111] R. J. Morris, J. Höffner, F.-J. Lübken, T. Viehl, B. Kaifler and A. K. Klekociuk. "Experimental evidence of a stratospheric circulation influence on mesospheric temperatures and ice-particles during the 2010-11 austral summer at 69° S". *J. Atmos. Solar-Terr. Phys.*, (2012), 54–61.

[112] M. Rapp, I. Strelnikova, Q. Li, N. Engler and G. Teiser. "Charged aerosol effects on the scattering of radar waves from the D-region". In F.-J. Lübken, editor, "Climate And Weather of the Sun-Earth System (CAWSES): Highlights from a priority program", Springer, Dordrecht, The Netherlands (2012).

[113] T. Renkwitz, W. Singer, R. Latteck, G. Stober and M. Rapp. "Validation of the radiation pattern of the Middle Atmosphere Alomar Radar System (MAARSY)". *Adv. Radio Sci.*, (2012).

[114] J. Röttger, N. Engler and M. T. Rietveld. "EISCAT's contributions to high latitude ionosphere and atmosphere science within CAWSES in Germany". In F.-J. Lübken, editor, "Climate And Weather of the Sun-Earth System

(CAWSES): Highlights from a priority program", Springer, Dordrecht, The Netherlands (2012).

[115] C. von Savigny, C. Robert, N. Rahpoe, H. Winkler, E. Becker, H. Bovensmann, J. P. Burrows and M. T. DeLand. "Impact of short-term solar variability on the polar summer mesopause and noctilucent clouds". In F.-J. Lübken, editor, "Climate And Weather of the Sun-Earth System (CAWSES): Highlights from a priority program", Springer, Dordrecht, The Netherlands (2012).

[116] A. Schneidereit, S. Schubert, P. Vargin, F. Lunkeit, X. Zhu, D. Peters and K. Fraedrich. "Large Scale Flow and the Long-lasting blocking high over Russia: Summer 2010". *Mon. Weather Rev.*, (2012).

[117] W. Singer, P. Hoffmann, G. Kishore Kumar, N. J. Mitchell and V. Matthias. "Atmospheric coupling by gravity waves: Climatology of gravity wave activity, mesospheric turbulence and their relations to solar activity". In F.-J. Lübken, editor, "Climate And Weather of the Sun-Earth System (CAWSES): Highlights from a priority program", Springer, Dordrecht, The Netherlands (2012).

[118] G. R. Sonnemann, P. Hartogh, U. Berger, F.-J. Lübken and M. Grygalashvyly. "Anthropogenic effects on the distribution of minor chemical constituents in the mesosphere/lower thermoshere - a model study". *Adv. Space Res.*, **50** (2012), 598–618.

[119] M. H. Stevens, S. Lossow, J. Fiedler, G. Baumgarten, F.-J. Lübken, K. Hallgren, P. Hartogh, C. E. Randall, J. Lumpe, S. M. Bailey, R. Niciejewski, R. R. Meier, J. M. C. Plane, A. J. Kochenash, D. P. Murtagh and C. R. Englert. "Bright Polar Mesospheric Clouds formed by Main Engine Exhaust from the Space Shuttle's Final Launch". *J. Geophys. Res.*, (2012).

[120] M. H. Stevens, L. E. Deaver, M. E. Hervig, J. M. Russell III, D. E. Siskind, P. E. Sheese, E. J. Llewellyn, R. L. Gattinger, J. Höffner and B. T. Marshall. "Validation of upper mesospheric and lower thermospheric temperatures measured by the solar occultation for ice experiment". *J. Geophys. Res.*, (2012).

[121] G. Stober, C. Jacobi, V. Matthias, P. Hoffmann and M. Gerding. "Neutral air density variations during strong planetary wave activity in the mesopause region derived from meteor radar observations". *J. Atmos. Solar-Terr. Phys.*, **74** (2012), 55–63.

[122] G. Stober, R. Latteck, M. Rapp, W. Singer and M. Zecha. "MAARSY-The new MST radar on Andøya: First results of spaced antenna and Doppler measurements of atmospheric winds in the troposphere and mesosphere using a partial array". *Adv. Radio Sci.*, (2012), 291–298.

2.5 Leibniz-Institute for Baltic Sea Research Warnemünde – Department of Physical Oceanography and Instrumentation

Director of the institute: Prof. Dr. U. Bathmann

Head of the department: Prof. W. Fennel
Deputy: Prof. H. Burchard

2.5.1 Introductory Remarks

The Leibniz-Institute for Baltic Sea Research Warnemünde is a member of the Science Association Gottfried Wilhelm Leibniz and is jointly funded by the federal government and the state of Mecklenburg-Vorpommern. The institute has an interdisciplinary profile comprising the basic disciplines of marine sciences. The IOW is associated with the University of Rostock where the IOW department heads are Professors and contribute to the teaching of Biology, Chemistry and Physics. Similarly, the section 'Marine Geology' is associated with the University of Greifswald.

The research of the IOW is focused on marine systems in coastal and marginal seas using the Baltic Sea as an example. For more detailed information we refer to the annual reports of the IOW and invite the reader to visit our web site: (www.io-warnemuende.de).

The department of physical oceanography is linked to the Institute of Physics of the Faculty of Mathematical and Natural Sciences of the University of Rostock. During the last three years, six members of our department, Prof. Fennel, Prof. Burchard, Dr. Umlauf, Dr. Schmidt, Dr. Mohrholz, Dr. Neumann and Dr. Seifert were teaching at the University of Rostock.

The oceanographic research encompass four elements: Observations with research vessels and moored instruments, theoretical studies and numerical modeling, satellite oceanography and work in of the Baltic Monitoring Programme. Further activities outside the Baltic are mainly focused on the Benguela Current System off Namibia, South Africa and Angola. The department is also strongly involved in multidisciplinary modeling of marine ecosystems.

2.5.2 Dynamics of Upwelling Ecosystems

V. Mohrholz, M. Schmidt, T. Junker and W. Fennel

As a mile stone in our longterm research activities in the eastern boundary upwelling system off the South Atlantic the first phase of the BMBF project GENUS (**G**eochemistry and **G**cology of the **N**amibian **U**pwelling **S**ystem) was finished suc-

cessfully in April 2012. A special focus is the forcing of upwelling and its impact on organisms in the higher trophic levels of the ecosystem. Key questions a are:

- How are the variations in the eastern boundary current and upwelling related to the atmospheric forcing?
- How do changes in eastern boundary current dynamics affect the oxygen and nutrient conditions in the Benguela upwelling system? How will this impact the lower trophic levels of the ecosystem?
- What are the budgets of matter fluxes between the Benguela upwelling system and the adjacent ocean basin?
- Which processes generate the mixed bottom layer on the Namibian shelf, and how impacts the turbulent mixing the vertical matter transports in the bottom boundary layer?

The Northern Benguela upwelling system is forced remote processes in the equatorial Atlantic and the local trade wind system. Both forcing components show pronounced seasonal and interannual variability with a strong impact on the hydrographic conditions on the Namibian shelf. We could demonstrate that the intensity of the trade wind as well as the spatial structure of the wind field determines strength and location of upwelling and the associated current field. As a feedback the stabilization of the atmospheric boundary layer above the upwelled coastal cold water belt and the impact of the land mass cause a weakening of the wind stress towards the coast. This cross shelf gradient of the strength of meridional windstress forces curl driven upwelling. With an analytical model [1] investigated the impact of the wind field structure on the strength and distribution of upwelling. The basic properties of the pole-ward undercurrent and the coastal jet and their relation to the spatial structure of the wind field are revealed by the model. It highlights also the important role of Kelvin waves for generation of the observed pattern of the poleward undercurrent off Namibia. North of the Kunene mouth the decreasing wind intensity causes a westward current belt, which coincides with the observed detachment of the Angola-current from the coast. Depending on the spatial structure of the actual wind forcing, the Kunene upwelling cell acts like a valve for the pole-ward undercurrent and controls the transport of South Atlantic Central Water into the northern Benguela.

The seasonal variation of the distribution of central water masses off Namibia and the related oxygen conditions were investigated during three field campaigns. The observations in austral summer have shown a poleward transport of SACW along the coast down to Lüderitz and a contemporary northward transport of ESACW along the shelf edge, Fig. 2.60. The area between the Kunene mouth and the Lüderitz upwelling cell can act as transition and mixing zone between both central water masses. The mixing is supported by mesoscale dynamics, development and decay of

filaments and the cross shelf Ekman flux. The advection of both central water masses and their mixing ration determines the oxygen supply to the northern Benguela. High fraction of SACW goes along with hypoxic and anoxic conditions at the shelf, whereas high fraction of ESACW enhances the ventilation.

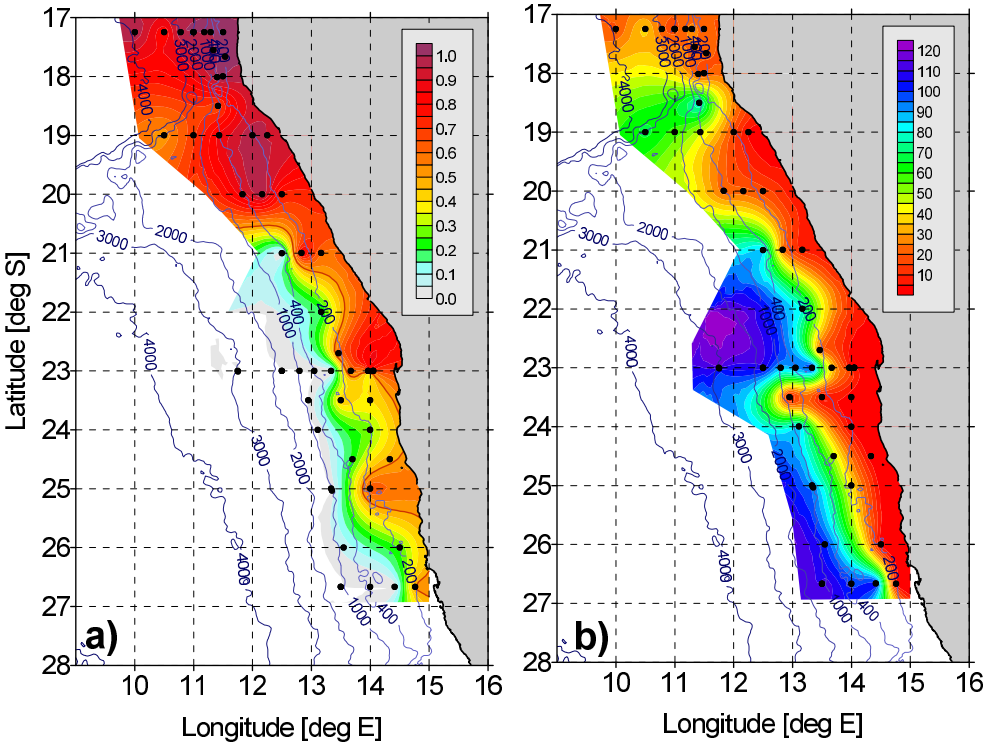

Fig. 2.60: Spatial distribution of SACW fraction (a) and oxygen concentration (b) during the austral summer in the northern Benguela at 100 m depth (Jan/Feb 2011).

Fig. 2.61 shows an example for the simulated ecosystem structure emerging within the nutrient and oxygen environment formed by the current pattern on the Namibian shelf [2]. It shows the contribution of different groups of organisms to the total oxygen consumption.

The main results of the first phase of GENUS can be summarized as follows:

- The Lüderitz and the Kunene upwelling cells are the boundaries of the transition zone between SACW and ESACW and act like hydrographic barriers in the upper central water.
- The distribution and the mixing stage of the central water masses control the available oxygen concentration at the shelf.
- The interannual variability of atmospheric forcing is mainly expressed in the meridional current component at the shelf.

- Upwelling filaments tend to intensify the exchange of matter between the shelf area and the adjacent ocean basin.
- Small scale processes, like internal waves, swell and turbulence, have a significant impact on the ecosystem, and must be quantified and parameterized for numerical modelling.

The BMBF had approved the funding of the second phase, that runs until April 2015.

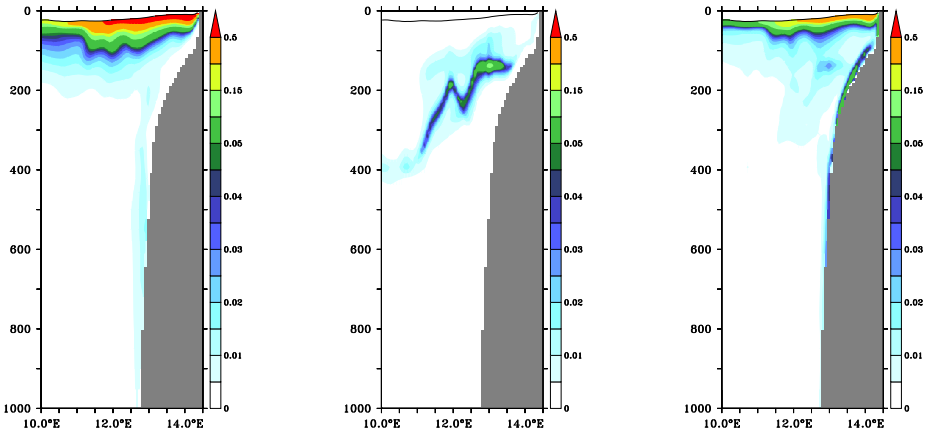

Fig. 2.61: Major contributions to oxygen consumption in μmol/kg/d at 23°S for January 2004 below the mixed layer. Left: small zooplankton respiration, middle: large zooplankton respiration, right: nitrification. The black line marks the mixing layer depth.

2.5.3 Ecosystem Model

T. Neumann, H. Radtke and W. Fennel

Eutrophication imposes a high pressure on the Baltic Sea ecosystem. When high concentrations of nutrients are available, this increases the net primary production in the surface layers. The biomass is then transferred to the deep basins of the Baltic Sea, where it is oxidized by microorganisms. This increases the extent of the naturally occurring hypoxic and anoxic areas in the Baltic Sea where no higher organisms can survive [3]. To counteract this problem, stake holders agreed on the Baltic Sea Action Plan which forces the states around the Baltic to reduce nutrient loads in the rivers. But since the problem of hypoxia and anoxia occurs in the open basins, the question arises how the nutrients which enter the Baltic Sea from the rivers are transported to this area of interest. Nutrients can hardly get from the coast to the central basins by passive advection only, as the geostrophically adjusted mean currents are directed parallel to the topography, which generates a "coast to basin

barrier". However, they are not passive substances like salt, but are also transported in the phase-space of the food web. As they are transformed into particulate organic matter, they show a vertical motion (sinking) which modifies their transport in physical space. The question of how these biological processes modify the pathways of the nutrients was addressed in a DFG project "BEST" (Baltic EcosyStem matter Transport). For this purpose, the ecosystem model was extended by the possibility to mark nutrients according to their input source and trace them in the food web. This diagnostic numerical method introduced by Menesguen in 2006 was combined with a method of "age attribution" by to allow the estimation of timescales for the nutrient transports and residence times. The results of the study showed that the biological influence on the pathways is totally different for nitrogen and phosphorus. The spreading of nitrogen is inhibited by the process of denitrification which removes it from the ecosystem on a timescale of 1.4 years. As a result, only a small fraction of riverine nitrogen reaches the open basins, it only dominates the coastal rim, while the nitrogen supply in the open basins is from dinitrogen fixation and direct atmospheric deposition. This is in accordance with findings of 15N isotope studies. As for phosphorus no process comparable to denitrification exists, its residence time in the Baltic Sea is much larger. According to our model, it exceeds the simulated period of 35 years, and therefore also that of water which is around 21 years. The reason for that is not only the storage of phosphorus in the sediments, but especially an active coast-to-basin transport which is the net effect of the biological cycling. This largely takes place as a sediment transport of particulate matter and generates a "trapping" of phosphorus in the deep basins. To highlight the influence of the biological effects on the transport of matter we show in Fig. 2.62 an example of the spreading of phosphorous with and without the impact of biogeochemical processes. The findings have implications on the effects of nutrient load reduction measures; while nitrate load reductions may show immediate effects, but mostly confined to the coastal region near the river mouth, the effects of phosphorus load reductions may be seen after several decades only. This stresses the importance of phosphorus load reductions for achieving a good environmental status of the Baltic Sea ecosystem [4].

Another challenge for ecosystem modeling is the inclusion of higher trophic levels. Usually the models end at the level of zooplankton, its mortality is used as a truncation parameter and parametrizes the effect of consumption by fish. However, fish may affect the lower trophic levels in ways which are not represented by this simple parametrization. Firstly, they can store biomass in their bodies and release it in a different time of the year, and thereby modify the seasonal cycle of nutrients. Secondly, they can swim actively and cause a horizontal transport of biomass which deviates from simple advection with the current. Finally, fishery extracts biomass from the food web and therefore represents a net sink of nutrients and counteracts eutrophication. In the last years we managed to include our stage-resolving fish model for the Baltic Sea [5] into the advanced NPZD (nutrient-phytoplankton-zooplankton-detritus) model ERGOM, generating an end-to-end NPZDF model. For this purpose we developed a swimming algorithm which makes the model fish

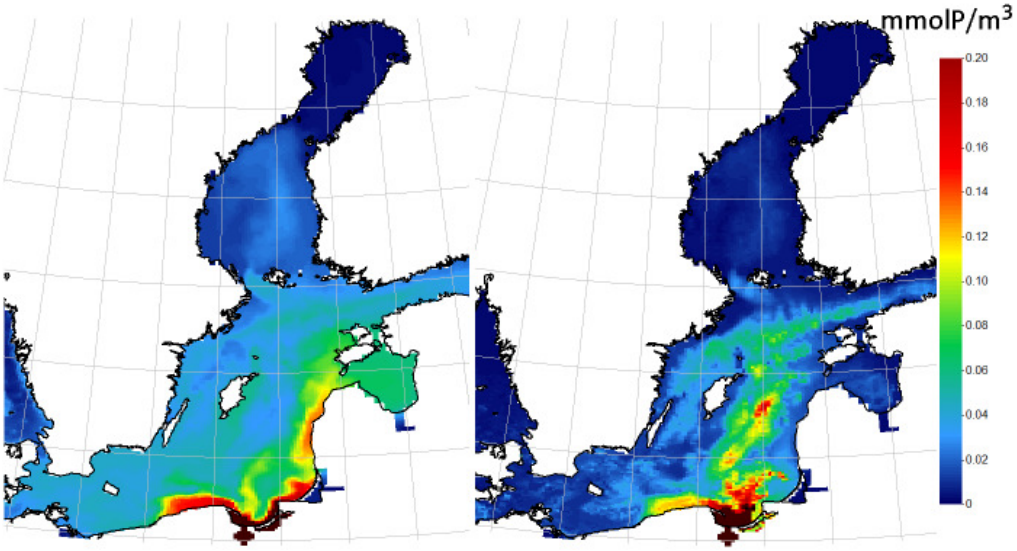

Fig. 2.62: Distribution of phosphorus from the Vistula after 7 years of simulation, (left) without biology–passive advection, (right) with biology–full ecosystem model. Vertical average over the whole water column. The net effect of biological processes on the phosphorus distribution is a coast-to-basin transport.

follow their food and migrate to their prescribed spawning grounds during spawning season. Contrary to most other fish models which are individuals-based, our model is described in a Eulerian way, that is, the fish population exists as biomass concentrations on the same horizontal grid as the state variables of the lower food web, which allows one to integrate the fully coupled model without a large extent of additional numerical effort. In a first test case simulation we investigated the question how fish which have their spawning grounds located in the deep basins of the Baltic Sea (sprat and cod) contribute to the coast-to-basin nutrient transport, as the biomass they lose during spawning was mostly accumulated in the food-rich coastal areas, and larval and egg mortality is high. Our results suggest that the transport to the deeps of the Eastern Gotland Basin amounts to $0.5 - 1.6\,\mathrm{kt/a}$ of nitrogen. This is about one order of magnitude below the input by dinitrogen fixation in the same region. However, the seasonal pattern of detritus production at Gotland deep changed significantly when fish were introduced, with its peak moving from spring to autumn. This provides a significantly better fit to the observations by sediment traps. So, even though our nutrient-to-fish model is in a very early state of development, the results are encouraging that a better representation of the ecosystem can be gained by the inclusion of fish. An example that shows how fish arranged almost proportional to their food is shown in Fig. 2.63, [6].

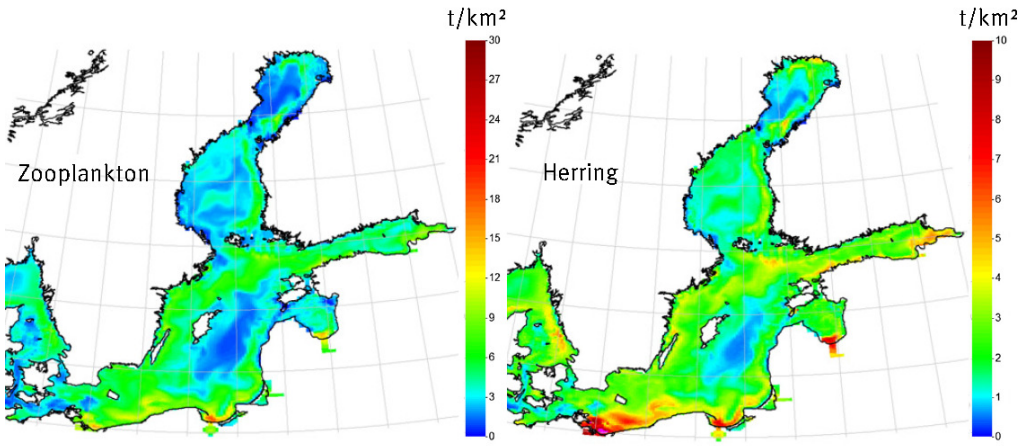

Fig. 2.63: Vertically integrated concentration of zooplankton (left) and herring (right), averaged over the first 10 days of August 1963. The fish arranged almost proportional to their food.

2.5.4 Thermodynamics of Seawater

R. Feistel

The need for accurate, consistent and comprehensive descriptions of the thermodynamic properties of seawater and its equilibria in contact with ice and humid air gave rise to the development of the new oceanographic standard TEOS-10, the Thermodynamic Equation of Seawater 2010 [7] which was adopted for marine sciences by the IOC in Paris 2009 and by the IUGG in Melbourne 2011 [8]. The formulation and successful international adoption of TEOS-10 consists of a novel salinity scale and recently developed, highly accurate and mutually consistent thermodynamic potential functions for water, ice, seawater and humid air [9–11], and is the result of a close cooperation between the SCOR/IAPSO WG127 and IAPWS in the years 2006–2011, until WG127 was disbanded in accordance with the rules governing SCOR/IAPSO Working Groups [12].

However, in addition to solving a number of problems, the development of TEOS-10 has also re-directed scientific attention again to several demanding fundamental, century-old and yet largely unsolved problems regarding the description and measurement of the chemical composition of the oceans and the atmosphere, and several related questions. In order to address pending urgent problems related to observables that are key to global climate-change monitoring, selected options and targets are considered for an intended cooperation between BIPM, the organisation that defines and maintains the international system of units (SI), and IAPWS, the international standards developing organisation for properties of water and aqueous systems. IAPWS documents laid the foundation of the recent seawater standard, TEOS-10. While TEOS-10 was being developed in close cooperation between the

oceanographic SCOR/IAPSO Working Group 127 (WG127) and IAPWS, it became evident that within that framework alone, certain fundamental problems could not be resolved yet in a satisfactory way. A longer-lasting and wider international cooperation is required for that purpose.

The new Joint Committee on Seawater (JCS), established by SCOR and IAPWS in the fall of 2012, will consider the task of introducing a new procedure updating the current salinity scale PSS-78 internationally in cooperation with the BIPM (to provide proper traceability to the SI and support by the National Metrological Institutes such as the PTB in Germany), IAPWS (to formulate a revised standard correlation equation between the conductivity and salinity to be used to embody the new salinity definition) and IAPSO (to support implementation of the new practice by the Standard Seawater Service and the oceanographic institutions). At the WMO-BIPM Workshop in Geneva 2010, WMO and BIPM signed the Mutual Recognition Arrangement (MRA) and formulated a number of recommendations regarding metrological aspects of climate change monitoring [13]. Of the recommendations with respect to ocean salinity (Section H of the Workshop), three are of central relevance for the planned activity of JCS, the need for SI-traceable, worldwide uniform and long-term stable international standards for seawater salinity [14]) and pH [15], as well as for relative humidity [11].

Fig. 2.64: BIPM-IAPWS meeting at the BIPM, Pavillon de Breteuil, Sevres, France, in February 2012 for preparation of international cooperation between BIPM, IAPWS, SCOR, IAPSO and WMO regarding novel SI definitions of oceanic salinity and pH, and atmospheric humidity.

Abbreviations:
BIPM: Bureau International des Poids et Mesures
IAPSO: International Association for the Physical Sciences of the Oceans
IAPWS: International Association for the Properties of Water and Steam
IOC: Intergovernmental Oceanographic Commission of Unesco
IUGG: International Union of Geodesy and Geophysics
JCS: SCOR/IAPWS Joint Committee on Seawater
MRA: CIPM Mutual Recognition Arrangement
SCOR: Scientific Committee on Oceanic Research
TEOS-10: International Thermodynamic Equation of Seawater - 2010
WG127: SCOR/IAPSO Working Group 127
WMO: World Meteorological Organization

2.5.5 Diapycnal Mixing Study in the Central Baltic Sea

P. Holtermann, H. Burchard, and L. Umlauf

The quantification of mixing processes within the density stratified water column of the Baltic Sea is essential to understand the fluxes of compounds. A prominent example for the importance of vertical mixing processes is the transport of the nutrient-rich deep waters into the upper layers, where the combination of sunlight and availability of nutrients allows for biological primary production. Mixing at the bottom boundary layer is one of the main candidates for basin-wide mixing [16–18]. During the Baltic Sea Tracer Release Experiment (BaTRE), we focused on the mixing processes in the deeper waters of the central Baltic Sea between 150 m and 240 m by analyzing the spreading behavior of a new type of tracer gas, CF_3SF_5 [19]. The tracer study included data from long-term moored instrumentation, shear microstructure-turbulence profilers [20], and the output of a numerical model of the central Baltic Sea, using newly developed vertically adaptive coordinates [21, 22]. The inert tracer gas was purposefully released in September 2007 in 200 m depth and was detected by means of gas chromatography at concentrations as low as $0.8\,\mathrm{fmol{\cdot}kg^{-1}}$ over times spans of several years, Fig. 2.65. This approach required, due to the extremely low solubility of the tracer, a specially designed ocean tracer injection system (OTIS), which was built up in collaboration with Woods Hole Oceanographic Institution (USA) and the GEOMAR in Kiel. The subsequent spreading of the tracer cloud was observed during 6 ship-based field surveys until February 2009 and used to infer diapycnal as well as lateral mixing rates. One main result of the experiment was the observed dramatic increase of the vertical mixing rates after the tracer had reached the lateral boundaries of the basin, suggesting that mixing processes in the vicinity of the bottom boundaries dominate overall mixing rates in the deeper Baltic Sea [19]. Long-term moored instrumentation was deployed throughout the deep basin, measuring salinity, temperature and velocities.

The analysis of the data showed that basin-scale topographic waves, a deep-rim current, and near-inertial waves are the most important energy sources for turbulence and thus for deep-water mixing. Direct measurements of the dissipation of kinetic energy with a shear-microstructure turbulence profiler showed that, in agreement with the tracer experiment, mixing activities are rather low and intermittent in the interior of the basin, but strongly increase inside the bottom boundary layer [20].

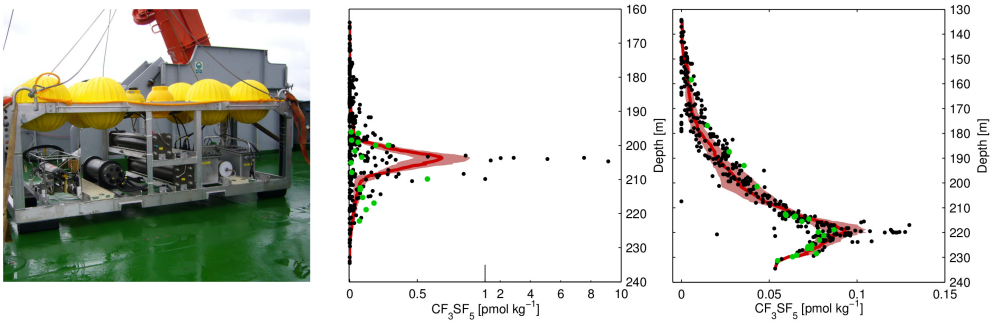

Fig. 2.65: Ocean tracer injection system (left panel), vertical mixing profile 44 days after the injection and before it reached the boundaries (center panel). Black and green dots are measurements, whereas green dots are within the vicinity of the boundary. Red line is the laterally averaged profile. The right panel shows the due to the beginning of boundary mixing processes distorted Gaussian shaped profile 140 days after the injection.

These findings are in contrast to the prevailing idea that mixing processes within the water column, for example the breaking of internal waves [23], dominate deep-water mixing. The importance of boundary mixing also implies that transport pathways of dissolved compounds have to be reconsidered. If vertical mixing happens mainly at the boundaries, a chain of processes, including boundary mixing and lateral redistribution of mixed fluid into the interior is responsible for the vertical transport of compounds. A detailed analysis based on the numerical model is ongoing work and focuses on the transition time of the tracer patch being influenced by interior or boundary mixing processes as well as the quantification of single processes on the overall mixing budget.

2.5.6 Mixing and Sediment Transport in Tidally Energetic Estuaries

H. Burchard, J. Becherer, V. Mohrholz, E. Schulz, L. Umlauf

Theoretical considerations [24–26] have shown that tidal straining (an asymmetry in tidal stresses and mixing due to tides interacting with horizontal density gradients) is relevant in well-mixed estuaries such as the Wadden Sea of the German

Bight. Horizontal density gradients are typically present due to net precipitation and run-off, and due to differential warming in spring. The relevance of this mechanism is the generation of net sediment transports towards the coast, a process which might explain why the Wadden Sea tidal flats have so far kept pace with sea level rise [27]. In two studies of last year, we could for the first time prove from field observations in the Wadden Sea that this process is really present. [28] showed by means of microstucture observations that flood turbulence is significantly enhanced compared to ebb turbulence, with consequently vertically more homogeneous velocity, salinity, temperature and suspended matter profiles during flood (see figure 2.66). [29] analysed long-term ADCP data at various locations in the Wadden Sea to show that flood velocity profiles are significantly more homogeneous than ebb profiles. They could show that the rate of flood to ebb difference depended on the horizontal density gradient, non-dimensionalised by water depth and tidal velocity amplitude, as predicted by theory.

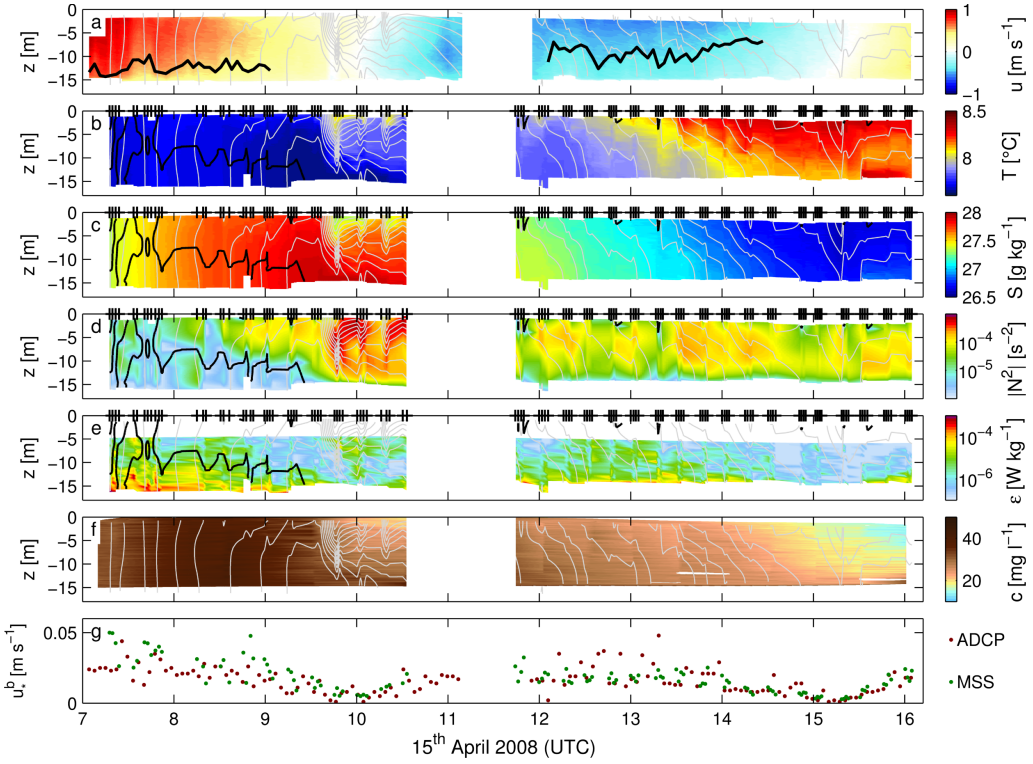

Fig. 2.66: Observed profiles on April 15, 2008 in The Lister Deep, with (a) showing the current velocity. (b) and (c) illustrate the temperature and salinity, respectively, (d) the buoyancy-frequency, N^2, and (e) the dissipation-rate of TKE. (b)-(e) are based on MSS-profiles, which are marked by black crosses atop the panels. (f) displays the SPM concentration. (g) shows the temporally resolved bottom friction velocity, u_*^b, based on ADCP-data (red) and dissipation rates from the MSS (green). Figure taken from [28].

2.5.7 Satellite Oceanography

H. Siegel, M. Gerth, T. Ohde, and I. Stottmeister

Synoptic remote sensing data in the visible and infrared spectral range and the high repeating rates allow the mapping of variable structures in space and time. The application of satellite data in the IOW was focused on studies of the development of sea surface temperature (SST) and phytoplankton, dynamical processes, and coastal discharge in the Baltic Sea. The experiences from the Baltic are transferred to other regions, NW- and SW- Africa, Indonesia, and Beibu Gulf (China). SST maps are derived from infrared channels of the Advanced Very High Resolution Radiometer (AVHRR) of the NOAA weather satellites and from the European Weather satellite MetOp-2. The LAC data with a spatial resolution of 1 km was received from the German Federal Maritime and Hydrographic Agency Hamburg (BSH). Ocean colour satellite data of SeaWiFS, MODIS and MERIS provided by NASA and ESA are used to derive optically active water constituents. Unfortunately, ESA lost the contact to ENVISAT satellite in April 2012. SeaWiFS and MODIS level 2 and 3 products were implemented to study river discharge, phytoplankton and in particular the cyanobacteria development and its inter-annual variation. The reflectance at 550 nm is a parameter representing the maximum of the spectral reflectance and by that the maximum light penetration depth in the Baltic Sea. Variations are produced by backscattering of particle, i.e. cyanobacteria in summer.

SST data are evaluated to investigate seasonal and inter-annual variations in the temperature development of the Baltic Sea. The seasonal development in each year is described in the yearly hydro-chemical assessments of the state of the Baltic Sea prepared by IOW [30, 31] and in the HELCOM indicator fact sheets [32, 33]. After the maximum value in 2008 the annual mean temperature of the entire Baltic Sea decreased and in 2010 below the long-term average of the period 1990-2010. This period was characterised by a positive linear trend in the yearly mean SST with an increase of 0.620°C per decade, see Fig. 2.67. In contrast to the global temperature

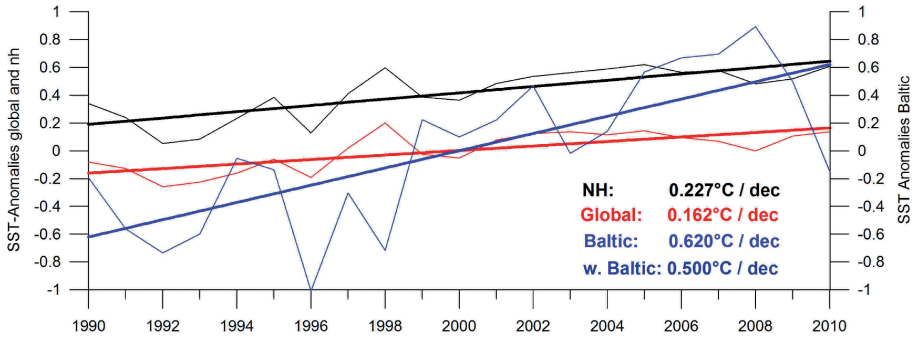

Fig. 2.67: Anomalies of yearly mean SST of the western and entire Baltic Sea including the linear trends

development and that of the northern hemisphere the increase in the Baltic Sea is much stronger and the variations are more pronounced in this confined region. In the annual average SST the shallower western Baltic Sea belongs to the warmest regions of the entire Baltic but the trends is with 0.500°C per decade lower. Reasons could be strong influences of dynamical processes, like water exchange between North and Baltic Seas as well as wind induced mixing and upwelling processes on the mean SST of the western Baltic. The trend was positive in all seasons except March and strongly depending on seasons and regions, see Fig. 2.68. The highest temperature increase occurred in July in the Bothnian Sea, Bothnian Bay, and Eastern Gotland Sea. Negative trends in May along the Polish coast and in autumn along the Swedish east coast indicate an increase in upwelling in the last years.

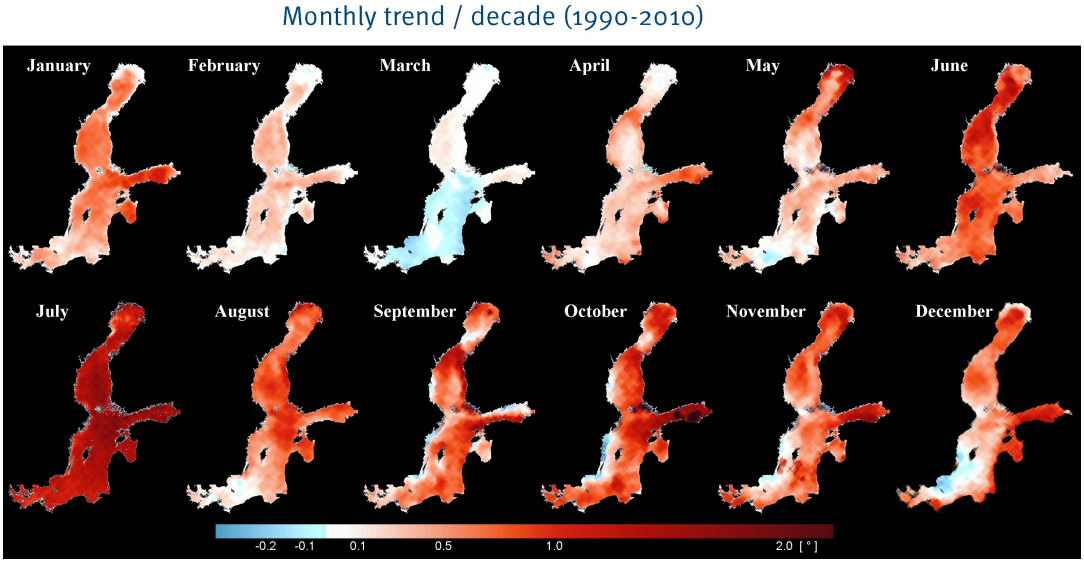

Fig. 2.68: Monthly SST trend / decade for the period 1990- 2010

The spatio-temporal development of phytoplankton in the Baltic Sea characterised by a spring and summer bloom is a main topic in the application of ocean colour satellite data [34]. The spring bloom is dominated by diatoms and dinoflagellates and after a stagnation period in June a summer bloom of toxic cyanobacteria occurs. Satellite derived chlorophyll is used for the investigation of the spring bloom of strong absorbing species. Quasi-true colour images and reflectances at 555 nm are used for the investigation of cyanobacteria in summer. Daily quasi real-time satellite data support local authorities in the observation of the potentially influenced German coast regions. The reflectance at 555 nm gives not only information about the surface accumulations but also inside into the upper water column. Because of their gas vacuoles in the cells the cyanobacteria have buoyancy and float up to the surface during low wind conditions. These are also the conditions for the development of a diurnal thermocline and a further fast heating of the surface water. That means, colder months belong to stronger wind mixing which may interrupt or

stop the development of cyanobacteria. In the Baltic Sea July is the month with the most intense cyanobacteria development in the year. Monthly mean values of the reflectance R555 and SST for July show in colder years lower cyanobacteria development and warmer years are related to higher concentrations see Fig. 2.69.

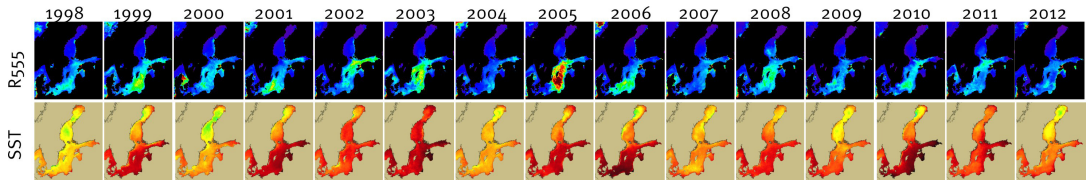

Fig. 2.69: Monthly mean distribution of R555 and SST of the Baltic Sea for the month July in the period 1998-2012

Satellite derived SST data supported geological investigations on the reconstruction of palaeo-temperature. The SST data were used to calibrate the TEX86 index reflecting temperature-induced changes in the composition of lipids. This calibration was then applied to sediment cores to reconstruct the temperature of the last 1000 years. The warm years were related laminated sediments due to anoxic conditions. The sediments have a high carbon content caused by re-mineralised cyanobacteria [35].

The second phase of the BMBF funded interdisciplinary pollution project SPICE II studied the 5 major rivers of South-East-Sumatra (Indonesia) ended in December 2010. Remote sensing data was combined with *in situ* measurements of optically active water constituents and water colour to identify different sources of water masses in the tributaries and estuaries. The variation in water colour allows one to follow the discharge into Malacca and Karimata Straits and to investigate the transport processes in relation to the driving forces. Sources of CDOM (peat draining rivers), area of high suspended matter concentration (erosion) and limited bio-production in the rivers and tributaries were identified. The rivers discharge into the Malacca and Karimata Straits east of Sumatra Island. The transport of the northern rivers in the Malacca Strait occurs north-westwards during all seasons. The distribution patterns of the southern rivers in the Karimata Strait are strongly related to the wind direction (monsoon phases). Tides strongly influence the distribution patterns of river discharge into the estuaries and establish the Estuarine Turbidity Maximum Zone. The Archipelago of Riau with tourist centres and coral reefs can be strongly influenced during southerly winds. In SPICE III the project "Carbon sequestration in the Indonesian Seas and its global significance: Generation of scientific knowledge for formulating strategies for adaptation to climate change (CISKA)" started March 2012. The aim is to quantify the carbon storage in and the CO_2 emission from the Indonesian Seas for the development of sustainable mitigation strategies to reduce CO_2 emissions.

Within the BMBF funded joint project SOPRAN II (Surface Ocean Processes in the Anthropocene, February 2009 — January 2013) the optical subproject of

IOW is dealing with the influence of Sahara dust on the solar radiation. Sahara dust strongly modifies the intensity and spectral solar radiation, photosynthetically available radiation and optical characteristics in the water column and induces a biological reaction of the ecosystem [36–38]. Furthermore, dust has a strong influence on the determination of wind and chlorophyll-a from satellite data [39].

In the BMBF funded Beibu-Project (Holocene environmental evolution and anthropogenic impact of Beibu Gulf, South China Sea) (June 2009 – May 2012) satellite data were used to investigate the climatology, distribution pattern of different water masses, their biological activity and the suspended matter transport in relation to driving forces. Beibu Gulf is a complex and highly dynamic system related to reversing wind directions, overlaid by tidal modes and typhoons. During SW monsoon clear ocean water is transported into the Gulf from the South. During NE monsoon mixed waters from NE with contributions from Perl River enter the gulf through the Qiongzhou Strait. Typhoons mix the water column, reduce the SST by up to 2°C, and increase SPM. Tidal influence leads to increasing resuspension in coastal areas. Highest bio-productivity occurs from December to February and after tropical storms.

In the BMBF funded GENUS II Project (Geochemistry and Geology of the Namibian Upwelling System) which started in May 2012 satellite data will be used to investigate the evaluation of persistent filaments in relation to possible driving forces. In 2003, a coccolithophore bloom was already observed for more than 10 days using satellite data and *in situ* measurements confirmed the special growth conditions in this persistent filament like shallow top layer, high solar radiation etc. This study continues the investigation to give insight into the mechanism of formation and development of persistent filaments containing coccolithophore a final stadium of the phytoplankton succession in the region. The main questions are: Is the succession developing within that single filament or does the filament developing after the first steps of succession and deliver special conditions for the final stage, the coccolithophores.

References

[1] W. Fennel, T. Junker, M. Schmidt and V. Mohrholz. "Response of the Benguela Upwelling Systems to spatial variations in the wind stress". *Cont. Shelf Res.*, **45** (2012), 65 –77.

[2] M. Herzfeld, M. Schmidt, S. M. Griffies and Z. Liang. "Realistic test cases for limited area ocean modeling". *Ocean Model.*, **37** (2011), 1–34.

[3] T. Neumann, K. Eilola, B. Gustafsson, B. Müller-Karulis, I. Kuznetsov, H. Meier and O. Savchuk. "Extremes of Temperature, Oxygen and Blooms in the Baltic Sea in a Changing Climate". *AMBIO*, **41** (2012), 574–585.

[4] H. Radtke, T. Neumann, M. Voss and W. Fennel. "Modeling pathways of riverine nitrogen and phosphorus in the Baltic Sea". *J. Geophys. Res.*, **117** (2012), DOI: 10.1029/2012JC008119.

[5] W. Fennel. "A nutrient to fish model for the example of the Baltic Sea". *J. Mar. Sys.*, **81** (2010), 184–195.

[6] H. Radtke, T. Neumann and W. Fennel. "A Eulerian nutrient to fish model of the Baltic Sea - A feasibility-study". *J. Mar. Syst..*, (2012), DOI: 10.1016/j.jmarsys.2012.07.010.

[7] IOC, SCOR and IAPSO. "The international thermodynamic equation of seawater - 2010: Calculation and use of thermodynamic properties. Intergovernmental Oceanographic Commission, Manuals and Guides No. 56, UNESCO (English), 196 pp., Paris" (2010). `http://www.teos-10.org/`.

[8] IUGG. "International Union of Geodesy and Geophysics, XXV General Assembly, 27 June - 7 July 2011, Melbourne, Australia, Comptes Rendus" (2011). `http://iahs.info/melbourne/2011_Melbourne_Comptes_Rendus.pdf`.

[9] R. Feistel, D. Wright, H.-J. Kretzschmar, E. Hagen, S. Herrmann and R. Span. "Thermodynamic Properties of Sea Air". *Ocean Sci.*, **6** (2010), 91–141.

[10] IAPWS. "Guideline on an Equation of State for Humid Air in Contact with Seawater and Ice, Consistent with the IAPWS Formulation 2008 for the Thermodynamic Properties of Seawater. The International Association for the Properties of Water and Steam. Niagara Falls, Canada, July 2010" (2010). `http://www.iapws.org/`.

[11] R. Feistel. "TEOS-10: A New International Oceanographic Standard for Seawater, Ice, Fluid Water and Humid Air". *International Journal of Thermophysics*, **33** (2012), 1335–1351.

[12] R. Pawlowicz, T. McDougall, R. Feistel and R. Tailleux. "Preface: An historical perspective on the development of the Thermodynamic Equation of Seawater - 2010". *Ocean Sci.*, **8** (2012), 161–174.

[13] BIPM. "WMO-BIPM workshop on measurement challenges for global observation systems for climate change monitoring: Traceability, stability and uncertainty. 30 March–1 April 2010, WMO Headquarters, Geneva, Switzerland" (2010). `www.bipm.org/utils/common/pdf/rapportBIPM/2010/08.pdf`.

[14] S. Seitz, R. Feistel, D. Wright, S. Weinreben, P. Spitzer and P. D. Bievre. "Metrological traceability of oceanographic salinity measurement results". *Ocean Sci.*, **7** (2011), 45–62.

[15] G. M. Marion, F. J. Millero, F. Camoes, P. Spitzer, R. Feistel and C.-T. A. Chen. "pH of Seawater". *Mar. Chem.*, **126** (2011), 89–96.

[16] L. Umlauf and H. Burchard. "Diapycnal transport and mixing efficiency in stratified boundary layers near sloping topography". **41** (2011), 329–345.

[17] J. Becherer and L. Umlauf. "Boundary mixing in lakes. 1. Modeling the effect of shear-induced convection". *J. Geophys. Res.*, **116** (2011), C10017.

[18] C. Lorrai, L. Umlauf, J. Becherer, A. Lorke and A. Wüest. "Boundary mixing in lakes. 2. Combined effects of shear-induced and convective turbulence on basin-scale mixing". *J. Geophys. Res.*, **116** (2011), C10018.

[19] P. Holtermann, L. Umlauf, T. Tanhua, O. Schmale, G. Rehder and J. Waniek. "The Baltic Sea Tracer Release Experiment. 1. Mixing rates". *J. Geophys. Res.*, **117** (2012), doi10.1029/2011JC007439.

[20] P. Holtermann and L. Umlauf. "The Baltic Sea Tracer Release Experiment. 2. Mixing processes". *J. Geophys. Res.*, **117** (2012), doi10.1029/2011JC007445.

[21] R. Hofmeister, H. Burchard and J.-M. Beckers. "Non-uniform adaptive vertical grids for 3D numerical ocean models". *Ocean Model.*, **33** (2010), 70–86.

[22] R. Hofmeister, J.-M. Beckers and H. Burchard. "Realistic modelling of the exceptional inflows into the central Baltic Sea in 2003 using terrain-following coordinates". *Ocean Model.*, **39** (2011), 233–247.

[23] E. M. van der Lee and L. Umlauf. "Internal-wave mixing in the Baltic Sea: Near-inertial waves in the absence of tides". *J. Geophys. Res.*, **116** (2011), C10016.

[24] H. Burchard and R. D. Hetland. "Quantifying the contributions of tidal straining and gravitational circulation to residual circulation in periodically stratified tidal estuaries". *J. Phys. Oceanogr.*, **40** (2010), 1243–1262.

[25] H. Burchard, R. Hetland, E. Fischer and H. Schuttelaars. "Drivers of residual circulation in tidally energetic estuaries: Straight and irrotational estuaries with parabolic cross-section". *J. Phys. Oceanogr.*, **41** (2011), 548–570.

[26] H. Burchard and H. Schuttelaars. "Analysis of tidal straining as driver for estuarine circulation in well mixed estuaries". *J. Phys. Oceanogr.*, **42** (2012), 261–271.

[27] Z. Wang, P. Hoekstra, H. Burchard, H. Ridderinkhof, H. de Swart and M. Stive. "Morphodynamics of the Wadden Sea and its barrier island system". *Ocean. Coast Manage.*, **68** (2012), 39–57.

[28] J. Becherer, H. Burchard, G. Flöser, V. Mohrholz and L. Umlauf. "Evidence of tidal straining in well-mixed channel flow from micro-structure observations". *Geophys. Res. Lett.*, **38** (2011), L17611.

[29] G. Flöser, H. Burchard and R. Riethmüller. "Observational evidence for estuarine circulation in the German Wadden Sea". *Cont. Shelf Res.*, **31** (2011), 1633–1639.

[30] G. Nausch, R. Feistel, L. Umlauf, V. Mohrholz and H. Siegel. "Hydrographisch-chemische Zustandseinschätzung der Ostsee 2010". *Meereswissenschaftliche Berichte Warnemünde*, **84** (2011), 1–99.

[31] G. Nausch, R. Feistel, L. Umlauf, V. Mohrholz, K. Nagel and H. Siegel. "Hydrographisch-chemische Zustandseinschätzung der Ostsee 2011". *Meereswissenschaftliche Berichte Warnemünde*, **86** (2012), 1–130.

[32] H. Siegel and M. Gerth. "Development of Sea Surface Temperature in the Baltic Sea in 2010". *HELCOM Indicator Report*, (2011). `http://www.helcom.fi/BSAP_assessment/ifs/ifs2011/en_GB/sst/`.

[33] H. Siegel and M. Gerth. "Development of Sea Surface Temperature in the Baltic Sea in 2011" (2012). `http://www.helcom.fi/BSAP_assessment/ifs/ifs2012/en_GB/sst/`.

[34] N. Wasmund, F. Pollehne, L. Postel, H. Siegel and M. Zettler. "Biologische Zustandseinschätzung der Ostsee im Jahre 2010,". *Leibniz Institute for Baltic Sea Research Warnemünde, Meereswiss. Ber.*, **85** (2011).

[35] K. Kabel, M. Moros, C. Porsche, T. Neumann, F. Adolphi, T. J. Andersen, H. Siegel, M. Gerth, T. Leipe, E. Jansen and J. S. S. Damsté. "Impact of climate change on the Baltic Sea ecosystem over the past 1,000 years". *Nature Climate Change*, **2** (2012), 871–874.

[36] T. Ohde and H.Siegel. "Biological response to coastal upwelling and dust deposition in the area off Northwest Africa". *Cont. Shelf Res.*, **30** (2010), 1108–1119.

[37] T. Ohde and H. Siegel. "Impacts of Saharan dust and clouds on photosynthetically available radiation in the area off Northwest Africa". *Tellus B*, **64** (2012), DOI: 10.3402/tellusb.v64i0.17160.

[38] T. Ohde and H. Siegel. "Impacts of Saharan dust on downward irradiance and photosynthetically available radiation in the water column". *Adv. Oceanogr. Limnol.*, **3** (2012), 99–131.

[39] T. Ohde. "Impact of Saharan Dust on Ocean Surface Wind Speed Derived by Microwave Satellite Sensors". *Journal of Infrared, Millimeter, and Terahertz Waves*, **31** (2010), 1225–1244.

2.6 Physics Education

Head: PD Dr. Heidi Reinholz

Staff: Dr. Viola von Oeynhausen, Falk Eberlein, Dipl.-Des. Wiebke Loseries, Matthias Hofstetter, Dipl.-Paed. Christa Nier, Adrian Lehrmann, Marion Pauer, Christine Prühs, Christian Schmidt

The goals of our activities are multilayered. Both sides of the teaching-learning interface are addressed and interrelated. While providing lectures and seminars for the future teacher generation is the primary focus, we also want to reach out to the broader community as well. We base our activities on empirical research with respect to teaching methods and media.

Teaching

The curriculum for the courses in physics education has been rewritten over the last few years in order to include new developments with respect to teaching methods and media. Questions of students' motivation, diagnostics of teaching, and interdisciplinary teaching are discussed as well as practically oriented seminars and activities have been introduced. School related lab work and first teaching experiences are seen as particularly helpful to students and teaching staff. Teaching experiences are organized in close collaboration with schools. Recently newly introduced units *Physics and technology* and *IT-media in teaching* have been established as popular units. A new bill on teacher education in Mecklenburg-Vorpommern (*Lehrerbildungsgesetz*) has been issued in July 2011. Student now enroll in 10 semester course work which is completed passing a final state examination (*1. Staatsexamen*).

Research

The illustration of directional physical quantities in school is commonly used to construct the resultant of forces, angular moments and the Lorentz force. However, taking this pictorial illustration up to the level of a symbolic (mathematical) description of scalar and vector product is rarely followed up allthough it is requested by the commonly agreed base curriculum.While investigations have shown that the iconic representation enhances the learning success, research on the application of symbolic representations is in the beginning and questions of learning improvements are left open. Based on current workon the overall concept of mechanics and dynamics a learning unit which includes a test design is in preparation.

Working with computers in order to get information is more and more in the focus for students as well as for teachers. 76 % of students use the computer for making enquiries with respect to school related tasks.Also scientific explorations and investigations using multimedia are considered relevant within the teaching profession.

We are aiming at the implementation of interactive simulations in the classroom provided by the University of Colorado [1]. We then focus on the investigation of the learning success comparing interactive simulations to the use of hands on experiments in the classroom.

Another project focuses on the connection of magnetism and special relativity [2]. Magnetism is one of the longest known physical phenomenon but the least generally understood mechanism. The consideration of different reference systems of electons and ions in parallel conducting wires illustrates nicely that magnetism is related to moving charges. Thanks to the very strong desire for electrical neutrality in nature, the small relativistic effect of moving charges implements itself as magnetism. The explanation is possible with very little mathematical prerequisites. A learning unit for school students is in preparation.

Outreach Activities

Jointly we - scientists, teachers, parents, students - look for new ways to take science into the classroom and beyond. We started various projects on different interfaces between teachers and learners which interrelate and complement each other. By involving future science teachers in particular, we are creating highly qualified multiplicators of science. What we want to achieve with all these activities is to reach out to a broad public audience and get them interested and excited about science. For this, the specialists have to explain complex structures and how it all works in an easy way. It is a great challenge to communicate with the audience via generally understandable explanations and not using too detailed scientific terminology. At outreach activities, we like to present good examples and encourage more and more scientists to get involved in presentations and activities for the general audience.

Since 2003, the Institute of Physics has organized the yearly **Lighthouse competition** [3] for the schools of Mecklenburg-Vorpommern which compete against each other for the lighthouse cup. After a prequiz about the main topic of the year (2010: magnetism, 2011: time, 2012: plus-minus), the best teams have to find good scientific explanations for experiments which are presented on the stage. Afterwards, the *Experimentarium* with hands on activities can be explored and the labs of the institute are open to visit. Last but not least, a lecture with lots of impressive experiments repacked in a new story every year (2010: Die 3 Fragezeichen, 2011: Die Simpsons, 2012: Indiana Jones Monopol) is been prepared and presented by a group of physics students, including teachers students.

lighthouse cup

Science is fun. This is the reason, why a group of scientists and students came together in 2005 to work on this project. Every year in August, Rostock welcomes 1.5 Mio visitors to the Hanse Sail, a meeting of large sailing boats.

During this time, our event **Science@Sail** [4] has been a yearly runner for young and old. They have an opportunity to learn about science, interesting facts and fascinating experiments. Close to the sea you can smell the salt in the air - can I really trust my nose? Under the water tap you can see a floating drop - but is it really true or are my eyes mistaken? The visitors of Science@Sail can probe their senses on more than 70 experiments and get the science behind them explained. In recent years the topic follows the theme of the physics day.

PhySch (*Phy*sik und *Sch*ule) [5] is a project on the interface between science and schools. University students who are trained to become science teachers are involved. They design experiments which complement the school curriculum in two possible ways. Either by an experiment which can not easily be done in schools, e.g. Franck-Hertz experiment, or experiments which go beyond the school curriculum but contain various aspects already taught at school, e.g. intelligent glass (heat absorption/emission), hydrogen vehicles, or a black box demonstrating how the scientific knowledge is achieved. Instructions for the school students are prepared at an appropriate level. The university students are also responsible to lead the school students through the projects which are offered at the university venues or in the schools.

Recently, a new project has been developed and established for primary school students. They are encouraged to explore a specific topic (energy, light [6], time [7]) by doing experiments or exploring every day materials excitedly guided by students who take on a specific role (e.g. Mr. Moon, Miss Second or Miss Spring). Students are encouraged to explore, investigate, find out differences or similarities. The project also aims to investigate the scope of this approach to empower the kids for scientific and technical subjects later in school.

Fig. 2.70: Students explore experiments around the topic *time*

References

[1] http://phet.colorado.edu/.

[2] H. Reinholz, C. Schmidt and S. Strauß. "Magnetismus relativistisch betrachtet". In "GDCP-Jahrestagung", Hannover (2012).

[3] http://www.physik.uni-rostock.de/physiktag/.

[4] http://www.scienceatsail.uni-rostock.de/.

[5] http://www.physik.uni-rostock.de/physch/.

[6] W. Loseries. "Entdeckerkids – eine naturwissenschaftliche Reise in die Welt des Lichtes". booklet, Rostock (2010).

[7] W. Loseries. "Entdeckerkids – eine Entdeckerkidsreise in die Zeit". booklet, Rostock (2011).

3 Collaborative Research

3.1 Collaborative Research Center (SFB 652) "Strong Correlations and Collective Effects in Radiation Fields: Coulomb Systems, Clusters and Particles"

Executive Board: Prof. Dr. Stefan Lochbrunner [a]
Prof. Dr. Karl-Heinz Meiwes-Broer [b]
Prof. Dr. Ronald Redmer
Prof. Dr. Heinrich Stolz

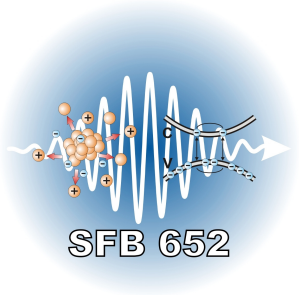

Homepage: http://web.physik.uni-rostock.de/sfb/

[a] leader of the intergrated graduate school
[b] spokesman

Collaborative Research Centers (Sonderforschungsbereiche) are long-term (up to 12 years) research centers at German universities devoted to topics at the frontier of science. The innovative and cross-disciplinary research program is treated in various projects in a coherent approach coordinated by the executive board. Funding is provided by the Deutsche Forschungsgemeinschaft (DFG).
The first funding period of the SFB 652 ended on June 30, 2009. The DFG has granted a second funding period that started on July 1, 2009 and ranges to June 30, 2013. The proposal for the third period has been submitted by the end of 2012.

3.1.1 Projects and Project Leaders (status 31.12.2012)

A1	Matter exposed to VUV- and X-ray radiation	Prof. Dr. Karl-Heinz Meiwes-Broer Prof. Dr. Ronald Redmer PD Dr. Josef Tiggesbäumkker
A2	Thomson-scattering and correlations in warm dense matter	Prof. Dr. Ronald Redmer

A3	Correlated processes in laser-excited trapped cluster ions	Prof. Dr. Lutz Schweikhard* Dr. Gerrit Marx* Prof. Dr. Karl-Heinz Meiwes-Broer
A4	Impact of dynamical correlations on optical properties in dense Coulomb systems and clusters	PD Dr. Heidi Reinholz
A5	Controlled strong-field excitation of clusters and particles by shaped laser pulses	PD Dr. Josef Tiggesbäumker Prof. Dr. Karl-Heinz Meiwes-Broer
A6	Quantum kinetics of dense Coulomb systems in laser fields	Prof. Dr. Manfred Schlanges* PD Dr. Thomas Bornath
A8	Microscopic description of atomic clusters in intense laser fields	Dr. Thomas Fennel
A9	Simulation of quantum dynamics in strong laser fields using density functional theory	Prof. Dr. Dieter Bauer
B1	Exciton matter in external potentials	Prof. Dr. Heinrich Stolz
B2	Generation and detection of non-classical light in semiconductor lasers and nanostructures	Prof. Dr. Werner Vogel Prof. Dr. Heinrich Stolz
B5	Optical signatures from excitons, biexcitons, polaron-excitons and collective excitonic phases in strongly correlated electron-hole systems	Prof. Dr. Holger Fehske*
B6	Radiation-induced correlations in ultracold droplets	Prof. Dr. Karl-Heinz Meiwes-Broer
B9	Dynamics of correlated excitons in molecular aggregates	Prof. Dr. Stefan Lochbrunner
B10	Laser-driven multi exciton dynamics in molecular aggregates	Prof. Dr. Oliver Kühn
B11	Structural correlations in liquid Coulomb systems	Prof. Dr. Ralf Ludwig Prof. Dr. Oliver Kühn Prof. Dr. Stefan Lochbrunner
B12	Quantum correlations in light and matter: characterization and verification	Prof. Dr. Werner Vogel
MGK	Integrated Graduate School	Prof. Dr. Stefan Lochbrunner

* Physics Department, University of Greifswald

3.1.2 Overview

The common goal of the research activities is to contribute to a deeper fundamental understanding of the role of strong correlations and collective phenomena for the interaction of radiation fields with matter. Characteristic for the SFB 652 are the joint experimental and theoretical efforts to investigate these issues in a broad spectrum of systems including ultracold quantum condensates, exciton clusters in semiconductor quantum films, atomic clusters and nanoparticles, as well as warm dense matter and molecular systems so that new frontiers in light-matter research are being explored. Along this line the centre connects topical issues from various subjects, including physics of correlated Coulomb systems, semiconductor physics, quantum and molecular optics, and cluster physics in an interdisciplinary manner. State-of-the art light sources, such as stabilized optical cw-lasers, ultra-intense femtosecond lasers, as well as the DESY VUV free-electron laser (FLASH) are used for the experimental investigations. In perspective, to attack new regimes regarding to the parameters of the radiation field, also the DESY X-ray free-electron laser (X-FEL) will be used for the experimental program. Some projects (A1, A2) participate in first experimental campaigns at the LCLS X-ray free-electron laser in Stanford/USA.

3.1.3 Structure

Thematically the projects are classified in two research complexes. Project complex A is devoted to the investigation of optical excitations of existent strongly correlated Coulomb systems while complex B addresses the generation of correlations by the radiation field itself. About 50 scientists collaborate on the above outlined topics, including several colleagues from the University of Greifswald. The central topic in the project complex A is the excitation and analysis of dense Coulomb systems, i.e. clusters and particles, warm dense matter, dense electron-ion systems, and particle-hole systems in semiconductors. The theoretical investigations in projects A1, A2, A4, A6, A8 and A9 are accomplished in close collaboration with the main three experimental topics which are: (i) the excitations of clusters and particles by radiation from free-electron lasers (A1, A5), and (ii) the controlled coupling of intense optical laser pulses to clusters and particles (A3, A5). For the analysis of the systems as well as the exploration of new routes for future application of light-matter correlations cutting-edge control techniques such as pulse optimization through genetic algorithms and pump-probe control schemes with phase-stabilized pulses are utilized. For the theoretical description state-of-the-art many-body techniques such as quantum particle-in-cell methods (A1, A8, A9), quantum kinetic equations (A6), linear response theory (A2, A4), density functional theory and quantum molecular dynamics simulations (A1, A2, A9) are applied.

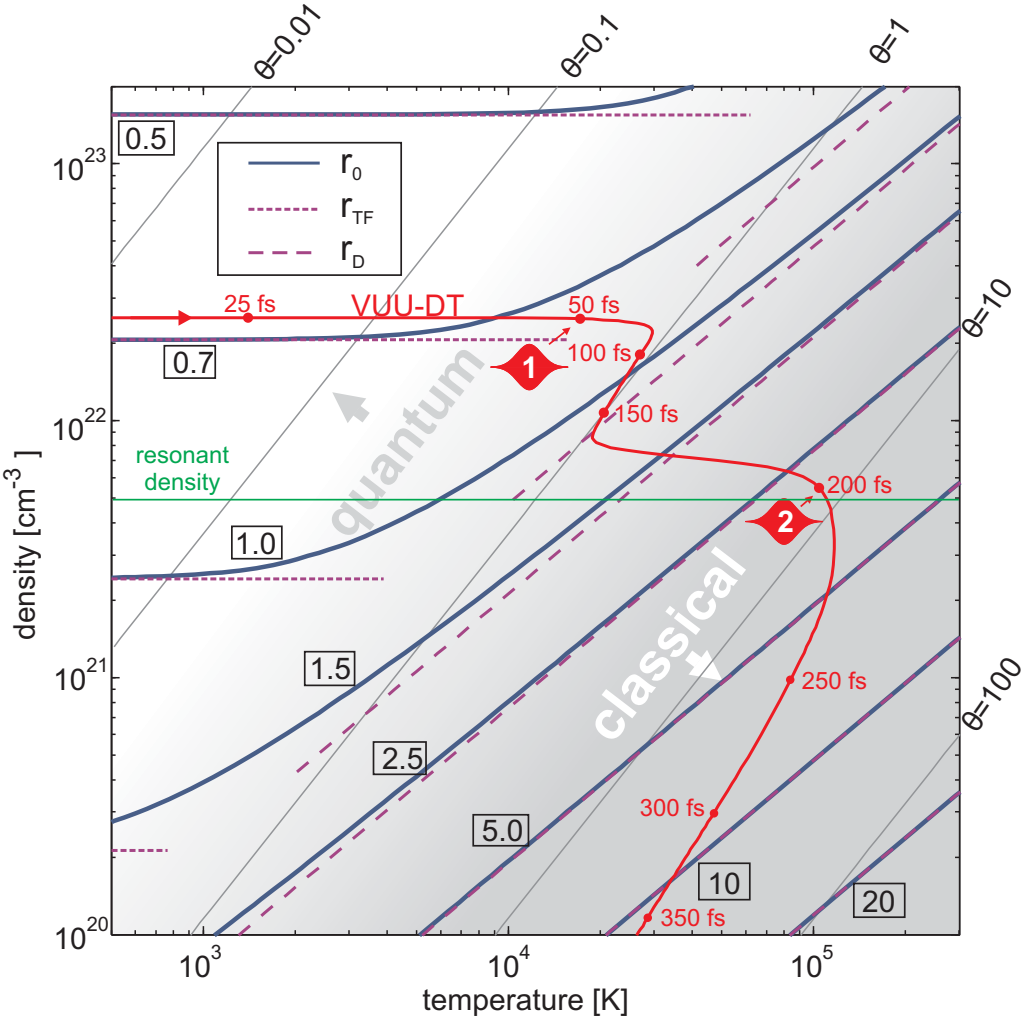

Fig. 3.1: Calculated nanoplasma evolution for Na_{55} subject to two laser pulses [$\lambda = 800\,\mathrm{nm}$, $\tau = 25\,\mathrm{fs}$ (FWHM), $I_0 = 8 \times 10^{12}\,\mathrm{W/cm^2}$] in the density-temperature plane (red curve, times as indicated). For the chosen pulse delay of $\Delta t = 150\,\mathrm{fs}$ the second pulse is resonant with the Mie plasmon of the expanding cluster (resonant density as indicated). Screening length r_0 (selected values indicated in boxes in units of Å) for an ideal electron gas as function of temperature and density. Results of Thomas-Fermi (r_{TF}) and Debye theory (r_{D}) are shown for the same set of screening lengths in the respective limits (violet lines). Thin diagonal lines indicate levels of constant degeneracy parameter Θ. From [Köhn, Redmer, Fennel, New Journal of Physics **14**, 055011, (2012)], Projects A1, A2 and A8.

Project complex B concentrates on the build-up of correlations in semiconductors, atom condensates, clusters, optical and molecular systems. Semiconductors and molecules represent ideal targets for the study of many-particle effects in a wide density range because of the well-controlled elementary excitation of the exci-

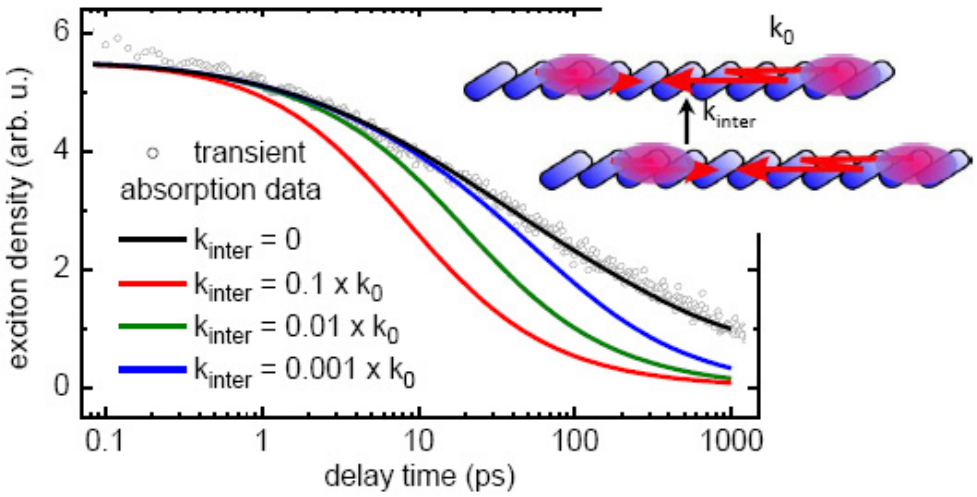

Fig. 3.2: Femtosecond pump/probe dynamics of the population of perylenbisimid aggregates. The data can theoretically be modelled only when one assumes an exciton transport along the molecular strands, black curve. As soon as hopping is allowed with a vertical component strong deviations appear between the measured dynamics and the theoretical results. From [Wolter, Aizezers, F. Fennel, Seidel, Würthner, Kühn, Lochbrunner, New Journal of Physics **14**, 105027 (2012)], Projects B9, B10

tons. In semiconductors a limiting factor is the finite lifetime of the excitons which, however, can be tuned by the choice of the material or tuning an external confinement potential. Corresponding studies are a major issue within the projects B1-B2. Excitons in mesoscopic potential wells are investigated in project B1, being very promising candidates in this context. Essential for the realization and the control of the light-induced correlations is the development of theoretical concepts that provide a consistent connection of quantum optics with many-particle theory. This is the subject of the project B2. In project B5 the formation of exciton-polariton quasiparticles through cooperative effects and the build-up of correlations at high pressures are investigated. Within project B6 the light-field induced formation of novel metal atom condensates in exotic and ultracold environments, such as suprafluid helium droplets, is studied.

During the course of the 1st funding period it became possible to include the field of exciton dynamics in molecular systems, within the project B9. This comprises experimental as well as theoretical activity on molecules as an additional basis of the collaborative research centre. In the current funding period these activities are extended within the project B9 and B10. The new projects B9-B11 emphasize the importance of correlation effects in the dynamics in molecular systems. In particular, it became possible to build a bridge to physical chemistry (B11) by including research

on ionic liquids. With the new projects A8, A9 and B12, methods of many-particle and density functional theory as well as problems of quantum correlations of light and matter are stronger emphasized within the SFB.

For its second period (2009-2013) the SFB 652 could significantly be strengthened by the inclusion of several new aspects. 16 scientific projects and an integrated graduate school constitute an internationally high-ranked research centre with a lively academic service which reaches out into the Faculty of Mathematics and Natural Sciences as well as into the whole university, especially via the Department of Life, Light and Matter of the Interdisciplinary Faculty. This interdisciplinary research platform was founded at the University of Rostock in 2007, also based on the SFB 652 with its scientific competence and its long-term missions.

The two results sketched above give an impression of current collaborative activities in the SFB. The first example illustrates results of theoretical work in the projects A1, A2 and A8 of the strong laser field interaction with sodium clusters. Fig. 3.1 demonstrates how a sodium cluster subject to a strong femtosecond laser pulse can be treated as a dense plasma. In the setting chosen the nanoplasma evolves in short times, see the red trace. It can practically reach any point in the temperature-density plane.

The second example concerns experimentally investigated ultrafast dynamics in ordered molecular organic systems (B9, B10). Organic materials have attracted strong scientific attention with respect to potential applications in photonics and electronics. The result in Fig. 3.2 demonstrates that the population of perylen-bisimid aggregates shows pronounced dynamics when investigated with fs pump/probe schemes. The data can theoretically be modelled only when one assumes an exciton transport along the molecular strands. As soon as hopping is allowed with a vertical component strong deviations appear between the measured dynamics and the theoretical results.

4 Department of Science and Technology of Life, Light and Matter

4.1 Overview

In a world which is becoming ever more complex, innovative or even revolutionary solutions primarily require two things: An extremely high specialization and a conceivably close interaction of various scientific areas. More than ever before, new ideas and technologies are being based on interdisciplinary thinking. On these grounds in 2007, the Department 'Science and Technology of Life, Light and Matter' (LL&M) has been established within the Faculty of Interdisciplinary Research of the University of Rostock. Its activities search to connect scientific effort of the faculties of natural sciences and mathematics, agriculture, engineering sciences as well as medicine. Three further departments 'Maritime systems', 'Ageing of individuals and society' and 'Knowledge – Culture – Transformation' together with LL&M currently constitute the Interdisciplinary Faculty (INF), which is supported by the University and the state of Mecklenburg-Western Pomerania. The aim is to identify and strengthen fruitful research fields through an appointment policy that is consequently oriented towards profile and strategy in order to foster international competitiveness.

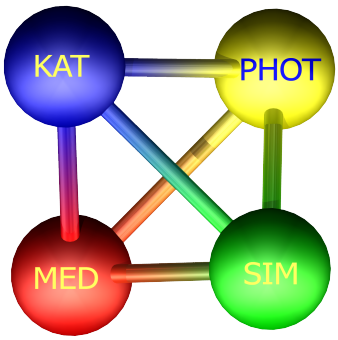

Fig. 4.1: Catalysis, Photonics, Medicine, and Simulation technology are in the core of the Department of Life, Light and Matter.

4.2 Program of the Department

The department LL&M aims at interdisciplinary research and training in the fields of photon sciences, engineering and catalysis, regenerative medicine and numerical simulations. The program comprises activities within several faculties and institutes of Rostock University. Among those are the basic sciences — chemistry, physics and mathematics — as well as the more applied mechanical and electronic engineering, informatics, and life sciences. In addition, the Leibniz–Institute for catalysis (LIKAT), the Leibniz–Institute for atmospheric research (IAP), as well as the Gesellschaft für Schweißtechnik International (GSI) are significantly involved.

The scope of the investigations reaches from fundamental problems like the interaction of light with matter via the development of chemical and agricultural as well as biologically relevant drug design for biomedical applications. Smart materials play an important role in all of these areas. One backbone of the Department LL&M is research on the impact of atomic and molecular properties onto macroscopic systems. Another focus is the question how atomic and molecular properties affect in macroscopic systems. Linked to this is the study of microscopic mechanisms that allow control by, e.g. light or molecular active substances. These operations on the atomic or nanometer scale can be used for the development and modification of new methods and materials. Potential applications in biomedical and technical areas are as numerous as fundamental insights into a highly interdisciplinary field.

The University of Rostock already has established competences at the intersection of natural, engineering and life sciences. They serve as solid basis for the Department LL&M, being a condensation nucleus of an interdisciplinary high-technology field. Moreover, as the research has many links to technical applications it bears potential for a sustainable future growth sector.

4.3 Contribution of the Physics Institute to LL&M

Among the over 40 research groups within LL&M, 10 belong to the Physics institute. These are:

Prof. Dr. Thomas Gerber	Physics of Nano- and Biomaterials
Prof. Dr. Boris Hage	Experimental Quantum Optics
Prof. Dr. Oliver Kühn	Molecular Quantum Dynamics
Prof. Dr. Stefan Lochbrunner	Dynamics of Molecular Systems
Prof. Dr. Franz-Josef Lübken	Leibniz Institute for Atmospheric Physics
Prof. Dr. Karl-Heinz Meiwes-Broer	Clusters and Nanostructures
Prof. Dr. Fedor Mitschke	Nonlinear Optics
Prof. Dr. Ronald Redmer	Statistical Physics
Prof. Dr. Christoph Schick	Polymer Physics
Prof. Dr. Heinrich Stolz	Semiconductor Optics

4.4 Current Activities

In the period under review one focal point of LL&M has been the enhanced networking among the workgroups in different scientific disciplines. At first, the members had to recognize their own benefits when participating in this interdisciplinary effort. With strong support by the University and the local government PhD scholarship funds could be granted to 14 students. All of them work on interdisciplinary topics and were coached by two supervisors from separate institutes. It is a success that numerous personalities have made an application for admission in the department as well as have written down research subjects suitable to LL&M. Members from five faculties as well as the IAP, LIKAT and GSI-SLV GmbH could be admitted thus after confirmation by the leading board of the Interdisciplinary Faculty and the Rector of the University, Prof. Schareck.

LL&M defines itself as a research department. Hence its main aim is the identification and establishment of topical research subjects in order to attract high-level scientists and enhanced third-party funding. In this respect the PhD scholarships serve as a glue money to strengthen initiatives setting up new research projects. Some major projects as well as few smaller ones could be either continued in the proximity of the department or be started. One major success has been the funding of a laboratory building specific for the Department LL&M. Approved by the German Council of Science and Humanities (Wissenschaftsrat) the scientific building will provide additional 2400 sqm of extensively equipped space. The topical focus of LL&M and the high standard of the contributing research groups made it possible to acquire 20 Mio. EUR funding for the new building and for equipment. With this an appropriate environment will be established for the interdisciplinary research and education in the Department LL&M. Activities within the disciplines Physics, Chemistry, Biology, Medicine and Engineering will be bundled in order to pursue the research on complex molecular systems. A central topic is the analysis, control and design of systems which are governed through processes on the molecular level. While most research groups are presently and will remain consistently located in their home institutions, the Department LL&M will get in the future additional capacity especially for Core Facilities and temporary project laboratories.

Several larger projects with the contribution of LL&M research groups include:

- Collaborative Research Center DFG-SFB 652 *Strong correlations and collective effects in radiation fields: Coulomb systems, clusters and particles*, see Sec. 3.1 for the overview. This project is centered at the Institute of Physics, with one project leader being from the Chemistry Department of the University of Rostock and three project leaders from the Institute of Physics of the University of Greifswald.

- The Graduate School *welisa - Analysis and Simulation of Electrical Interactions of Implants with Bio-Systems* increases the communication among the

Fig. 4.2: Architect's view of the scientific building LL&M

PhD students within weekly colloquia, workshops, and other social activities. The doctoral students have the possibility to do their doctorate at the interface among electrical engineering, materials science, medicine, biology, physics and scientific computing. Along with this, occupational perspectives in research and industry of the medical technology are introduced to the young scientists through the high interdisciplinarity of their research topic.

- The Helmholtz Zentrum München has set up a *Virtual Institute for Complex Molecular Systems in Environmental Health* (HICE) together with the University of Rostock and additional research partners. The project is funded by the Initiative and Networking Fund of the Helmholtz Association. HICE examines the biological effects of aerosols from relevant anthropogenic sources. Background are the health effects of aerosols from combustion processes (so-called *particulate matter*, i.e., emissions from car and/or truck traffic and heating) known from epidemiological studies. In addition to the exact chemical and physical analysis of aerosol composition, their biological effects are investigated using primarily innovative *in vitro* models of lung tissue.

- The project *Metrology for Biofuels* aims to provide validated and reliable methods with ensured traceability of the measurement results for physical and chemical parameters of liquid biofuels, focusing on customer and industry needs, particularly on the automotive and aviation industry. A metrology infrastructure that underpins appropriate policies, stressing more sustainable use

Fig. 4.3: Status of the construction in the end of 2012. In front: the physics teaching building. In the back: completed shell of LL&M.

of natural resources, by the way of provision of sufficiently rigorous, independent, accurate and robust measurements, above dispute and legal challenge, usable by interested parties for compliance testing and regulatory enforcement, forms the basis of this project. This is of prime importance to consolidate a sustainable contribution of biofuels to the European energy supply sources.

- The combined research project *Ionische Flüssigkeiten als Abschreckmedien in der Wärmebehandlung metallischer Werkstoffe* is funded through the DFG and connects activities of the physics, chemistry and engineering (Keßler, Kragl, Schick)

Furthermore, physics research groups and members of the department are involved in two cutting-edge Research and Innovation Projects in East Germany ('Spitzenforschung in den Neuen Ländern'):

- *Regionale Entwicklung durch Medizintechnische Innovation und Spitzenforschung* (REMEDIS). This collaborative project focuses onto the development of new implants for clinical applications. The consortium unites competence in the areas of the engineering sciences, medicine and natural sciences from the university. Other local, national and international institutes and companies are involved.

- *Light2Hydrogen - Energy for the Future.* This research project explores new ways for hydrogen generation, boosting efficiency using nanotechnology and other novel technologies for a post-oil society. The production of hydrogen with the sole use of solar power would be a magnificent contribution to the generation of energy, which will not access fossil resources and will not pollute

the atmosphere. Co-funding by the state M-V is provided through the project *Nano4Hydrogen*. In close connection and intensive exchange with the sister project Light2Hydrogen, a unique basis upon the research topic photo-catalysis has been established.

A variety of additional smaller and larger research projects constitute interdisciplinary work connecting the Physics Institute with other institutes and groups. The Department LL&M strives for increasing such concerted activities in order to strengthen the international competitiveness of the University of Rostock.

5 Academic Qualifications, Colloquia, and Workshops

5.1 PhD Theses

Author	*Date*	*Title of PhD Thesis*
Andreas Przystawik	29.01.2010	Dynamik von Metallclustern in suprafluiden Heliumtropfen
Jörg Köhn	23.02.2010	Wechselwirkung von intensiven Laserfeldern mit Metallclustern – Energieabsorption durch Streuprozesse
Gerolf Burau	28.04.2010	Räumliche und spektrale Untersuchung der Resonanzfluoreszenz von Halbleiterstrukturen
Christof Liebe	30.06.2010	Zur Physik des Straßenverkehrs: Empirische Daten und dynamische Modelle
Haldor Hartwig	16.07.2010	Zur Dynamik von nichtlinearen optischen Impulsen und Impulsstrukturen in Glasfasern mit alternierender Dispersion
Martin French	23.07.2010	Thermodynamische und Transporteigenschaften von Wasser bei hohen Drücken und hohen Temperaturen
Evgeny Zhuravlev	23.09.2010	Crystal nucleation and growth in poly(ϵ-caprolactone) studied by fast scanning calorimetry
Andrea Sengebusch	01.11.2010	Linienprofile von Röntgenübergängen komplexer Atome in dichten Plasmen
Kristofer Hallgren	19.11.2010	Mesospheric water vapor; Variability at different timescales observed by ground-based microwave spectroscopy
Serguei Adamovski	26.11.2010	A calorimetric study of non-equilibrium structures on fast cooling (100 000 K/s)
Yultuz Omarbakiyeva	30.11.2010	Cluster virial expansion for the equation of state of partially ionized Hydrogen plasma

Sven Radefeldt	10.12.2010	Entwicklung und Charakterisierung eines hochporösen Formkörpers zum Einsatz als Knochenaufbaumaterial
Kristian Sell	15.10.2010	Electronic and structural properties of deposited silver nanoparticles: a STM and GISAXS study
Thomas Raitza	17.01.2011	Dynamischer Strukturfaktor von Plasmen in hoch angeregten Clustern
Richard Hofmeister	02.02.2011	Numerical and diagnostic techniques for modelling stratified coastal seas
Bastian Holst	05.04.2011	Ab-initio-Simulationen für die Zustandsgleichung und Transportgrößen von dichtem Wasserstoff
Xuan Truong Nguyen	08.04.2011	Optimal Control of the Strong-Field Laser Ionization of Clusters in Helium Droplets
Thomas Hartmann	15.04.2011	Study of the decay $\overline{B}^0 \to \Lambda_c^+ \bar{p}\pi^+\pi^-$ and its intermediate states
Hannes Rennau	27.05.2011	Natural, numerical and structure-induced mixing in dense gravity currents: idealised and realistic model studies
Marcus Ebert	31.05.2011	Isospin analysis and study of the decay modes $\overline{B}^0 \to \Lambda_c^+ \bar{p}\pi^0$ and $\overline{B}^0 \to \Lambda_c^+ \bar{p}\eta$
Jan Sperling	29.06.2011	Characterization of Entanglement in Continuous Variable Systems
Thomas Kiesel	12.10.2011	Verification of nonclassicality in phase space
Qiang Li	21.10.2011	Multi-frequency radar observations of polar mesosphere summer echoes: Statistical properties and microphysical results
Mahmoud Abdel-Latif	11.10.2011	Infrared Laser Driven Quantum Dynamics of Double Proton Transfer Reactions and Collective Carbonyl Vibrations
Rahel Knöpfel	11.11.2011	An Idealized Radiative Transfer Scheme for Use in an Atmospheric General Circulation Model From the Surface up to the Mesopause Region
Alexander Hause	27.01.2012	Wechselwirkungen und Bindungsmechanismen von optischen Solitonen in Glasfaserne
Peter Holtermann	09.03.2012	The Baltic Sea Tracer Release Experiment. Mixing processes in the Gotland Basin
Sebastian Brune	20.04.2012	Analysis of the Global Spectrum of the Atmospheric Horizontal Kinetic Energy from the Boundary Layer to the Mesopause

Eefke Marijn van der Lee	11.05.2012	Observation of internal waves in the Baltic Sea: Motions near the inertial and buoyancy frequencies
Gunda Wieczorek	25.05.2012	Spatiotemporal Scales of the Deep Circulation in the Eastern Gotland Basin/ Baltic Sea
Winfried Lorenzen	20.06.2012	Phase Transitions in Hydrogen-Helium Mixtures
Hagen Radtke	04.10.2012	Einfluss biologischer Prozesse auf die Ausbreitungswege von Nährstoffen in der Ostsee
Henning Marciniak	24.10.2012	Spektroskopische Untersuchung der Exzitonendynamik in molekularen Systemen aus organischen Halbleitern
Anne Theuerkauf	21.12.2012	Stratospheric turbulence observations with the new balloon-borne instrument LITOS

5.2 Physics and SFB Colloquia

Date	*Speaker, Affiliation, Title*
14.01.10	PD Dr. Ralf Röhlsberger, Hasylab, DESY Hamburg: Mit Synchrotronstrahlung in den Nanokosmos: Magnetischen Strukturen beim Wachstum zugeschaut
21.01.10	Prof. Dr. Manfred Lein, Universität Hannover: Zeitliche Struktur der Emission hoher Harmonischer aus Molekülen
04.02.10	Prof. Dr. Alexander Meister, Institut für Mathematik, Universität Rostock: Antrittsvorlesung
08.04.10	Prof. Dr. Markus Drescher, Universität Hamburg: Molekulare Dynamik mit ultrakurzen Röntgenpulsen: Zeitauflösende Röntgen- Photochemie am FLASH
15.04.10	Prof. Dr. Heike Rauer, DLR und Technische Universität Berlin: CoRoT Mission und extrasolare Planeten
06.05.10	Prof. Dr. Roland Sauerbrey, Dresden-Rossendorf: Relativistische Optik und Laser-Teilchen-Beschleunigung (100 Jahre Physikhaus: Erinnerung Optik in Rostock, Gustav Mie)
27.05.10	Prof. Ulrich Uwer, Heidelberg: Von den B-Fabriken zum LHC
03.06.10	Prof. Dr. Marc Vrakking, Max-Born-Institut Berlin: Connecting Lab-Based Attosecond Science with FEL research (Jubiläumsvortrag: Erinnerung an Friedrich Hund)
15.06.10	Prof. Dr. Dr. h.c. Paul-Gerhard Reinhard, Universität Erlangen: Observablen der Elektronenemission aus Clustern: Winkelverteilungen und Photoelektronenspektren
17.06.10	Prof. Dr. Horst Schmidt-Böcking, Goethe-Universität Frankfurt/M: Von Otto Sterns Molekularstrahlmethode zum COLTRIMS-Reaktionsmikroskop (Jubiläumsvortrag zur Erinnerung an Otto Stern)
01.07.10	Prof. Dr. Angelika Brückner, Inst. für Chemie und LIKAT: Operando-Spektroskopie – Innovativer Zugang zu Struktur-Wirkungsbeziehungen in der Katalyse
05.07.10	Prof. Dr. Thomas Fennel, Universität Rostock: Cluster in intensiven Laserpulsen: Nanolabore für ultraschnelle Vielteilchendynamik
08.07.10	Prof. Dr. Jörg P. Kotthaus, LMU München: Manipulation Licht-induzierter Ladungen auf einem Chip - Photonische Fallen und Förderbänder (Jubiläumsvortrag: Erinnerung an W. Schottky)
14.10.10	Prof. Dr. Mark Maroncelli, Pennsylvania State University: Solvation and Dynamics in Ionic Liquids
28.10.10	Prof. Dr. Jörn Manz, Freie Universität Berlin: Panta rhei - electronic fluxes during chemical reactions

18.11.10	PD Dr. Matthias Wollenhaupt, Universität Kassel: Ultraschnelle Laserkontrolle
09.12.10	Prof. Dr. Gerhard Paulus, Universität Jena: Nichtlineare Optik mit ultrakurzen Laserpulsen
16.12.10	Prof. Dr. Michael Vollmer, FH Brandenburg: Von der Fee Morgana, dem Hof des Mondes und weiteren farbenprächtigen Erscheinungen der Atmosphäre.
06.01.11	Prof. Dr. Thomas Klinger, MPI für Plasmaphysik Garching, Außenstelle Greifswald: Das Fusionsprojekt Wendelstein 7-X - Aufbau und Physik
19.01.11	Prof. Dr. Lutz Schön, HU Berlin: Phänomen als Zugang zur Physik - Physikuntericht als "Erkenntnisbiographie"
20.01.11	Prof. Dr. Peter Toschek, Institut für Laserphysik, Universität Hamburg: Wozu sind einzelne Atome gut?
12.05.11	Prof. Dr. Robin Santra, Zentrum für Freie-Elektronen-Laser CFEL, Hamburg: Ultrafast processes at high x-ray intensity
19.05.11	Prof. Dr. Theodore Shepherd, Dept. of Physics, University of Toronto, Kanada: The role of atmospheric dynamics in ozone-climate coupling
24.05.11	Dr. Michael Briggs, University of Alabama, Huntsville, USA: Positrons from Thunderstorms
26.05.11	Prof. Dr. Matias Bargheer, Universität Postsdam: Ultrafast x-ray diffraction
07.06.11	Prof. Dr. Dieter Hoffmann, MPI für Wissenschaftsgeschichte Berlin: Pascual Jordan — der gute Nazi
09.06.11	Dr. Achim Franz, Brookhaven National Laboratory, USA: Mit Schwerionen zurück zu den ersten Mikrosekunden des Universums
16.06.11	Frau Renate Wirth, Universität Passau: PArcours: Stationen der Eignungsdiagnostik für das Lehramtsstudium
23.06.11	Prof. Dr. Selim Jochim, MPG und Universität Heidelberg: Ultrakalte Quantengase
30.06.11	Prof. Dr. Lutz Schweikhard, Universität Greifswald: Präzisionsmassenspektrometrie kurzlebiger Nuklide
07.07.11	Ewa Weinert-Raczka, Faculty of Electrical Engineering, Stettin: Properties and possible applications of photorefractive waveguides based on AlGaAs Multiple-Quantum-Well structures
13.10.11	Prof. Dr. Markus Gerhards, Universität Kaiserslautern: Hydrogen-bonds in isolated clusters: From peptides to proton wires and metal containing aggregates
27.10.11	Prof. Dr. Frank Weinhold Madison, Wisconsin, USA: Thermodynamics and Geometry
03.11.11	Prof. Dr. Matias Bargheer, Universität Potsdam: Ultrafast X-ray diffraction

03.11.11	Prof. Dr. Rainer Blatt, Universität Innsbruck: The quantum way of doing calculations
17.11.11	Prof. Dr. P. Saalfrank, Universität Potsdam: Ultrafast, correlated dynamics of laser-driven electrons
08.12.11	Prof. Dr. Carlos Stroud Jr., Universität Rochester, New York, USA: Rydberg atomic electron wave packets: classical and quantum theory intertwined
12.01.12	Dr. Christian Bressler, European XFEL, Hamburg: Using femtosecond x-rays to study electronic and nuclear motion in complex molecules
19.01.12	Prof. Dr. Martin Aeschlimann, Universität Kaiserslautern: Simultaneous Spatial and Temporal Control of Nanooptical Fields
24.04.12	Prof. Dr. Girish Saran Agarwal, Oklahoma State University: Electromagnetically Induced Transparency and Quantum Memory in Nano Mechanical Systems
03.05.12	Prof. Dr. Stefan Scheel, Universität Rostock: Viel Lärm im Nichts - Quantenfluktuationen im Vakuum
10.05.12	Dr. Mikhail Eremets, MPI für Chemie, Mainz: Metallic hydrogen - experimental studies at few megabar
24.05.12	Prof. Dr. Rudolf Hilfer, Universität Stuttgart: Zeitentwicklung makroskopischer Zustände in statistischer Physik, Quantendynamik, Festkörperphysik, Biophysik und Polymerphysik abseits vom Gleichgewicht
07.06.12	Prof. Dr. Boris Hage, Universität Rostock: Experimente mit weniger als nichts. Gequetschtes und verschränktes Licht.
14.06.12	Prof. Dr. Klaus Sengstock, Universität Hamburg: Spektroskopie ultrakalter Quantengase
18.06.12	Prof. Dr. Winfried Denk, MPI für Neurobiologie, Heidelberg: Biomedizinische Optik: Der Blick ins Gehirn
21.06.12	Prof. Dr. Y. Tanimura, Universität Kyoto (z.Zt. Humboldt Preisträger in Hamburg): Modeling, calculating and analyzing multidimensional vibrational spectroscopies
28.06.12	Prof. Stephanie Hansmann-Menzemer, Universität Heidelberg: Mit B-Zerfällen neuer Physik auf der Spur
05.07.12	Prof. Dr. J. Peter Toennies, MPI für Dynamik und Selbstorganisation: Quantum Vortices in Helium Droplets
09.07.12	Prof. Dr. Hans A. Bachor, Australian National University, Wamboin Canberra: From Entanglement to Neuroscience - an unlikely link made possible by technology
18.09.12	Prof. Dr. Amulya Chandra Roy, Ramakrishna Mission Vivekananda University, currently at MPIPKS Dresden: Inverse bremsstrahlung heating rate in the interaction of femtosecond laser pulses with noble gas clusters

02.10.12	Dr. Christoph Merschjann, Helmholtz-Zentrum Berlin für Materialien und Energie: Transient optical spectroscopy of small polarons in organic and inorganic "semiconductors": Birth, life, and death of a localized quasiparticle
02.10.12	Prof. Dr. Nobuko Naka University of Kyoto: The electron-hole liquid in Diamond and cyclotron resonance in Cuprous Oxide
18.10.12	PD Dr. Roland Waldi, Universität Rostock: Entdeckung und Bedeutung des Higgs-Bosons
25.10.12	Prof. Dr. Rupert Klein, FU Berlin: Multi-scale asymptotic analyses of atmospheric motions
01.11.12	Prof. Dr. Ralf Ludwig, Institut für Chemie, Universität Rostock: Frieren, salzen, lösen, binden: Sieben Rostocker Geschichten über das Wasser
22.11.12	Dr. Christoph Marquardt, MPI for the Science of Light, Erlangen: Versatile sources of light for quantum information processing
29.11.12	Prof. Dr. Philip Russel, MPI for the Science of Light, Erlangen: Novel light-matter interactions in glass fibre microstructures
29.11.12	Prof. Dr. Roman Schnabel, Universität Hannover und MPI für Gravitationsphysik: Quantum entanglement in application
06.12.12	Prof. Dr. Kurt Busch, HU Berlin: Nano-Photonics: From photonic crystals to plasmonics
11.12.12	Prof. Dr. Werner Vogel, Universität Rostock: Messung und Manipulation individueller Quantensysteme - der Nobelpreis für Physik 2012
13.12.12	Prof. Dr. Karl Jakobs, Universität Freiburg: Discovery of a New Boson at the LHC
20.12.12	Dr. Stuth, Klostermuseum Rostock: Zeugnisse astronomischer Forschung in Rostock

5.3 Scientific Meetings and Workshops

Date	*Title*
01.04–30.04.10	Research Workshops Nucleation Theory and Applications, Dubna, Russia
06.06–11.06.10	Lähnwitzseminar on Calorimetry, Rostock
25.06.10	2nd Collaborative Research Centers Meeting - SFB 450 mit SFB 652
30.09–01.10.10	SFB Workshop 2010 in Plau am See
21.03–22.03.11	International Workshop on "Exciton Dynamics and Spectroscopy"
01.04–30.04.11	Research Workshops Nucleation Theory and Applications, Dubna, Russia
13.06–17.06.11	ECT* Workshop: Clusters in nuclei and nuclear matter: Nuclear structure, heavy ion collisions and astrophysics, Trento, Italy
15.06–17.06.11	Spectroscopy — Detective in Science, Rostock
12.09–16.09.11	International Conference on "Correlations in Radiation Fields" (CERF11), Rostock
01.04–30.04.12	Research Workshops Nucleation Theory and Applications, Dubna, Russia
13.06.12	Ganztägige Klausurtagung des SFB im Institut für Ostseeforschung, Warnemünde
10.06–15.06.12	Lähnwitzseminar on Calorimetry, Rostock
02.07–06.07.12	International Minisymposium on "Soliton Molecules", Rostock
30.08–31.08.12	2. International Workshop on "Exciton Dynamics and Spectroscopy"
09.09–14.09.12	International Conference "Physics of Non-Ideal Plasmas" (PNP14), Rostock

Universität Rostock

Traditio et Innovatio

Universität Rostock

MATHEMATISCH-NATURWISSENSCHAFTLICHE FAKULTÄT

Institut für Physik

D 18051 Rostock
Fon + 49 (0)381 498-67 00
Fax + 49 (0)381 498-67 02
institut.physik@uni-rostock.de

http://web.physik.uni-rostock.de